

THE USES OF THE SLIME MOLD LIFECYCLE AS A  
MODEL FOR NUMERICAL OPTIMIZATION

By

DAVID R. MONISMITH JR.

Bachelor of Science in Computer Science  
Tulane University  
New Orleans, LA  
December 2001

Master of Science in Electrical Engineering  
Oklahoma State University  
Stillwater, OK  
July 2008

Submitted to the Faculty of the  
Graduate College of the  
Oklahoma State University  
in partial fulfillment of  
the requirements for  
the Degree of  
DOCTOR OF PHILOSOPHY  
July, 2010

THE USES OF THE SLIME MOLD LIFECYCLE AS A  
MODEL FOR NUMERICAL OPTIMIZATION

Dissertation Approved:

Dr. Blayne E. Mayfield

---

Dissertation Adviser

Dr. John P. Chandler

---

Dr. Douglas R. Heisterkamp

---

Dr. Martin T. Hagan

---

Dr. Mark E. Payton

---

Dean of the Graduate College

## ACKNOWLEDGMENTS

There are many people to whom I am thankful for their help and guidance during my academic journey. First, I thank Dr. Mayfield for his guidance while I tried to decide on a topic and while I went about researching Slime Molds. Dr. Mayfield has always been kind to me and very patient, even when I took on extremely boring topics. For that I am most grateful. I applaud Dr. Hagan for doing such a wonderful job teaching. The courses I took with Dr. Hagan were thorough, most enjoyable, and they gave me much of the background I needed to study optimization. To Dr. Chandler, I am very grateful for all the help while I studied many different evolutionary computation topics. During all the independent study courses I took with him, he provided me with a wealth of knowledge, and introduced me to several algorithms I never would have thought to study. I thank Dr. Heisterkamp for his help with the graphs in this dissertation and for his help while I studied Computer Vision early into my Ph.D. He spent many hours with me in discussion of topics like 3D Reconstruction and Structure from Motion. Finally, I am especially thankful for the assistance I have received from Dana Brunson at the OSU High Performance Computing Center. Dr. Brunson was most helpful in setting up the software I needed to run simulations on the OSU supercomputer. Without her assistance, I would have spent many more months running simulations on my home computer and the computer science server.

During my time at OSU, I learned about much more than academics and research. I gained much real life experience. I have had the opportunity to teach, develop, and assist many courses. For those opportunities, I am thankful to all the members of the Computer Science Department. I also had the chance to spend four years in student government, much of which as an officer, where I helped to change for the better the way travel grants were distributed, how teaching assistants were compensated, and the way research grades were given. Student government taught me more about university politics than I ever wanted to know, but the experience was been very beneficial to me. I learned much about leadership, conflict resolution, event coordination, meeting management, and many other topics. To all the members of the GPSGA and the Graduate College, especially Philip Verghese, Shirley Vincent, Mark Payton, Gordon Emslie, Craig Satterfield, and Rosslyn Orcutt, I thank you for the time and experience.

Finally, I thank my wife, Andrea, and my family and friends for their support, love, and guidance. My wife, Andrea, and my parents, Linda and David, have supported me all throughout school and pushed me to get finished. My in-laws, Jerry and Louise, helped me by always offering me a place to stay and a meal while I traveled from Fort

Worth to Stillwater. My friends, Sunny, Andy, Doug, Robert, Erma, Amjad, and Tom, were always there for me to talk to about research or to just hang out and have fun. Thank you all for being there and thank God for helping me to finish this degree.

## TABLE OF CONTENTS

Chapter	Page
I. INTRODUCTION .....	1
II. REVIEW OF LITERATURE.....	7
Section 2.1 Optimization Algorithms .....	7
<i>Section 2.1.1 Pattern Search</i> .....	8
<i>Section 2.1.2 Razor Search</i> .....	11
<i>Section 2.1.3 Simplex Method</i> .....	15
<i>Section 2.1.4 Genetic Algorithm</i> .....	17
<i>Section 2.1.5 Particle Swarm Algorithm</i> .....	19
<i>Section 2.1.6 Differential Evolution</i> .....	21
Section 2.2 Biology.....	23
<i>Section 2.2.1 Vegetative Amoebae</i> .....	24
<i>Section 2.2.2 Aggregation</i> .....	26
<i>Section 2.2.3 Mound</i> .....	28
<i>Section 2.2.4 Slug</i> .....	28
<i>Section 2.2.5 Fruiting Body and Spore Dispersal</i> .....	29
Section 2.3 Slime Mold Simulations .....	31
<i>Section 2.3.1 Cellular Automata</i> .....	31
<i>Section 2.3.2 Biological Simulations</i> .....	34
<i>Section 2.3.3 Educational Simulations</i> .....	38
<i>Section 2.3.4 Moving to Optimization</i> .....	42
III. SLIME MOLD OPTIMIZATION ALGORITHM .....	45
Section 3.1: Initialization and Preliminary Data Structures.....	47
Section 3.2: Vegetative Search .....	49
Section 3.3: Aggregative Search.....	51
Section 3.4: Slime Mold World .....	54
Section 3.5: Mound Formation .....	56
Section 3.6: Slug Search .....	58
Section 3.7: Slime Mold Optimization Algorithm.....	62
IV. VARIATIONS ON THE SLIME MOLD OPTIMIZATION ALGORITHM.....	64
Section 4.1: Variations on the Vegetative State.....	65
<i>Section 4.1.1: Downhill Simplex for the Vegetative State</i> .....	65

<i>Section 4.1.2: Razor Search Algorithm for the Vegetative State</i> .....	67
Section 4.2: Variations on the Slug State.....	68
4.2.1 <i>Differential Evolution</i> .....	70
4.2.2 <i>DE + Followers</i> .....	70
Section 4.3 Conclusion .....	73
 V. RESULTS AND ANALYSIS .....	74
Section 5.1: Test equations and testing procedures .....	74
Section 5.2 Original Algorithm Results.....	78
Section 5.3 Comparisons between the Original Algorithm, HJ, DE, RCGA, and PSO	84
Section 5.4 Results from Modifying the Slime Mold Algorithm .....	86
Section 5.5 Comparisons to the Original Algorithm and other EAs.....	88
 VI. CONCLUSION.....	91
Section 6.1 Concluding Remarks.....	91
Section 6.2 Future Work.....	92
<i>Section 6.2.1 Further Variants on the Vegetative State</i> .....	92
<i>Section 6.2.2: Population dynamics</i> .....	92
<i>Section 6.2.3: Theoretical Research of Slime Mold Optimization</i> .....	94
 REFERENCES	96
 APPENDICES	101
APPENDIX A: OBJECTIVE FUNCTION APPENDIX .....	102
APPENDIX B1: SMOA AVERAGE RESULTS .....	118
APPENDIX C1: SMOA AVG. RESULTS FROM VARYING PSEUDOPODS .....	127
APPENDIX C2: SMOA ST. DEV. FROM VARYING PSEUDOPODS .....	130
APPENDIX C3: SMOA RUNTIMES FROM VARYING PSEUDOPODS .....	133
APPENDIX D1: AVG. RESULTS FOR SMOA WITH RAZOR VEG. STATE.....	136
APPENDIX D2: ST. DEV. FOR SMOA WITH RAZOR VEG. STATE.....	139
APPENDIX D3: AVG. RUNTIMES FOR SMOA WITH RAZOR VEG. STATE...	142
APPENDIX E1: AVG. RESULTS FOR SMOA WITH SIMPLEX VEG. STATE...	145
APPENDIX E2: ST. DEV. FOR SMOA WITH SIMPLEX VEG. STATE.....	148
APPENDIX E3: AVG. RUNTIMES FOR SMOA WITH SIMPLEX VEG. STATE	151
APPENDIX F1: AVG. RESULTS FOR SMOA-HTDE .....	154
APPENDIX F2: ST. DEV. FOR SMOA-HTDE .....	157
APPENDIX F3: AVG. RUNTIMES FOR SMOA-HTDE .....	160
APPENDIX G1: AVG. RESULTS FOR SMOA-HTDER.....	163
APPENDIX G2: ST. DEV. FOR SMOA-HTDER.....	166
APPENDIX G3: AVG. RUNTIMES FOR SMOA-HTDER.....	169
APPENDIX H1: EA AVERAGE RESULTS .....	172
APPENDIX H2: EA ST. DEV. OF RESULTS .....	173
APPENDIX H3: EA AVERAGE RUNTIMES .....	174
APPENDIX I: PARAMETER VALUE LIST FOR SMOA AND VARIANTS.....	175

## LIST OF TABLES

Table	Page
Table 4.1: List of states from the Slime Mold Optimization Algorithm .....	64
Table 5.1: Objective Functions Used.....	75

## LIST OF FIGURES

Figure	Page
Figure 1.1: Slime Mold from Fort Worth, TX .....	4
Figure 2.1: Simplex example .....	16
Figure 2.2: $\alpha$ -Blend Crossover Operator (BLX- $\alpha$ ) .....	18
Figure 2.3: Lifecycle of Dictyostelium discoideum .....	23
Figure 2.4: Example of amoeboid cell movement. ....	25
Figure 2.5: Example of cAMP waves .....	27
Figure 2.6: Example of a Fruiting Body. ....	30
Figure 2.7: 1-D and 2-D von Neumann neighborhoods. ....	33
Figure 2.8: Moore Neighborhoods.....	34
Figure 2.9: Amoebae as modeled by Glazier and Graner [1993]. ....	38
Figure 2.10: Example grid for slime mold state space.....	39
Figure 2.11: Example from James Matthews' Slime Mold Program. ....	41
Figure 3.1: UML diagram of the Amoeba object. ....	48
Figure 3.2: Approximate Nearest Neighbor Mesh,.....	52
Figure 3.3: UML diagram of the Cell data structure. ....	55
Figure 3.4: UML diagram of the Slime Mold CA data structure.....	55
Figure 3.5: Approximate Nearest Neighbor Mesh and Mound Mesh .....	57
Figure 4.1: Modification to the slug state. ....	69
Figure 5.1: Log of Scaled Relative Error for Original SMOA .....	79
Figure 5.2: Original SMOA results from Rosenbrock's function.....	80
Figure 5.3: Original SMOA results from Spherical Contours Function 10D.....	81
Figure 5.4: Error in x for Griewangk 10D Function.....	82
Figure 5.5: Original SMOA results from Griewangk Function 10D.....	83
Figure 5.6: LSRE for Original SMOA, EAs, and Hooke Jeeves.....	85
Figure 5.7: Simplex SMOA results from Rosenbrock's function.....	86
Figure 5.8: Simplex SMOA results from Modified Rosenbrock 1 function.....	87
Figure 5.9: HTDER SMOA results from Storn's Chebyshev function .....	87
Figure 5.10: LSRE for all SMOA methods .....	89
Figure 5.11: LSRE for all optimization methods.....	89



## CHAPTER I

### I. INTRODUCTION

Past years have seen the introduction of new and difficult optimization problems. Many creative algorithms have been devised to solve these problems. Such algorithms include components from fields including evolution, biology, chemistry, and ecology. These fields have inspired researchers to devise algorithms with names such as Genetic Algorithms, Differential Evolution, Ant Colony Systems, and Particle Swarms [Goldberg 1989, Price et al. 2005, Dorigo and Stützle 2004, Kennedy and Eberhart 1995]. Still, the main driving force behind this creativity is to solve optimization problems that are considered hard or intractable quickly and efficiently.

This work's purpose is to conceptualize slime mold as a viable optimization algorithm, provide evidence of its usefulness, and introduce modifications and possible improvements to the existing slime mold optimization algorithm. The final product of this work will be an algorithm capable of solving a vast array of single-objective optimization problems to optimal or near optimal values in a reasonable amount of time. Study of *Dictyostelium discoideum* (Dd), a popular slime mold in biological literature, was necessary to devise the optimization algorithm presented in this work [Kessin 2001].

Before discussing Dd, it is important to understand the problem that will be undertaken. The focus of this work is solving numerical single objective function optimization problems; therefore, a definition of the problem is provided here. Within a single objective optimization problem, it is assumed that there exists a function  $f$  or set of piecewise functions  $\{f_1, \dots, f_n\}$  that define a single function  $f$  that need not be continuous. From here on the (se) function(s) will be referred to as an objective function. It is also assumed that the objective function is composed of a set of variables  $\{x_1, \dots, x_n\}$  that form the search (or decision) space. These variables will be referred to as the decision variables. Typically, it is assumed that these variables are constrained to some area and that one or more maxima or minima exist for the objective function. The solution to such an optimization problem is, without loss of generality, the minimization of the objective function. The optimum value  $f^*$  for a function  $f$  can be expressed formally as follows:

$$\begin{aligned} f^* &= f(x_1^{\min}, x_2^{\min}, \dots, x_n^{\min}) \text{ such that} \\ f^* &= f(x_1^{\min}, x_2^{\min}, \dots, x_n^{\min}) < f(x_1, x_2, \dots, x_n) \\ &\forall \{x_1, x_2, \dots, x_n\} \end{aligned}$$

within the bounds of the search space. Minimization may be used without loss of generality because minimizing  $-f(x)$  is equivalent to maximizing  $f(x)$ . I.e. any maximization problem may be turned into one of minimization [Deb 2001].

Many methods exist to solve an optimization problem for a single objective function. Given a function that is continuous and has a first and second derivative, its minimum can be found directly. Many problems exist in real life, which however, do not meet these qualifications. Therefore, more advanced methods are necessary to solve problems that are not continuous or do not have a derivative. Methods such as Steepest Descent, Newton's method, Levenberg-Marquardt, and others make use of the first or second derivative or a compromise between the two, to progressively or quickly move close to a local minimum by moving opposite direction of the gradient or via the Hessian toward a solution [High 2005]. Other existing classical methods offer a direct search within the bounds of the space in an attempt to find a solution. Most classical methods are not guaranteed to find a global optimum unless some criterion is met (such as a continuous function with multiple derivatives or a function of low order, i.e. quadratic) [Corne et al. 1999]. Such methods typically find only a local optimum for most problems and can typically be improved by using multiple starting points for the algorithms.

Artificial Intelligence (AI) inspired methods have been implemented in the past 50 – 60 years to offer differing methods with different advantages to solve the optimization problem. Most AI inspired methods are based on some man-made or biological process that occurs in the real world. Many of these methods are population based as well. Genetic algorithms try to mimic the real life process of crossover and mutation that occurs when cells undergo meiosis [Goldberg 1989, Mitchell 1998]. Ant colony systems make use of the idea of pheromones that ants use to follow each other to a food source [Dorigo and Stützle 2004]. Simulated annealing was inspired by the process of heating and cooling metal then reheating it to make metal stronger [Chen 1997]. Particle swarm algorithms use the idea of bird flocking [Kennedy and Eberhart 1995]. Each of these algorithms yielded interesting and promising results. Still research is ongoing and often AI inspired algorithms are only used when direct approaches and algorithms such as Steepest Descent and Levenberg-Marquardt are inefficient or fail [Corne et al. 1999]. Provided this short history of optimization, we go on to discuss *Dictyostelium discoideum* and its uses as a model for numerical optimization.

In this dissertation, the lifecycle of *Dictyostelium discoideum* (Dd) is presented as a model for numerical optimization. Before discussing this model, the lifecycle is explained. Dd is an amoeba that can undertake a complex lifecycle involving several stages. Such amoebae begin their life from binary fission – the splitting of one cell into two. These amoebae are vegetative; that is, they forage in their environment. Vegetative Dd typically live in peat and humus and they eat bacteria such as *Escherichia coli* that live in such environments. Once vegetative amoebae expend the resources in their area (i.e. the bacteria), they begin to starve. After a 4 to 6 hour period of starvation, Dd enter a new stage in their lifecycle. One of the starving amoebae begins to emit a pheromone called cyclic Adenosine Monophosphate (cAMP). This amoeba is referred to as a pacemaker [Kessin 2001]. Provided there are a number of the same amoebae within the

same localized area (a 1 cm<sup>3</sup> area), a signal cascade begins [Dallon and Othmer 1997]. Other starving amoebae are stimulated to release cAMP and move toward the pacemaker. This phase of the Dd lifecycle is referred to as aggregation. The signal cascade of the aggregative phase draws amoebae in the locality of the pacemaker near it. The attraction of the amoebae toward a cAMP gradient is so strong that "streams" are formed. As the amoebae are moving toward the pacemaker in streams, they begin to release cellulose, which has a slimy consistency. The amoebae move closer and closer toward the pacemaker until they form a mound. Amoebae within the mound enclose themselves in cellulose and self-organize into a head and a tail. Once self-organization is complete the group of amoebae is a slug. The slug head directs movement of the tail toward a light source. Movement toward a light source is with the intent of moving all amoebae within the slug to the top of the soil or humus they previously inhabited. As the slug reaches a lit area, it culminates to form a fruiting body. Members of the slug's tail die to form a stalk, and members of the head climb the stalk to form spores at the top of the stalk. At this point, the fruiting body is almost like a dandelion. Various environmental factors cause the spores to be removed from the fruiting body and distributed to new locations in the environment. These include spores being eaten by worms and birds and being redistributed in their droppings. Another environmental factor allowing for redistribution is that spores may be washed away by rain or blown away by wind. Once a spore has been dispersed in the environment, upon germination it becomes a vegetative amoeba again, and the Dd lifecycle begins anew [Kessin 2001, Segel 2001].

Literature shows three different classes of studies of the Dd lifecycle using computational models. These are educational simulations, biological simulations, and discrete optimization tasks. Many of the educational simulations in literature are quite simple. While very informative, they present a simulation of only a portion of the Dd lifecycle "usually the aggregative, mound, and slug stages. Both the simulations presented by Resnick [1994] and Matthews [2002] present 2D simulations of the slime mold lifecycle starting with starving, randomly dispersed amoebae and allow them to aggregate and form slugs using simulated cAMP that is deposited on a 2D cellular automaton. The only difference between the two algorithms is the implementation. The Resnick [1994] slime mold simulation was implemented in StarLogo as an example of parallelism whereas the Matthews [2002] simulation was implemented in Java as an example of a cellular automaton. In comparison to the biological simulations, Matthews' and Resnick's simulations appear quite simple.

Of the biological simulations, the earliest reviewed in this work is that of Glazier and Graner [1993]. In 1993, they proposed a Cellular Automata (CA) model for cell sorting and differentiation. This is of particular importance because later models for the slug phase of *Dictyostelium discoideum*, such as those of Maree and Hogeweg, use cell sorting as a major portion of their simulation [2001]. The models of Segel [2001] and Maree, Panfilov, and Hogeweg [1999, 2001] take from the Glazier and Graner model to form a hybrid CA/Partial Differential Equation (PDE) model to allow for visualization of Dd movement during the mound, slug, and fruiting body stages of the Dd lifecycle. More recent work presented by Erban and Othmer [2007] provides insight into the use of PDEs to model the movement of amoebae during the aggregative stage, and suggests that

movement under the conditions where no chemical stimulus exists occurs at random. Movement of amoebae during the vegetative stage is assumed to follow similar equations to those presented in the work of Erban and Othmer, though on a smaller scale [2007].

Few efforts outside of educational studies or biological simulations have focused on the use of Dd or other slime molds as an optimizer. In fact, the author does not know of any numerical optimization algorithms based upon slime molds other than his own [Monismith and Mayfield 2008]. Existing studies of slime molds as optimizers focus on its uses as a discrete optimizer. Rothermich presents a study of slime mold as an optimizer for a resource allocation problem for an information ecosystem in his thesis [2002]. Rothermich's [2002] model is primarily based upon the educational simulations of Resnick [1994]. Another researcher, Yokoi, in 1995, devised a slime mold based optimization algorithm for the traveling salesman problem. His model is based upon the Potts Hamiltonian like the biological simulation of Glazier and Graner [1993]. Although, it appears to work well, no follow up work has been based upon it. Another interesting effort at optimization using slime molds exists, although it is not computer based. In 2000, Nakagaki was able to get a live slime mold of the genus *Physarum polycephalum* to find its way through a maze to food using the shortest path. Each of these examples shows that slime molds have the potential to be optimizers.



**Figure 1.1: Slime Mold from Fort Worth, TX, possibly *Physarum*.**

To investigate slime mold as a numerical optimizer, the cellular slime mold Dd was chosen for study. Its lifecycle exhibits two of the key elements of an evolutionary algorithm — exploration and exploitation [Goldberg 1989]. The first stage of this lifecycle — the vegetative stage, in which, individual amoebae search for food, can be contrasted with exploration. Amoebae in this stage follow folate gradients in a search for bacteria (food) [Pollitt et al. 2006]. Similarly, in many optimization algorithms such as

the Downhill Simplex Algorithm, Evolutionary Strategy, and Pattern Search, movement in a downhill and explorative manner is performed at the beginning of a search [Corne et al. 1999, Spendley et al. 1962, Hooke and Jeeves 1961]. Once Dd amoebae deplete their food source, they begin to starve. Several hours after starvation, Dd amoebae emit cAMP in an effort to aggregate [Marée et al. 1999 □Migration□]. The combination of a directed search algorithm such as PSO and a nearest neighbor data structure upon which a virtual attractant representing cAMP may be stored closely mimic the movement seen during the aggregative phase. Next, amoebae join together tightly in a mound and shield themselves from the rest of the environment with a slime sheath [Marée et al. 1999 □Phototaxis□ Kessin 2001]. This life stage could be mimicked in a numerical optimization algorithm as the formation of a data structure representing multiple individual search agents with similar goals. Thereafter, in biology, the mound becomes a slug that moves the amoebae toward a lit area where a fruiting body may be formed [Marée et al. 1999 □Phototaxis□ Segel 2001, Kessin 2001]. An analogous structure in optimization would be the aforementioned mound data structure with movement attributed to all its members. Finally, biological amoebae are redistributed in the environment as spores [Kessin 2001, Segel 2001]. Similarly, a slime mold numerical optimization algorithm could relocate the members of a slug data structure and reset their movement to that of vegetative individuals.

This dissertation includes a detailed study of the elements that were briefly discussed above. The literature review presented herein provides a detailed view of the lifecycle of Dd. The biology of Dd is reviewed first. Next, the educational simulations by Resnick [1993] and Matthews [2002] are presented. In conjunction with these simulations, a review of cellular automata (CAs) is provided [Ilachinski 2001]. The biological simulations of Dd for each portion of its lifecycle are discussed in detail. Both the educational and biological simulations give rise to the necessity of one additional tool. This is the  $\epsilon$ -Approximate Nearest Neighbor ( $\epsilon$ -ANN) algorithm [Arya and Mount 1998]. Additionally, in the literature review, existing optimization algorithms are discussed. These include classical algorithms, direct search algorithms, and evolutionary algorithms. In particular, Differential Evolution (DE), Particle Swarm Optimization (PSO), a Real Coded Genetic Algorithm (RCGA), Pattern Search, Downhill Simplex, and Razor Search are presented in detail [Price et al. 2005, Corne et al. 1999, Kennedy and Eberhart 1995, Coello Coello and Lechuga 2002, Herrera et al. 1998, Hooke and Jeeves 1961, Spendley et al. 1962, Bandler and MacDonald 1969]. After completing the literature review, the steps used to convert Dd from a lifecycle to an algorithm are shown. The Slime Mold Optimization Algorithm is then defined.

Following the explanation of the Slime Mold Optimization Algorithm, several updates to the Vegetative, Mound, and Slug states are introduced that allow for new variations of the existing algorithm. These include replacing the Vegetative state with modified versions of the Razor Search and Downhill Simplex algorithms. Furthermore, a new form for the slug is introduced that is closer to the true biological form. With the Slime Mold Optimization Algorithm and its variants defined, results are introduced. To illustrate the value of the Dd lifecycle as an optimization algorithm, results from this algorithm for a sizeable function suite are provided [Monismith and Mayfield 2008].

Comparisons are made between the Slime Mold Optimization Algorithm and existing Evolutionary Algorithms (EAs) including DE, PSO, and RCGA. Comparisons are also made to the Hooke-Jeeves Pattern Search Algorithm. Thereafter, results from the variants of the Slime Mold Optimization Algorithm are presented. These results are compared against the EAs and the original Slime Mold Optimization Algorithm. Results as presented are competitive with those of the RCGA and PSO algorithms, but the DE results are significantly better than most of those obtained from the Slime Mold Optimization Algorithm. Analysis of the results includes discussion of averages of minimum objective function values obtained from the algorithms, average runtimes, and error of results. Following analysis and comparisons, possible future works are presented. These include updates to improve the existing algorithm, the addition of population dynamics to the Slime Mold Optimization Algorithm, and the need for theoretical study of the algorithm to verify its efficacy [Monismith and Mayfield 2008].

## CHAPTER II

### II. REVIEW OF LITERATURE

Optimization using slime mold as its basis requires multi-disciplinary study. First, a study of existing optimization algorithms is necessary to provide background, insight, and inspiration. The algorithms studied are of the same class as the one being created. They are all direct search algorithms of one form or another that do not require the computation of a derivative [Corne et al. 1999]. Many of these algorithms have taken inspiration from biology, and they serve as a natural starting point for the creation of a new optimization algorithm based in biology [Passino 2005]. Next, study of the organism *Dictyostelium discoideum* (Dd) is necessary as it is the basic unit of the type of slime mold that will be scrutinized. Its lifecycle will be dissected to illustrate the portions necessary for building an optimization algorithm [Kessin 2001]. Finally, simulations of the slime mold are investigated. Existing biological simulations that use both cellular automata and differential equations are discussed [Glazier and Graner 1993, Erban and Othmer 2007, Marée et al. 1999 □Migration□ Marée et al. 1999 □Phototaxis□ Dallon and Othmer 1997, Marée and Hogeweg 2001, Segel 2001]. Educational simulations of slime molds provide some insight as to how a slime mold optimization algorithm might be created, and initial trials for optimization with slime mold and previous works build the final foundation for a slime mold optimization algorithm [Resnick 1994, Matthews 2002]. Thus, the literature review for this work is divided into three sections: Optimization, Biology of Dd, and Slime Mold Simulations.

#### ***Section 2.1 Optimization Algorithms***

In this section, several existing single-objective numerical optimization algorithms will be discussed. These algorithms have provided both inspiration and new ideas for the author's work. Since the focus of this work is to explore numerical optimization in a generalized sense, discussion of numerical optimization algorithms that are derivative-based will be omitted. Such algorithms include Steepest Descent, Newton's Method, Levenberg-Marquardt Method, and many others [Corne et al. 1999, Passino 2005]. The discussion of algorithms in this chapter will include Direct Search methods and Evolutionary Algorithms.

Direct Search methods refer to those optimization methods that do not require computation of a derivative [Hooke and Jeeves 1961]. Rather, these methods rely on some type of heuristic to search for an optimum value. Such heuristics typically rely on moving in the direction of a peak (for maxima) or a valley (for minima). This can be accomplished by random exploration, pattern based movement, or combinations thereof. Since these methods do not rely on the computation of a derivative, they can solve optimization problems that are not differentiable. Direct Search methods often use only a single starting point or very few starting points. As a result, these methods often become trapped in local optima like derivative-based methods. So when using these methods many programmers run a direct search algorithm from multiple starting points and choose the best result [Hooke and Jeeves 1961, Spendley et al. 1962, High 2005].

Evolutionary Algorithms (EAs) refer to a class of optimization algorithms that draw inspiration from nature and typically make use of a population that uses cooperation or competition to search for an optimum function value [Corne et al. 1999]. These algorithms are similar to Direct Search algorithms in that they typically do not require computation of a derivative during the search. These algorithms are, however, more advanced than direct search in that they use populations of starting points, hereafter referred to as individuals, that work together to search for an optimum objective function value. The heuristics used in an Evolutionary Algorithm vary widely and may include ideas such as population dynamics, genetic evolution, population evolution, bird flocking, etc. Each of these algorithms all, however, has the following similarities: an EA starts with a population of individuals that are initialized in some random fashion, the algorithm iterates and allows some or all of the individuals contribute toward the search, and the best objective function value is retained after each iteration. EAs build on this basic outline and can be very simple or quite complex depending upon the heuristic used [Arabas et al. 1994, Corne et al. 1999, Passino 2005, Price et al. 2005].

Included in this chapter are several existing Direct Search and Evolutionary Algorithms. First, the Pattern Search of Hooke and Jeeves is discussed along with the transformations to it to create the Razor Search algorithm. Next, the Simplex Algorithm of Hext and Spendley is considered. These direct search algorithms are considered in a later chapter for use in the first stage of the author's Slime Mold Optimization Algorithm. Next, evolutionary algorithms are discussed. These include a Real-Coded Genetic Algorithm, the Particle Swarm Optimization Algorithm, and Differential Evolution. These will be used both for comparisons and inspirations to the author's algorithm in later chapters.

### *Section 2.1.1 Pattern Search*

The Pattern Search algorithm was one of the first optimization algorithms that allowed for optimization without computation of a derivative. This is one of the algorithm's main advantages over classical approaches. Search for a minimum or maximum function value is performed by exploring in multiple directions (i.e. dimensions) using a fixed or varying step size. The algorithm makes use of a direction vector to decide whether to search forward or backward by one step in each dimension.



Once a suitable direction is achieved, the algorithm attempts a pattern step. That is, a second move is made in the same direction as the successful move. The reason for doing so is heuristic. Given the fact that a successful move was made in a particular direction, it is reasonable to assume that continuing to search in the same direction might yield positive results (i.e. the move should be at least partially in the direction opposite the gradient) [Hooke and Jeeves 1961]. A variant of this method exists using a line search in the pattern move direction. The line search attempts to find the best value in that direction, so a different pattern move in a different direction will be necessary on the next iteration of the algorithm [High 2005].

The pattern search method of Hooke and Jeeves is detailed below in Algorithm 2.1: PatternSearch. This algorithm iterates until either a convergence criterion is met or until a fixed number of objective function evaluations has occurred. Initially, a starting point  $x_0$  is selected and evaluated as  $f_0$ ; then, iterations begin. During iteration, the starting point and starting objective function value are both copied into temporary variables, and an exploration is performed. If the exploration succeeds, a pattern move is attempted by determining the search direction,  $\theta$ , and moving further in that direction [Hooke and Jeeves 1961]. Further explorations and pattern moves are attempted as long as the results of such moves are significant (i.e. they pass the Bell-Pike Test) and progress toward better function values [Bell and Pike 1966]. Once a pattern move fails, the magnitude of the search, denoted as  $\delta$ , is decreased by a factor of  $\alpha$ . Note that  $\alpha$  is a constant in the range (0, 1) and is typically set to a value between 0.1 and 0.2. Iterations continue until the convergence criterion is met or until the maximum number of function evaluations has been met [Hooke and Jeeves 1961]. Pseudocode for the pattern search algorithm is provided below.

---

#### Algorithm 2.1: PatternSearch

---

```

Do,
    x      x0 (copy x0 and f0 into x and f)
    f      f0
    Explore(ref f, x)

    While (f < f0 and numEvals < MAX_EVALS and Bell-Pike Test Passes),
         $\theta$     x - x0 (compute the direction of the valley)
        x0    x
        x      x0 +  $\theta$ 
        f0    f
        Evaluate f(x) and count the evaluation.
        Explore(ref f, x)
        Perform the Bell-Pike Test for progress.
    End while.

    If(f < f0)
        f0    f
        x0    x
    Else If(not converged and numEvals < MAX_EVALS),
         $\delta$      $\delta * \alpha$ 
    End if.

```

While not converged and numEvals < MAX\_EVALS.

---

During pattern search it is necessary to search for a good direction in which to move. Exploration in multiple directions allows for such movement. In Algorithm 2.2: Explore, a vector  $S$  is initialized to one and used to indicate the direction of an exploratory move using the values 1 or -1 to denote a positive or negative direction along each dimension. Movements are attempted in the direction of each dimension, one dimension at a time, using this module. After a movement is attempted, the module checks to see if the move improved the previous function value. If the move was indeed an improvement, that move is saved and the next dimension is tested. Otherwise, a move is made in the opposite direction and tested for improvement. This move is saved if it is an improvement; however, in the case of a move forward or backward resulting in no improvement in function value, both moves are ignored and the next dimension is tested [Hooke and Jeeves 1961]. Pseudocode for the Explore module is provided below.

Pattern search is an effective search algorithm when searching for an optimum in a function that is singly modal. Problems occur with this algorithm in multi-modal functions. Using a poor starting point may result in the function being trapped within local minima. Multiple starting points may alleviate this problem; however, minima that lie along a line or point with a narrow opening angle may have a low probability of being found. For many functions, whether differentiable or not, using pattern search with multiple starting points will deliver optimal or near optimal results as long as reasonable step sizes are used [Hooke and Jeeves 1961, High 2005].

---

**Algorithm 2.2:** Explore (ref  $f_0$ ,  $x$ )

---

```
For I = 1 to NUM_DIM
    Si = 1
End for.

For I = 1 to NUM_DIM,
    xi = xi + Si * |  $\delta$  |
    Evaluate f at x.

    If (f < f0),
        f0 = f
    Else,
        Si = -Si
        xi = xi + 2 * Si * |  $\delta$  |
        Evaluate f at position x.

        If (f < f0),
            f0 = f
        Else,
            xi = xi - Si * |  $\delta$  |
        End if.
    End if.
End for.
```

---

### Section 2.1.2 Razor Search

Razor search is an extension of the "Direct Search" method of Hooke and Jeeves [1961]. Razor search attempts to improve upon the Pattern Search method by allowing for random search in a different direction once direct search does not yield improved results. This method is interesting because it can make direct search effective on functions with an extremely narrow opening angle to a minimum. In such functions, it can be quite difficult to achieve optimization using non-classical methods such as genetic algorithms, particle swarm, ant colony optimization, etc. Razor search is divided into four major parts. These are the Razor Search module itself and three additional modules to perform a modified version of the pattern search of Hooke and Jeeves. These additional modules perform the pattern search via the use of a main module and two additional modules to perform the exploration move and to find a reliable starting point for a pattern move [Bandler and MacDonald 1969].

In razor search, first, the objective function is evaluated at a starting point. This point may be chosen at random. Pattern search is performed at this starting point. Additionally, criteria are set for the maximum number of iterations  $\kappa$  and reductions in the current minimum step size  $\varepsilon$  using the formula below.

$$\varepsilon \leftarrow \varepsilon_{\min} \cdot \eta^{\kappa} \quad (2.1)$$

Note that  $\eta$  is a constant that is set heuristically, and  $\varepsilon_{\min}$  is the smallest step size that may be taken during a pattern search. Furthermore, if a finishing criterion is not met, the program iterates until a finishing criterion is met or until a fixed number of iterations has been completed; whichever comes first. During an iteration, a point nearby the last best point found is generated using the following formula:

$$x \leftarrow x_0 + \rho \cdot \text{Rand}(1, -1) \cdot \varepsilon, \quad (2.2)$$

Where  $x$  contains the generated point,  $x_0$  is the variable containing the last best point,  $\rho$  is a scaling factor,  $\varepsilon$  is the minimum magnitude of the current move, and  $\text{Rand}(1, -1)$  is a pseudorandom number generator that produces values between 1 and -1 with uniform probability. Using this new point, a pattern search is conducted in a different direction. If the results of the pattern search yield a better function value, the new value is saved. Additionally, a new valley (search) direction  $\theta$  is computed using the following formula:

$$\theta \leftarrow x_0 - x. \quad (2.3)$$

Thereafter, a pattern move is performed using this direction. So long as this pattern move is beneficial, additional pattern moves are performed and the best location and function value are updated. Finally, the finishing criterion is checked. If the finishing criterion is not satisfied and the maximum number of iterations has not been expended, the program

continues iterating [Bandler and MacDonald 1969]. Pseudocode for Razor Search is provided in Algorithm 2.3: RazorSearch.

---

**Algorithm 2.3:** RazorSearch

---

```

 $\varepsilon \leftarrow \varepsilon_{\min} * \eta^k$ 
Evaluate  $f_0$  at its initial position  $x_0$ .
PatternSearch( $x_0$ , ref  $f_0$ )

If the finishing criterion is satisfied,
    End program.
End if.

For  $j = 1$  to  $k$ ,
    Obtain a new position  $x$  in a random direction using (Eq. 2.3).
    Evaluate  $x$  and store its result in  $f$ .
     $\varepsilon \leftarrow \varepsilon / \eta$  (Decrease the smallest allowable step size)
     $\delta \leftarrow ||x - x_0||$ 

    If  $x$  is out of bounds,
         $F \leftarrow \infty$ 
    End if.

    PatternSearch( $x$ , ref  $f$ )

    If ( $f < f_0$ ),
         $f_0 \leftarrow f$ 
         $\theta \leftarrow x - x_0$ 
         $x_0 \leftarrow x$ 
    Else,
         $f \leftarrow f_0$ 
         $\theta \leftarrow x - x_0$ 
    End if.

    conv2  $\leftarrow$  true

    While(conv2),
         $x \leftarrow x_0 + \theta$ 
         $\delta \leftarrow ||\theta||^2$ 
        PatternMove(ref  $f$ ,  $x$ ,  $x_0$ )
        If ( $f < f_0$ ),
             $f_0 \leftarrow f$ 
             $x_0 \leftarrow x$ 
        Else,
            conv2  $\leftarrow$  false
        End if.
    End while.

    If the finishing criterion is satisfied,
        End program.
    End if.
End for.

```

---

The Pattern Search method used as part of Razor Search is used in place of the second call to Algorithm 2.2: `Explore` in the Hooke and Jeeves Pattern Search [1961]. As a method of determining the step size, the magnitude of the search direction,  $\theta$ , denoted as  $\delta$  is used when an exploratory or pattern move is performed. This value is also used as the stopping criteria for the pattern search in conjunction with  $\varepsilon$ , which is the smallest allowable step size. This is the main difference between the Pattern Search of Hooke and Jeeves and the one used here. While the pattern search iterates, first an exploration is performed using copies of the point and function value passed in as parameters. Then, so long as the exploration is beneficial, the direction of the valley is computed and pattern moves are performed in that direction. If the move is not beneficial, the magnitude of the exploration is decreased. Iteration for pattern search continues until the magnitude of the exploration becomes too small (less than  $\varepsilon$ ) [Bandler and MacDonald 1961].

During Razor Search exploration is necessary to achieve reasonable pattern moves and improvements in objective function values. This exploration is, in fact, performed in the same fashion as that of Algorithm 2.2: `Explore`. Therefore, the exploration module presented in Section 2.1.1 will be used again here as part of the Pattern Search for Razor Search presented in Algorithm 2.4 [Hooke and Jeeves 1961].

---

**Algorithm 2.4:** `PatternSearch(x0, ref f0)`

---

```

While ( $\delta > \varepsilon$ ),
    x    x0 (copy x0 and f0 into x and f)
    f    f0
    Explore(f, x)

    If (f < f0),
        While (f < f0),
             $\theta$     x - x0 (compute the direction of the valley)
            x0    x
            x      x0 +  $\theta$ 
             $\delta$     ||  $\theta$  ||2 (compute the magnitude of the step)
            PatternMove(f, x, x0)
        End while.
    Else,
         $\delta$      $\delta * \alpha$ 
    End if.
End while.

```

---

The pattern move module presented below serves to find a suitable exploration move for use in a following pattern move. Obviously, the method used in Razor Search for a pattern move is slightly different than that of Hooke and Jeeves [1961]. Notably, a variable  $m$  is used to provide three tries at possible explorations. Algorithm 2.5: `PatternMove` starts by assigning  $m$  a value of one. Thereafter,  $\delta$  is compared to  $\varepsilon$  to ensure the exploration size is large enough. Next, a loop begins that will cycle at most

three times. In this loop the objective function is evaluated at its current position. Then, an exploration move is attempted [Bandler and MacDonald 1969]. If the exploration succeeds (i.e. the move was an improvement and passes the Bell-Pike Test), the method returns because of its success [Bell and Pike 1966, Bandler and MacDonald 1969]. Otherwise, the value of  $m$  is checked. If  $m$  is one and the previous move was unsuccessful, the current pattern is not immediately thrown away. Rather,  $m$  is set to two and a move closer to the base point is attempted by decreasing the variable  $\delta$ . If this closer move is unsuccessful,  $m$  is set to three and a move in the opposite direction is attempted. If the third try fails, the method is terminated [Bandler and MacDonald 1969].

---

**Algorithm 2.5:** PatternMove (ref  $f_0$ ,  $x$ ,  $x_0$ )

---

```

m      1

If ( $\delta < \varepsilon$ )
    Return;
End if.

While (true)
    Evaluate f at position x
    Explore(f, x)

    If ( $f < f_0$ )
        For I = 1 to NUM_DIM,
            If(  $|x_i - x_{0i}| > 10^{-6}|x_{0i}|$  )
                 $f_0 \leftarrow f$ 
                Return.
            End if.
        End for.
    End if.

    If ( $m = 1$ )
        m      2
         $\delta \leftarrow \delta / 2$ 
         $x \leftarrow x_0 + 0.5 * \theta$ 

        If ( $\delta < \varepsilon$ )
            Return;
        End if.
    Else if ( $m = 2$ )
        m      3
         $S \leftarrow -S$ 
         $x \leftarrow x_0 - 0.5 * \theta$ 
    Else
        Return;
    End if.
End while.
```

---

### Section 2.1.3 Simplex Method

The Simplex Method of Spendley, Hext, and Himsworth is another direct search algorithm [1962]. It makes use of a geometric shape known as a simplex to perform numerical optimization. The shape of a simplex depends upon the dimensionality of the function as a simplex consists of  $N+1$  points, where  $N$  is the number of dimensions in the objective function being considered. Creation of a simplex starts by choosing a base point  $x^{(0)}$ . Then  $N$  additional points are created based upon the formula below. Note that  $j$  represents a dimension;  $i$  represents the index of the point in question; and both  $i$  and  $j$  are in the range  $[1, N]$ .

$$x_j^{(i)} = \begin{cases} x_j^{(0)} + \delta_1 & j = i \\ x_j^{(0)} + \delta_2 & j \neq i \end{cases} \quad (2.4)$$

These  $N+1$  points form the simplex. Spendley, Hext, and Himsworth suggest  $\delta_1$  and  $\delta_2$  be chosen such that all points are equidistant from the base point  $x^{(0)}$  [1962]. For a two dimensional objective function, the result is a simplex that is a triangle. For a three dimensional function the result is a tetrahedron. To ensure the points are equidistant, the following formulas may be used.

$$\delta_1 = \frac{(N+1)^{1/2} + N - 1}{N\sqrt{2}} \quad (2.5)$$

$$\delta_2 = \frac{(N+1)^{1/2} - 1}{N\sqrt{2}} \quad (2.6)$$

The user may multiply both  $\delta_1$  and  $\delta_2$  by a constant  $\alpha$  to scale the distances between these points up or down; however, this constant should be the same for all points created as part of the simplex and may cause unexpected results during optimization [Spendley et al. 1962].

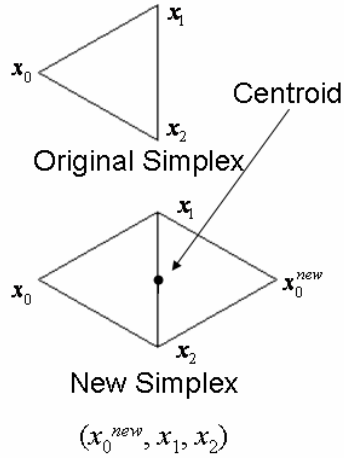


**Figure 2.1: Simplex example [High 2005].**

The objective function is evaluated at all  $N+1$  points in the simplex, and the point that has the worst objective function value in the simplex is marked as the new base point,  $x^{(0)}$ . The simplex is then reflected about this worst point. The centroid of the remaining points, where  $i$  is in the range  $[1, N]$ , is computed as follows.

$$x_c = \frac{1}{N} \sum_{i=1}^N x^{(i)} \quad (2.7)$$

The base (i.e. worst) point is then reflected about the centroid using the following formula.

$$x^{(new)} = x^{(0)} + \lambda(x_c - x^{(0)}) \quad (2.8)$$

A symmetric reflection is typically used and may be achieved by setting  $\lambda$  to 2. Reflection typically moves the new base point in the direction of a valley. This occurs because moving away from the worst point in a simplex is typically at least partially in the opposite direction of the gradient. To perform optimization via the Simplex Algorithm, this process is repeated until either the simplex reflects back upon itself or a single point within the simplex is repeated for  $M$  iterations, where  $M$  is defined in the formula below.

$$M = 1.65N + 0.05N^2 \quad (2.9)$$

Once the one of the aforementioned criteria is met, the size of the simplex is reduced (typically by half) and iteration continues. Iteration stops when the simplex becomes too small or the number of iterations surpasses a preset limit [Spendley et al. 1962].



Many variations upon the Simplex Algorithm exist. One of the most famous is the Nelder-Mead method. This method allows for both expansion and contraction of a simplex and is an excellent optimizer for some functions with low dimensionality [Torczon 1989]. Unfortunately, this optimizer fails in certain circumstances. In her dissertation, Virginia Torczon proved that the Nelder-Mead method fails on functions with a high degree of multidimensionality [1989]. For example, the Nelder-Mead method may fail on a 32-dimensional sphere function. Therefore, even though the Spendley [1962] method may converge to a local minimum, the simplex used therein will not collapse when used for general purpose optimization.

---

#### **Algorithm 2.6:** Simplex

---

```

Choose a base point.
Create the initial simplex using formulas (2.4), (2.5), and (2.6).
Evaluate and store  $f(x)$  at all simplex points.

While(numIterations < MAX_ITERATIONS)
    Find the simplex point  $j$  with the worst objective function value.
    Swap  $x^{(0)}$  and  $x^{(j)}$ .
    Obtain the centroid using formula (2.7).
    Create  $x^{(new)}$  using formula (2.8).
    Evaluate and store  $f(x^{(new)})$ .

    If( $f(x^{(new)}) = f(x^{(0)})$ ),
        Decrease the size of the simplex and continue.
    Else if repetitions for any simplex point are greater than  $M$ ,
        Decrease the size of the simplex and continue.
    Else,
         $x^{(0)} \quad x^{(new)}$ 
    End if.
    Retain the best objective function value.
End while.
```

---

#### *Section 2.1.4 Genetic Algorithm*

A Genetic Algorithm is an algorithm based upon population evolution. The theory behind population evolution is that fit individuals are selected to mate and during mating their genes are recombined and mutated to produce offspring. The best or fittest of these offspring survive to pass on their genes to a new generation. The same concepts are used in a Genetic Algorithm for optimization. For numerical optimization, an individual may be represented as a location within the search space and the corresponding objective function value [Goldberg 1989, Mitchell 1998, Passino 2005]. Many options then exist to "evolve" a population of individuals toward an optimal objective function value. In a Real-Coded Genetic Algorithm, individuals are selected from the population to produce children. Such individuals can be recombined in many ways. Typically this involves random selection from a subspace near or in between the locations of the parents. Mutation can be achieved by adding a small random value to the

children. Finally, survival of the fittest can be realized by only retaining the children with the best objective function values [Herrera 1998, Mitchell 1998]. To better visualize the real-coded Genetic Algorithm, an example algorithm is provided.

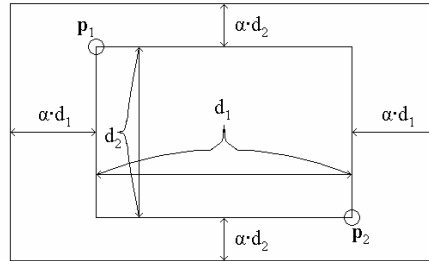


**Figure 2.2:  $\alpha$ -Blend Crossover Operator (BLX- $\alpha$ ), redrawn from [Tsutsui et al. 1999].**

The example of a real-coded GA presented in Algorithm 2.7: `RealCodedGA` includes four basic components of a GA: selection, recombination, mutation, and elitism (survival of the fittest) [Goldberg 1989]. First, tournament selection was used to choose parent individuals. Parents were chosen by comparing two randomly chosen individuals and selecting the one with the better fitness value. After choosing two parents, two children were produced by recombination [Goldberg 1989, Mitchell 1998]. For simplicity, the same number of children as parents is created in the example algorithm. The probability of recombination may be set near 60% for the algorithm presented in this work, though values between 50% and 95% will definitely be effective. During recombination, a real-coded crossover operator named the  $\alpha$ -Blend Crossover (BLX- $\alpha$ ) operator is used [Herrera et al. 1998]. This crossover operator creates a bounding box using the locations of the two parents to form bounds. The bounding box is extended to a size of  $1.\alpha$  times the distance between the locations of the two parents. Note that  $\alpha$  is in the range  $[0,1)$ , and if  $\alpha$  is equal to zero the crossover is referred to as Arithmetic Crossover. So, if  $\alpha = 0.5$ , the bounding box would be 1.5 times the distance between the parents in each dimension [Herrera et al. 1998]. An example of this is shown in Figure 2.2 above [Tsutsui et al. 1999]. In Algorithm 2.7: `RealCodedGA`, each pair of children is chosen from random locations within this bounding box. A mutation operator may be applied to the children after recombination. With, for example, a 0.5% probability, the mutation operator adds a small random value to a child [Herrera et al. 1998]. Once a generation is completed, a child population and a parent population exist. Pairs of parents that were not recombined are retained in the next generation. Children are compared to their parents, and those that exhibit better fitness are retained in the new population otherwise, their parents are retained [Goldberg 1989, Mitchell 1998].

These steps are performed on a population of a fixed size (e.g. 100 individuals), which is updated over a fixed number of generations (e.g. 1000 generations) or for a fixed number of function evaluations (e.g. 200,000 function evaluations). Each of the

choices above builds a simple genetic algorithm that works quite well for single objective optimization [Goldberg 1989, Mitchell 1998]. That is not to say that this algorithm is without deficiencies. The GA algorithm presented here has difficulties with functions that have narrow opening angles to minima. Moreover, the crossover operator presented here may cause the algorithm to ignore dimensions in the search space; however, different arithmetic crossover operators exist that correct this problem [Herrera et al. 1998, Kita et al. 1999, Takahashi and Kita 2001]. Even with these deficiencies, for most problems the GA provides a simple, yet efficient comparison algorithm and will be used as such in the results section of this work.

---

#### **Algorithm 2.7:** RealCodedGA

---

Initialize a random location and evaluate the function value at that location for each individual in a parent population of size NP.  
Archive the best individual in the parent population.

```

For the number of generations,
  For i = 1 to floor(NP/2),
    Select a pair of parents to form children using a
    tournament selection.
    Create a pair of children by performing recombination on
    the parents with a fixed probability (e.g. 60%).
    If a pair of children was created,
      Perform mutation on the children with a fixed
      probability (e.g. 0.5%).
      Evaluate the function values of the children.
      Add the children to the child population.
    Else,
      Add the parents to the child population.
    End if.
  End for.

  For i = 1 to NP,
    If child[i].fitness < parent[i].fitness)
      parent[i] = child[i]
    End if.
  End for.
End for.

```

---

#### *Section 2.1.5 Particle Swarm Algorithm*

Creation of the Particle Swarm Optimization (PSO) algorithm was inspired by bird flocking and the "boids" simulation by C. W. Reynolds [1987]. Kennedy and Eberhart discovered that simulated bird flocking could be used for optimization purposes [1995]. The PSO algorithm makes use of a population of "birds" that are called particles. These particles consist of current and personal best locations and objective function values. Particles typically have a velocity as well. A population of particles mimics some of the properties of bird flight such as following a leader and individuality.

Particles follow the leader by moving in the direction of the particle with the best objective function value. They also exhibit individuality by moving in the direction of their personal best objective function value. Based on these properties, the PSO algorithm has been adapted to discrete and continuous optimization in both single and multi-objective functions [Kennedy and Eberhart 1995, Coello Coello and Lechuga 2002].

Numerical Particle Swarm Optimization makes use of a population of particles that start with uniformly distributed, randomly selected locations from the search space of a particular problem. Each of these points is moved about the decision space via the formulas below.

$$v_i(t+1) = \chi( v_i(t) + c_1 \cdot \text{rand}(0,1) \cdot (p_{\text{best}_i}(t) - x_i(t)) + c_2 \cdot \text{rand}(0,1) \cdot (g_{\text{best}}(t) - x_i(t)) ) \quad (2.10)$$

$$x_i(t+1) = x_i(t) + v_i(t+1) \quad (2.11)$$

In the formulas above,  $x_i(t)$  is the location of particle  $i$  within the state space at time  $t$ ,  $\chi$  is a constant used to avoid exorbitant velocity,  $v_i(t)$  is the velocity of particle  $i$  at time  $t$ ,  $p_{\text{best}_i}(t)$  is the personal best location of particle  $i$  at time  $t$ ,  $g_{\text{best}}(t)$  is the global best location at time  $t$ , and  $c_1$  and  $c_2$  are constants determined heuristically. With each time step, the position and the velocity of each particle is updated with respect to the formulas above. In addition, with each time step, the personal best of each particle is updated as necessary. Similarly, is the global best is updated for the entire set of particles [Kennedy and Eberhart 1995, Clerc and Kennedy 2002].

An example implementation of PSO similar to that of Algorithm 2.8: ParticleSwarmOptimization could make use of 100 particles that are updated through 1000 iterations. The standard PSO formula explained above for  $g_{\text{best}}$  may be used. In this formula, constants may be set to  $c_1 = 2$  and  $c_2 = 2$  as recommended by Kennedy and Eberhart [1995]. Smaller values such as  $c_1 = 0.2$  and  $c_2 = 0.2$  may be chosen to allow for additional exploration of the search space over the published constants [Coello Coello and Lechuga 2002]. The constant  $\chi$  should be set to a number slightly less one such as 0.9 to allow for exploration and to prevent explosion of the population. This constant may be decreased as the algorithm converges to allow for smaller and finer movements near an optimal function value [Clerc and Kennedy 2002]. Like any stochastic optimizer, this one does, however, have problems finding minima in narrow valleys and in regions where there is an extremely low probability of finding a minimum. Even so, implementation of the algorithm as described above results in a decent optimizer with few deficiencies.

---

#### **Algorithm 2.8:** ParticleSwarmOptimization

---

```
Initialize random values for each particle.
Compute the  $p_{\text{best}}$  for each particle.
Find the  $g_{\text{best}}$  from the set of particles.
```

```
For the number of iterations,
```

```

For each particle i,
  -Evaluate the following formulas:
     $v_i(t+1) = \chi( v_i(t) + c_1 \cdot \text{rand}(0,1) \cdot (p_{\text{best}_i}(t) - x_i(t)) + c_2 \cdot \text{rand}(0,1) \cdot (g_{\text{best}}(t) - x_i(t)) );$ 
     $x_i(t+1) = x_i(t) + v_i(t+1).$ 
  -Evaluate the function value for particle i.
  -If the new function value for particle i is
    better than particle i's pbest, update particle
    i's pbest.
End for.

Update the  $g_{\text{best}}$  if necessary.
End for.

```

---

### Section 2.1.6 Differential Evolution

Differential Evolution (DE) is a population-based Evolutionary Algorithm (EA) that was created by Kenneth Price and Rainer Storn [Corne et al. 1999]. Much like other Evolutionary Algorithms, it makes use of mutation, recombination, and selection. The main difference between this algorithm and other EAs is that it uses the difference between two randomly selected vectors (i.e.  $x_{r1} \ominus x_{r2}$ ) for mutation. Much of the rest of the algorithm is quite similar to other EAs. It is important to note, however, that discrete recombination is used in the version of DE presented in this work, and selection based upon the better function value is used to determine whether a parent or a child vector is retained in the population [Price et al. 2005]. The details of this algorithm are described below.

Initialization of the Differential Evolution algorithm begins with a population of fixed size  $NP$ . In this population, each individual  $i$  is initialized to a uniformly distributed random location within the search space, and its objective function value is evaluated and stored within that individual. Additionally, a temporary individual is created for use when creating "child" individuals. Differential Evolution iterates for a fixed number of generations or until some finishing criteria is met. During each generation, a "child" is created for each individual  $i$  in the population. This is done by selecting 3 individuals at random from the population. These individuals, indexed  $r1$ ,  $r2$ , and  $r3$ , are used in combination for both mutation and recombination. Indices are chosen such that  $r1 \neq r2 \neq r3 \neq i$ . Mutation occurs by the formula listed below.

$$temp_j = p_j^{r3} + F \cdot (p_j^{r1} - p_j^{r2}) \quad (2.12)$$

Note that  $j$  represents a dimension,  $r1$ ,  $r2$ , and  $r3$  are indices, and  $F$  represents a mutation factor in the range (0,1+). Recombination, as noted before, is discrete. This recombination is performed using a crossover factor  $CR$ .  $CR$  is a constant probability factor in the range [0,1) used to make a decision whether to keep the value from dimension  $j$  of the parent  $i$  or to use the mutated value for dimension  $j$  from equation (2.12). In this work, at least one dimensional value within the child will contain a mutated value. After a child vector is created, its objective function value is evaluated.

If the child vector has a better function value than the parent with index  $i$ , the child replaces the parent. Otherwise, the parent is retained. This process occurs for each individual  $i$  within the population over a number of generations or until some finishing criterion is met [Price et al. 2005].

The DE algorithm, presented as Algorithm 2.9: DifferentialEvolution below, is one version (DE/rand/1/bin) presented in [Corne et al. 1999]. Reasonable values for the constant  $F$  range between 0.4 and 0.9 as indicated by graphs in [Corne et al. 1999]. Similarly, the decent values for the crossover constant  $CR$  range from 0.8 to 1.0, and the population size should be between 2 to 100 times the number of dimensions in the problem with 20 times the number of dimensions typically working best. Finally, the number of generations should be set to a reasonably large number such as 1000. This algorithm works quite well as a general purpose optimizer so long as initialization is uniform over the search space and parameters are set appropriately [Price et al. 2005].

---

### Algorithm 2.9: DifferentialEvolution

---

```

Initialize a population "pop" of NP individuals each with a random
location.
Compute and store the objective function at each location.
Create an individual called temp.

For the number of generations,
    For each individual i,
        Choose 3 unique individuals at indices r1, r2, and r3 from
        the population at random.

        Assign j a random value between 0 and NUM_LOC-1, inclusive.

        For k = 0 to NUM_LOC-1,
            If( rand(0,1) < CR | k = NUM_LOC-1 ),
                temp[j] = pop[r3].location[j] +
                F * (pop[r1].location[j] - pop[r2].location[j]);
            Else
                temp[j] = pop[i].location[j];
            End if.

            Ensure temp[j] is within the bounds of the problem
            specification.

            j = (j + 1) mod NUM_LOC;
        End for.

        Compute the fitness of temp.

        If(temp.fitness < pop[i].fitness),
            pop[i].fitness = temp.fitness;
            pop[i].location = temp.location;
        End if.
    End for.

```

Archive the individual with the best fitness.  
End for.

---

## Section 2.2 Biology

In this section we discuss the biological aspects of slime mold. A commonly studied slime mold is the species *Dictyostelium discoideum*. Dd is of biological interest because it is one of a small group of amoeba that exhibit self-organizing behavior. This interest in Dd and other amoeba with self-organizing behavior exists in biological communities because these organisms exhibit behavior that represents a step between multicellular organisms (e.g. animals) and single celled organisms like bacteria and non-organizing amoeba [Kessin 2001]. Slime molds have also provided interest to computer scientists. The self-organizing behavior of slime mold lends itself to easily implemented parallel systems and to cellular automata [Resnick 1994, Matthews 2002].

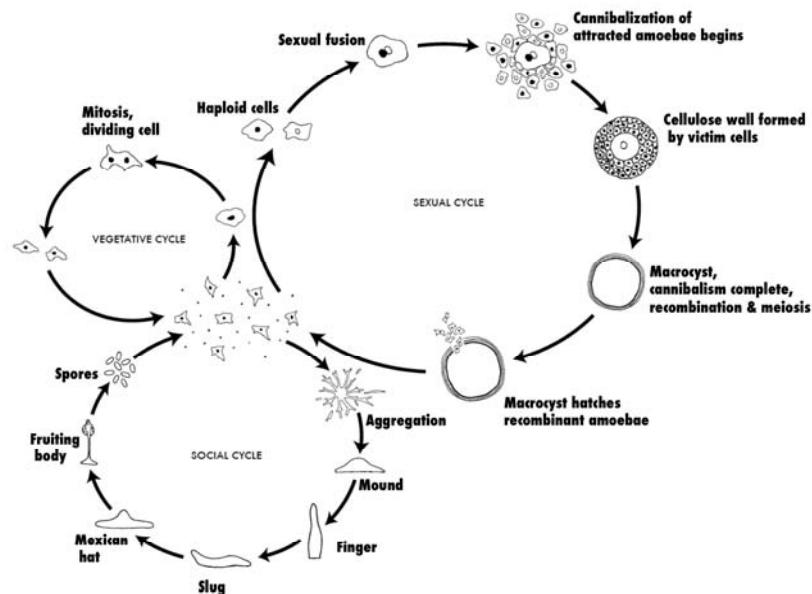


Figure 2.3: Lifecyle of *Dictyostelium discoideum*  
[Brown and Strassman 2009]. Image used under the terms of the Creative Commons Attribution 3.0.

Computer scientists have built simple interactive models of slime mold in the past 15 years, and a few have attempted to use slime mold for discrete optimization [Rothermich 2002].

The lifecycle of Dd will be studied to better understand this amoeba and how it and other amoeba like it form slime molds. Dd takes on a number of states in its life cycle, as shown in the figure above. When food is readily available, Dd exists in a vegetative state. It uses pseudopods for its movement and forages for bacteria and decaying materials such as logs. In the absence of live food, Dd may attempt to attract

food by releasing folic acid, a typical nutrition source for bacteria. Dd act as individuals in this stage of their lifecycle and exhibit no self-organizing or swarm-like behavior. They may also procreate in this stage by binary fission or they may hibernate as a microcyst (small group of dormant cells) or macrocyst (large group of dormant cells) [Kessin 2001]. This stage of the Dd lifecycle is relatively uninteresting when compared to the other stages.

Dd exhibit cooperative swarm-like behavior only upon starvation. During extended starvation, Dd amoebae release a chemical called cyclic Adenosine Monophosphate (cAMP). This chemical is like a pheromone and attracts the amoebae. Movement of the amoeba is opposite the gradient of cAMP and detection of this chemical during starvation causes a Dd amoeba to release additional cAMP [Dallon and Othmer 1997, Kessin 2001, Erban and Othmer 2007]. When released in a group of starving amoeba, cAMP causes the nearby amoeba to initiate a signaling cascade that causes a streaming effect toward the first amoeba, called a pacemaker, which released cAMP. This step is referred to as aggregation [Kessin 2001, Erban and Othmer 2007]. Dd move in streams toward this pacemaker until a mound is formed. Dd amoebae in the mound engulf themselves in slime to provide protection for the group [Kessin 2001]. The Dd also organize themselves into motile slug with a head and a tail, which represent the amoeba that will form a stalk and spores respectively [Marée et al. 1999 □Migration□ Marée et al. 1999 □Phototaxis□ Kessin 2001]. The slug moves toward a light source so a fruiting body consisting of a stalk and spores may be formed. Spores from the fruiting body are eaten and deposited as waste by animals or deposited by wind [Kessin 2001, Pollitt 2006]. Stimulus from a food source causes these spores to activate as new vegetative cells [Kessin 2001]. Each of these steps is elaborated upon in this section, beginning with the vegetative state and ending with the fruiting body state [Kessin 2001]. In further sections their simulations and applications will be discussed.

### *Section 2.2.1 Vegetative Amoebae*

Vegetative amoebae are individual amoebae that are independent and have little or no interaction with other amoebae in the environment. When Dd are vegetative, they exist in soil, humus, and decaying logs. Dd hunt bacteria in these environments as they are as much as 1000 times bigger than their prey. Dd may also eat yeast. In most cases, Dd hunt their bacterial prey by detecting folate gradients. They do so because folate (Vitamin B9) is a common food source of bacteria. Dd even possess the ability to emit folate to attract their prey [Kessin 2001, Pollitt 2006, Erban and Othmer 2007].



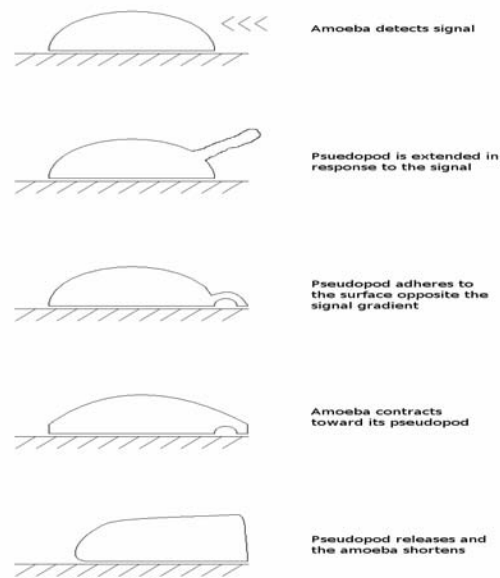


**Figure 2.4: Example of amoeboid cell movement.**  
Redrawn from [Kessin 2001].

Movement of these amoebae is similar to the movement in some mammal cells such as leukocytes (white blood cells). This is one of the reasons that Dd is well studied. During movement Dd amoebae may move at a speed up to  $20\text{ }\mu\text{m}/\text{min}$  [Dallon and Othmer 1997, Erban and Othmer 2007]. Movement is achieved through the use of pseudopods. These pseudopods are similar to arms, but they have chemical sensitivity at the ends and are also capable of adhering to surfaces at the ends. Movement is typically preceded by sensory perception. First, an amoeba receives a signal such as stimulus from a folate gradient. Dd are able to ascertain the approximate direction of a gradient across their cell bodies. Depending on the type of signal, the amoeba may decide to move in the direction of the gradient or to move opposite it. If, for example, the initial stimulus was folate, the amoeba would decide to move opposite or nearly opposite the folate gradient. Dd have a similar response to cyclic Adenosine Monophosphate (cAMP). *Ammonia* elicits a movement in the direction of the gradient, to direct Dd away from this noxious substance [Kessin 2001, Marée and Hogeweg 2001]. After ascertaining the appropriate direction of movement, the amoeba then extends a pseudopod, which has the appearance of a protrusion [Kessin 2001].

The pseudopod adheres to a surface in the direction of the stimulus or opposite it depending upon the type of stimulus. Chemotactic sensors at the end of the pseudopod provide additional sensory information. Depending on the type of signal and the direction of movement, the amoeba may decide to move in that direction or to retract the pseudopod. During movement, a Dd amoeba contracts its body wall in the direction of the pseudopod. Thereafter, the tension in the direction of the pseudopod in conjunction with cell motility would cause the amoeba to de-adhere from its previous location and move toward the new location. An example of the movement previously described is

shown in the figure above. It is important to note that such movement may not occur if detection of a negative stimulus occurs at the end of the protrusion [Kessin 2001]. Interestingly, several versions of the simplex optimization method described in section 2.1.3 have been based upon this type of movement [Torczon 1989].

Of further interest are the differing stages of life Dd may enter in response to environmental stimuli while in the vegetative state. The first of these is the microcyst. A microcyst is an amoeba that is encapsulated in cellulose. It is in most cases dormant and is formed in response to multiple conditions. These are the simultaneous presence of starvation and either increased osmotic pressure (too much water in the environment) or ammonia (a negative stimulus) [Kessin 2001, Marée and Hogeweg 2001]. These stimuli cause a Dd amoeba to form a cellulose coating in place of its cell wall and to go dormant until environmental conditions are more suitable. The second of these life stages is the macrocyst. This stage is typically elicited by two or more well fed amoebae that are of different sexual types. The cells fuse together and form a large cyst with a cellulose wall. Additional amoebae may be attracted to join the cyst prior to formation of the cellulose wall by the cyst's release of cAMP. The cells within the macrocyst reproduce to form new Dd amoeba through meiosis. The third and final life stage vegetative Dd may enter is the aggregation stage [Kessin 2001]. Entrance into this stage will be described in the next section.

### *Section 2.2.2 Aggregation*

Aggregation is initiated by starvation of a group of Dd that are in close proximity. It is the first step that Dd take involving self-organizing activity. The self organizing activity taken on by amoebae is multi-faceted. First, amoebae must realize that they are starving. Next, one amoeba, referred to as a pacemaker, must begin signaling that it is starving. Other nearby amoebae follow suit by aggregating toward the pacemaker. A cascading signaling process then occurs causing more and more starving amoebae to aggregate. Finally, the aggregate realizes when to shut off the signal when enough amoebae converge [Kessin 2001]. The details of each of these steps are quite interesting and are explained in this subsection.

Aggregation is initiated by a single Dd amoeba called a pacemaker within 6 to 10 hours after starvation. The aggregative process occurs over a  $1\text{ cm}^3$  area in which as many as one million Dd amoebae may exist. Pacemaker amoebae occur at a frequency of 1 in 1000 to 10000 amoebae; however, the mechanism by which an amoeba is chosen to be a pacemaker is unknown [Dallon and Othmer 1997, Kessin 2001]. It is known that the amoeba chosen as the pacemaker begins to emit a chemical called cyclic adenosine monophosphate (cAMP). This chemical is a normal attractant of Dd amoebae. While the pacemaker is emitting cAMP, other starving Dd within close proximity of the pacemaker become highly receptive to cAMP. This receptivity is initiated by a genetic factor that initiates this receptivity in response to starvation [Kessin 2001]. Note that without the existence of a pacemaker, movement of Dd amoebae may be aberrant during starvation [Pollitt 2006].

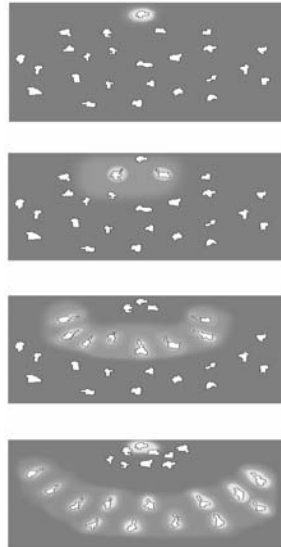


**Figure 2.5: Example of cAMP waves and amoeboid cell movement during aggregation.**  
Redrawn from [Kessin 2001]

The genetic factor that causes high receptivity to cAMP also causes amoebae to extend their pseudopods in the direction of cAMP (i.e opposite a cAMP gradient) at a high frequency (approximately 95% of the time) [Erban and Othmer 2007]. The cAMP emitted by the pacemaker disperses over a small (in terms of micrometers) area only attracting amoebae in its immediate vicinity. This is only enough cAMP to attract a few amoebae. To form a mound, the amount of cAMP dispersed must cover a larger area ( $1 \text{ cm}^3$ ), and, as expected, starving Dd within the vicinity of the pacemaker move toward the pacemaker and begin releasing cAMP [Dallon and Othmer 1997, Kessin 2001]. This process repeats with starving Dd further from the pacemaker. Because detection of cAMP by Dd degrades cAMP, the process of aggregation occurs in waves as shown in the figure below [Dallon and Othmer 1997, Kessin 2001].

cAMP waves continue outward from the pacemaker in a progressive fashion as shown in the figure above. The directedness of the waves also causes amoebae to aggregate as in streams as shown above. The process of signal uptake, movement, and further expression of cAMP increases the amount of cAMP in an area exponentially. The expression of cAMP eventually may become too high and attract too many Dd. To prevent this occurrence, Dd amoebae employ a genetic cell counting factor which enables them to stop expressing as much cAMP when a significant number of cells begin aggregating to form a mound. The expression and exponential growth of a chemical by cells until equilibrium or a limiting factor is reached is also known as the signal transduction pathway (STP) [Dallon and Othmer 1997, Kessin 2001, Erban and Othmer 2007].

### *Section 2.2.3 Mound*

The third stage in the slime mold lifecycle is the mound. As the aggregation stage ends, *Dd* amoebae are located in close proximity to each other. There are typically thousands of amoebae in close proximity in a group that is so tightly packed that it looks like a mound. As the amoebae aggregated toward the pacemaker they also began to excrete a slime-like substance consisting of cellulose and a glycoprotein. This substance is used to form a sheath that will encapsulate the amoebae within the mound. The sheath serves several purposes: it protects the mound from nematodes (predators of *Dd*); it serves to conserve the volume of the mound; and it also allows for containment of signaling molecules pertinent to the mound's movement when it becomes a slug [Kessin 2001].

While in the mound, amoebae also begin organizing themselves. The *Dd* amoebae sort themselves into two different types: prestalk and prespore. These types obviously determine whether a particular amoeba will become a spore or will die to become part of the stalk of the fruiting body. These two types always occur at a rate of 1/5 prestalk and 4/5 prespore. The way that amoebae are chosen to become prestalk or prespore is also quite interesting. The fittest amoebae are always chosen to become spores [Segel 2001, Kessin 2001]. These amoebae are those that had previously led a good life; that is, they consumed a large amount of resources. Unfortunately, those amoebae that did not eat as much are chosen to be prestalk, and interestingly those amoebae that were the result of binary fission (asexual reproduction from one cell splitting into two) are also chosen to be prestalk because they appear to have eaten less during their lifetimes [Segel 2001]. Organization has a second purpose that is even more interesting. Prestalk amoebae move toward one end of the mound to become a head in the slug stage. They become sensitive to light and particular chemicals. They are also able to send chemical messages to the prespore amoebae that make up the tail of the slug. The mound becomes a mobile slug once amoeboid organization is complete [Savill and Hogeweg 1997, Marée et al. 1999 □Migration□ Marée et al. 1999 □Phototaxis□ Kessin 2001, Marée and Hogeweg 2001].

### *Section 2.2.4 Slug*

The slug stage of the *Dd* lifecycle is quite interesting. It is of particular interest to biologists because the slug has the outside appearance of a multicellular organism, but is not actually a multicellular organism. This stage in the *Dd* lifecycle represents an intermediate ecological step between a single celled organism and a multicellular one [Kessin 2001]. The slug is an aggregate of individual amoebae that are self-organizing. These amoebae are organized into a head and tail. Of great interest to biologists are the movement of the slug and its reactions to various environmental stimuli [Savill and Hogeweg 1997, Marée et al. 1999 □Migration□ Marée et al. 1999 □Phototaxis□ Marée and Hogeweg 2001, Kessin 2001]. These interesting facets of the slug stage will be discussed in this subsection.

We know that the slug is divided into a head and tail, but of particular interest is the composition of these portions of the slug and their reactions to various stimuli. The head is composed of 1/5 of the amoebae within the slug. It consists solely of prestalk amoebae, and these amoebae direct the movement of the slug. The amoebae in the head move in a scroll wave (vortex) pattern and primarily react to light (phototactic) and chemical (chemotactic) stimuli [Marée et al. 1999 □Migration□ Marée et al. 1999 □Phototaxis□ Kessin 2001]. The head directs movement toward light in an attempt to ensure amoebae are in an open area when culmination and formation of the fruiting body occurs. Chemotactic movement primarily occurs to move the slug away from noxious chemicals such as ammonia [Marée and Hogeweg 2001, Segel 2001, Kessin 2001]. The head directs the movement of the remaining 4/5 of amoebae by emitting cAMP signals. All of these tail amoebae are prespore cells. Since the slug is encapsulated in cellulose and glycoproteins, the cAMP signals will only stimulate cells within the slug. This causes directed movement of the tail amoebae in a column-like fashion. This movement is similar to the treads of a tank [Kessin 2001].

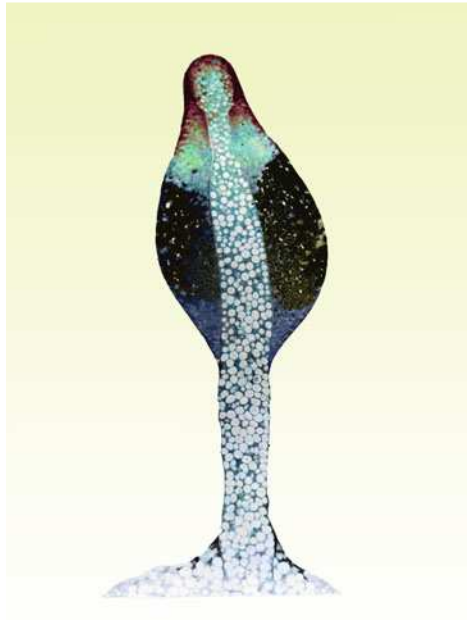
Timely movement of the slug toward an area where culmination may occur is essential as the amoebae within it are expending resources without the ability to eat. The amount of time required for such migration may be a matter of hours or days; however, if a suitable area cannot be found, all amoebae within the slug may perish. Some experiments have indicated continued slug movement toward a light source until death. This can occur if the light source is continually moved away from slug. Thus, stability within the slug's environment is essential for formation of the fruiting body [Kessin 2001].

#### *Section 2.2.5 Fruiting Body and Spore Dispersal*

The fruiting body is the final self-organizing stage that starving *Dd* amoebae undertake. During this stage, prestalk amoebae, which were the head of the slug, slow their movement and reorganize themselves into a stalk. As each prestalk amoeba becomes part of the stalk, it dies. While prestalk amoebae are becoming stalk, the prespore amoebae also reorganize themselves. The prespore amoebae surround the prestalk amoebae as they become the stalk, and slowly climb the stalk. As they climb, the prestalk amoebae undergo metamorphosis that changes them from amoebae to spores. These spores are then eaten by nematodes or other animals and are deposited in new locations. Spores may also be blown away by wind, eaten and redeposited in the droppings of birds or nematodes, or washed away [Kessin 2001].

The fruiting body stage begins with culmination, the point at which movement of the slug stops and begins formation of the fruiting body. According to Kessin, the exact cause for culmination is unknown, but it is suggested that possible build-up of ammonia from developing prespore cells causes the expression of two genes (*ecmA* and *ecmB*) known to be expressed during culmination [2001]. Once the slug culminates, it begins to form a shape similar to a Mexican Hat. During formation of the Mexican Hat, the head, which contains prestalk cells, begins to point vertically, and the prespore cells

move beneath the head to form a mound-like structure. The mound centers itself beneath the prestalk amoebae. Thereafter, prestalk amoebae from the head move down through the center of the prespore mound. Prestalk cells then extend downward through the mound of prespore amoebae. The prespore cells also begin moving up the stalk as it is being formed. Once the prestalk cells reach the bottom of the prespore mound, they begin to form a basal disc along with rearguard cells. This disc anchors the stalk to the ground. The stalk continues extending upwards and thinning. As prestalk amoebae take their place in the stalk, they die. Prespore amoebae move toward the top of the stalk and metamorphosis to spores (dormancy) by encapsulating themselves [Kessin 2001].



Copyright, M.J. Grimson & R.L. Blanton, Biological Sciences Electron Microscopy Laboratory, Texas Tech University [Grimson and Blanton 2009].

**Figure 2.6: Example of a Fruiting Body.**

The Dd lifecycle does not end with the fruiting body. Spores are dispersed so the vegetative stage may begin anew. Dispersal typically happens in one of two ways. Infrequently, spores may be dispersed by wind; although this is not considered by many researchers to be a normal cause of spore dispersal. More often, spores are eaten by the natural predators of Dd – nematodes. Nematodes are small worms, and they will eat Dd amoebae and Dd spores. Interestingly, Dd spores pass through the digestive tract of nematodes without disruption or degradation. Eaten spores are deposited as waste from nematodes allowing for their dispersal. After dispersal, spores must be germinated to activate spores to become vegetative amoebae [Kessin 2001]. In the next section, simulations of slime molds in various forms are discussed. In particular, a continuation of the biological discussion is provided in the next section in the form of biological simulations of the different stages of the lifecycle.

### ***Section 2.3 Slime Mold Simulations***

In this section the means to transform *Dictyostelium discoideum* (Dd) from biology to simulation and later to an optimization algorithm are discussed. This process is neither simple nor easy. We know from the previous section that there are many steps to the Dd lifecycle from single celled amoeba to fruiting body. Simulations for each of these portions of the lifecycle exist and vary in complexity, but most share common traits. Many models employ a grid or lattice on which Dd exist or where portions of the cell surface are modeled. Most allow this grid or lattice to be a cellular automaton and allow amoeba to interact with it if it is the world in which they exist. Models of cell surfaces allow for interactions between amoeba surfaces (i.e. between CAs) and for self interactions. Some model amoeba as CAs or a combination of some CA/PDE/statistical model. In this section, we first investigate some of these models, and then we move to educational models for additional study.

Biological studies involving simulation of Dd are quite diverse. These studies include those of single celled amoeba and their vegetative movement, aggregative movement, mound formation, slug chemotaxis and phototaxis, and fruiting body formation. Each of these will be discussed in this section. Additionally, several educational studies of Dd as CA have been made. Resnick introduced a model of aggregation and slug formation to teach high school students about parallelism using the StarLogo language. Matthews also created an educational model of Dd. His model is intended to provide an example of how CAs work. Both of these models will also be discussed in this section even though these models primarily deal with the aggregation and slug states. Discussion of many of these models necessitates preliminary information on CA.

So, in this section we will first discuss CA, including a formalism for the types of CAs used in the rest of this work. Then, we will discuss existing models for differing portions of the Dd lifecycle. Next, the educational models will be discussed. Initial suggestions will be made about how Dd could be used as an optimization algorithm. Finally, the nearest neighbor and approximate nearest neighbor algorithms will be discussed in the context of their possible use in Dd simulations. These algorithms will be used in the next chapter as part of the presented optimization algorithm.

#### ***Section 2.3.1 Cellular Automata***

So, what is a cellular automaton? The answer is a complicated one because so many variations of CAs exist. In fact, there is no single formalism to define all CA. Nevertheless, CAs do share some traits. They are automata and are deterministic and typically discrete in both space and time. CAs were invented by John von Neumann. He conceived them in the 1950s as a tool to model biological systems. Since then they have been used as such, but they have also been used for many other systems. On the same note, most CAs share five traits that are explained in Ilachinski's book on CA [2001]. For informational purposes those traits are listed here.

- A grid/lattice of cells (typically 1, 2, or 3-Dimensional)
- Homogeneous cells (all cells share the same properties)
- Interactions between individual cells are only local (referred to as neighborhood)
- Cells take on only discrete values or states
- Update of cell states is based upon a set of rules

So, knowing these facets of a CA, a formalism for CAs used in this work will be created. This will serve as the basis for the CAs that will be described throughout this work [Ilachinski 2001].

To provide the formalism for the CAs used in this work, we will divide the CA into several parts similar to those listed above. These parts are provided in the list below.

- State space
- Rules
- Neighborhood
- Boundary conditions
- Starting State

In our description, the state space will be first to be described. Then, we will describe cell locations, states, and boundaries. Finally, we will discuss neighborhoods and rules to complete the formalism [Ilachinski 2001].

We know that a CA uses a lattice or grid as its state space. It is also known that these spaces are of low dimensionality. Furthermore, this grid may be viewed as a discrete space. As such, it may be bounded or infinite. The space may also be toroidal, have holes, etc. The locations within the grid will be referred to as cells. Their values will be taken from a discrete set. These values may be anything, but since they are discrete, they may be mapped to the range 0, 1, ...,  $q$ , without loss of generality. Thus, we may define a set  $\Gamma$  to contain this range.

$$\Gamma \equiv \{0, 1, \dots, q\} \quad (2.13)$$

This set of values will serve as the possible values each cell may take on [Ilachinski 2001, Monismith and Mayfield 2008].

Given our set of values, we may now investigate cell locations. A cell location is a discrete location in the grid. This location may be represented as a tuple that typically indicates the location along each dimension of the grid; for example, a tuple may be listed as  $(i, j, k, \dots)$ . Each of these locations represents a cell that may take on a value from the set  $\Gamma$  at each discrete time step. We denote single cells as  $\sigma$  using a tuple to denote their location and a time  $t$  to denote their value at the current time step. A formal definition of  $\sigma$  is provided below.

$$\sigma_{i,j,k,\dots}(t) \in \Gamma \quad (2.14)$$



Now the grid,  $\Sigma$ , also referred to as the state space, may be defined as the set containing all cells  $\sigma_{i,j,k,\dots}$  as shown below.

$$\Sigma \equiv \{..., \sigma_{i,j,k,\dots}, ...\} \quad (2.15)$$

Note that the bounds of this space may be defined as necessary to the problem in question. They may be limits upon the number of cells along each dimension, intermittent limits, etc. These bounds will be referred to as  $B$ . Discussion of bounds will always be specific to the problem in question and as such will not be discussed further here [Ilachinski 2001, Monismith and Mayfield 2008].

Of additional importance are the local interactions between each cell. Relationships between each cell  $\sigma_{i,j,k,\dots}$  are defined first by a neighborhood. As the word implies, these neighborhoods typically consist of relationships between nearby grid locations. These may be applied to any  $N$ -dimensional CA. Typically, two different types of neighborhoods are used with CAs. These are called von Neumann and Moore neighborhoods. A Neumann neighborhood only uses the immediate nearest neighbors as the neighborhood for each cell. An example is shown in Figure 2.7 below.

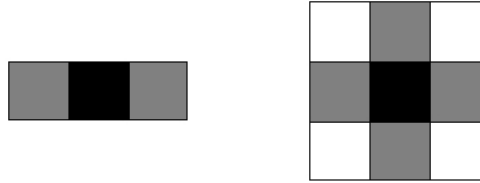


**Figure 2.7: 1-D and 2-D von Neumann neighborhoods.**  
Grey cells are the neighborhoods of black cells  
Redrawn from [Auer and Norris 2001].

A Moore neighborhood uses as neighbors the cells with centers within distance  $nHD$  of the center of the cell in question. Note that  $n$  is an integer with value greater than or equal to one, and  $D$  is the number of dimensions in the state space. Examples of the Moore neighborhood are provided in the figure below. The neighborhood used in a CA in this section will be referred to as  $N$  [Ilachinski 2001, Monismith and Mayfield 2008]

Now, we will discuss rules. Rules for a CA determine the update of the entire CA grid  $\Sigma$  with each discrete time step. Rules must also take into account the neighborhood and dimensionality of the state space used. A single rule will be denoted as  $\phi$ . Rules work as mappings. They typically map a group of cell values (e.g. those from a neighborhood) to a single cell value as shown below.

$$\phi : \Gamma \times \Gamma \times \dots \times \Gamma \rightarrow \Gamma \quad (2.16)$$

In many cases  $\phi$  is a function; however, this is not required. Rules may be grouped together into a set that represents all possible rules for a CA. This set will be denoted as  $\Phi$ , and it will be used to complete our formalism [Ilachinski 2001, Monismith and Mayfield 2008].

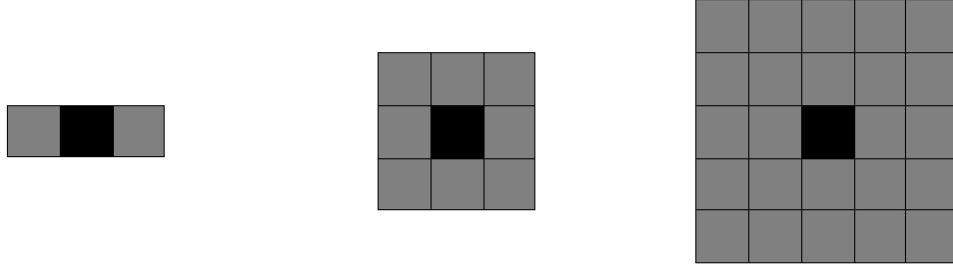


**Figure 2.8: Moore Neighborhoods.**  
**1-D Moore neighborhood and 2-D Moore neighborhoods of size one and two, respectively.**  
**Grey cells are the neighborhoods of black cells [Auer and Norris 2001].**

We may now complete our formalism for the CA. We have defined the state space (grid),  $\Sigma$ , the neighborhood,  $N$ , the set of rules,  $\Phi$ , and boundaries,  $B$ . A starting state however, has not yet been defined. This is the set of initial values for all cells. We will denote the starting state as  $S$  and it will be defined as shown below.

$$S \equiv \{..., \sigma_{i,j,k,...}(0), ...\} \quad (2.17)$$

Given this definition, the basic formalism for the CAs used in this work may be constructed. A CA,  $C$ , may be defined as a combination of a state space  $\Sigma$ , neighborhood,  $N$ , rules,  $\Phi$ , boundaries,  $B$ , set of values for each cell,  $\Gamma$ , and starting state  $S$  as shown below.

$$C \equiv \{\Sigma, B, \Phi, S, N, \Gamma\} \quad (2.18)$$

This concludes the discussion of the formalism. In the next section, existing models of Dd will be discussed [Ilachinski 2001, Monismith and Mayfield 2008].

### *Section 2.3.2 Biological Simulations*

Computer simulations and formulaic representations of the movement and formation of key steps in the Dd lifecycle have been of great interest to the biological community in the past 50 years. The reasoning behind such interest is that these simulations allow biologists to verify that their models of movement and chemical uptake are correct and to compare them against biological observations. Such simulations are available for all portions of the Dd lifecycle, but particular interest has been paid to the

aggregative, slug, and fruiting body stages as many of the mechanisms present in these stages of the Dd lifecycle are highly correlated with the mechanisms of human cell interaction and motility. Modeling of the vegetative stage is lumped together with the aggregative stage in the work of Erban and Othmer because the mechanics used in both the vegetative and aggregative stages are extremely similar [2007]. Models of these two stages are by PDEs. The mound, slug, and aggregative stages have been modeled in several different studies including those of Marée and Hogeweg [2001], Savill and Hogeweg [1997], and Segel [2001]. Dispersion, on the other hand, is not well studied from a modeling perspective. The relatively chaotic aspects of dispersion, including wind, rain, and birds, effectively prevent any model, other than random relocation of amoebae, from being accurate. Because of the importance of such models to the biological community and the possibility of obtaining insight into their use or modification as a part of a numerical optimization algorithm, the primary focus of this subsection will be the study of biological simulations of Dd amoebae.

The first of the simulations investigated in this subsection are the cell taxis models of Erban and Othmer. Recall that taxis is the movement of a cell in response to a stimulus. As previously noted, Dd exhibits taxis in response to chemical stimuli such as cAMP, referred to as chemotaxis. This response is available to Dd amoebae because they are able to sense chemical gradients across their cell walls. Using this sensor information Dd amoebae are able to ascertain the correct direction of motion. Erban and Othmer note that during chemotaxis Dd undergoes four stages of movement. These are first extending a pseudopod at the amoeba's front edge, then, attaching to a substrate, next, squeezing its cytoplasm forward through contraction of the cell body, and finally detaching its tail from the substrate to squeeze the rest of the cell body toward the pseudopod's location. Their model of this movement is through a series of partial differential equations, some of which are presented here, in brief.

With the description of motion, we may go on to discuss how motion may be modeled in a formulaic sense. First, it is important to note that eukaryotic cells such as amoebae and some mammalian cells move on a substrate (surface) by modifying the shape of their cell bodies, e.g. by extending a pseudopod. During this movement volume and density of the cell as a whole is conserved. Thus, any equation representing amoeboid cell movement must take this into account. Erban and Othmer note this fact from previous works when defining a formula for cell movement [2007]. They define cell movement based upon the flux of a cell (its change in volume over time) as in the formula below.

$$\mathbf{j} = -D\nabla n + n\mathbf{u}_c \quad (2.19)$$

In this formula,  $\mathbf{j}$  is the amoeboid cell's flux,  $D$  is the diffusion constant of the chemical stimulus,  $n$  is the density of the amoeba, and  $\mathbf{u}_c$  is the velocity of the amoeba. Since an amoeba's velocity is dependent upon the presence and gradient of a chemical signal, the velocity  $\mathbf{u}_c$  may be defined as shown below.

$$\mathbf{u}_c = \chi(S)\nabla S \quad (2.20)$$

In the equation above,  $S$  represents the chemical stimulus and  $\chi(S)$  is the function representing the amoeba's sensitivity to chemical stimulus. Since cell density is conserved if we assume no change in osmotic pressure and no cell death, the flux equation may be differentiated to present a formula for conservation of density as shown below.

$$\frac{\partial n}{\partial t} = \nabla(D\nabla n - n\chi(S)\nabla S) \quad (2.21)$$

Erban and Othmer explain that an additional formula for the change in distribution of the chemical stimulus may be necessary in addition to the equation above [2007].

To completely model the Dd and chemical stimulus environment, much additional information is required. Work presented by Erban and Othmer shows that with the inclusion of equations to represent the position, velocity, and chemical signal strength, it is possible to produce a velocity transport jump equation that represents most of the factors Dd amoebae and like cells encounter in their environments as they chemotaxis [2007]. Such extended equations include internal Dd variables and chemical stimulus evolution equations. Furthermore, Erban and Othmer derive simplified equations to simulate the movement of amoebae in the presence of a chemical stimulus such as cAMP [2007]. The extended equations are beyond the scope of this work; however, the simulation equations from the Erban and Othmer paper are presented below [2007].

$$\frac{dx}{dt} = v, \quad \frac{dv}{dt} = \frac{\gamma q - v}{\tau_d}, \quad (2.22)$$

$$\frac{dq}{dt} = \frac{\nabla S(x, t) - q}{\tau_a} \quad (2.23)$$

In the equations above,  $x$  represents the position of the amoeba,  $v$  represents its velocity,  $q$  represents the amoeba's internally sensed gradient of the signal,  $\tau_a$  represents the decay rate of the chemical signal, and  $\tau_d$  represents the time necessary for the amoeba to orient itself toward the signal. Since Dd and other cell types occasionally exhibit random errors in the sensing of chemical stimuli, a small percentage of movements in the model are purposefully random [Erban and Othmer 2007]. Additionally, the model is useless to represent Dd in the presence of no chemical stimulus. In fact, Dd amoebae are assumed to extend pseudopods randomly if no stimulus is available [Pollitt 2006, Erban and Othmer 2007].

Of the models used for the mound and slug stages, that of Glazier and Graner appears to hold the most merit in a classical sense [1993]. It is often cited and used or modified to build models for mound formation and slug movement. This 2-D model was created in 1993 to provide solid evidence that only portions of the Dd cell body need be used to model the cell sorting that occurs during Dd mound formation and between animal cells. The Glazier and Graner [1993] model makes use of a discrete Potts

Hamiltonian equation to represent the total surface energy of a single amoeboid cell as represented on a lattice. Note that the Potts Hamiltonian is typically used to model magnetic spins on a lattice. This Hamiltonian attempts to represent many amoebae or other types of cells as groups of like spins on a lattice. In the Glazier and Graner [1993] model usually only two different types of cells are considered such as prespore and prestalk amoebae. This equation is presented below.

$$H_{Potts} = \sum_{(i,j),(i',j') \text{ neighbors}} J(\tau(\sigma(i,j)), \tau(\sigma(i',j'))) \cdot (1 - \delta_{\sigma(i,j), \sigma(i',j')}) + \lambda \sum_{\text{spins } \sigma} (a(\sigma) - A_{\tau(\sigma)})^2 \cdot \Theta(A_{\tau(\sigma)}) \quad (2.24)$$

In the equation above, the Hamiltonian,  $H_{Potts}$ , represents the total surface energy of a lattice point,  $\sigma(i,j)$  represents the spin of one lattice site (which amoeba it belongs to),  $\tau(\sigma)$  represents the cell type associated with the spin  $\sigma$  (e.g., prespore or prestalk),  $J(\tau, \tau')$  represents the surface energy between different cell types,  $a(\sigma)$  is the area (number of lattice sites) occupied by the amoeba,  $A_{\tau}$  is the number of lattice sites amoebae of type  $\tau$  should occupy, and  $\lambda$  is a Lagrange multiplier used to indicate the strength of the conservation of volume.  $\Theta(x) = \{0, x < 0; 1, x \geq 0\}$  is a step function used to turn the area constraint on or off as a third cell type with no area constraint is used to represent the lattice in the Glazier and Graner model [1993].

Glazier and Graner [1993] implemented a simulation of their model using three cell types. The first two types referred to as light and dark types have high and low surface energies, respectively. The third type has no area constraint and is used to represent the area upon which the amoebae exist (i.e. the lattice). Note that this third type is actually a cellular automaton (CA), and the other types are automata that interact with the CA. Lattice sites occupied with a light or a dark cell contained a number corresponding to the unique spin of that particular cell. As shown in Figure 2.9, use of these spins allowed for edges between different cells to be identified. Simulation of this model is actually quite simple. A large number of lattice sites are selected at random, and their spins are switched to a neighboring spin located within a Moore neighborhood according to an annealing schedule. This schedule is based upon the Hamiltonian in Equation 2.24. Results of the Glazier and Graner [1993] simulation show that the differing surface tensions between light and dark cells causes those of each type to migrate toward one another and bundle with like types, effectively allowing for cell sorting without any centralized form of intelligence. More recent simulations make use of Potts Hamiltonian equation as part of a CA and a PDE model to create a 3D representation of the slug and fruiting body stages of the slime mold life cycle [Savill and Hogeweg 1997, Marée et al. 1999 □Migration□ Marée et al. 1999 □Phototaxis□ Marée and Hogeweg 2001, Segel 2001]. Both the Erban and Othmer model [2007] and the Glazier and Graner model [1993] provide interesting cues for future work, which will be discussed in Chapter 4.

2	2	2	2	2	3	3	3	3	3	3	3
2	2	2	2	1	1	1	3	3	3	3	3
2	2	2	1	1	1	1	1	1	3	3	3
2	2	1	1	1	1	1	1	1	1	3	3
8	8	1	1	1	1	1	1	1	1	4	4
8	8	8	1	1	1	1	1	1	4	4	4
8	8	8	1	1	1	1	1	1	4	4	4
7	7	1	1	1	1	1	1	5	4	4	4
7	7	1	1	1	1	5	5	5	5	4	4
7	7	1	1	1	5	5	5	5	5	5	4
7	7	7	1	6	6	5	5	5	5	5	5
7	7	7	6	6	6	6	5	5	5	5	5

**Figure 2.9: Amoebae as modeled by Glazier and Graner [1993].**

### Section 2.3.3 Educational Simulations

Two educational studies of slime mold have been previously noted in this chapter. Those noted were Matthews' [2002] study from Generation5.org and Resnick's [1993] study in *Turtles, Termites, and Traffic Jams*. Resnick [1993] employed a parallel version of Logo called StarLogo in his work, and Matthews [2002] used Java along with a visual interface in his work. The examples provided in both studies are similar in form and application. Therefore, we will only discuss one in this section. Since Matthews' example is more detailed, we will discuss it and formalize his model [2002]. This model will divide the slime mold and its environment into a state space with cells and neighborhoods and will include rules by which amoeba may update this space and exist within it.

The models used by both Resnick [1993] and Matthews [2002] are cellular automata and begin with a state space (i.e. environment) for the slime mold to live in and modify. This state space is two dimensional in both models and is represented as a toroidal space. One may visualize this space as a grid or image as shown in the figure below, with sides that wrap around. Amoebae populate this state space and interact with it. As one might expect, this state space is a cellular automaton and may be updated at discrete time steps; i.e. it will be updated after every amoeba in the state space takes one step [Resnick 1993, Ilachinski 2001, Matthews 2002]. Additionally, if a grid is used as the state space it will be bounded to a fixed size.

The model used by both Matthews [2002] and Resnick [1993] assumes that the amoebae have already begun starvation. At this point in the lifecycle, it is known that amoebae deposit cAMP. Matthews' [2002] model assumes that the state space is represented as a color image. Note that RGB values for color images each range from zero to 255 as triples with zero representing the absence of a color and 255 representing the full intensity of a color. Empty cells are represented as black, i.e. the triple (0, 0, 0).

Cells containing an amoeba are represented as red, (255, 0, 0). Amoebae interact with their world by depositing cAMP, but different amounts may be deposited in different locations. Therefore, it makes sense to allow amoebae within our state space to deposit cAMP within cells in the search space. cAMP values could be represented by arbitrary values, but since Matthews is using an image to represent the state space, cAMP values are allowed to range from 0 to 255 and will be represented as green [2002]. If an amoeba is located in a cell that contains cAMP, only the color green will show (i.e. cAMP will not be shown in this case). Additionally, at most one amoeba may occupy a single cell at any given time step [Matthews 2002].

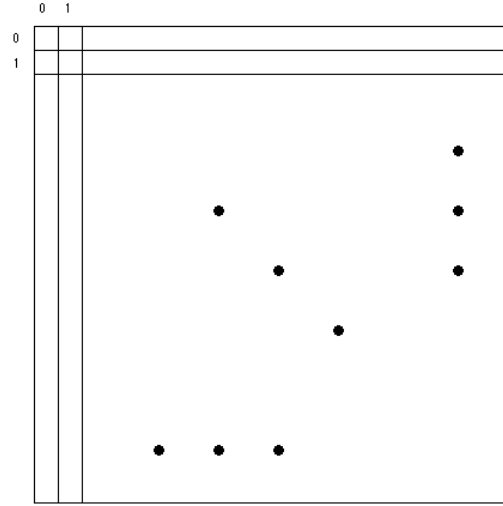


**Figure 2.10: Example grid for slime mold state space.  
Redrawn from [Monismith and Mayfield 2008]**

A number of rules are employed to make the slime mold state space appear to act as a real slime mold world. First, it is assumed that amoebae move one from one cell to another cell in the Moore neighborhood of size one in a single time step. An amoeba may not move into a cell that is occupied by another amoeba. This movement occurs at random in the simulation if there is no cAMP in the Moore neighborhood. If there is cAMP in the Moore neighborhood of an amoeba, that amoeba moves to the empty cell containing the most cAMP (verify). If there are no empty neighboring cells, the amoeba cannot move. Amoebae deposit cAMP at their previous location after each move. The amount that they deposit is a fixed integer. Because cAMP values will be displayed as green with their values ranging from zero to 255, adding cAMP to a cell should be done using a small integer value  $x$  in the range [2, 10]. Formally, each cell that contained an amoeba in the previous time step is updated according to the formula below, where  $k$  is the maximum cAMP value for a cell.

$$\sigma_{i,j}(t+1) = \begin{cases} \sigma_{i,j}(t) + x, & \text{result} \leq k \\ k, & \text{result} > k \end{cases} \quad (2.25)$$

cAMP is also assumed to evaporate from every cell after each time step. Evaporation should be slower than deposit, so less cAMP is assumed to evaporate than is deposited. Matthews implemented evaporation using the following formula.

$$\sigma_{i,j}(t+1) = \begin{cases} \sigma_{i,j}(t) - 1, & \sigma_{i,j}(t) > 0 \\ 0, & \sigma_{i,j}(t) = 0 \end{cases} \quad (2.26)$$

Note that once there is no more cAMP within a cell, no more evaporation may occur. The last rule that is used within the state space is a spreading rule. It is assumed that cAMP spreads from one cell to another after each time step. This is related to the dissipation and evaporation that occurs with cAMP in the wild. To implement cAMP spreading, a smoothing operator is applied to the Moore neighborhood of every cell. The operator works by averaging all the cAMP values in the Moore neighborhood of a cell, including the value in that cell. This allows a portion of every cell's cAMP to spread out over its Moore neighborhood. In areas where there is a high concentration of cells containing cAMP, this will have little effect, but in those areas where there are low concentrations of cAMP, smoothing will attract amoeba and cause them to form mounds. The smoothing operator rule is defined below.

$$\sigma_{q,r}(t+1) = \begin{cases} \sum_{i=q-1}^{q+1} \sum_{j=r-1}^{r+1} \frac{1}{9} \sigma_{i,j}(t), & \text{result} \leq k \\ k, & \text{result} > k \end{cases} \quad (2.27)$$

The smoothing operator has another interesting effect. On the outer edges of mounds, a cAMP gradient is formed. This effect can be seen in the images below as a green halo surrounding a group of amoeba. The gradient on the outer edges of a mound causes the mound to attract additional amoeba toward it. Movement of the amoebae within the mound eventually causes the mound to eventually move like a slug [Matthews 2002, Monismith and Mayfield 2008].

The images below depict different time steps in Matthews' simulation of the slime mold [2002]. The first image depicts the starting state consisting of starving amoebae, which are all colored red. Empty space is shown as black. These amoebae begin moving, making one move per time step and depositing cAMP along the way. After 100 time steps, small mounds are formed. After 1000 time steps, few individuals are left. The small mounds have generated large halos of cAMP that engross groups of amoebae. At times 5000 and 10,000, the small mounds have joined together to form slugs. Eventually, all of the slugs will join together to form a single slug in this simulation.

The educational simulation provided here may be formalized to provide added insight as to the process of creating a CA-based simulation of a population. Such simulations involve two major parts □ a world in which the amoeba exist and the amoeba themselves. We will refer to the world as  $W$  and the set of amoeba as  $A$ . First, the world consists of a state space  $\Sigma$  consisting of all the cells in which the amoebae exist. The



world also has limiting boundaries  $B$  that define the size and shape of the space [Ilachinski 2001, Monismith and Mayfield 2008].

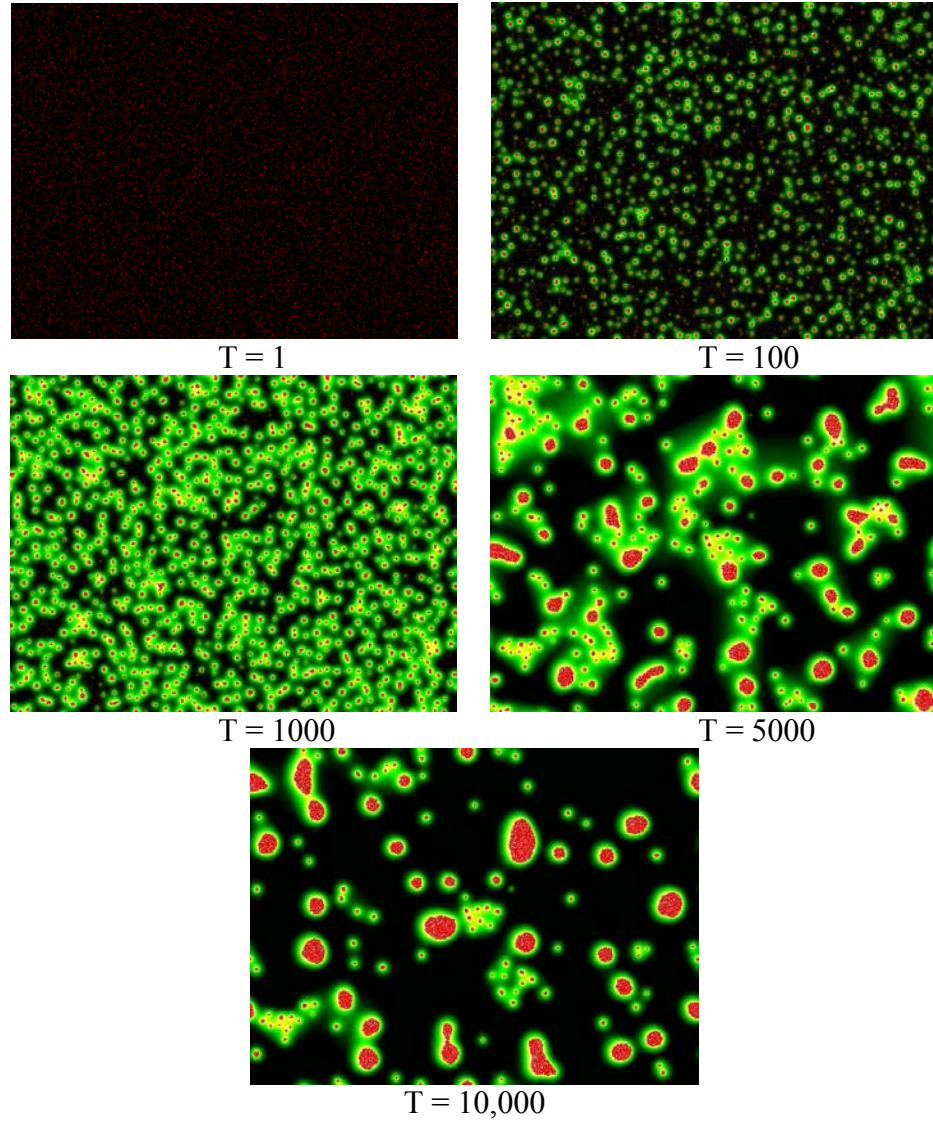


**Figure 2.11: Example from James Matthews' Slime Mold Program.**  
Results from time steps  $T = 1$  through  $T = 10000$  [Matthews 2002].

Additionally, the world uses a Moore Neighborhood,  $N$ , and a set of local values for each cell,  $\Gamma$ , that are in the discrete range  $[0,255]$ . Finally, the world has a starting state,  $S$ , with all cells being initially set to zero and rules that apply to it alone; those being the evaporative and smoothing rules explained above, which could be included in a set  $\Phi$ . Each of these properties defines a world  $W$  that fits the definition of a CA as explained in section 2.3.1.

$$W \equiv \{\Sigma, B, \Phi, S, N, \Gamma\} \quad (2.28)$$

The world is, however, uninteresting without amoebae that will interact with it and deposit cAMP. Therefore, amoebae must be defined and formalized as well as an addition to the CA,  $W$ . Note that an amoeba may exist within a cell in the state space, and it has additional rules to interact with the state space. As explained above, each amoeba deposits cAMP with each time step; it also attempts to move to another cell in its neighborhood after each time step; lastly, only one amoeba may exist in one cell at any given point in time. These rules may be contained within a set  $R$ . Each amoeba has a location within the state space denoted as  $L$  and an initial location denoted as  $L_0$ . Thus, a single amoeba  $a_i$  may be defined as follows below.

$$a_i = \{R, L, L_0\} \quad (2.29)$$

The set of amoeba  $A$  that interacts with the world  $W$  may then be defined as follows below.

$$A = \{\dots, a_i, \dots\} \quad (2.30)$$

Thus, the complete CA for the slime mold world and its amoeba would consist of a set containing the world  $W$  and the set of amoebae  $A$ .

$$\text{Slime Mold CA} = \{W, A\} \quad (2.31)$$

With this formalism, one can easily construct a simulation of a slime mold [Ilachinski 2001, Monismith and Mayfield 2008].

### *Section 2.3.4 Moving to Optimization*

In this final section of chapter 2, initial attempts to convert the lifecycle of Dd to a numerical optimization algorithm are discussed in brief. The first attempt made by the author was completely based upon the algorithm presented in the previous section [Matthews 2002]. This implementation was somewhat effective, but introduced several problems. The first of these problems was the use of a grid as an overlay onto the search space of the objective function. In short, this approach proves effective for functions of low dimensionality; however, it is quite obvious that this approach requires  $O(n^d)$  operations at minimum where  $n$  is the least number of cells along one dimension of the CA and  $d$  is the dimensionality of the search space [Lu and Yen 2003, Yen and Lu 2003]. Grids using an adaptive size may work, but the same problems will be faced, only on a slightly smaller scale.

A slightly faster approach to the grid problem would be to use a sparse 1-dimensional grid based upon uniformly distributed initial search locations. This can be accomplished by producing a grid based upon a nearest neighbor algorithm. This process limits the number of operations performed upon the grid with each iteration to  $O(kn)$  where  $k$  is the number of neighbors of each grid point, and  $n$  is the number of grid points. This process has a cost of  $O(kdn^3)$  operations for a naïve implementation where  $n$  is the number of initialization points,  $d$  is the dimensionality of the problem, and  $k$  is the

number of neighbors. This process is also costly because the grid locations may need to be reassessed after several iterations [Arya et al. 1998]. A less costly grid can be created using the  $\epsilon$ -Approximate Nearest Neighbor algorithm. This algorithm has a lower initialization cost of  $O(dn \log(n))$ , making it more suitable for use as part of an optimization algorithm. Thus, in this section the nearest neighbor and approximate nearest neighbor algorithms will be discussed to better familiarize the reader with them [Arya et al. 1998, Mount and Arya 2006].

First, the nearest neighbor algorithm is investigated. This algorithm is a brute force algorithm used to find the nearest neighbors of all the points in a set. Any distance measure may be used in the algorithm; however, we will only consider the  $L_2$  distance measure in this work. The  $L_2$  distance measure is defined as follows below.

$$dist = \|\bar{x} - \bar{y}\|_2 = \sqrt{\sum_i (x_i - y_i)^2} \quad (2.32)$$

The nearest neighbor algorithm is quite simple. Given a set  $S$  of  $n$  vectors, all with the same dimensionality, the user of the algorithm chooses an integer value  $k$  that must be in the range  $[1, n]$ . Typically,  $k$  is chosen to be less than or equal to  $D$ , the dimensionality of each vector. The algorithm then ascertains the  $k$  vectors from  $S$  that are closest in distance to each of the  $n$  vectors in  $S$ , using the prescribed distance measure. The brute force method of doing this is to compute the distance from each vector to every other vector in the set and store the distances in a table. Then for each vector  $v$  in the set  $S$ , choose the  $k$  vectors with the shortest distances to  $v$  [Arya et al. 1998].

---

**Algorithm 2.10:** K\_NearestNeighbors( $k$ ,  $S$ )

---

Create a table  $T$  of distances from each vector to every other vector.  
Create an array  $L$  of size  $S.size$  containing empty lists.

```

For each vector  $v$  in  $S$ ,
    For  $i = 0$  to  $k-1$ ,
        Find the nearest vector  $x$  to  $v$  using  $T$ .
        Add  $x$  to  $L[v]$ .
        Mark  $x$  as used.
    End for.
End for.
```

---

Because the time costs of the  $k$ -nearest neighbor algorithm are high, many attempts have been made to improve upon it. The  $\epsilon$ -Approximate Nearest Neighbor ( $\epsilon$ -ANN) algorithm of Mount and Arya has proven to be an effective algorithm for finding neighbors in a reasonable amount of time, and the authors of the algorithm have provided a package form so that researchers need not go to the trouble of recreating this complex algorithm [Mount and Arya 2006]. Therefore, discussion of this algorithm will be limited to a short description of the data structures used, benefits, and fallacies.

The  $\epsilon$ -ANN algorithm offers substantial time savings over the naïve nearest neighbor algorithm through the use of box-decomposition trees and allowances for nearest neighbors to be approximated. Box-decomposition trees are similar to KD-trees and allow for partitioning of a space based upon its dimensionality and the number of points that lie within the space. Partitions are made along each dimension to divide sets of points, and data structure linkages are made between divisions to indicate divisions when neighbors are to be found. Divisions in the tree are made until the number of points contained within each node is few. Doing so allows for a search for neighbors in the tree to be executed quickly. Actual creation of a box-decomposition tree is more complicated than the previous discussion, but the discussion is enough for the reader to grasp an understanding of how  $\epsilon$ -ANN works. After creation of the tree, the algorithm may ascertain the  $k$  approximate nearest neighbors of any given point. These neighbors are referred to as approximate because the algorithm searches for neighbors within a hypersphere of radius  $(1 + \epsilon)r$ , where  $r$  is the distance to the nearest neighbor of the point in question. Using this property,  $\epsilon$ -ANN can find the  $k$  approximate nearest neighbors of a point with relatively good accuracy for spaces having upwards of 16 dimensions [Arya et al. 1998, Mount and Arya 2006].

In the next chapter, the creation of the Slime Mold Optimization Algorithm will be discussed [Monismith and Mayfield 2008]. Results and some comparisons to existing algorithms will also be provided. Continuing work on this optimization algorithm will be discussed in a further chapter. Consequently, each of the previously discussed topics is of importance to the creation, testing, or comparison to the algorithm that will be discussed in the next chapter and to future work to be completed upon the algorithm.

## CHAPTER III

### III. SLIME MOLD OPTIMIZATION ALGORITHM

In the previous chapter, discussion of the lifecycle of *Dictyostelium discoideum* (Dd) and simulations thereof was provided. Additionally, many examples of existing optimization algorithms were reviewed. This information laid the groundwork for the discussion of a new optimization algorithm. In this chapter, the move is made from biology and simulation to an algorithm capable of numerical optimization. Here the Slime Mold Optimization Algorithm is presented and discussed in detail. This algorithm uses a multi-step process for optimization with each step being related to a stage in the lifecycle of Dd [Monismith and Mayfield 2008].

Briefly, the portions of the Slime Mold Optimization Algorithm are presented below. This algorithm is able to solve single objective optimization problems using a multi-step approach mimicking the lifecycle of the slime mold [Monismith and Mayfield 2008]. The approach begins with the vegetative state, which allows for directed random movement of agents representing amoebae. This movement is similar to that of a slug searching for food along a folate gradient [Kessin 2001]. These agents, referred to as amoebae, search for new personal optima within the search space of an optimization problem. Before amoebae begin moving, their initial locations are stored and used as the nodes in a grid [Monismith and Mayfield 2008]. This grid and the linkages between its nodes are built using the  $\epsilon$ -Approximate Nearest Neighbor ( $\epsilon$ -ANN) algorithm [Arya et al. 1998]. The vegetative stage ends when a significant number of amoeboid agents have difficulty finding new optima. At this point amoebae enter the aggregative state. They begin depositing an arbitrary amount of "cAMP" (represented as an integer value) at each node (i.e. cell) within the grid. Cells are attracted in the direction of their personal best and in the direction of the nearest cAMP source. These amoebae are drawn toward a pacemaker amoeba that is chosen as the best location within the group [Monismith and Mayfield 2008].

---

**Algorithm 3.1: Slime Mold Optimization Algorithm**

---

1. For each amoeba,
  2.     Assign the amoeba a random location within the search space.
  3.     Evaluate the objective function at that location.
  4.     Initialize the amoeba's personal best objective function value and location.
  5.     Set the amoeba's state to VEGETATIVE.
  6. End for.
  7. Archive the best objective function value from the population of amoebae.
  8. Input the locations of each amoeba to  $\varepsilon$ -ANN and create a mesh based on the results.
  9. For each time step ,
  10.    For each amoeba,
  11.     Switch (Amoeba state)
  12.     Case VEGETATIVE: VegetativeMovement; End Case.
  13.     Case AGGREGATIVE: Aggregation; End Case.
  14.     Case MOUND: MoundFormation; End Case.
  15.     Case SLUG: SlugMovement; End Case.
  16.     Case DISPERSAL: Dispersal; End Case.
  17.     End switch.
  18.    End for.
  19.    Convert an aggregate to a mound if such an aggregate exists.
  20.    Convert a mound to a slug if a mound exists.
  21.    Disperse any slugs that have not updated their personal bests for a significant amount of time.
  22.    Update the grid if necessary.
  23. End for.
- 

Once most of the aggregative amoebae are densely populated about the pacemaker, these agents are allowed to enter the mound stage. The mound stage encompasses the formation of a new data structure relating all the previously aggregative amoebae to each other through the use of another  $\varepsilon$ -ANN grid. This grid separates the mound from the other elements of the population that may be in different states. After this data structure is created, all amoebae within the mound are converted to the Slug state. In the slug state, amoebae are limited to make smaller movements in relation to the size of the slug and distances between each of its members. After improvements fail for a number of time steps, the amoebae within the slug are dispersed randomly through the search space. Their states are set back to vegetative and the cycle begins again [Monismith and Mayfield 2008]. Pseudocode for the Slime Mold Optimization Algorithm is provided above in Algorithm 3.1.

This chapter provides a detailed discussion of the slime mold optimization algorithm. It is based upon existing algorithms including stochastic random search, particle swarm, and  $\varepsilon$ -ANN [Corne et al. 1999, Kennedy and Eberhart 1995, Arya et al. 1998]. The algorithm provides a multi-tiered approach to solve single objective

optimization problems. Detailed discussion of this algorithm begins with its initialization and the data structures used therein, including the  $\epsilon$ -ANN grid. Additionally, each of the stages of the Dd lifecycle, as used in the algorithm, is described. We start with the vegetative stage to describe the random search used. Next, the data structure and methodology used for the aggregative state are provided. Finally, the data structure for the mound stage and movement for the slug stage are detailed. Results for the slime mold optimization algorithm and their analysis are provided in the final section of this chapter [Monismith and Mayfield 2008].

### ***Section 3.1: Initialization and Preliminary Data Structures***

The Slime Mold Optimization Algorithm begins, much like other EAs, with initialization. Initialization includes several key data structures: an  $\epsilon$ -Approximate Nearest Neighbor tree that will represent the grid, a population of amoebae, a list of mounds, a list of pacemakers, the individual amoebae, and an archive [Corne et al. 1999, Monismith and Mayfield 2008]. Additionally, various calculations are made and random number generators are initialized. These steps are detailed in this section.

Initialization begins with the amoebae themselves, but before their initialization can be discussed their structure must be described. An amoeba is represented as an object, and as such it has many important member variables and methods. Since an amoeba is a representation of an individual in an evolutionary algorithm it has as its most important parts a search space location and an objective function value [Corne et al. 1999]. Each amoeba also has a personal best location and a personal best objective function value [Kennedy and Eberhart 1995]. In addition to the normal EA individual variables, each amoeba includes a grid position and a state. These are used to denote the amoeba's position in the  $\epsilon$ -ANN grid and its current functional state, which may be VEGETATIVE, AGGREGATIVE, MOUND, SLUG, or DISPERSIVE. Amoebae each contain additional variables pertinent to their current state. These indicate movement via pseudopodia and "hunger" in the vegetative state; time spent aggregating in the aggregative state; and velocity in the slug state [Kennedy and Eberhart 1995, Kessin 2001, Monismith and Mayfield 2008]. State specific variables will be discussed in detail in respective sections later in this chapter.

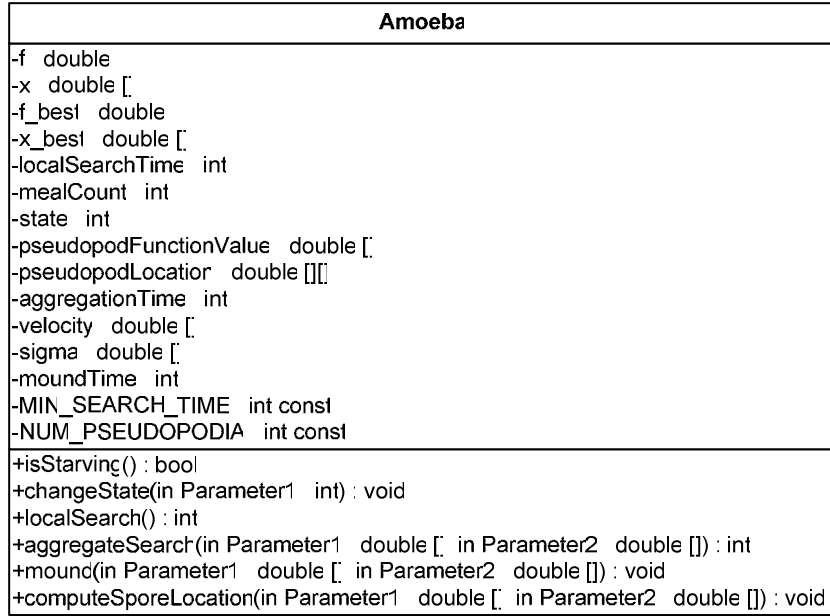


**Figure 3.1: UML diagram of the Amoeba object.**

Given the data structure for each amoeba, population initialization can be examined. The population is an array of amoebae. Its size is fixed at initialization. Each amoeba in the population is initialized with a random starting location chosen from a uniform distribution, and its objective function value is computed. Likewise the personal bests are set based upon the initialization values. Each amoeba's state is initialized to vegetative, and its grid position is set to be the same as its index in the population array. All other amoeba variables are initialized to zero or empty [Monismith and Mayfield 2008].

After the amoeba population has been initialized, several additional steps must be taken to ensure proper functionality during iteration. First, an array is created to allow for counting of amoebae at each  $\epsilon$ -ANN grid point during aggregation. This will allow for an aggregate (mound) to be created once a size threshold has been met. Additionally, an array is created to contain the initial amoeba positions. This array of positions is used to initialize the  $\epsilon$ -ANN data structure and to retain the locations for this data structure throughout the runtime of the program. Indices of each data point relate to a grid position. These indices also match with the previously created aggregation count array. After the  $\epsilon$ -ANN data structure has been initialized, approximate nearest neighbors may be found. These neighbors may be used to compute the average distance between data points along each dimension. They may also be used to direct movement during the aggregation phase when cAMP is being deposited at positions in the grid. Finally, an archive is created, and the best position from the initial population is stored within the



archive [Monismith and Mayfield 2008]. Thereafter, the iteration portion of this evolutionary algorithm begins.

### ***Section 3.2: Vegetative Search***

Iteration of the slime mold optimization algorithm begins with the vegetative search. This search is based upon the vegetative state of the Dd amoeba. Vegetative amoebae are independent agents that search for food. Models of their movement when searching for food are abundant. These range from simple random movement to complicated statistical models or differential equations. Choosing a search strategy to represent the vegetative stage of the Dd lifecycle thus includes many possibilities [Kessin 2001, Erban and Othmer 2007]. These choices include directed random search, simplex search [Spendley et al. 1962], and variants of direct search, especially that of [Hooke and Jeeves 1961]. Each of these can be or is shaped to represent the type of search carried out by a live amoeba. That is, these types of searches can represent searching for food independently via the use of a pseudopod, and they are good at finding local minima. For the slime mold optimization algorithm, a directed random search will represent the vegetative search [Monismith and Mayfield 2008]. Other search variants will be considered in the next chapter.

Initial reading about slime molds from a modeling perspective presented movement during the vegetative state as a directed random search for food [Matthews 2002, Resnick 1994]. Information about amoebae and their movement, however, indicates otherwise. Amoebae have pseudopods that they extend to perform a search for food. Modeling the exact movement of an amoeba is a difficult task, though. Thus, the approach used here is a directed random search that is intended to represent pseudopod extension. Additionally, amoebae transition from a vegetative state to an aggregative state. This transition is made through starvation. An adequate representation of starvation from the standpoint of numerical optimization is time spent searching. The ratio of updates to personal bests to time spent searching is a good representation of an amoeba's food intake [Monismith and Mayfield 2008].

We now provide a run through of the steps taken by an amoeba during its vegetative state. Using a fixed number of pseudopodia, the directed random search chooses a new location for a pseudopod along each dimension using the formula below [Corne et al. 1999, Monismith and Mayfield 2008].

$$pop_i(t).pseudopod_k.x_j = c \cdot N(0,1) \cdot E_j(d_{neighbor}) + pop_i(t-1).x_j, \quad (3.1)$$

This formula is evaluated for each pseudopod  $k$  of an amoeba. In the formula above,  $E_j(d_{neighbor})$  is the average distance to a neighbor along dimension  $j$ , and the constant  $c$  may be reduced as time progresses. After each pseudopod has been created, the result  $pop_i(t).pseudopod_k.f$  is evaluated for each pseudopod. Performing this search for each pseudopod is equivalent to performing a local search about the amoeba, which is what a real amoeba does with its pseudopodia. Once the objective function has been evaluated, the best result from the pseudopodia is compared to  $pop_i(t).f^*$ , the best objective function

value for the amoeba, and, if the best pseudopod result is better than  $pop_i(t).f^*$ , it replaces  $pop_i(t).f^*$ . Likewise,  $pop_i(t).x^*$  is replaced with the search space location of the best pseudopod [Monismith and Mayfield 2008].

Provided with all the pseudopodia and their results, we must determine if the amoeba is starving and obtain new values for the amoeba's location and objective function value, i.e.  $pop_i(t).f$  and  $pop_i(t).x$ , respectively. These values are chosen either at random or using a roulette wheel. The decision between making a random move and a roulette wheel is based upon a probability  $p$ . With probability  $p$ , a pseudopod is chosen at random for a move, and with probability  $1 - p$ , a pseudopod is chosen based upon the strength of its objective function value to replace  $pop_i(t).f$  and  $pop_i(t).x$ . Additionally, with every time step, the local search time counter is incremented. If one of the pseudopodia provided an improvement to  $pop_i(t).f^*$  and  $pop_i(t).x^*$ , then a "meal" counter is incremented to indicate that the amoeba was "fed" during that time step. The use of these counters allows for starvation to be determined by a formula. Starvation may be represented as the ratio of the time the amoeba has spent without improvement (i.e. without a meal) to the total time spent searching. We can decide if an amoeba is starving via the probability equation below [Arabas et al. 1994, Yen and Lu 2003, Monismith and Mayfield 2008].

$$p \left( x < \frac{t_{\text{unimproved}}}{t_{\text{lifetime}}} \right) \quad (3.2)$$

$$g(x) = 1, \text{ for } 0 \leq x \leq 1,$$

In the equation above, which is employed for an amoeba after it has searched for a fixed number of time steps,  $x$  is a random variable with uniform distribution  $g(x)$ ,  $t_{\text{unimproved}}$  is the time spent without a meal and  $t_{\text{lifetime}}$  is the total time spent performing local searches. Provided  $x$  is less than the ratio above, the amoeba is determined to be starving; otherwise, the amoeba is assumed to be well fed. Once an amoeba is starving, its state is changed to AGGREGATIVE [Monismith and Mayfield 2008].

---

### Algorithm 3.2: Vegetative Movement

---

1.  $pop_i(t).localSearchTime \leftarrow pop_i(t).localSearchTime + 1$
2. For each pseudopod  $k$ ,
3.     For each dimension  $j$ ,
4.          $pop_i(t).pseudopod_k.x_j \leftarrow c * E_j(d_{\text{neighbor}}) * N(0,1) + pop_i(t-1).x_j$
5.         Ensure that the result above is within the bounds of the problem space.
6.     End for.
7.      $pop_i(t).pseudopod_k.f \leftarrow f(pop_i(t).pseudopod_k.x)$
8.     Retain the best pseudopod as  $pop_i(t).pseudopod.f^*$  and its location as
9.      $pop_i(t).pseudopod.x^*$ .
10. End for.
11. If (  $pop_i(t).pseudopod.f^* < pop_i(t).f^*$  )
12.      $pop_i(t).f^* \leftarrow pop_i(t).pseudopod.f^*$

13.  $pop_i(t).x^* \leftarrow pop_i(t).pseudopod.x^*$
  14.  $pop_i(t).mealCount \leftarrow pop_i(t).mealCount + 1$
  15. End if.
  16. If (  $rand(0,1) < p$  )
  17.     Select a pseudopod,  $n$ , by its fitness  $f$  using a roulette wheel.
  18. Else,
  19.     Select a pseudopod with index  $n$ , at random.
  20. End if.
  21.  $pop_i(t).f \leftarrow pop_i(t).pseudopod_n.f$
  22.  $pop_i(t).x \leftarrow pop_i(t).pseudopod_n.x$
  23. If ( $rand(0,1) < (pop_i(t).localSearchTime - pop_i(t).mealCount)/pop_i(t).localSearchTime$
  24.     and  $pop_i(t).localSearchTime > MIN\_SEARCH\_TIME$ ),
  25.     Change the state of the amoeba to AGGREGATIVE.
  26.     Update the amoeba's grid location using the  $\epsilon$ -ANN grid.
  27. End if.
- 

Algorithm 3.2: Vegetative Movement, provided above, details the sequence of events that occur during vegetative movement. To recap, this algorithm allows for a local search by one amoeba. That amoeba searches in a fixed number of directions for at least  $MIN\_SEARCH\_TIME$  time steps. If a pseudopod is an improvement over the personal best of the amoeba in question, the best location,  $pop_i(t).x^*$ , and objective function value,  $pop_i(t).f^*$ , are updated. Update in the position of the amoeba is provided through random selection of a pseudopod with probability  $p$  and selection of a pseudopod by roulette wheel with probability  $p-1$ . Starvation occurs when the local search time has surpassed the minimum starvation age,  $MIN\_SEARCH\_TIME$ , and a random variable is less than the ratio of lack of meals to local search time, i.e. Eq. (2) is met. Provided these circumstances, the amoeba is converted to the AGGREGATIVE state and its  $\epsilon$ -ANN grid location is recorded [Monismith and Mayfield 2008].

### ***Section 3.3: Aggregative Search***

Aggregative search is the first state in which amoebae are involved in a cooperative effort. This state begins with a search for the nearest grid location with the most cAMP. Once this location is found, it is tagged for use while searching. Next, the search begins. The aggregative search allows amoebae to move in a directed fashion toward the area with the most cAMP. Amoebae make movements in a similar fashion to particle swarm following their own personal bests and being attracted to the area with the most cAMP. As amoebae in this state move, they drop cAMP on the grid [Resnick 1994, Matthews 2002, Monismith and Mayfield 2008]. The closer they are to reaching a minimum, the more cAMP is dropped. Once enough amoebae have aggregated about a single location, the aggregate becomes a mound. Cells that exist in an aggregative state for too long a time will revert to the vegetative state. The steps of the aggregative state are discussed in detail below [Monismith and Mayfield 2008].

At the beginning of an aggregative search step, a search must be made for the nearest grid location with a large amount of cAMP. To do so, an  $\varepsilon$ -ANN search is made for the nearest neighbors about the closest grid point to the amoeba's current location,  $pop_i.x$ . An example of an  $\varepsilon$ -ANN grid is provided below.

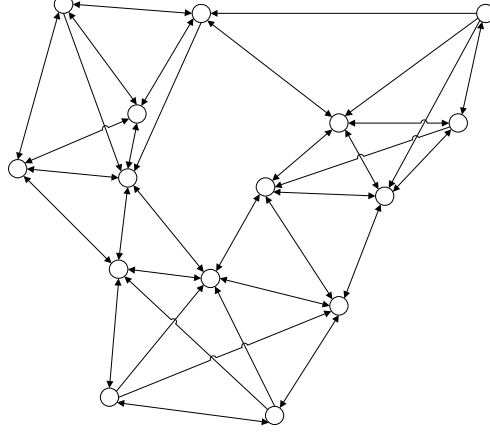


**Figure 3.2: Approximate Nearest Neighbor Mesh, 2-D with 4 neighbors per node [Monismith and Mayfield 2008].**

Next, out of these nearest neighbors a search is made for the grid location with the most cAMP. This location is tagged for later use. After finding the largest cAMP source, a move is made [Monismith and Mayfield 2008].

Making a move during the aggregative phase is a multi-step process. It is quite similar to the process used during particle swarm, as both velocity and position update formulae are used. First, the elapsed aggregation time is incremented. Next, a velocity is computed based upon the direction of the cAMP source and the direction of the previous best location found. A small value from a normally distributed pseudorandom number generator is added to this velocity to protect against a null velocity. The formula for velocity update is provided below [Kennedy and Eberhart 1995, Monismith and Mayfield 2008].

$$pop_i(t+1).v_j = c_1 \cdot pop_i(t).v_j + c_2 \cdot (grid_{best\_cAMP\_Neighbor}(t).x_j - pop_i(t).x_j) + c_3 \cdot (pacemaker(t).x_j - pop_i(t).x_j) + c_4 \cdot E_j(d_{neighbor}) \cdot N(0,1) \quad (3.3)$$

In this formula the velocity for amoeba  $i$  at dimension  $j$  is represented as  $pop_i(t).v_j$  for time  $t$ . The grid location containing the amoeba's neighboring  $\varepsilon$ -ANN grid point is provided as  $grid_{best\_cAMP\_Neighbor}.x_j(t)$  at dimension  $j$ . The location of the best aggregating amoeba is represented as  $pacemaker.x_j(t)$  at dimension  $j$  and time  $t$ . The average distance between grid locations along dimension  $j$  is represented as  $E_j(d_{neighbor})$ . Constants  $c_1$ ,  $c_2$ ,  $c_3$ , and  $c_4$  are set to values less than one to reduce the population explosion effect that may occur when using particle swarm formulae. After the new velocity has been

computed, the velocity is used to update the current position. The formula for position update is provided below [Kennedy and Eberhart 1995, Monismith and Mayfield 2008].

$$pop_i(t+1).x_j = pop_i(t).x_j + pop_i(t+1).v_j \quad (3.4)$$

At this point the algorithm must ensure that the new location is within the bounds of the problem space. If it is not, the location must be adjusted to the bounds of the space along the appropriate dimension. The location may then be evaluated using the objective function to provide a new objective function value. Provided the new objective function value is a new personal best for the amoeba, the personal best for that amoeba is updated, and the maximum amount of cAMP is deposited at the closest grid location. If a new personal best is not found, cAMP proportional to the strength of the amoeba's new objective function value is deposited at the nearest grid location. The formula for cAMP deposit at a grid location is provided below [Matthews 2002, Monismith and Mayfield 2008].

$$grid_i(t+1).cAMP = \begin{cases} grid_i(t).cAMP + c \cdot \left( norm \left( \frac{pop_i(t+1).f}{pop_i(t+1).f^*} \right) \right), & grid_i(t+1).cAMP < k \\ k, & grid_i(t+1).cAMP \geq k. \end{cases} \quad (3.5)$$

In this formula, we see that the grid update is provided based upon the ratio of the amoeba's personal best to its current location. The maximum amount of cAMP in that may be deposited in a single state space location at a particular time step is provided as the constant  $c$ , and the total amount of cAMP at a grid location may not exceed the constant  $k$  [Matthews 2002, Monismith and Mayfield 2008].

Once a new location for the amoeba has been found, the grid is updated, and transition to another state must be considered. Amoebae can transition to the mound state if two conditions are met. First, there must be at least as many amoeba in the AGGREGATIVE state as there are possible neighbors at one particular grid location. Next, the amoebae must pass the following formula test.

$$p \left( x < \frac{grid_i(t).aggregateCount - minAggregateCount}{aggregateCountThreshold} \right) \quad (3.6)$$

$g(x) = 1$ , for  $0 \leq x \leq 1$ .

In the equation above,  $x$  is a random variable with distribution defined by  $g(x)$ . Additionally,  $minAggregateCount$  is the fewest number of amoebae that may exist as an aggregate, and  $aggregateCountThreshold$  is the preferred minimum number of amoebae that may exist as an aggregate. This is calculated as the population size (number of amoebae) divided by the number of neighbors and causes formula (3.6) to have little effect when large numbers of neighbors are used.  $grid_i(t).aggregateCount$  is the current

number of amoebae that exist at position  $i$  in the grid. If the criterion above is met, a mound is created at the grid location in question. All amoebae within the vicinity of the grid location are converted to the MOUND state, and a data structure for the mound is created. If said criteria are not met, the group of aggregating amoebae are not converted to the mound state. Amoebae that stay in the aggregative state for too long a time and for which the following criterion is met are reverted to the vegetative state.

$$p\left(\frac{grid_i(t).aggregateCount}{pop_i(t).aggregationTime} < x\right) \quad (3.7)$$

$$g(x) = 1, \text{ for } 0 \leq x \leq 1$$

In the equation above,  $x$  is a random variable with distribution defined by  $g(x)$ . This allows for the amoebae to continue with further local searches and gives them a chance to join another aggregate [Arabas et al. 1994, Yen and Lu 2003, Monismith and Mayfield 2008].

---

### Algorithm 3.3: Amoeba Aggregation

---

1. Find the grid location nearest the amoeba's current location,  $pop_i(t).x$  in the  $\epsilon$ -ANN tree and store said location in  $pop_i(t).gridLocation$
  2. Performing the previous search also yields the amoeba's nearest neighbors in the grid. Determine which of those neighbors has the most cAMP. Retain the index of that neighbor as *neighborWithMostCAMP*.
  3. If more than one neighbor has the same amount of cAMP as the previously chosen neighbor, choose one of the neighbors with the largest amount of cAMP at random, and store that grid location's index as *neighborWithMostCAMP*.
  4.  $pop_i(t).aggregationTime = pop_i(t).aggregationTime + 1$
  5. Evaluate equations (3.3) and (3.4) for each dimension of the decision space.
  6. Determine the amount of cAMP to deposit using equation (3.5), and deposit that amount of cAMP at grid index *neighborWithMostCAMP*.
  7. If the new objective function value is a personal best, update  $pop_i(t).f^*$ .
  8. If the personal best of  $pop_i(t)$  has been updated check to see if the archive should be updated as well.
  9. If  $pop_i(t)$  fails either equation (3.6) or (3.7), revert to the VEGETATIVE state.
  10. Otherwise, increment the aggregate count at grid index *neighborWithMostCAMP*.
- 

### Section 3.4: Slime Mold World

Up to this point, references have been made to the grid, but it has not been discussed in detail. The grid is a cellular automaton that is the focal point for interaction between aggregating amoebae. This interaction is facilitated by the deposit of cAMP on the grid and its spread and evaporation similar to that explained in Section 2.3.3 [Matthews 2002]. Therefore, updates to these equations will be provided. Moreover, in

this section the data structure used to create the grid and the modifications to the grid update functions will be provided.

The base unit of the cellular automaton is the cell. Cells of the state space in this work are represented as an object with a number of attributes [Ilachinski 2001]. For the algorithm in this work, these include a cAMP value, a neighborhood derived from the  $\epsilon$ -Approximate Nearest Neighborhood, a location within the bounds of the problem space, and a count of the number of amoebae attempting to aggregate at a given cell. Additionally, constants are provided as a part of this data structure to place upper and lower limits on the cAMP values and the aggregate count [Monismith and Mayfield 2008]. A UML diagram of this structure is presented below.

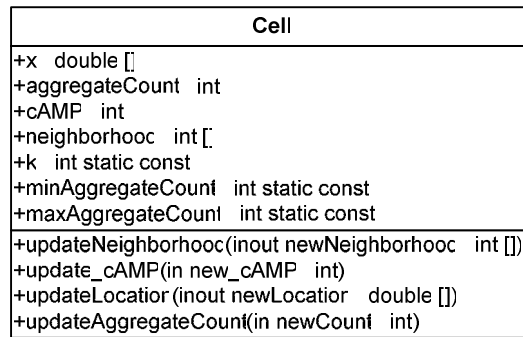


Figure 3.3: UML diagram of the Cell data structure.

The helper methods provided in the UML diagram above allow for the update of cells as needed by the amoebae and the automaton.

The Cellular Automaton (CA), which may be referred to as the Slime Mold World, consists of a grid of cells, represented as an array, with its neighborhood represented based upon data obtained from an  $\epsilon$ -ANN tree [Monismith and Mayfield 2008]. After its construction, the  $\epsilon$ -ANN tree may be queried to find the approximate nearest neighbors of each cell [Mount and Arya 2006]. During initialization of the slime mold optimization algorithm, locations are stored in the  $\epsilon$ -ANN data structure as an array in the same order they are stored in the grid, which is also an array. Thus, their array indices are the same. Therefore, initialization of the neighborhood via  $\epsilon$ -ANN queries is straightforward  $\square$  it only requires the index values returned be stored in the corresponding grid location. A UML diagram of the Slime Mold CA is provided below.

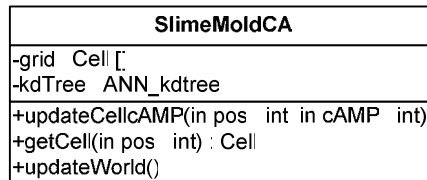


Figure 3.4: UML diagram of the Slime Mold CA data structure.

In the diagram above, functions to update the grid are provided. Of the provided functions, the first serves to allow the amoebae to update the amount of cAMP in a cell by depositing it during the aggregative state. The next function allows for access to the values of particular cell. The last function allows for update of the entire CA via the evaporation and spreading functions explained in section 2.3.3 [Matthews 2002]. Evaporation for the CA is carried out using the formula below.

$$grid_i(t+1).cAMP = \begin{cases} grid_i(t).cAMP - 1, & grid_i(t).cAMP > 0 \\ 0, & grid_i(t).cAMP = 0 \end{cases} \quad (3.8)$$

The formula above allows for the slow removal of cAMP from the grid via evaporation in the same manner as the evaporation formula of section 2.3.3 [Matthews 2002, Monismith and Mayfield 2008]. The formula for spreading or smoothing of cAMP, which is also quite similar to that of the previous chapter, is provided below.

$$grid_i(t+1).cAMP = \begin{cases} \frac{1}{q+1} \sum_{j=0}^q grid_{h(j)}(t).cAMP, & grid_i(t+1).cAMP \leq k \\ k, & \text{otherwise} \end{cases} \quad (3.9)$$

$$h(j) = \begin{cases} grid_i(t).neighborhood_j, & j < q \\ i, & j = q \end{cases}$$

Note that in the formula above,  $q$  represents the number of neighbors used in the algorithm, and the function  $h(j)$  allows for computation of the indices of the approximate nearest neighbors, which are needed to complete the smoothing function. This formula is different than the smoothing formula of section 2.3.3 in only one aspect; it makes use of the CA's  $\varepsilon$ -ANN information to allow for update of cAMP [Matthews 2002, Monismith and Mayfield 2008].

### **Section 3.5: Mound Formation**

At the end of the aggregative stage, Dd amoebae begin to form a mound. These amoebae encapsulate themselves in a slime sheath, thus separating them from the rest of the world [Kessin 2001]. For the slime mold optimization algorithm, mound formation is represented as the formation of the data structure to encapsulate a group of aggregating amoebae that will later emulate the slug stage of Dd. Since mound formation is represented by the formation of a single data structure, this step in the algorithm only requires one time step. For mound formation to begin, a cell and group of amoebae must meet the criterion of formula 3.6. In form, this data structure is much like the neighborhood, CA, and population of the entire slime mold algorithm because it is simply a smaller version of the automata in which the main population exists [Monismith and Mayfield 2008].

During formation of the mound, there are several important initialization steps that must be taken before conversion to the slug state. To amortize the costs of creating



$\epsilon$ -ANN trees across iterations, only one mound is created per time step. To create the mound, first, a search is made for the grid location (cell) with the largest number of associated amoebae. The number of amoebae in the aggregative state at this grid location is tested using formula 3.6. Provided this grid location satisfies formula 3.6, each amoeba in the aggregative state that is associated with that grid location has its state changed to the mound state. The mound data structure is then created including a reference to each of these amoebae as part of the data structure. Continuing with the mound formation, an amoeba is chosen from the members of the mound to become the head of the slug. The amoeba chosen as the head is the amoeba with the best function value out of all the amoebae that are part of the mound. During the slug stage, the head of the slug will be represented as the amoeba with the best objective function value. The location of this amoeba will be used in a particle swarm formula to drive other amoebae in the slug (i.e. the members of the tail) toward better objective function values [Monismith and Mayfield 2008].

The last part of forming the mound involves creating a neighborhood for the amoebae of the mound to move about when they become part of the slug. This neighborhood may be represented as an  $\epsilon$ -Approximate Nearest Neighborhood, with the  $\epsilon$ -ANN tree, which is either a KD-tree or Box Decomposition Tree, as the key data structure of the neighborhood [Arya et al. 1998]. The new neighborhood that is created is separate from that of the main population of the slime mold optimization algorithm; although, it functions in a similar manner. Just like the  $\epsilon$ -ANN data structure of the main algorithm, this data structure is used as a mesh overlaid on the decision space. The main purpose of this mesh is to compute distances between amoebae within the mound and to establish a quick means of locating an amoeba's neighbors while in the slug stage. An example of the mesh used for the mound and slug stages is presented below in conjunction with the mesh used for the population of all amoebae.

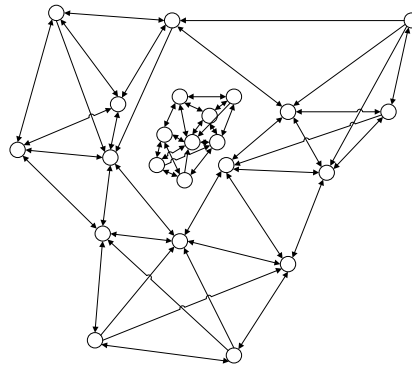


**Figure 3.5: Approximate Nearest Neighbor Mesh and Mound Mesh (inner mesh), 2-D with 4 neighbors per node [Monismith and Mayfield 2008].**

Above, in Figure 3.5, the smaller mesh represents the mound and the larger mesh represents the mesh for the entire population of amoebae. This figure also shows that there are no linkages between the mound and population meshes [Monismith and Mayfield 2008].

Once the necessary pieces for the mound data structure are intact, it may be used as part of the slug. The mound consists of a population of amoebae, a mesh representing neighborhoods, and the average distance between mesh locations. It is quite similar to the data structures used for the main population [Monismith and Mayfield 2008]. In the next section, when it is used as the attributes of the slug its functionality will become quite different than that of the population as a whole.

---

**Algorithm 3.4:** Mound Formation

---

1. If there are any aggregating amoebae and  $\text{grid}_{\text{maxAggInd}}.\text{aggregateCount} > \text{numNeighborsFind}$  the grid location nearest the amoeba's current location,  $\text{pop}_i(t).x$  in the  $\epsilon$ -ANN tree and store said location in  $\text{pop}_i(t).\text{gridLocation}$
  2. Performing the previous search also yields the amoeba's nearest neighbors in the grid. Determine which of those neighbors has the most cAMP. Retain the index of that neighbor as *neighborWithMostCAMP*.
  3. If more than one neighbor has the same amount of cAMP as the previously chosen neighbor, choose one of the neighbors with the largest amount of cAMP at random, and store that grid location's index as *neighborWithMostCAMP*.
  4.  $\text{pop}_i(t).\text{aggregationTime} = \text{pop}_i(t).\text{aggregationTime} + 1$
  5. Evaluate equations (3.3) and (3.4) for each dimension of the decision space.
  6. Determine the amount of cAMP to deposit using equation (3.5), and deposit that amount of cAMP at grid index *neighborWithMostCAMP*.
  7. If the new objective function value is a personal best, update  $\text{pop}_i(t).f^*$ .
  8. If the personal best of  $\text{pop}_i(t)$  has been updated check to see if the archive should be updated as well.
  9. If  $\text{pop}_i(t)$  fails either equation (3.6) or (3.7), revert to the VEGETATIVE state.
  10. Otherwise, increment the aggregate count at grid index *neighborWithMostCAMP*.
- 

**Section 3.6: Slug Search**

From a biological perspective, once Dd mound formation is complete, Dd amoebae have organized themselves into two separate and equally important sections. These are the head and tail of the slug. The head and tail allow for the slug to become motile. Amoebae in the head emit cAMP to direct motility in the tail [Hogeweg and Savill 1997, Marée et al. 1999 □Migration□ Marée et al. 1999 □Phototaxis□ Marée and Hogeweg 2001, Kessin 2001]. The equations of such movement, however, are still being researched by the author. Therefore, slug movement for the Slime Mold Optimization Algorithm is simplified. Instead of using multiple amoebae for the head, a single amoeba is used. The remaining amoebae in the slug perform similar movements to those used in the aggregative stage, with some modification [Monismith and Mayfield 2008]. This section details the slug data structure and the search methodology therein.

The slug object consists of the mound structure discussed in the previous section and two important update methods. The first of these is a method to update the  $\epsilon$ -ANN mesh, for which two possible implementations are presented. One of these is based upon the change in spread of the amoeba populating the slug, and the other simply updates the mesh and its associated tree with each time step. The second is a method to provide information about the slug to the amoebae that are part of it as they move. This method is necessary because the amoebae operate independently using the slug data structure only as a means of communication. The information provided includes the average distance between slug members based upon the  $\epsilon$ -ANN mesh, the location of the amoeba representing the head of the slug, and the location of the approximate nearest neighbor with the best current objective function value. This search includes the aforementioned information, which is used as part of a search formula similar to equations 3.3 and 3.4 [Monismith and Mayfield 2008]. The two methods described above are presented below in detail.

In many aspects, the search methodology for the slug is similar to that used by the individual amoebae of the slime mold world. It makes use of an  $\epsilon$ -ANN mesh for a nearest neighbor search and it makes use of a population, although the population is smaller than that of the main population and a slightly different nearest neighbor search. The slug search also makes use of particle swarm formulae for its movement. There are some slight differences between the amoebae of the slug and the amoebae of the entire slime mold world. First, the slug population is isolated from the rest of the slime mold world. Thus, there are no cAMP interactions between members of the slug and the rest of the world population. Instead, interactions only occur between members of the slug. During each time step, each member of the slug is given an opportunity to move from its current location to a new one. Before movement begins, an approximate best neighbor is found using the slug's  $\epsilon$ -ANN tree that was created in the mound stage. The best neighbor and head of the slug are used together as part of a particle swarm velocity formula as described below.

$$\begin{aligned} slug_i(t+1).v_j = & c_1 \cdot slug_i(t).v_j + c_2 \cdot (slug_{bestANNNeighbor}(t).x_j - slug_i(t).x_j) + \\ & c_3 \cdot (slug_{head}(t).x_j - slug_i(t).x_j) + c_4 \cdot E_j(d_{neighbor}) \cdot N(0,1) \end{aligned} \quad (3.10)$$

In the formula above, the velocity for the  $i$ th amoeba of the slug along dimension  $j$  of the search space at time  $t$  is represented as  $slug_i(t).v_j$ . Similarly, the location for the same amoeba in the objective function space is represented as  $slug_i(t).x_j$ . The locations of the head amoeba and best neighboring amoeba are represented using the same notation but with the subscripts *head* and *bestANNNeighbor*, respectively. To recap, the head amoeba is the amoeba within the slug having the best objective function value and corresponding location. The average distance to a neighboring amoeba along dimension  $j$  is represented as  $E_j(d_{neighbor})$  [Kennedy and Eberhart 1995, Coello Coello and Lechuga 2002, Monismith and Mayfield 2008]. Since the Clerc and Kennedy work has shown that large constants for PSO equation will cause population explosion, constants  $c_1$ ,  $c_2$ ,  $c_3$ , and  $c_4$  are chosen such that they sum to one to prevent amoebae from overshooting the coverage area of the slug by a large distance [2002]. This formula allows for the amoeba to move both in the direction of its best neighbor and the slug's pacemaker with slight jitter from the random

component to continue movement during those cases where the positions of an amoeba and its neighbor or the head might be one and the same. The position update formula is presented below. It allows for the update of the position of the amoeba using the velocity formula above.

$$slug_i(t+1).x_j = slug_i(t).x_j + slug_i(t+1).v_j \quad (3.11)$$

This formula is the same as equation 3.4 and serves the same purpose. Once the location vector,  $slug_i(t+1).x$ , has been computed, its dimensional values are compared to the bounds of the decision space along each dimension. Any dimensional value of  $slug_i(t+1).x$  that falls outside of the decision space bounds is clamped to the bound. Thereafter, the objective function is evaluated at  $slug_i(t+1).x$  and its result is stored in  $slug_i(t+1).f$ . Such movement occurs for each amoeba that is part of the slug [Kennedy and Eberhart 1995, Monismith and Mayfield 2008].

Although equations (3.10) and (3.11) are similar to (3.3) and (3.4), their purposes are quite different. The equations of this section serve along with the  $\epsilon$ -ANN mesh to provide a dense search that exploits the coverage area of the slug. Conversely, equations 3.3 and 3.4 serve as a middle ground to drive amoebae from the exploration search as explained in section 3.2 toward an area that should be exploited because a possible minimum exists in that location [Goldberg 1989, Mitchell 1998, Corne et al. 1999].

The second method tied to the slug stage is the  $\epsilon$ -ANN mesh update method. This method is necessary to locate the approximate nearest neighbors of the amoebae within the slug. When implementing the algorithm, the author devised two different methods for locating neighbors of an amoeba. For the first method, the  $\epsilon$ -ANN data structure is recalculated with each time step. By updating this data structure after each time step, the location of each amoeba within the slug corresponds exactly to the locations of the nodes of the kd-tree within the  $\epsilon$ -ANN data structure. Since these nodes are the points from which nearest neighbors are computed, the neighborhood of the amoebae within the slug is exact. The location of the best nearest neighbor is found by querying the  $\epsilon$ -ANN tree for each amoeba's approximate nearest neighbors then choosing the one with the best current objective function value. This method accurately assesses the locations of the amoebae but is quite costly in terms of system resources. When using the method above, the  $\epsilon$ -ANN data structure must be recomputed after each time step for each slug that is used in the algorithm. Due to this problem, a second method is presented that is similar to the method used in Section 3.3 for the aggregate. In this method, the same  $\epsilon$ -ANN tree is used for several time steps before being updated. Amoebae within the slug must update their positions with respect to the  $\epsilon$ -ANN tree so that requests during a search for the nearest neighbor produce the correct result. This same principle is used with the  $\epsilon$ -ANN tree of Section 3.3; however, the current version of the algorithm does not include cAMP deposit. Rather, it simply picks the best nearest neighbor amoeba. Update of the  $\epsilon$ -ANN tree is necessary when the positions of the amoebae within the slug significantly differ from those in the  $\epsilon$ -ANN tree. To check for a significant change, the centroid and standard deviation of the points within the slug are computed. These values are then used to compare the centroid of the  $\epsilon$ -ANN mesh to the centroid of the points. If a significant

change has occurred, the  $\epsilon$ -ANN tree is updated to the current locations of the slug amoebae. An example of a formula that may be used to make this comparison is presented below.

$$p\left(x < \frac{\|\mu_{Slug\ \epsilon-ANN} - \mu_{Slug\ Amoebae}\|}{\sigma_{Slug\ \epsilon-ANN}}\right) \quad (3.12)$$

$$f(x) = 1, \text{ for } 0 \leq x \leq 1$$

In the formula above, the distance between the centroid of the slug's  $\epsilon$ -ANN mesh and the slug's amoebae (computed as means) is normalized by the standard deviation of the slug's  $\epsilon$ -ANN mesh. Thus, the formula causes an update to the mesh as the distance between the centroids of the points nears the standard deviation of the  $\epsilon$ -ANN mesh [Monismith and Mayfield 2008].

As the slug moves, two important values are tracked. The first of these factors is the number of time steps that the slug has spent moving. The second is the number of updates to the best result obtained by the slug. These variables can be used to determine when the slug data structure should be disposed. The reasoning behind this is simple — as the number of updates to the slug becomes fewer, the need for dense search over the coverage area of the slug lessens. A simple formula to decide when to end the slug stage is presented below.

$$p\left(x > \frac{\text{Number of slug best updates}}{\text{Time spent in the slug stage}}\right) \quad (3.13)$$

$$f(x) = 1, \text{ for } 0 \leq x \leq 1$$

The author's implementation of the slime mold optimization algorithm allows for a constant number of updates to any particular slug before the above formula is used [Monismith and Mayfield 2008].

In nature, the end of the slug stage is followed by the beginning of culmination, i.e. formation of a fruiting body. The members of the tail of the slug would then die to form the stalk of the fruiting body, and members of the head would crawl up the stalk to be dispersed to new locations as spores [Kessin 2001, Segel 2001]. A simplification of these processes for optimization purposes is to restart the algorithm for all members of the slug. This means that each member of the slug is dispersed (i.e. randomly distributed) throughout the search space once the slug stage is complete. That is, once equation (3.13) is satisfied, members of the slug revert to the vegetative state and are placed at random positions in the search space. They do, however, retain a memory of their personal bests as obtained during all the previous stages of their lifecycles. These amoebae begin searching for new optima and continue to follow through the slime mold lifecycle [Monismith and Mayfield 2008].

### ***Section 3.7: Slime Mold Optimization Algorithm***

Having explained how each of the stages in the slime mold optimization algorithm work, we can now explain how they are put together. We first review initialization detailing its importance during the algorithm. After initialization, iteration begins. For a fixed number of iterations, each amoeba is given an opportunity to perform operations based upon its current state. Additionally, data structures including mounds and slugs are updated at the end of each iteration, if necessary. Update to the mesh, as described in section 3.4 is also performed at the end of each iteration [Monismith and Mayfield 2008]. We further elaborate upon the composition of the algorithm in this section.

During initialization a fixed number of amoebae data structures, as described in section 3.1, are allocated and initialized to random locations. Their objective function values are then evaluated, and the current location and objective function value is stored as the best location and objective function value, respectively, for each amoeba. Thereafter, the  $\varepsilon$ -ANN algorithm is used to create a mesh based upon the initial locations of each amoeba with a fixed number of neighbors for each vertex of the mesh. Each vertex in this mesh corresponds to one amoeba's location. These vertices are also used as locations at which cAMP may be stored during the aggregative state. Each amoeba's counters are initialized to zero and each amoeba's state is initialized to VEGETATIVE. After each amoeba is initialized and the  $\varepsilon$ -ANN data structure has been created, the best location in the population is archived [Monismith and Mayfield 2008].

After initialization is complete, iteration begins. A fixed number of objective function evaluations is used during the Slime Mold Optimization Algorithm. This value is chosen heuristically. Once per iteration, each amoeba is given a chance to perform an operation based upon its current state of VEGETATIVE, AGGREGATIVE, MOUND, SLUG, or DISPERSIVE. Amoebae archive new global bests as necessary after executing the actions appropriate to their states. While an amoeba is in a particular state it performs appropriate actions corresponding to its state. That is, if an amoeba is in the vegetative, aggregative, or slug state, it moves according to the appropriate equations for that state. Amoebae in the dispersive state act slightly differently □ they are relocated to a new random position. Amoebae in the mound state perform no actions as they are to be incorporated into a data structure. Therefore, there must be some action performed after iteration [Monismith and Mayfield 2008].

Several actions are carried out after each iteration. During an iteration, every amoeba is allowed to carry out its own state based action appropriate to its state. The actions executed after an iteration are to deal with the creation and destruction of data structures as amoebae aggregate, form a mound, move as a slug, and are ultimately dispersed to restart their lifecycle. So, the first of these steps after iteration is to take the world location at which there is the highest concentration of aggregating amoebae, and to decide if those amoebae need to be converted from an aggregate to a mound. This decision is made using equation 3.7. If the aggregate passes equation 3.7, the cell within the aggregate having the best objective function value is chosen as the pacemaker and all

amoebae in the aggregative associated with the world position with the highest concentration of amoebae are converted to the MOUND state. Finally, a mound is created at that location. The next step taken after iteration is an update of the slug's  $\epsilon$ -ANN data structure. Depending on the type of implementation this either occurs after each iteration or after the iteration during which the slug has made significant movement. Thereafter, the kd-tree contained within the slug's  $\epsilon$ -ANN data structure is reformulated based upon the current locations of the amoebae within the slug. After mound creation and slug updates are considered, any slugs that have existed for more than a fixed number of iterations and have not had updates to their personal bests according to equation 3.13 are cleared. Then, the archive that is maintained to keep track of the overall bests throughout the algorithm is updated, if necessary. Finally, the slime mold world is updated. These updates are performed according to equations 3.8 and 3.9, which cause evaporation and smoothing to occur. Thus a number of important actions are carried out after each iteration [Monismith and Mayfield 2008].

So far we see that we have an algorithm with multiple stages — those being Vegetative, Aggregative, Mound, Slug, and Dispersal states. We have also seen that the algorithm also makes use of a grid based on the  $\epsilon$ -ANN algorithm and that it requires several ancillary data structures to facilitate the aggregative, mound, and slug stages [Monismith and Mayfield 2008]. Having a full description of the algorithm, we move on to variants of the algorithm in Chapter 4 and testing, results, and analysis in Chapter 5.

## CHAPTER IV

### IV. VARIATIONS ON THE SLIME MOLD OPTIMIZATION ALGORITHM

Genetic algorithms, particle swarm optimization, and differential evolution have all led to many variants [Goldberg 1989, Arabas et al. 1994, Mitchell 1996, Clerc and Kennedy 2002, Coello Coello and Lechuga 2002, Price et al. 2005]. For example, there are many variations on the recombination operator in genetic algorithms [Goldberg 1989, Herrera et al. 1998]. A first look at the Slime Mold Optimization Algorithm along the same lines would be view it as a heuristic for building an evolutionary algorithm. The lifecycle of Dd, when used as a model for an optimization algorithm, lends itself to many possible variants. A top level look at the algorithm is provided in the figure below.

Vegetative State	Initial search algorithm using many individuals
Aggregative State	Force individuals that are no longer fruitful to converge around a "best location"
Mound State	Converging individuals are grouped together as part of a data structure
Slug State	Make use of another search algorithm for the individuals in the data structure designed to exploit their area of coverage
Dispersal State	Reset the members of the slug data structure

**Table 4.1: List of states from the Slime Mold Optimization Algorithm [Monismith and Mayfield 2008].**

Using this strategy, a variety of search algorithms could be substituted for those used in the vegetative and slug states. For the vegetative state, two such methods are presented. These include the use of the Razor Search Method and the Downhill Simplex Method in place of the random search methodology presented in section 3.2 [Bandler and MacDonald 1969, Spendley et al. 1962]. For the slug state a method using Differential Evolution is presented to use in place of the method in section 3.6 [Price et al. 2005]. Each of these modifications is discussed and elaborated upon in this chapter. Discussion of testing methods and results is provided in Chapter 5.



### ***Section 4.1: Variations on the Vegetative State***

The original Slime Mold Optimization Algorithm makes use of a directed random search for the vegetative state. While this search is simple and attempts to model the pseudopod-based movement of actual Dd amoebae, it is lacking in several aspects [Monismith and Mayfield 2008]. First, the distribution used in the random search is not amenable to rotation in the contours of the search space. This search methodology turns out to be similar to Evolutionary Strategy and faces the same limitations because of its distribution [Corne et al. 1999]. One possible improvement to it is to modify the strategy to take the covariance of the distribution into account when performing a search. Since this methodology may be quite time consuming, it is prudent to consider other search strategies that make movements similar to amoebae [Corne et al. 1999].

In this section, in an attempt to address some of the deficiencies of the original vegetative state, two variations on the vegetative state are presented. These include the use of the Downhill Simplex Algorithm for the first variant, and the Razor Search Algorithm for the second variant. These two algorithms were presented previously in Chapter 2. The use of such algorithms in the Slime Mold Optimization Algorithm requires modification for use in a single timestep. Thus, in the following subsections the modified versions of the timestep-based Downhill Simplex Algorithm and Razor Search Algorithm are provided [Spendley et al. 1962, Bandler and MacDonald 1969]. Furthermore, the reasoning for the use of such algorithms is presented.

#### ***Section 4.1.1: Downhill Simplex for the Vegetative State***

The Downhill Simplex search presents an interesting option for use in the vegetative state because simplex movement is amoeboid. A simplex is a hyper-triangle, so it consists of  $D+1$  points, where  $D$  is the number of dimensions. Another point is added to the simplex by reflecting the worst point in the simplex about the centroid of the other  $D$  points. Before the next timestep, the worst from the old simplex is discarded to create a new simplex. This movement is similar to the pseudopod movement that real amoebae use, wherein amoebae are able to measure a gradient across their body wall and make movement opposite that direction. One caveat we must consider is that real amoebae occasionally make mistakes when searching [Spendley et al. 1962]. Thus, to allow for the new algorithm to more closely match Dd movement and to allow some randomness that may allow escape from local minima, the Simplex search used as part of the Slime Mold Optimization Algorithm allow for incorrect movements to be made occasionally (5% of the time) [Erban and Othmer 2007].

To use the Downhill Simplex Algorithm in the vegetative state, several modifications are made to it. First, to fit in the timestep-based approach used in the Slime Mold Optimization Algorithm, the Simplex Algorithm is cut down to what amounts to a single timestep. This is effectively one simplex step. That is, determination of the worst point, the centroid of the remaining points, and movement opposite the direction of the worst point through the centroid. Algorithm 4.1 details the necessary steps to make one simplex step, and is quite straightforward. These involve determining

whether to make a random move or an actual simplex move, finding the centroid of the points, ensuring the new point is not out of bounds, counting for repeats, decreasing the simplex size if necessary, and finally keeping track of any new personal or global bests [Spendley et al. 1962, Monismith and Mayfield 2008].

---

**Algorithm 4.1:** Vegetative Simplex Movement

---

1.  $pop_i(t).localSearchTime \leftarrow pop_i(t).localSearchTime + 1$
  2. If  $Rand(0.0 \leq 1.0) < 0.95$ ,
  3.     Find the centroid of all simplex points,  $simplexPoints_{0:D}$ , except the worst point.
  4. Else
  5.     Find the centroid of all simplex points,  $simplexPoints_{0:D}$  except for a randomly chosen point, and swap that point with  $simplexPoints_0$ .
  6. End If.
  7. Do
  8.      $isOutOfBounds \leftarrow false$
  9.     Find  $x^{new}$  (This is based on Formula 2.8)
  10.    If  $x^{new}$  is outside the search space
  11.      $isOutOfBounds \leftarrow true$
  12.      $\lambda \leftarrow \lambda / 2$
  13.    End If
  14. While ( $isOutOfBounds$ )
  15.    Reset  $\lambda$  if  $\lambda \leq 2$
  16.     $oldSimplexPoints \leftarrow simplexPoints$
  17.     $simplexPoints_0 \leftarrow x^{new}$
  18.    Compute the objective function result
  19.    Find the new worst point in the simplex and swap it with  $simplexPoints_0$
  20.    Count any repeats
  21.    If any repeats have occurred more than M times or if the newly created point,  $x^{new}$ , is equal to  $oldSimplexPoints_0$ ,
  22.     Decrease the simplex size.
  23.    End if.
  24.    If the size must be decreased,
  25.     Compute a new set of simplex points of the appropriate size and evaluate their objective function values.
  26.     Reset the repeat counts.
  27.     Find the worst point in the simplex and swap it with  $simplexPoints_0$ .
  28.    End if.
  29.    If an improvement was made,
  30.      $pop_i(t).mealCount \leftarrow pop_i(t).mealCount + 1$
  31.     Retain the improvement
  32. End If.
-

### *Section 4.1.2: Razor Search Algorithm for the Vegetative State*

Razor Search is an interesting algorithm that will be investigated for use in the Vegetative State. This algorithm is interesting because it allows for both step based movement like that of the Hooke and Jeeves Pattern Search and random movement when Pattern Search stalls. Often, such random movements can be made along a narrow valley, if one exists in the solution space. This search is also similar to amoeboid movement because it allows for step based movement to be made in a direction near the opposite of the gradient in many objective functions [Hooke and Jeeves 1961, Bandler and MacDonald 1969, Kessin 2001]. Promising results are apparent upon testing of this algorithm, as will be shown in Chapter 5.

To use this algorithm in the vegetative state, modifications must be made to the Razor Search algorithm. These modifications are similar to those used in the previous section for the Simplex Algorithm. That is, Razor Search must be modified for use on a timestep basis. In its form as presented in Algorithm 2.3, the method is ill suited for use in the Slime Mold Optimization Algorithm. Of particular importance is the lack of short iterative units that would correspond to single timesteps. As shown below in Algorithm 4.2, the modification involves dividing Razor search into several steps. The first of these involved is a Pattern Search based upon Algorithm 2.1 and limited to a small fixed number of iterations (e.g. 100). This step, though sometimes cumbersome in terms of performance, accounts for one timestep. The second step in the Vegetative State Razor Movement starts a typical razor search iteration as would be used in Algorithm 2.3. In this step, a random location is obtained based upon the end point of the previous pattern search. Thereafter, the third step begins. In the third step, another pattern search is performed from the previous random move. This is done to test the random move for effectiveness. The fourth step begins after the pattern search is complete. In this step, a valley direction is ascertained and a pattern move is attempted in the direction of the valley. Then, the fifth step begins. In the fifth step pattern moves are attempted to exploit the direction of movement toward the valley until such movement is no longer fruitful. Once movement is no longer fruitful, the algorithm returns to the second step where timestep based Razor Search movement begins again [Bandler and MacDonald 1969, Monismith and Mayfield 2008].

---

**Algorithm 4.2: Vegetative Razor Movement**

---

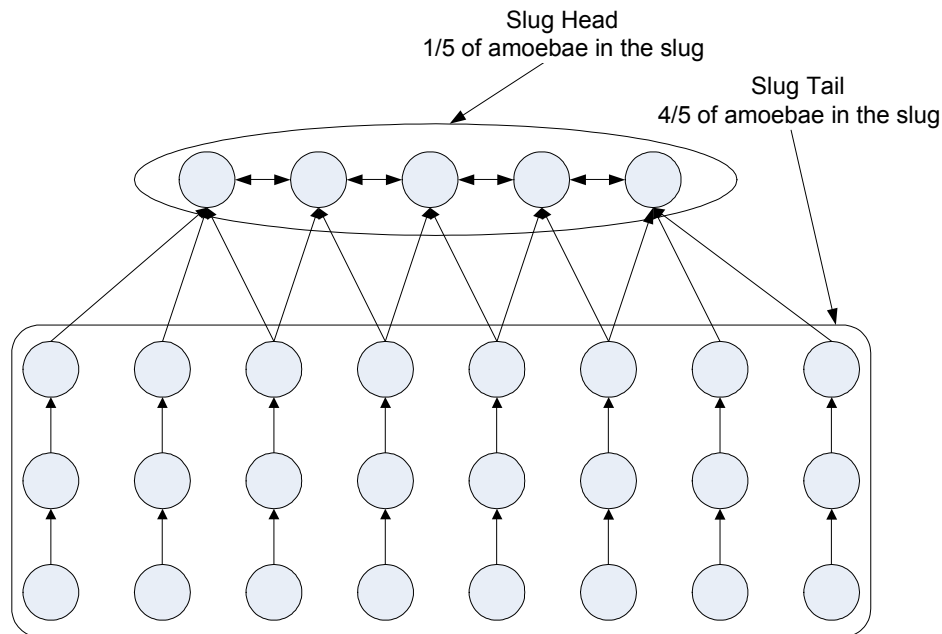
1.  $pop_i(t).localSearchTime \leftarrow pop_i(t).localSearchTime + 1$
- 2.
3. Switch ( RazorState )
4.     Case 0: (in 1st pattern search)
5.     Run one pattern search iteration based on Algorithm 2.1.
6.     If the first pattern search is complete,
7.         Set RazorState to 1.

8. End If.
9. Break.
10. Case 1: (beginning a Razor Search iteration)
11. Get a random location using equation (2.2).
12. Change RazorState to 2.
13. Break.
14. Case 2: (running a  $\square$ test $\square$ Pattern Search as part of the Razor Search iteration)
15. Run one Pattern Search iteration based on Algorithm 2.1.
16. If the pattern search is complete,
17.     Set RazorState to 3.
18. End If.
19. Break.
20. Case 3: (Once the pattern search is complete perform pattern moves)
21. Find the new valley direction using equation (2.3)
22. Perform one Pattern Move using Algorithm 2. .
23. Change RazorState to 4.
24. Break.
25. Case 4: (Exploit the direction of movement by performing more pattern moves)
26. Perform a Pattern Move using Algorithm 2. .
27. If the Pattern Move yielded no improvement to the objective function value,
28.     Change RazorState to 1.
29. End If.
30. Break.
31. End Switch.
32. If an improvement to the objective function value was made,
33.      $pop_i(t).mealCount \leftarrow pop_i(t).mealCount + 1$
34.     Retain the improvement
35. End If.

---

#### ***Section 4.2: Variations on the Slug State***

The form of the slug state as presented in sections 3.4  $\square$  6 is quite different from what is presented in biology. The main reasons for this difference were lack of inspiration and limited biological research on the part of the author. As a quick fix, the data structure created in the mound state was originally based upon the structure of the aggregative state. This data structure and the related equations were used to ensure amoeba movement during the slug state was similar to movement during the biological aggregative state over a localized area [Monismith and Mayfield 2008]. To ensure a better correlation with what is found in nature, heavy modification was made to this portion of the algorithm. Implementation includes a search methodology that focuses on both the biological head and tail elements. Recall from section 2.2.4 that the head of the slug consists of 1/5 of the slug's population and the remaining 4/5 of the amoebae compose the tail [Kessin 2001]. The modifications to the slug stage in the Slime Mold Optimization Algorithm include this construct.



Simplified example of communication during slug movement  
Arrows indicate possible lines of communication between amoebae

**Figure 4.1: Modification to the slug state.**

The focus of this portion of research is to modify the slug to better follow equations in biology literature. To do so, the slug will be divided into a head and tail. The Dd slug head consists of the 1/5 of the slug population that are to become spores. Recall from Chapter 2 that these are the best fed amoebae from the mound [Kessin 2001]. An analogous formation for optimization purposes is a head consisting of the 1/5 of the slug population with the best objective function values. These individuals should direct the movement of the remainder of the slug, i.e. the tail. A simple way of doing this would be to let the head perform a search that can accurately determine the contours of the search space and allow the tail to perform a dense search of the area behind the head to ensure nearby minima are found. Forcing the amoebae in the tail to follow the head is simple, Equations similar to those used in the PSO are sufficient to elicit such movement [Janson and Middendorf 2005]. Choice of the proper movement in the head may prove much more difficult. Using Differential Evolution or a Genetic Algorithm should be suitable for the search being carried out by the head; therefore, DE will be tested for use in the head as part of this work. Another more interesting improvement to the head would be to try to implement the chaotic whorl movement used by real Dd slugs to move toward light [Kessin 2001, Marée et al. 1999 □Phototaxis□]. The author is currently researching the whorl movement; thus, such research will not be included as part of this work.

#### 4.2.1 Differential Evolution

Replacement of the original slug algorithm with the Differential Evolution algorithm is quite simple. To start, a single instance of the DE algorithm may be used for each slug member (an amoeba with index  $i$ ). This algorithm begins by choosing three random slug members (amoebae with indices  $a1$ ,  $a2$ , and  $a3$ ). These amoebae are assumed to be passed as parameters to Algorithm 4.3 as shown below. As in the standard DE algorithm, a random index, representing dimension  $k$ , is chosen to begin application of the DE algorithm to the amoeba's location. A random value is tested against the crossover probability,  $CR$ , to cause either a crossover with a mutation factor  $F$  or to keep the original location along dimension  $k$ . Next, the algorithm ensures the new location for dimension  $k$  is not out of bounds. This process is repeated for each dimension  $k$ . At least one dimension in the new location is forced to include a crossover as shown in Algorithm 4.3. Finally, the algorithm computes a result based upon the new location and updates the location only if the new location results in a better objective function value. Additionally, the personal best of the amoeba with index  $i$  is updated if necessary. Although use of this portion of the DE algorithm does not fit directly into the scope of the movement shown in Figure 4.1, it will be used in the next section as part of the head movement for the slug [Price et al. 2005, Monismith and Mayfield 2008].

---

**Algorithm 4.3:** DE (Used for Head Movement)

---

```
1. Parameters:  $a1, a2, a3$  : Integer
2.  $j \leftarrow \text{Rand}(0 \leq D - 1)$ 
3. for  $k \leftarrow 0$  to  $D - 1$ ,
4.   if( $\text{rand}(0.0 \leq 1.0) < CR$  or  $k = D - 1$ )
5.      $\text{temp}_j \leftarrow \text{pop}_{a1}(t).x_j + F \cdot (\text{pop}_{a2}(t).x_j - \text{pop}_{a3}(t).x_j)$ 
6.   else
7.      $\text{temp}_j \leftarrow \text{pop}_i(t).x_j$ 
8.   End if.
9.   Ensure  $\text{temp}_j$  is not out of bounds.
10.   $j \leftarrow (j + 1) \bmod D$ 
11. End for.
12.  $\text{tempF} \leftarrow f(\text{temp})$ 
13. If ( $\text{tempF} < \text{pop}_i(t).f$ )
14.   $\text{pop}_i(t+1).f \leftarrow \text{tempF}$ 
15.   $\text{pop}_i(t+1).x \leftarrow \text{temp}$ 
16. End If.
17. Update the personal best of  $\text{pop}_i(t+1)$  if necessary.
```

---

#### 4.2.2 DE + Followers

The DE + Followers slug search algorithm is a heavily modified version of the slug search as explained in sections 3.4 – 3.6. It begins with creation of the slug data

structure through the mound stage. The slug is initialized to the appropriate size and number of nearest neighbors, and a new sizing algorithm to determine the best head and tail sizes is applied. During the Mound stage, as amoebae are added to the slug, the DE + Followers algorithm inserts amoebae into the head and tail. During the slug search phase, instead of using the PSO equations, DE is used for the head of the slug, and a simple following algorithm is applied to force the tail amoebae to follow the amoebae pursuing the DE strategy in the head [Monismith and Mayfield 2008]. Details are presented for this algorithm in this subsection.

Creation of the slug begins at the end of the aggregative phase as presented in Chapter 3. Upon satisfaction of equation (3.6), the slug object is created based upon a number of amoebae that have aggregated at a particular grid location. The "normal" operations for slug initialization may be carried out at that point (i.e. memory allocation for the  $\epsilon$ -ANN tree and array of slug amoebae) [Monismith and Mayfield 2008]. Additionally, the head and tail may be sized. The preferred sizes for the head and tail are 1/5 of the amoebae in the slug for the head and 4/5 of the amoebae in the slug for the tail [Kessin 2001]. Issues may occur when there are too few amoebae within the slug. For example, the DE algorithm requires at least four locations to work. Thus there must be at least four amoebae in the head. Moreover, the slug must contain at least four amoebae, and in the case where there are less than twenty amoebae in the slug the numbers of amoebae in the head and tail must diverge from the biological requirements. To deal with this issue, the algorithm allows for a larger head than tail when there are too few members in the slug to meet the 1:4 head tail ratio. Additionally, initialization may be performed for head and tail counts and memory for the head and tail amoebae used when adding amoebae to the head and tail of the slug [Kessin 2001, Price et al. 2005]. Algorithm 4.4 briefly indicates the necessary instructions to determine the size of the head and tail.

---

**Algorithm 4.4:** DE + Followers Slug Movement (Head and Tail Sizing)

---

```

1. headCount    0, tailCount    0
2. If  $0.2 * \text{slugSize} < \text{numNeighbors}$ 
3.   headSize    numNeighbors
4.   tailSize    slugSize - numNeighbors
5. else
6.   headSize     $0.2 * \text{slugSize}$ 
7.   tailSize    slugSize - headSize
8. End If.
9. Allocate memory for head, tail, and centroids

```

---

The next part of the DE + Followers slug update is to add amoebae to the head and tail. This occurs in the mound stage after the slug object has been created. The mound algorithm from Chapter 3 is used to add these amoebae to the slug [Monismith and Mayfield 2008]. Additionally, amoebae must be placed in the data structures

representing the head and tail. Initially, the head and tail are empty. Amoebae are placed in the head until it is filled. Once the head data structure is full, the algorithm attempts to replace amoebae in the head one at a time, moving the worst amoebae to the tail. A short algorithm to add amoebae to the head and tail is provided below as Algorithm 4.5.

---

**Algorithm 4.5:** DE + Followers Slug Movement (Adding amoebae to the Head and Tail)

---

```

1. If headCount < headSize
2.   headAmoebae[headCount]  popi
3.   headCount  headCount + 1
4. Else
5.   worstAmoeba  popi
6.   worstPosition  -1
7.   for j  0 □ headSize □ 1
8.     if headAmoeba[j].f < popi(t).f
9.       worstPosition  j
10.    End if.
11.  End for.
12. End if.
13. If worstPosition != -1
14.  tailAmoebae[tailCount]  headAmoebae[worstPosition]
15.  headAmoeba[worstPosition]  popi
16. Else
17.  tailAmoeba[tailCount]  popi
18. End if.
19. tailCount  tailCount + 1

```

---

DE based movement was provided in section 4.2.1, and that same movement as shown in Algorithm 4.3 may be used for members of the slug's head. To complement this movement, an additional algorithm is provided below for tail movement. Amoeboid tail movement is driven by two factors. The first of these is the direction of the head. This is determined by the difference between the centroid of the head and the centroid of the tail. This value is normalized and then scaled by the average distance between all members of the slug. The second factor used is the nearest neighbor direction. Each amoeba has a nearest neighbor, and the one closest to the tail direction is used to aid in the computation of each tail amoeba's new location. These two factors are multiplied by a random value, each scaled by half, and added to the amoeba's old location to determine its new location. Algorithm 4.6 provides the details for amoeboid tail movement.

---

**Algorithm 4.6:** DE + Followers Slug Movement (Tail Movement)

---

```

1. Find the nearest neighbor, with index nn, in the direction nearest the TailDirection.

```



2. Compute the NearestNeighborDirection as the distance between  $pop_i(t).x$  and  $pop_{nn}(t).x$
  3. for  $j = 0 \square D \square 1$
  4.  $pop_i(t+1).x_j = pop_i(t).x_j + 0.5 * Rand(0.0 \square 1.0) * E_j[d_{slugNeighbor}] * TailDirection_j + 0.5 * Rand(0.0 \square 1.0) * NearestNeighborDirection_j$
  5. Ensure that  $pop_i(t+1).x_j$  is within bounds.
  6. End for.
  7. Compute the new objective function value and update personal best if necessary.
- 

Lastly, as part of the Slime Mold Optimization Algorithm, each slug must be updated after all amoebae have completed one timestep's worth of movement. The majority of updates for the slug presented in this section follow similar algorithms as that of the original slug update algorithm [Monismith and Mayfield 2008]. There is, however, one additional update that is required for the slug, as presented in this section. Before continuing to another iteration of amoeboid movement, the centroids for the members of the head and tail must be found. Once these values are determined, the general direction of tail movement is ascertained and normalized so it may be used in subsequent amoeboid movement. Algorithm 4.7 details the necessary updates for DE + Followers slug movement.

---

**Algorithm 4.7:** DE + Followers Slug Movement (Slug Update)

---

1. Compute centroids of the head and tail as headCentroid and tailCentroid.
  2. Compute the tail direction (referred to as tailDirection) as the difference between the head and tail centroids.
  3. Normalize tailDirection by the square root of its dot product.
- 

### ***Section 4.3 Conclusion***

In this chapter, several modifications to the Slime Mold Optimization Algorithm were introduced. These included modification to the vegetative state to allow for the use of the Downhill Simplex and Razor Search algorithms as vegetative search algorithms [Spendley et al. 1962, Bandler and MacDonald 1969]. Additionally, the slug state was modified to allow for use of Differential Evolution as a search algorithm and to allow for DE's use as part of a slug containing a head and a tail [Kessin 2001, Price et al. 2005]. In the following chapter, results for the algorithms presented in Chapter 3 and those presented in this chapter will be provided and analyzed.

## CHAPTER V

### V. RESULTS AND ANALYSIS

In this chapter, results are provided for the Slime Mold Optimization Algorithm. Before discussing results, the test equations and testing procedures are discussed. Next, the Slime Mold Optimization Algorithm, as presented in Chapter 3, is tested against a large function suite provided in the Objective Function Appendix (Appendix A). This first round of testing is carried out using different numbers of amoebae, pseudopods, neighbors, and function evaluations. Analysis of results is presented, and results are then compared against those of existing algorithms, including Hooke Jeeves (HJ), DE, RCGA, and PSO. Thereafter, results for variations on the Slime Mold Optimization Algorithm are presented. These include replacement of the vegetative state with the Razor Search and Downhill Simplex algorithms. Additionally, results for the DE + Followers method (as described in section 4.2) using both Razor Search and the standard vegetative search are provided. Comparisons are provided for each modified algorithm using the same criteria as the standard slime mold optimization algorithm.

#### *Section 5.1: Test equations and testing procedures*

The first portion of the results includes testing each of the optimization algorithms over a variety of parameters using many objective functions. The objective functions include variation in dimensionality and contours, some feature high levels of multimodality, discrete steps, or minima that are cut off at a bound. Additionally, parameters for the Slime Mold Optimization Algorithm are varied so comparisons within the algorithm may be made. Furthermore, direct comparisons are made to results from other algorithms such as Differential Evolution, Particle Swarm Optimization, and Real-Coded Genetic Algorithms. Performing such a comparison as part of this work will give a better feel for the strengths and weaknesses of the slime mold optimization algorithm. Therefore, the focus of this section includes a discussion of the various test functions used, the method of testing functions using varying parameters, and comparisons to variations of the slime mold optimization algorithm and other existing algorithms.

The test function suite used in this work includes functions with varying degrees of difficulty including multi-modality, variation in dimensionality, discrete steps, and minima cut off at bounds. The reader is referred to the Objective Function Appendix (Appendix A) for formulae, bounds, and optimal objective function values and locations

for the functions to be optimized. A list of these functions is also provided in Table 5.1. Of the functions, several are included which are unimodal and present little difficulty to general optimizers. These are the DeJong or Spherical Contours function which is a simple parabolic function that slopes downward toward a single optimum, the Easom function, which is a Gaussian centered at  $(\pi, \pi)$ , and the functions S1, S2, and S3 which are downward sloping functions of two variables that have a minimum at a bound [Chen 1997, GEATbx 2007, Choi and Mayfield 2009]. Each of these functions should present little difficulty to a general optimizer.

The McCormic, Goldstein and Price, Bohachevsky, Engvall, Branin rcos, and Six Hump Camel functions all present multiple modes. These functions are smooth, but include local and global minima across their search spaces. As such they are slightly more difficult to optimize than unimodal functions. Likewise, the Rosenbrock function and the Downhill Step Function are slightly more difficult to optimize than the Spherical Contours or Easom functions. Classical optimization methods may not work on these functions; therefore, the use of direct search methods such as EAs, Pattern Search, or Downhill Simplex is necessary [Chen 1997, GEATbx 2007]. Thus, it is expected that the Slime Mold Optimization Algorithm should have little difficulty in optimizing the functions above even as variations in dimensionality and bounds are introduced.

Rosenbrock 2D (1)	McCormic (2)	Box and Betts (3)	Goldstein (4)	Easom (5)	Mod. Rosenbrock 1 2D (6)
Mod. Rosenbrock 2 2D (7)	Bohachevsky (8)	Powell (9)	Wood (10)	Beale (11)	Engvall (12)
DeJong 2D (13)	Rastrigin 2D (14)	Schwefel 2D (15)	Griewangk 2D (16)	Ackley (17)	Langermann (18)
Michalewicz (19)	Branin (20)	Six Hump Camel (21)	Osborne 1 (22)	Osborne 2 (23)	Mod. Rastrigin 2D (24)
Mineshaft 1 (25)	Mineshaft 2 (26)	Mineshaft 3 (27)	Spherical Contours 32D (28)	S1 (29)	S2 (30)
S3 (31)	Downhill Step (32)	Salomon 2D (33)	Whitley 2D (34)	Odd Square 2D (35)	Storn Chebyshev 9D (36)
Rana 2D (37)	Rosenbrock 10D (38)	Rosenbrock 30D (39)	Mod. Rosenbrock 1 10D (40)	Mod. Rosenbrock 1 30D (41)	Mod. Rosenbrock 2 10D (42)
Mod Rosenbrock 2 30D (43)	Spherical Contours 10D (44)	Rastrigin 10D (45)	Rastrigin 30D (46)	Schwefel 10D (47)	Schwefel 30D (48)
Griewangk 10D (49)	Griewangk 30D (50)	Salomon 10D (51)	Salomon 30D (52)	Odd Square 10D (53)	Whitley 10D (54)
Whitley 30D (55)	Rana 10D (56)	Rana 30D (57)			

**Table 5.1: Objective Functions Used**

Testing of the Slime Mold Optimization Algorithm will also involve many functions that are more difficult than those explained above. The Rastrigin, Schwefel, Griewangk, and Ackley's Path functions all present different variants of a pincushion function. That is they all have high numbers local minima that make the function appear as if it is a pincushion that has been molded to a particular form. Rastrigin's function is a pincushion overlaid upon a parabola as is the Griewangk function, although it has a tighter pincushion [Price et al. 2005]. The Ackley's Path function has a Gaussian conformation with a pincushion applied to it, and the Schwefel function has an almost random appearance to its pincushion [Price et al. 2005]. Since these functions have multiple minima they offer many positions in which an optimizer may become trapped, but since there are always other "pins" (i.e., minima) nearby, a good optimizer will be

able to escape these traps that lie throughout the search space. The Modified Langermann's function also presents multiple minima that are located in a close space, and thus, optimizers act similarly when working upon it [Chen 1997, Price et al. 2005]. The Wood, Beale, and Powell functions are all deceptively simple. For example, though the Powell function appears simplistic, Chen notes that it has a singular Hessian matrix at its minimum [1997]. These functions each present combinations of parabolic functions of varying powers. Instead of creating a pincushion landscape, they create a landscape with a few valleys that cause Direct Search methods to sometimes become trapped within a valley that is a local minimum [Chen 1997]. Two other functions that offer similar effects with different conformations are also included. These are the Michalewicz and Mineshaft 3 functions. The Michalewicz function offers a few minima that are hidden within nearly flat valleys, and the Mineshaft 3 function offers two extremely narrow Gaussian minima that are shaped like mineshafts and located within a flat plane. Both of these functions provide some difficulty to direct search methods and EAs because they offer locations far from the actual minima at which such optimizers may become trapped [GEATbx 2007, Monismith and Mayfield 2008]. Though the functions explained above present a moderate amount of difficulty to EAs, many such algorithms are able to optimize these functions provided enough time.

The next group of functions that will be tested on the Slime Mold Optimization Algorithm are quite difficult to optimize. The first pair of difficult functions is a pair of modified versions of Rosenbrock's function. Such modification in the function changes the nearly planar valley of the original function to an edge via square root and absolute value operators. Using these operators yields two functions—a flat ground bent knife edge function and a hollow ground bent knife edge function. Since the optimum in both of these functions lies along an edge within a valley having a narrow opening angle, stochastic methods that are unable to correctly judge contours may take an infinite amount of time to reach the optimum or may converge incorrectly [Chen 1997]. Next, the discussion of difficult functions includes a group of functions that the author has modified and developed. These are the Mineshaft 1, Mineshaft 2, and Modified Rastrigin functions, and they were crafted using root functions for Mineshaft 1 and Modified Rastrigin and a Gaussian for Mineshaft 2. The low order roots and the narrow Gaussian cause these functions to exhibit minima that are located at the bottom of areas with extremely narrow openings, which makes optimization very difficult [GEATbx 2007, Monismith and Mayfield 2008]. Two other interesting functions are the Osborne 1 and 2 functions, which are least squares problems of 5 and 11 dimensions respectively. In his thesis, Chen notes that these functions may provide difficulty to stochastic optimizers, and the reason for such difficulty is as of yet unknown [1997]. In unpublished work, the author has verified that the Osborne functions do indeed prove difficult to optimize with both RCGAs and PSO algorithms. Several additional functions are included for testing from [Price et al. 2005]. These are Salomon's function, Whitley's function, Storn's Chebyshev function, the Odd Square function, and the Rana function. These functions are noted for their difficulty, high multimodality, and many of them may be scaled to varying degrees of dimensionality. The reader is directed to the Objective Function Appendix for formulae and 3D views (where applicable) of the functions described above.

The functions explained above will be used as part of a suite to test the Slime Mold Optimization Algorithm. Testing of the algorithm will be based upon several factors – variation in the number of amoebae, maximum number of iterations, and number of neighbors. The results provided are the averages of the smallest objective function values obtained during attempts at finding the true minima over a fixed number of trials or runs of a particular optimization algorithm. Unless otherwise denoted, these averages will be over 100 runs or trials of an algorithm and the generic term, “result” will refer to such an average. In addition, relative error is used to compare the Slime Mold Optimization Algorithm, its variants, the Hooke Jeeves algorithm, and Evolutionary Algorithms. Relative error is defined as the difference between an approximate and actual value divided by the actual value [Abramowitz and Stegun 1972]. The formula for the relative error between an actual minimum  $f^*$  and an approximate minimum  $f_{est}^*$  is provided below.

$$\text{Relative Error} = \frac{|f_{est}^* - f^*|}{|f^*|} \quad (5.1)$$

The percent error may also be calculated by multiplying the relative error by 100 [Abramowitz and Stegun 1972]. When  $f^* = 0$ , it is impossible to calculate the relative error. In that case, adding one to both the estimated minimum and true minimum allows for calculation of the relative error. Such calculation is used because doing so is equivalent to calculating the absolute error [Abramowitz and Stegun 1972]. Graphs in the latter sections of this chapter include variations in error of high orders of magnitude. To deal with this a variant of relative error called Log of Scaled Relative Error was devised and is defined below.

$$\text{LSRE} = \log\left(\frac{|f_{est}^* - f^*|}{|f^*|} + 1\right) \quad (5.2)$$

The LSRE is the logarithm of one plus the relative error. This is needed to avoid taking the logarithm of zero when dealing with exact estimates of minima.

First, results for the algorithm, as presented in Chapter 3, will be provided with objective function evaluations limited to maximums of 100,000, 500,000, and 1,000,000 evaluations, respectively. Additionally, the algorithm will be tested by varying the number of amoebae in the population using the values 50, 100, 250, and 500 as population sizes. Within those results, the number of neighbors will be varied as a fixed four neighbors, the number of search space dimensions limited to a maximum of 10 neighbors, 2 times the number of search space dimensions with no limit, and the square of the search space dimensions. Furthermore, selected population sizes of 50 and 500 will be tested using the original algorithm using a maximum of 500,000 evaluations while allowing the number of pseudopods to vary from 2 to 10 in steps of two. Results from these runs will be graphed to show the effect of varying population size and objective function evaluation limits on each set of algorithm parameters. The reason for such

testing is to evaluate the effect of varying parameters so that the number of function evaluations needed to optimize the various objective functions explained above [Price et al. 2005, Monismith and Mayfield 2008].

The next portion of the testing procedures involves comparison of the slime mold algorithm's results against those of the Hooke Jeeves Pattern Search, DE, PSO, and RCGA. Each of the four algorithms will be tested on all the functions presented in the Objective Function Appendix. This testing will include limitations of 100,000, 500,000, and 1,000,000 objective function evaluations, respectively. The specific versions of the Evolutionary Algorithms planned for use are the DE current-to-rand algorithm with fixed values for the F and K parameters, the standard PSO algorithm, and an RCGA algorithm with a 90% crossover rate and a 0.5% mutation rate [Price et al. 2005, Kennedy and Eberhart 1995, Herrera et al. 1998]. These EAs will have population sizes of 200 (DE), 100 (PSO), and 500 (RCGA). Such sizes were used because of their effectiveness on the Objective Function Appendix. Code for the EAs was written by the author. Results from the Hooke Jeeves algorithm will be provided using starting step sizes of 10% of the distance across the bounds of the objective functions, and the step size reduction factor will be set to 0.2. Additionally, each trial of the Hooke Jeeves Pattern Search used 100 randomly chosen starting locations from which the algorithm was allowed to start. The best result out of the 100 was used as the result for each trial of the algorithm. This implementation was used as a way to simulate having a population like an EA. Code for this algorithm was provided by John Chandler and updated by the author for use in this work. Results from these algorithms using similar limits on function evaluations should provide a reasonable basis for comparison to the Slime Mold Optimization Algorithm.

The final portion of the testing procedures includes testing the variants of the Slime Mold Optimization Algorithm. There are four of these variants to be tested, and each will be tested using the same parameters as the Original Algorithm where applicable. This includes limitations of 100,000, 500,000 and 1,000,000 objective function evaluations, amoeba population sizes of 50, 100, 250, and 500, and the same four neighbor settings as listed above. The variants to be tested are Slime Mold Optimization Algorithms (SMOAs) with 1) a vegetative state that makes use of the Downhill Simplex Algorithm (Simplex SMOA), 2) a vegetative state that makes use of the Razor Search Algorithm (Razor SMOA), 3) a slug state that makes use of the DE + Followers algorithm (HTDE-SMOA), and 4) both a vegetative state using the Razor Search Algorithm and a slug state using the DE + Followers Algorithm (HTDER-SMOA). Results as explained above will be explained in the following sections and their graphs are provided in the appendices.

### ***Section 5.2 Original Algorithm Results***

In this section results from the version of the Slime Mold Optimization Algorithm as presented in Chapter 3 are presented. This algorithm will also be referred to as the "Original Algorithm" or "SMOA" in this section and thereafter. Results for the Original Algorithm are presented as tables in Appendix B1. Likewise similar tables are presented

in Appendices B2 and B3 for the standard deviations of the results and the runtimes of each test. Results are shown for 57 objective functions, all of which are presented in the Objective Function Appendix (Appendix A). For each objective function, 48 results are presented. These results are divided into three groups of 16 representing the tests of the SMOA with limits of 100,000, 500,000, and 1 million objective function evaluations, respectively. Each set of 16 is further divided into sets of four using population sizes of 50, 100, 250, and 500 amoebae (denoted as A50, A100, A250, and A500 in graphs and tables), respectively. Each of these sets of four uses one of the four neighbor strategies as numbered here: N1) four neighbors, N2) the number of decision variables limited to a maximum of ten neighbors, N3) two times the number of decision variables with no limit, and N4) the square of the number of decision variables. As an example, one point might represent 100,000 objective function evaluations with a population size of 250 (A250) and use neighbor strategy N1) four neighbors.

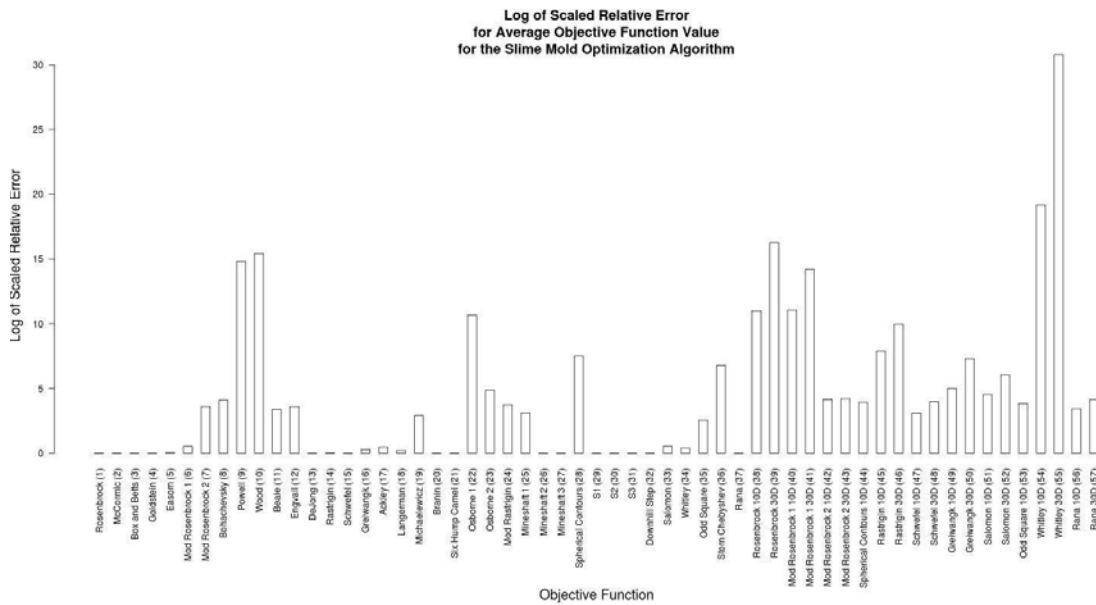


**Figure 5.1: Log of Scaled Relative Error for Original SMOA using the best of the average results across parameter variations.**

**Refer to Table 5.1 for names corresponding to function numbers.**

Before comparing results between parameter variations of the original algorithm, the overall performance of the algorithm is considered. That is, assuming the user of the algorithm had knowledge of appropriate parameters, how would said user's results appear. A first look at the best of our average results shows mediocre to good performance on low dimensional functions. Among the functions where the algorithm performed well are Rosenbrock (1), Rastrigin (14), Griewangk (15), Schwefel (16), Mineshaft 3 (27), and many other functions. In particular, the algorithm performs well on any function that is not of very high dimensionality or of very high difficulty as shown in Figure 5.1. The algorithm's performance on more difficulty functions such as the Powell (9), Wood (10), Osborne (22, 23), Mineshaft 1 (25), and Modified Rastrigin (24) functions is particularly poor. Many of the results appear to be approaching the optima,

but the algorithm needs more objective function evaluations to reach the optima. For example, in the appendices, one can see progress being made toward the minima for the 32D Spherical Contours (28), Storn Chebyshev (36), and Odd Square (35) functions. It appears as if many more evaluations are needed to reach optima on these functions.

Next, the algorithm's performance across the various evaluation limits is discussed. Such performance is as expected. The SMOA shows its best results at the 1,000,000 evaluation limit, mid-range results are at the 500,000 evaluation limit, and the worst results show up at the 100,000 evaluation limit. An example of this can be seen for Rosenbrock's function in Figure 5.2. Moreover, results become more consistent according to their standard deviation as evaluations are increased, but the time cost of the algorithm significantly increases as the evaluation limit is increased. What is odd is that improvement between the 100,000 and 500,000 limits and between the 500,000 and 1,000,000 limits is not always as strong as should be expected. This indicates the need for modification to the algorithm as currently designed. One possible change that could be made to the SMOA is to force the slug stage to retain the current global best within one of its members. This would effectively force all amoebae in the slug to move toward the current global best.

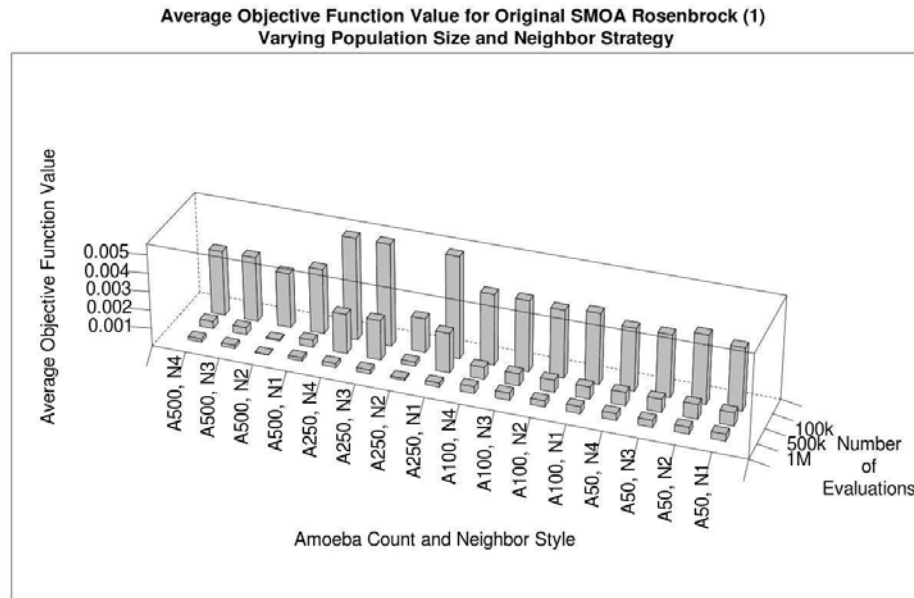


**Figure 5.2: Original SMOA results from Rosenbrock's function ( $f^* = 0$ ) across evaluations, population sizes, and neighbor strategies.**

Another interesting parameter of the SMOA is the number of amoebae used in algorithm. This parameter has strong effects on both results and runtimes. For objective functions of many dimensions, runtime costs increased as the number of amoebae were increased. The opposite was often true for objective functions of fewer dimensions. This occurred because the time cost in using the slug state with an objective function of few dimensions was quite low because of the small number of neighbors used, even in comparison to the cost associated with the vegetative state. In contrast, with a high



dimensional function, using many amoebae causes the slug state to become costly in terms of CPU usage because of the large number of links between neighbors.

Performance changes across by varying population size are quite noticeable across all evaluation limits. Of additional interest is that functions most affected (i.e. requiring more CPU time) were those that are difficult to optimize and/or of high dimension (5+). Lower population sizes improved results and standard deviations for the following functions: Goldstein, Powell, Wood, Langerman, Michaelewicz, Osborne 1 & 2, Modified Rastrigin, Mineshaft 1 & 2, Spherical Contours 10D & 32D, Storn Chebyshev (9D), Rana, Rosenbrock 10D & 30D and its modifications, Griewangk 10D & 30D, Rastrigin 10D & 30D, Schwefel 10D & 30D, Salomon 10D & 30D, Odd Square 10D & 30D, and Whitley 10D & 30D. An example of this for the 10D Spherical Contours function is provided in Figure 5.3. Note that all of the aforementioned

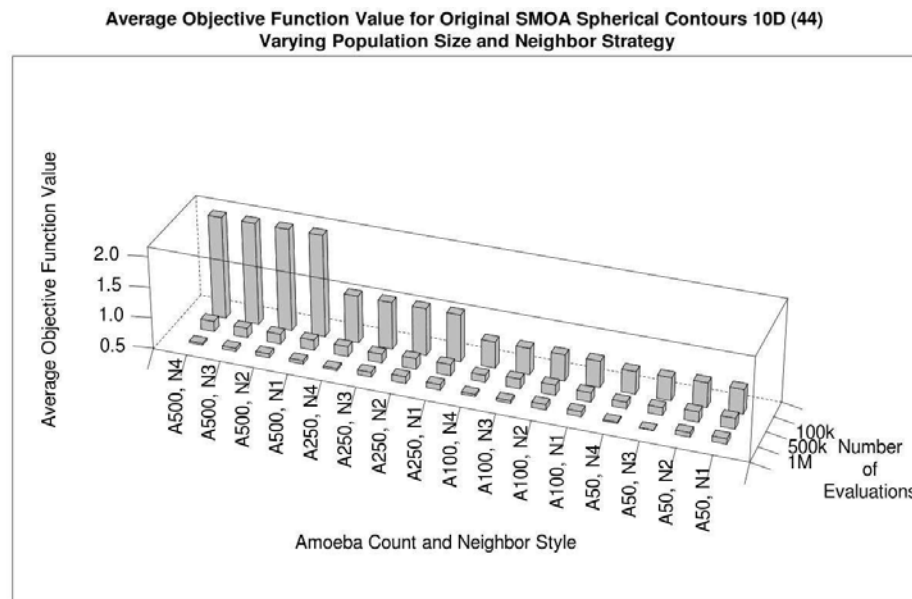


**Figure 5.3: Original SMOA results from Spherical Contours Function 10D ( $f^* = 0$ ) across evaluations, population sizes, and neighbor strategies**

functions listed may present considerable difficulty to optimization algorithms based on their dimensionality and/or multiple minima. Occasionally, one particular population size was best. This tendency can be seen in the Beale and Engvall functions. Additionally, there is a tendency for results to flatten across parameter variations with higher number of objective function evaluations (500k and 1M). This is to be expected because as results improve in many optimization algorithms, they tend to stabilize as they near optima. Such tendency can be seen in Figure 5.2 for Rosenbrock's function. Results for the Wood and Powell functions reversed their performance with respect to population size at the 100,000 and 1,000,000 evaluation limits. This is, however, not worth much merit since an optimum was not reached, and both results and standard deviations for these functions improved as population size was increased. Lastly, many objective functions that would be considered "easy" to optimize were relatively

unaffected by change in population size, especially at higher evaluation limits. This is to be expected because in many cases the number of evaluations was more than sufficient to produce reasonable results.

Objective function values provide much insight into the performance of the Slime Mold Optimization Algorithm. There are, however, limits to how well performance can be judged based upon this one indicator. To better gauge performance in functions where there are many local minima, it is helpful to look at the distance between the decision space values obtained from an optimization algorithm and the decision space values of the actual minima. This will be referred to as the "error in x". In Figure 5.4, the error in x is presented for the Griewangk function. From the box plots presented, it is easy to see that the Original SMOA falls between 20 and 70 units away from the actual minimum.

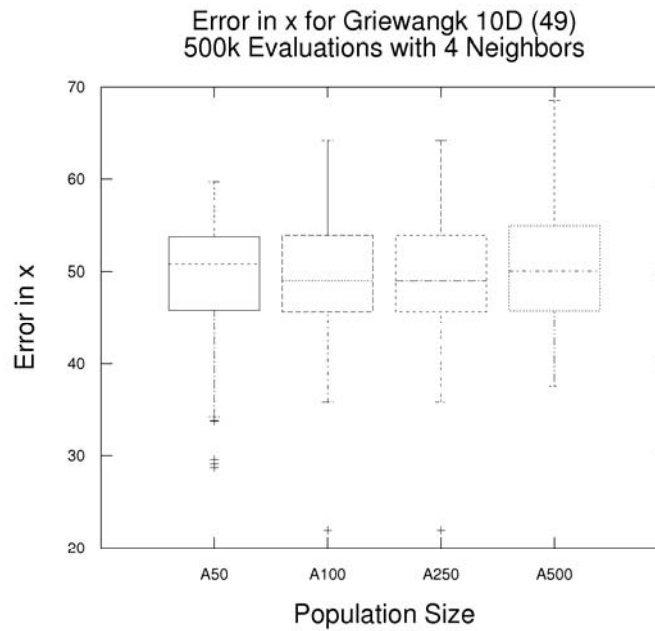


**Figure 5.4: Error in x for Griewangk 10D Function (49) using 4 neighbors and 500,000 evaluations.**

Looking at Figure 5.5 in conjunction with Figure 5.4, it is clear that the objective function values produced by the Original SMOA are nearing the actual minima of zero at decision space location (0, 0). Since it is known that the Griewangk function has many local minima, one can assume that the Original SMOA was caught in an area of local minima near the true minimum

Next, performance across neighborhood strategies is discussed briefly. Performance from varying neighbor strategies is more straightforward than that of varying population size. Simply put, increasing the number of neighbors has a tendency to improve performance (result and standard deviation) as the number of evaluations is increased and with higher dimensionality and difficulty of the objective function. Such improvement comes with a cost of increased runtime as the dimensionality of the objective function is increased. This should not come as a surprise since more neighbors

will provide more information when attempting to optimize functions of higher dimensions.

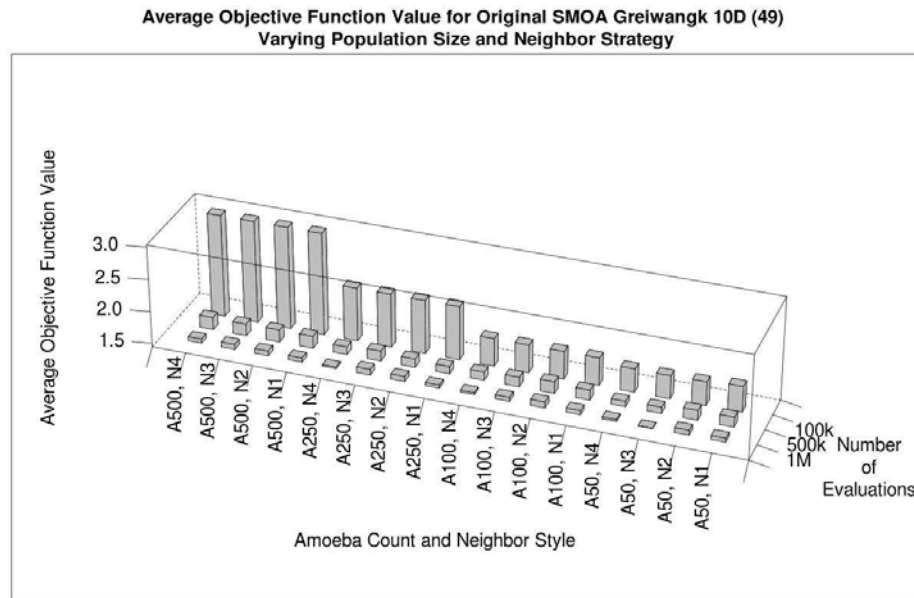


**Figure 5.5: Original SMOA results from Griewangk Function 10D ( $f^* = 0$ ) across evaluations, population sizes, and neighbor strategies**

Another of the parameters that was varied to ascertain performance was the number of pseudopods. For this set of parameters, the algorithm was fixed at a limit of 500,000 evaluations and was tested using each of the four neighbor strategies with population sizes of 50 and 500 amoebae. Performance from modifying number of pseudopods shows little variation. Perhaps slight preference is indicated for very few (2) or many (10+) pseudopods. Results, standard deviations, and runtimes for varying the number of pseudopods may be seen in Appendices C1, C2, and C3, respectively. Of more interest is that the results, regardless of the number of pseudopods show a definite preference for a smaller population size when optimizing high dimensional functions using a 500,000 evaluation limit.

The last of the data considered for the Original algorithm is its runtime. Runtimes for SMOA are provided in Appendix B3. Note that these runtimes are averaged over the 100 trials that were used for each objective function. The algorithm was executed as a 9 thread process with one `server` thread and each of a number of `client` threads running one instance of the SMOA with a particular parameter set. This program ran on a 1U Dell PowerEdge 1950 III with dual quad-core Intel E5430 processors. This was one node of the OSU Supercomputer called Pistol Pete. Run times ranged from less than 0.08sec for a 100,000 evaluation run of SMOA on function S1 to just over 6.5min for a 1,000,000 evaluation run of SMOA on the Storn Chebyshev (9D) function. The high cost associated with the Chebyshev function is due to a high amount of recursion and iteration required for its evaluation. Most runs of SMOA cost between 0.1sec and 10sec for

functions of low dimensionality and between 10sec and 6.5min for functions of high dimensionality (e.g. 9D  $\square$  32D).

### ***Section 5.3 Comparisons between the Original Algorithm, HJ, DE, RCGA, and PSO***

In this section, comparisons between the Hooke Jeeves, DE, RCGA, and PSO algorithms and the best of the average results from the original SMOA are discussed. This is done to get a baseline for the performance of the SMOA versus existing EAs. One might wonder why comparisons are not made against existing derivative-based classical algorithms (e.g. Steepest Descent). For such algorithms, it is not possible to test the entire function set to classical algorithms because many of them lack derivatives (e.g. Storn Chebyshev, Odd Square, Modified Rosenbrock 1, etc.). Such algorithms typically offer a better cost to performance ratio on differentiable functions as well. One direct search algorithm, Hooke Jeeves Pattern search is tested against the SMOA. Since this algorithm is different from EAs in that it does not have a population, a population-based heuristic is used whereby many Hooke Jeeves trials are used with starting points scattered randomly about the decision space. This was done to ensure fairness against EAs, because direct search algorithms using single starting points may become trapped in local minima. Even with such a population-based heuristic, direct search algorithms are typically not very costly in terms of run time. EAs also offer the possibility of global optimization, but this is often at the cost of hundreds of thousands or millions of objective function evaluations. Therefore, it is prudent to compare such algorithms based on fixed limits on evaluations.

Comparison of the algorithms begins with a look at the average performance from each of the algorithms. Such comparisons can be made easily by comparing the best of the average results from Appendix B1 against those of Appendix H1 at the 1,000,000 evaluation limits. These comparisons are also provided in a graph below using LSRE. Hooke-Jeeves performs surprisingly well on the function suite. It outshines the EAs on all but a few functions: Easom, Griewangk, Modified Rastrigin, Odd Square, Salomon, and Rana. Hooke-Jeeves, just like many of the EAs seems to have the most difficulty in areas where the minimum objective function value is hidden along a line or curve having a narrow opening angle. DE shows the best performance of the EAs on most functions in the entire suite, but even it fails to optimize several objective functions including the Michalewicz, Mineshaft1, Odd Square 2D and 10D, Modified Rosenbrock 1 10D and 30D, Rastrigin 10D and 30D, Schwefel 10D and 30D, Whitley 10D and 30D, and Rana 30D functions. In fact, out of the aforementioned functions the optimum of only one (Michalewicz) is found by one of the EAs  $\square$  PSO. PSO, RCGA, and SMOA all have worse performance than DE, but they perform in a similar fashion, each finding minima for about half the functions in the suite. All methods need more objective function evaluations to take on many of the high dimensional functions. There are, however, slight differences between the minima the algorithms find. SMOA has more obvious difficulty with high dimensional functions than any other algorithm. It even has the poorest performance on the 10D Spherical Contours function. PSO seems to have more problems with functions with minima  $\square$ hidden $\square$ on flat planes. This problem has to do

with its design as PSO relies on velocity to move about. RCGA doesn't seem to have any overall problems other than that it seems to be taking longer to reach optima, especially as the search space gets larger. Again this is simply due to the algorithm's design. RCGA is actually a semi-random search, and with a larger search area, the search time will be increased.

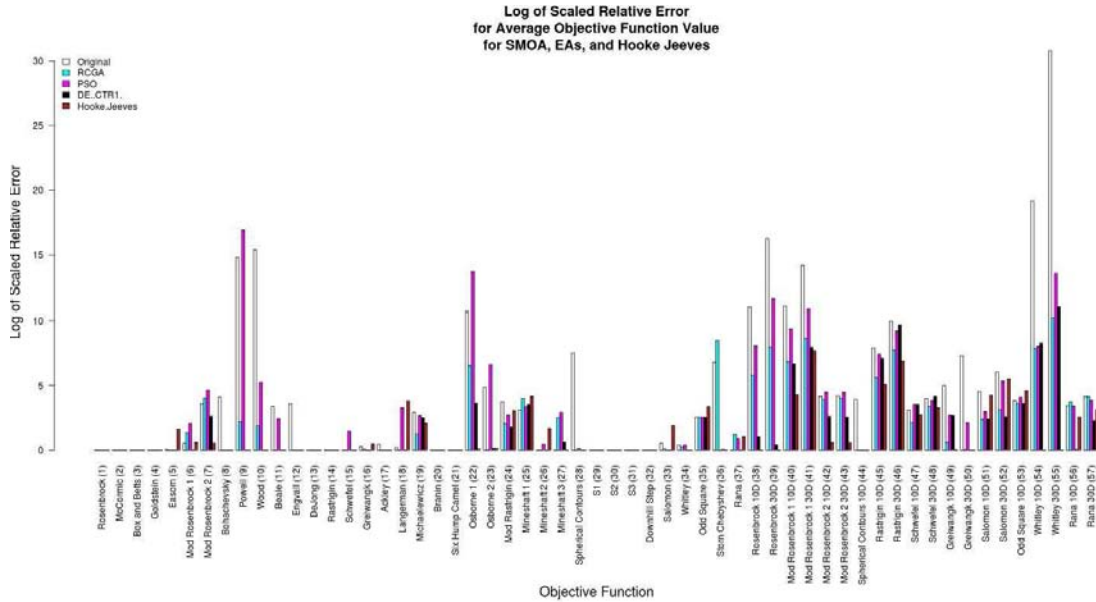


**Figure 5.6: LSRE for Original SMOA, EAs, and Hooke Jeeves for Average Objective Function Values.**

Given the comparisons in performance, it is also prudent to compare standard deviations and runtimes. The standard deviations of results were excellent for most results of EAs and Hooke-Jeeves, i.e. they were near zero for results near minima. SMOA also showed reasonable results standard deviations, but those standard deviations for results near minima were not as close to zero as those produced by the other EAs. For the entirety of the results considered in this section, standard deviations for poorer results were quite large. Such standard deviations are actually good because they indicate all of the algorithms have not converged on any location — the algorithms were still searching for minima when an evaluation limit was reached. Next runtimes for these algorithms are considered. These are not easily comparable as Hooke-Jeeves, PSO, and RCGA all ran as single processes on 1U on 1 core of 1 processor on the OSU Supercomputer with no context switching, SMOA ran on the same equipment as noted in the previous section, and DE results were produced as part of a process having 40 threads on the author's home computer, which has 1 processor with 2 cores. Obviously comparing these runtimes against each other could lead to false assumptions because of the overhead associated with context switching.

## Section 5.4 Results from Modifying the Slime Mold Algorithm

As noted in previous sections, four major variants of the SMOA were created. These are first, two algorithms that replace the vegetative state with the Downhill Simplex (Simplex SMOA) and Razor Search (Razor SMOA) algorithms, respectively, and two other algorithms that make use of a new slug state, those being the DE+Followers (HTDE-SMOA) and DE+Followers with Razor Search Vegetative State (HTDER-SMOA) algorithms. All of these algorithms provide at least some benefit over the SMOA; however, in some cases they may perform worse. In this section, the performance of these algorithms is explained.

First, the Simplex SMOA is analyzed. On first look, its performance appears to be quite good on many objective functions such as the Modified Rosenbrock 1 function, but occasionally the results are quite poor even for some “easier” objective functions such as the 2D Rosenbrock function. On closer analysis it becomes clear that the Simplex SMOA is highly dependent on population size and neighborhood strategy. With more difficult objective functions often a smaller population size with a reasonable neighbor strategy works well. Occasionally, with simpler high dimensional functions, a larger population size is more beneficial as with the 10D Spherical Contours function. The method is significantly faster than any of the other SMOA methods, but it is also the most sensitive to changes in population size and neighborhood strategy.

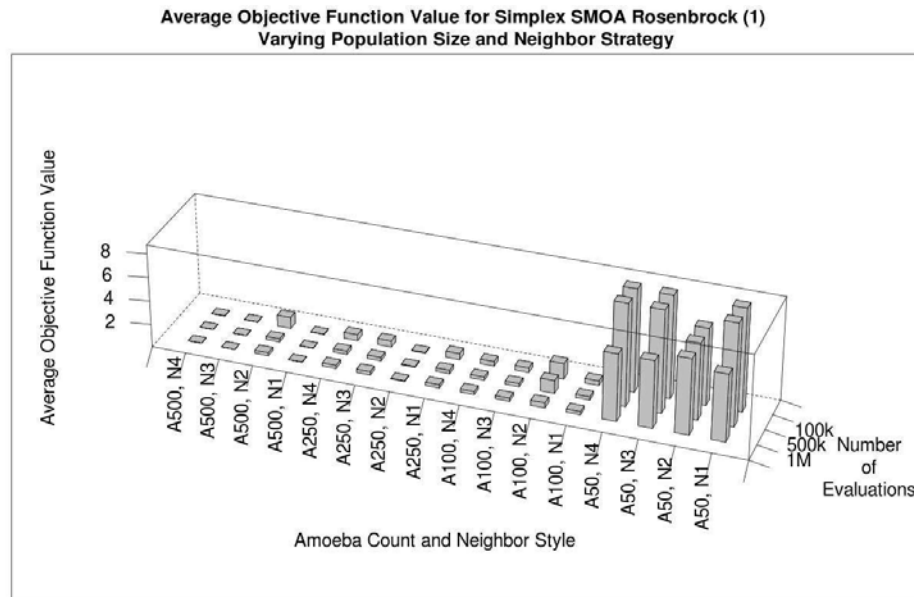


**Figure 5.7: Simplex SMOA results from Rosenbrock’s function ( $f^* = 0$ ) across evaluations, population sizes, and neighbor strategies.**

The HTDE-SMOA method seems to be quite stable. It is fairly consistent across most parameters changes, though there are slight variations that occur from parameter changes. The algorithm reacts better to having more neighbors with objective functions with higher dimensionality. Note the performance on the Storn Chebyshev function in Figure 5.9. For simpler functions, especially those with lower dimensionality, a smaller

population size seems to improve results. In comparison to the Original SMOA, many similarities are present. Varying evaluation limits often produces similar improvements and standard deviations are also quite similar, though improved.

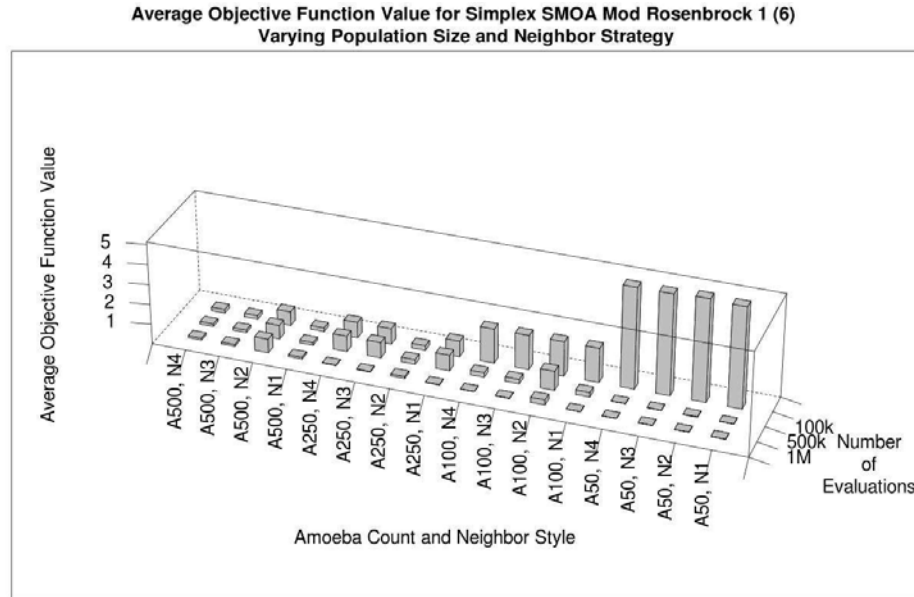


**Figure 5.8: Simplex SMOA results from Modified Rosenbrock 1 function ( $f^* = 0$ ) across evaluations, population sizes, and neighbor strategies.**

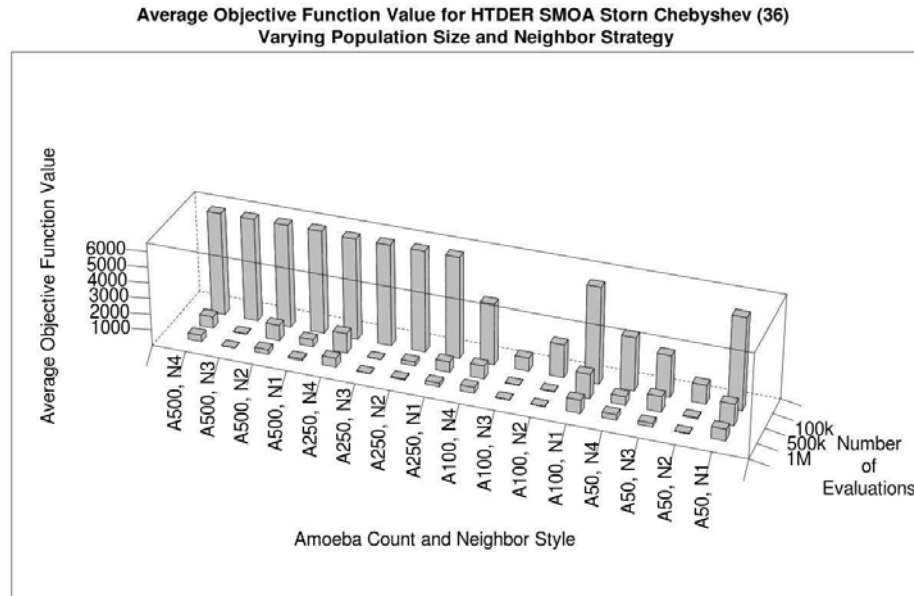


**Figure 5.9: HTDER SMOA results from Storn Chebyshev function (9D,  $f^* = 0$ ) across evaluations, population sizes, and neighbor strategies.**

Improvement to this algorithm is seen when the Razor Search is added in place of the vegetative search defined in Chapter 3. The Razor SMOA produces results similar to

those of the Original SMOA. It seems offer little performance boost over the Original algorithm on its own, but when added to the HTDE-SMOA significant improvements to results are visible. With this change to the vegetative state, the new algorithm is referred to as HTDER-SMOA. Results from this algorithm are better overall with a larger population size for objective functions of low dimensionality with a generous number of neighbors (i.e. neighbor strategy 3 or 4). Interestingly in many of the same situations, using very few neighbors and a small population (e.g. neighbor strategy 2 with 50 amoebae) also work well for simple functions of low dimensionality. For objective functions of many dimensions, results improve when using few neighbors and a moderate population size (e.g. neighbor strategy 2 with 100 or 250 amoebae). The HTDER-SMOA generally produces quality results with reasonable standard deviations for functions of dimension less than ten and is even able to near the optimum on the Storn Chebyshev (9D) function. More objective function evaluations would be necessary to improve its performance on the difficult, high dimensional functions in the suite.

### ***Section 5.5 Comparisons to the Original Algorithm and other EAs***

To simplify this section, the best of the averages at the 1,000,000 evaluation limit from the Original Algorithm, HTDE, HTDE-Razor, Razor, and Simplex algorithms were compared against each other and against the methods mentioned in Section 5.3. Initial observations are made from Figure 5.10. First, comparing the SMOA algorithms against themselves, it is obvious that the HTDE-Razor and Simplex SMOAs provide the best overall quality. The Original SMOA, HTDE SMOA, and Razor SMOA provide a slightly lower level of quality with slight variations between results. None of the algorithms work particularly well on the higher dimensional functions, but the HTDE and HTDE-Razor algorithms do tend to perform consistently and are better on the Storn Chebyshev (9D), Osborne 1 and 2, and many of the high dimensional functions. The Simplex SMOA tends to have varying performance that limits it, especially on some of the easier functions such as the 2D Rosenbrock function, but occasionally has excellent performance on objective functions with high dimensionality such as the 10D and 30D Griewangk functions and those with high difficulty like the 2D Modified Rosenbrock functions.



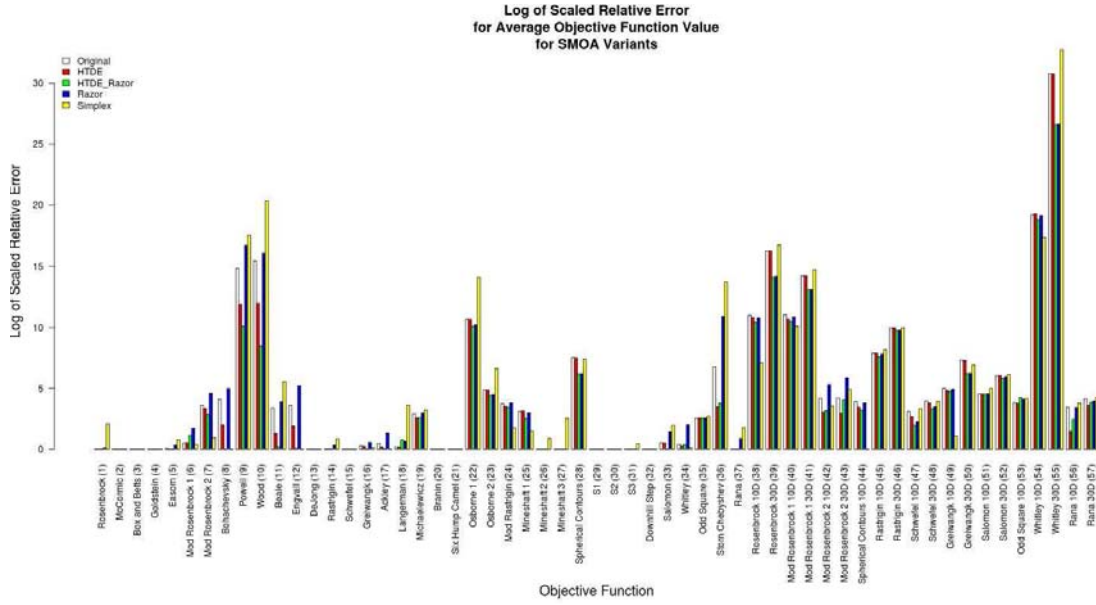


Figure 5.10: LSRE for all SMOA methods across all objective functions.

Next, comparisons are made of the best average results at the 1,000,000 evaluations limit to the EAs covered in Section 5.2 and to the Hooke Jeeves Pattern Search (HJ). Such comparison is made through Figure 5.10. The results show two obvious winners based upon average result: DE and Hooke Jeeves. Aside from this, the

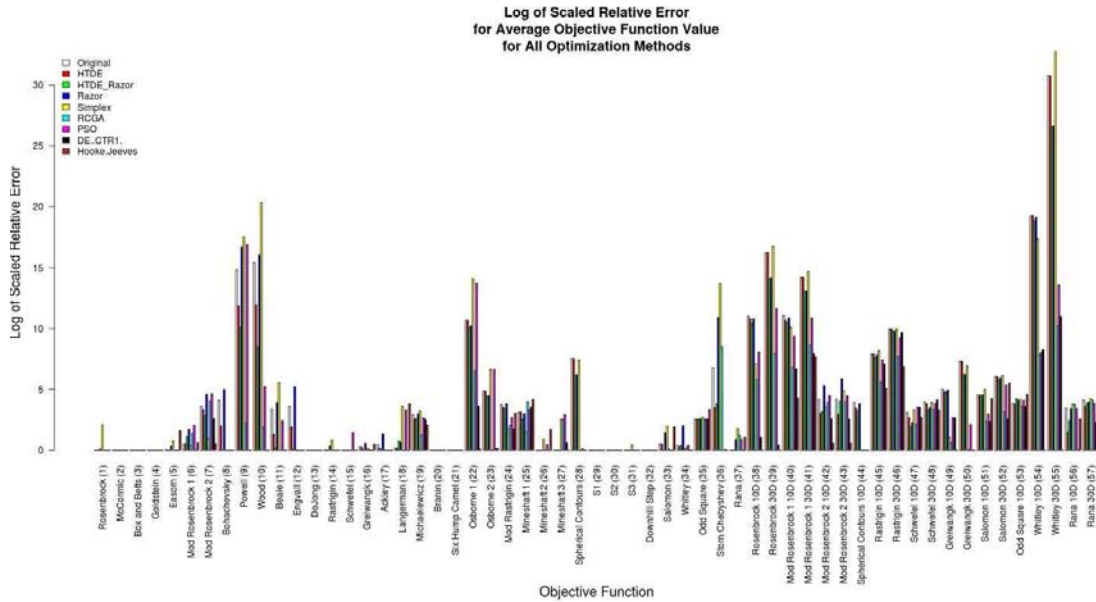


Figure 5.11: LSRE for all optimization methods across all objective functions.

next best quality in results where the algorithms work well is provided by RCGA, PSO, HTDE-SMOA, HTDER-SMOA, and the Original SMOA. Poorer performance is seen in all of these algorithms in functions of both higher dimensionality (esp. those of 30+ dimensions) and high difficulty. Time performance for Slime Mold algorithms may be a problem in comparison to other EAs. Unless context switching is having a significant effect on the time results of the various SMOAs, they appear to utilize as much as 5 to 10 times more CPU time than RCGA or PSO.

## CHAPTER VI

### VI. CONCLUSION

#### *Section 6.1 Concluding Remarks*

In the previous chapters, Slime Mold was taken from biology to simulation to an optimization algorithm. Review of existing Evolutionary Algorithms and Direct Search was provided as was review of the biology of *Dictyostelium discoideum* and its simulation. Educational simulation of the Slime Mold and several additional topics including Cellular Automata and Approximate Nearest Neighbors were reviewed as well. Portions of educational simulation, biological simulation, existing EAs, and existing Direct Search methods were combined to form the Slime Mold Optimization Algorithm. This algorithm was discussed in detail with special attention paid to its relation to the lifecycle of Slime Molds. The Slime Mold Optimization Algorithm was divided into states with each one being related to part of the Slime Mold lifecycle. Thereafter, variations on the algorithm's vegetative, mound, and slug states were introduced. The vegetative state modifications were based upon two Direct Search methods – Downhill Simplex and Razor Search. The modification to the mound and slug states was based upon biology and the Differential Evolution algorithm.

Using the many variations of the Slime Mold Optimization Algorithm (SMOA), results were generated. Results from each algorithm were provided for a variety of parameters including limits on objective function evaluations, various population sizes, different numbers of nearest neighbors, and various numbers of pseudopods for the Original algorithm. For Original SMOA, results improved when using more objective function evaluations, and they varied depending on the population size and number of nearest neighbors. Generally, better results were produced for more difficult objective functions with smaller population sizes (e.g. 50 or 100) and a generous number of nearest neighbors (e.g. two times the dimension of the objective function). Easier objective functions often yielded good results regardless of parameter choice. Results for objective functions with many dimensions were poor, though they improved as the limit on evaluations was increased. When comparing the Original algorithm to RCGA, PSO, and DE, results from RCGA and PSO were similar to those of the Original SMOA, whereas DE yielded much better results. Unfortunately, the SMOA seems to have much greater time requirements than DE, RCGA, or PSO. It is expected that further refinement of the Original SMOA to include a slug state that always uses the global best as a pacemaker will improve results.

Results from the variants of the SMOA were quite interesting. Overall, adding the DE+Followers (HTDE) strategy for the Slug State improvement over the Original algorithm as did the SMOA using the Downhill Simplex for the Vegetative State (Simplex SMOA). The Simplex SMOA, did however, perform quite poorly on some of the easier objective functions, such as Rosenbrock's function. The Razor Search for the Vegetative State (Razor SMOA) provided about the same level of performance as the Original SMOA; however, when combined with DE+Followers (referred to as HTDER-SMOA), significant improvements were seen. All of these algorithms were quite costly in terms of CPU usage, but they did provide similar, and sometimes better in the case of HTDER-SMOA and Simplex SMOA, performance to PSO and RCGA.

## ***Section 6.2 Future Work***

### *Section 6.2.1 Further Variants on the Vegetative State*

Many further variations on the vegetative state, aside from those presented in Chapter 4, are possible. The current vegetative and aggregative state equations are similar to the work of Erban and Othmer [2007]. The discretization of their functions suggests a function similar to the Particle Swarm Optimization functions with a random component to allow for incorrect movements, which is currently implemented in the Slime Mold Optimization Algorithm. A more interesting modification to the algorithm would be to replace the equations and data structure of the vegetative and aggregative states with a structure similar to that of the Glazier and Graner model [1993]. To implement this model multiple data points would be used to represent a single amoeba. The structure used should be similar to that used in the Downhill Simplex, but it would be slightly flexible in size and contain more data points to ensure such flexibility. Knowing that the Nelder-Mead Simplex is prone to collapse, the volume of this new data structure must be loosely conserved and the structure must retain data points in all dimensions of the search space, i.e. there must exist a set of coordinates within the data structure that span the entire search space [Torczon 1989]. Movement of this structure should follow that shown in Figure 2.4, where several data points would protrude from the main structure to search in a preferred direction. Were that direction an improvement in the structure's favor, the points would be moved in said direction with the rest of the structure to follow. Movements in flat directions or in a worse direction would follow an annealing schedule. Once implemented, an analysis of this structure will be needed. It should be evaluated alone, as a population, and finally as part of the Slime Mold Optimization Algorithm in the vegetative and aggregative states. Additionally, comparisons between the original algorithm and the modified one will be necessary.

### *Section 6.2.2: Population dynamics*

Variants of GAs and PSO algorithms often allow for the population to vary in size. Such variations are implemented through the use of operators that allow for birth and/or death of individuals [Arabas et al. 1994, Lu and Yen 2003, Yen and Lu 2003]. Birth operators for GAs vary greatly. They include simple crossover operators such as the  $\alpha$ -blend operator [Herrera 1998] and more complex ones such as the Unimodal

Normal Distribution Crossover (UNDX) and the Blend Crossover with Principal Components Analysis (BLXPCA) operators of Takahasi [2001]. Hybrid GA/PSO algorithms may also include such operators. As shown in Chapter 2, even DE includes a birth operator to create a fixed population of children [Price et al. 2005]. Recent research has shown that DE has been modified to include a dynamic population with success [Huang et al. 2006]. Death operators for population based EAs allow the population size to be reduced. Existing operators are typically two pronged. Such operators often make use of an aging operator and a likelihood function. The aging operator counts the number of time steps (iterations) for which an individual has existed in the population. After a fixed number of time steps the individual's continued existence in the population is contingent upon a likelihood function. This function is often based upon the number of iterations spent searching versus the number of updates said individual has made to its personal best or the population's global best. For many of such death operators, an individual is exempted from the likelihood function test if it is elite (i.e. the best of the population). This exemption is not necessary if an archive is used to record the best objective function values from the population [Arabas et al. 1994, Yen and Lu 2003].

Since GAs, PSO algorithms, and DE algorithms are population based and may allow for creation (procreation) and removal (aging) of individuals from the population and the Dd lifecycle includes birth and death, it follows that addition of birth and death operators to the Slime Mold Optimization Algorithm may be useful. With respect to birth operators, the Dd lifecycle allows for two different types of procreation. The first is an asexual birth referred to as binary fission or mitosis, which is the splitting of one amoeba into two. Procreation of this sort occurs after an amoeba has eaten numerous meals and becomes large enough to divide [Kessin 2001]. An algorithmic representation of this birth operator would be to allow for one amoeba to split into two after obtaining a certain number of new personal bests. The second type of Dd procreation is sexual and may be referred to as meiosis. Meiosis occurs when two Dd amoebae merge to form a macrocyst with a cellulose cell wall. This macrocyst emits cAMP much like the slug. Other amoebae are attracted to the macrocyst, and they are forced to become part of it because of their attraction to cAMP. Once a sufficient number of amoebae join the macrocyst, the contents of those cells are recombined and used to form new amoebae. Thereafter, the cellulose wall of the macrocyst bursts and new amoebae erupt out of it [Kessin 2001]. As of yet, the author has not determined an appropriate use for this construct. Amoeboid death in the slime mold optimization algorithm provides for several possibilities. The first of these is aging, which may be applied during the vegetative state after a fixed number of time steps. A likelihood function may be applied after amoebae have existed for a fixed number of time steps to determine if such amoebae should be removed from the population [Arabas et al. 1994, Monismith and Mayfield 2008]. Toward the end of the aggregative state, those amoebae that do not join a mound may be subjected to additional scrutiny for removal from the population. Additionally, before the dispersive state, Dd amoebae that are part of the tail of the slug die [Kessin 2001]. This may be implemented in the algorithm as well by forcing the 4/5 of the amoebae in the tail of the slug to be removed from the population before dispersal [Arabas et al. 1994, Kessin 2001, Monismith and Mayfield 2008]. For this portion of

future work, reasonable comparisons could be between the base algorithm, the algorithm with the improvements of Sections 4.1 and 4.2, and the above proposed changes.

### *Section 6.2.3: Theoretical Research of Slime Mold Optimization*

Several topics are of interest to the author with respect to theoretical research on Slime Mold Optimization and Evolutionary Algorithms in general. These topics are, however, only of interest as future research and not as part of the dissertation research. The first of these topics is research on the convergence of the Slime Mold Optimization Algorithm. It may prove interesting to investigate if the algorithm meets the criteria necessary to allow for convergence in an Evolutionary Algorithm and then to see if convergence may be proven outright or if it is objective function specific like DE [Rudolph 1996, Zaharie 2002]. Similarly, a study of the relationships between different evolutionary algorithms could be quite interesting. Particle Swarm Optimization and Differential Evolution share many similarities. Additionally, PSO and estimation theory share similarities. We would like to answer two questions in regards to the previous statements. Is DE a generalization of PSO and is PSO a special case of the estimation theory component referred to as a particle filter? Once answers to these questions are available, we would like to address them to the Slime Mold Optimization Algorithm to determine if the algorithm is unique or simply a specialization or generalization of another algorithm.



## REFERENCES

- [Abramowitz and Stegun 1972] M. Abramowitz, M. and I. A. Stegun, *Handbook of Mathematical Functions with Formulas, Graphs, and Mathematical Tables*, 9th printing, Dover Publications, New York, NY, 1972.
- [Arabas et al. 1994] J. Arabas, Z. Michalewicz, and J. Mulawka, "GAVaPS—a Genetic Algorithm with Varying Population Size", *IEEE World Congress on Computational Intelligence*, Vol. 1, pp. 73–78, June 27–29, 1994.
- [Arya et al. 1998] S. Arya, D. M. Mount, N. S. Netanyahu, R. Silverman, and A. Wu, "An Optimal Algorithm for Approximate Nearest Neighbor Searching in Fixed Dimensions", *Journal of the ACM*, Vol. 45, pp. 891-923, 1998.
- [Auer and Norris 2001] K. Auer and T. Norris, "ArrierosAlife—a Multi-Agent Approach Simulating the Evolution of a Social System: Modeling the Emergence of Social Networks with "Ascape", *Journal of Artificial Societies and Social Simulation*, Vol. 4, No. 1, January 31, 2001. URL: <http://jasss.soc.surrey.ac.uk/4/1/6.html>, date created: January 31, 2001, date accessed: October 11, 2007.
- [Bandler and MacDonald 1969] J. W. Bandler and P. A. MacDonald, "Optimization of Microwave Networks by Razor Search", *IEEE Transactions on Microwave Theory and Techniques*, Vol. MTT-17, No. 8, pp. 552–563, August 1969.
- [Bell and Pike 1966] M. Bell and M. Pike, "Remark on Algorithm 178: Direct Search", *Communications of the ACM*, Vol. 9, No. 9, p. 684, September 1966.
- [Brown and Strassman 2009] D. Brown and J. Strassman, *The Lifecycles of Dictyostelium discoideum*, URL: <http://www.dictybase.org/Multimedia/DdLifecycles/index.html>, date accessed: March 2009.
- [Chen 1997] D. Chen, *Comparisons Among Stochastic Optimization Algorithms*, Master's Thesis, Oklahoma State University, OK, 1997.
- [Choi and Mayfield 2009] S. Choi and B. E. Mayfield, "Particle Swarm Optimization in the Presence of Multiple Global Optima", *Proceedings of the 11<sup>th</sup> Annual Conference on Genetic and Evolutionary Computation (GECCO '09)*, Montreal, Québec, Canada, 2009.



- [Clerc and Kennedy 2002] M. Clerc and J. Kennedy, "The Particle Swarm – Explosion, Stability, and Convergence in a Multidimensional Complex Space," *IEEE Trans. on Evolutionary Computation*, Vol. 6, No. 1, Feb. 2002.
- [Coello Coello and Lechuga 2002] C. A. Coello Coello and M. S. Lechuga, "MOPSO: a proposal for multiple objective particle swarm optimization," *Proceedings of the 2002 Congress on Evolutionary Computation*, Vol. 2, pp. 1051 – 1056, 12-17 May 2002.
- [Corne et al. 1999] D. Corne, M. Dorigo, and F. Glover, *New Ideas in Optimization*, McGraw-Hill, London, 1999.
- [Dallon and Othmer 1997] J. C. Dallon and H. G. Othmer, "A Discrete Cell Model with Adaptive Signaling for Aggregation of *Dictyostelium discoideum*," *Phil. Trans. R. Soc. London B*, Vol. 352, pp. 391-417, 1997.
- [Deb 2001] K. Deb, *Multi-Objective Optimization using Evolutionary Algorithms*, John Wiley & Sons, Ltd., West Sussex, England, 2001.
- [Dorigo and Stützle 2004] M. Dorigo and T. Stützle, *Ant Colony Optimization*, Massachusetts Institute of Technology Press, Cambridge, MS, 2004.
- [Erban and Othmer 2007] R. Erban and H. G. Othmer, "Taxis Equations for Amoeboid Cells," *Journal of Mathematical Biology*, Vol. 54, pp. 847 – 885, 2007.
- [GEATbx 2007] GEATbx: Examples of Objective Functions, URL: [http://www.geatbx.com/docu/fcnindex-01.html#P86\\_3059](http://www.geatbx.com/docu/fcnindex-01.html#P86_3059), date created: unknown, date accessed: June 2007.
- [Glazier and Graner 1993] J. A. Glazier and F. Graner, "Simulation of the Differential Adhesion Driven Rearrangement of Biological Cells," *Physical Review E*, Vol. 47, No. 3, pp. 2128 – 2154, Mar. 1993.
- [Goldberg 1989] D. Goldberg, *Genetic Algorithms in Search, Optimization, and Machine Learning*, Addison-Wesley, Reading, MA, 1989.
- [Grimson and Blanton 2009] M. Grimson and R. Blanton, *Colorized Light Micrograph: Section Through Developing Culminant, Color Background*, URL: <http://www.dictybase.org/Multimedia/LarryBlanton/culm1.html>, date accessed: March 2009.
- [Herrera et al. 1998] F. Herrera, M. Lozano, and J. L. Verdegay, "Tackling Real-Coded Genetic Algorithms: Operators and Tools for Behavioral Analysis," *Artificial Intelligence Review*, Vol. 12, pp. 265 – 319, 1998.
- [High 2005] K. High, *Class Notes – Optimization Applications*, Oklahoma State University, Stillwater, OK, 2005.

- [Hooke and Jeeves 1961] R. Hooke and T. A. Jeeves, "Direct Search" Solution of Numerical and Statistical Problems, *Journal of the Association for Computing Machinery*, Vol. 8, No. 2, pp. 212–229, April 1961.
- [Huang et al. 2006] F. Huang, L. Wang, B. Liu, "Improved Differential Evolution with Dynamic Population Size", *Intelligent Computing*, Vol. 4113, pp. 725–730, Springer-Verlag, Berlin, 2006.
- [Ilachinski 2001] A. Ilachinski, *Cellular Automata: A Discrete Universe*, World Scientific Publishing Co., Singapore, 2001.
- [Janson and Middendorf 2005] S. Janson and M. Middendorf, "A Hierarchical Particle Swarm Optimizer and Its Adaptive Variant", *IEEE Transactions on Systems, Man, and Cybernetics-Part B: Cybernetics*, Vol. 35, No. 6, pp. 1272–1282, 2005.
- [Kennedy and Eberhart 1995] J. Kennedy and R. Eberhart, "Particle Swarm Optimization", *Proc. of the IEEE Int. Conf. on Neural Networks*, Vol. 4, pp. 1942–1948, Nov. 1995.
- [Kessin 2001] R. H. Kessin, *Dictyostelium: Evolution, Cell Biology, and the Development of Multicellularity*, Cambridge University Press, Cambridge, UK, 2001.
- [Kita et al. 1999] H. Kita, I. Ono, S. Kobayashi, "Multi-parental extension of the unimodal normal distribution crossover for real-coded genetic algorithms", *Proceedings of the 1999 Congress on Evolutionary Computation*, Vol. 2, 1999, pp. 1581–1588.
- [Lu and Yen 2003] H. Lu and G. Yen, "Rank-density-based multiobjective genetic algorithm and benchmark test function study", *IEEE Transactions on Evolutionary Computation*, Vol. 7, No. 4, pp. 325–343, 2003.
- [Madsen 2008] K. Madsen, Test problems for global optimization, June 2008, URL: [http://www2.imm.dtu.dk/~km/Test\\_ex\\_forms/test\\_ex.html](http://www2.imm.dtu.dk/~km/Test_ex_forms/test_ex.html)
- [Marée and Hogeweg 2001] A. F. M. Marée and P. Hogeweg, "How Amoeboids Self-Organize into a Fruiting Body: Multicellular Coordination in *Dictyostelium discoideum*", *Proceedings of the National Academy of Sciences*, Vol. 98, No. 7, pp. 3879–3883, March 27, 2001, URL: <http://www.pnas.org/cgi/content/abstract/98/7/3879>, date created: March 2001, date accessed, October 10, 2007.
- [Marée et al. 1999 "Migration"] A. F. M. Marée, A. V. Panfilov, and P. Hogeweg, "Migration and Thermotaxis of *Dictyostelium discoideum* Slugs, a model study", *Journal of Theoretical Biology*, Vol. 199, pp. 297–309, 1999.

- [Marée et al. 1999] □Phototaxis□ A. F. M. Marée, A. V. Panfilov, and P. Hogeweg, □Phototaxis during the slug stage of *Dictyostelium discoideum*: a model study□ *Proceedings of the Royal Society of London B*, Vol. 266, pp. 1351-1360, 1999.
- [Matthews 2002] J. Matthews, □Slime Mold Simulation □Java Applet□ URL: <http://www.generation5.org/content/2002/slimejava.asp>, date created: September 15, 2002, date accessed: October 10, 2007.
- [Mitchell 1998] M. Mitchell, *An Introduction to Genetic Algorithms*, MIT Press, Cambridge, MA, 1998.
- [Monismith and Mayfield 2008] D. R. Monismith Jr. and B. E. Mayfield, Slime Mold as a Model for Numerical Optimization, *IEEE Swarm Intelligence Symposium*, St. Louis, MO, September 21 □23, 2008.
- [Mount and Arya 2006] D. M. Mount and S. Arya, □ANN: A Library for Approximate Nearest Neighbor Searching□ University of Maryland, URL: <http://www.cs.umd.edu/~mount/ANN/>, date created: Aug 4, 2006, date accessed: Nov. 6, 2007.
- [Nakagaki et al. 2000] T. Nakagaki, H. Yamada, and A. Toth, □Maze-solving by an amoeboid organism□ *Nature*, Vol. 407, pp. 470, Sept. 28, 2000.
- [Passino 2005] K. M. Passino, *Biomimicry for Optimization, Control, and Automation*, London: Springer-Verlag, 2005.
- [Pollitt et al. 2006] A. Y. Pollitt, S. L. Blagg, N. Ibarra, and R. H. Insall, □Cell motility and SCAR localization in axenically growing *Dictyostelium* cells□ *European Journal of Cell Biology*, Vol. 85, pp. 1091 □1098, 2006.
- [Price et al. 2005] K. Price, R. Storn, J. Lampinen, *Differential Evolution: A Practical Approach to Global Optimization*, Springer-Verlag, Heidelberg, Germany, 2005.
- [Resnick 1994] M. Resnick, *Turtles, Termites, and Traffic Jams: Explorations in Massively Parallel Microworlds*, Massachusetts Institute of Technology Press, 1994.
- [Reynolds 1987] C. W. Reynolds, □Flocks, herds and schools: a distributed behavioral model□ *Computer Graphics*, Vol. 21, No. 4, pp. 25 □34, 1987.
- [Rothermich 2002] J. A. Rothermich, *From Multicellularity to Cell Based Optimization*, Master's Thesis, The University of Birmingham, Edgbaston, Birmingham, UK, September 2002.
- [Rudolph 1996] G. Rudolph, □Convergence of Evolutionary Algorithms in General Search Spaces□ *Proceedings of the IEEE International Conference on Evolutionary Computation*, pp. 50 □54, 1996.

[Savill and Hogeweg 1997] N. J. Savill and J. Hogeweg, "Modeling Morphogenesis: From Single Cells to Crawling Slugs" *Journal of Theoretical Biology*, Vol. 184, pp. 229-235, 1997.

[Segel 2001] L. A. Segel, "Computing an organism" *Proceedings of the National Academy of Sciences of the United States of America*, Vol. 98, pp. 3639-3640, March 27, 2001.

[Spendley et al. 1962] W. Spendley, G. R. Hext, and F. R. Himsworth, "Sequential Application of Simplex Designs in Optimization and Evolutionary Operation" *Technometrics*, Vol. 4, pp. 441-461, 1962.

[Takahashi and Kita 2001] M. Takahashi and H. Kita, "A Crossover Operator Using Independent Component Analysis for Real-Coded Genetic Algorithms" *Proceedings of the Congress on Evolutionary Computation*, pp. 643-649, 2001.

[Tang et al. 2008] Tang, L., Franca-Koh, J., Xiong, Y., Chen, M. Y., Long, Y., Bickford, R. M., Knecht, D. A., Iglesias, P. A., Devreotes, P. N. "Irsun, the *Dictyostelium* homolog of the Fused kinase, is required for polarization and chemotaxis" *Genes Dev* Vol. 22, pp. 2278-2290, 2008.

[Torczon 1989] V. J. Torczon, *Multi-Directional Search: A Direct Search Algorithm for Parallel Machines*, Ph. D. Thesis, Rice University, Houston, TX, May, 1989.

[Tsutsui et al. 1999] S. Tsutsui, M. Yamamura, T. Higuchi, "Multi-parent Recombination with Simplex Crossover in Real Coded Genetic Algorithms," *Proceedings of the 1999 Genetic and Evolutionary Computation Conference (GECCO-99)*, 1999, pp. 657-664.

[Yen and Lu 2003] "DMOEA" G. Yen and H. Lu, "Dynamic multiobjective evolutionary algorithm: adaptive cell-based rank and density estimation" *IEEE Transactions on Evolutionary Computation*, Vol. 7, pp. 253-274, June 2003.

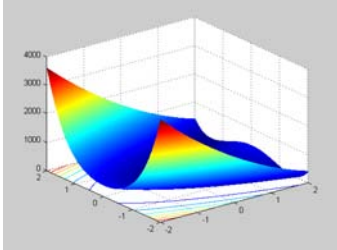
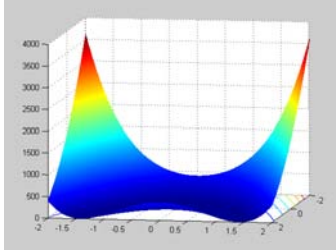
[Zaharie 2002] D. Zaharie, Critical Values for the Control Parameters of Differential Evolution Algorithms, *Proceedings of Mendel 2002, 8th International Conference on Soft Computing*, pp. 62-67, Brno, Czech Republic, 2002.

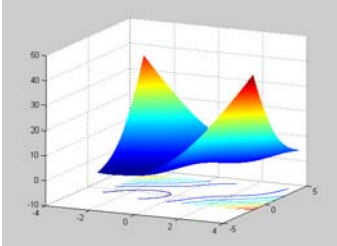
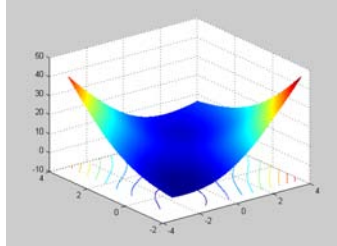
[Zimmerman and Siegert 1998] T. Zimmermann and F. Siegert, "Dictyostelium" *Homepage ZI - Munich*, Zoological Institute of Munich, Munich, Germany, URL: <http://www.zi.biologie.uni-muenchen.de/zoologie/dicty/dicty.html>, date created: January 1998, date accessed: October 10, 2007.

## APPENDICES

## APPENDIX A: OBJECTIVE FUNCTION APPENDIX

The Razor Search Algorithm, Real-Coded Genetic Algorithm, Particle Swarm Algorithm, Differential Evolution Algorithm, and Slime Mold Optimization Algorithm will be tested on a suite of 36 functions. These functions test different limitations of optimization algorithms. Some of the functions listed below contain plateaus, narrow valleys/peaks, and multiple local minima. Some functions lack derivatives, gradients, or Hessians especially near or at a global minimum. Some contain multiple global minima. Finally, some functions include a disproportionately large search area.

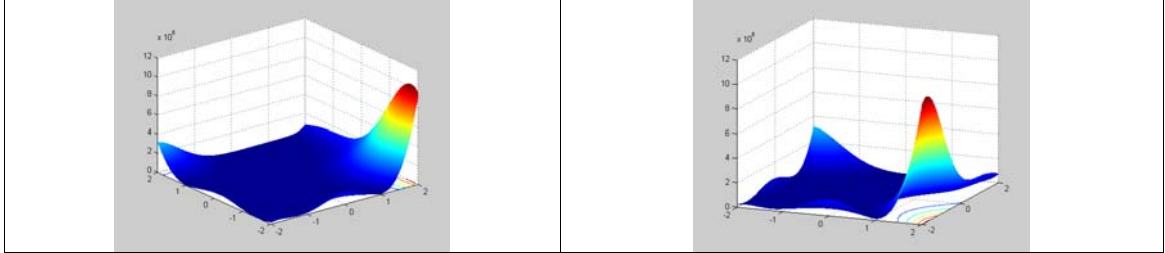
1. Generalized Rosenbrock's Function [Price et al. 2005]	
Objective Function	$f(\mathbf{x}) = \sum_{i=1}^{D-1} (100 \cdot (x_{i+1} - x_i^2)^2 + (x_i - 1)^2)$
Feasible Region	$-30 \leq x_i \leq 30$
Global Minima	$f(1, \dots, 1) = 0$
Number of Global Minima	1
Function Images	
	

2. McCormic's Function [Madsen 2008]	
Objective Function	$f(x) = \sin(x_1 + x_2) + (x_1 - x_2)^2 - 1.5x_1 + 2.5x_2 + 1$
Feasible Region	$-1.5 \leq x_1 \leq 4, -3 \leq x_2 \leq 4$
Global Minima	$f(-0.54719, -1.54719) = -1.9133$
Number of Global Minima	1
Function Images	
	

3. Box and Betts Exponential Quadratic Sum Function [Madsen 2008]	
Objective Function	$f(x) = \sum_{i=1}^{10} g(x)^2$ $g(x) = \exp(-0.1i \cdot x_i) - \exp(-0.1i \cdot x_i) - x_3 \cdot (\exp(-0.1i) - \exp(-i))$
Feasible Region	$0.9 \leq x_1, x_3 \leq 1.2, 9 \leq x_2 \leq 11.2$
Global Minima	$f(1,10,1) = 0$
Number of Global Minima	1
No function images are provided because its graph would be 4-dimensional.	

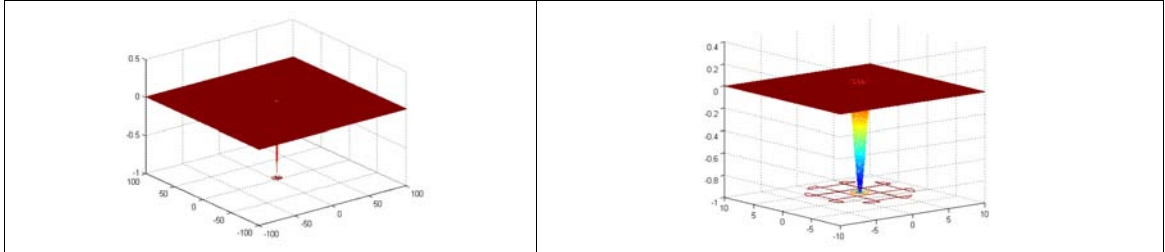
4. Goldstein and Price Function [GEATbx 2007]	
Objective Function	$f(x) = [1 + (x_1 + x_2 + 1)^2 \cdot (19 - 14x_1 + 3x_1^2 - 14x_2 + 6 \cdot x_1 \cdot x_2 + 3x_2^2)] \cdot$ $[30 + (2x_1 - 3x_2)^2 \cdot (18 - 32x_1 + 12x_1^2 + 48x_2 - 36 \cdot x_1 \cdot x_2 + 27x_2^2)]$
Feasible Region	$x_1, x_2 \in [-2, 2]$
Global Minima	$f(0, -1) = 3$
Number of Global Minima	1

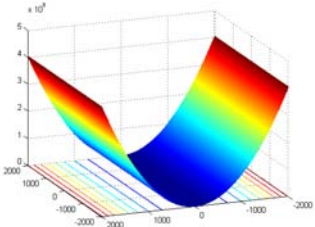
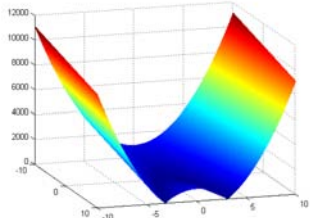
Function Images

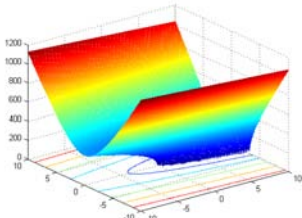
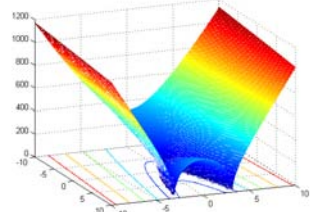


5. Easom's Function [GEATbx 2007]	
Objective Function	$f(x) = -\cos(x_1) \cdot \cos(x_2) \cdot \exp(-((x_1 - \pi)^2 + (x_2 - \pi)^2))$
Feasible Region	$-100 \leq x_1, x_2 \leq 100$
Global Minima	$f(\pi, \pi) = -1$
Number of Global Minima	1

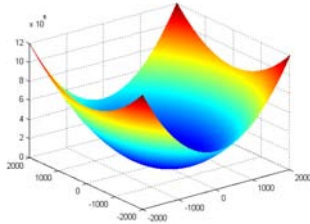
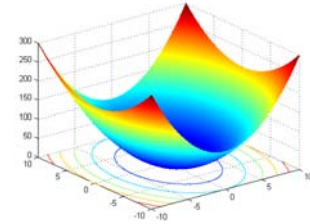
Function Images



6. Generalized Modified Rosenbrock's Function 1 [Chen 1997] Flat Ground Bent Knife Edge Function	
Objective Function	$f(x) = \sum_{i=1}^D (100 \cdot  x_{i+1} - x_i^2  + (1 - x_i)^2)$
Feasible Region	$-30 \leq x_i \leq 30$
Global Minima	$f(1, \dots, 1) = 0$
Number of Global Minima	1
Function Images	
	

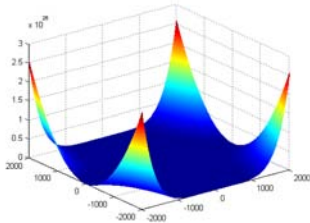
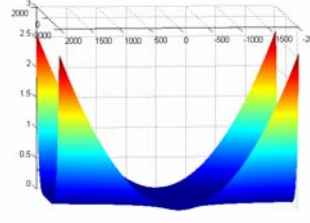
7. Generalized Modified Rosenbrock's Function 2 [Chen 1997] Hollow Ground Bent Knife Edge Function	
Objective Function	$f(x) = \sum_{i=1}^D (100 \cdot \sqrt{ x_{i+1} - x_i^2 } + (1 - x_i)^2)$
Feasible Region	$-30 \leq x_i \leq 30$
Global Minima	$f(1, \dots, 1) = 0$
Number of Global Minima	1
Function Images	
	

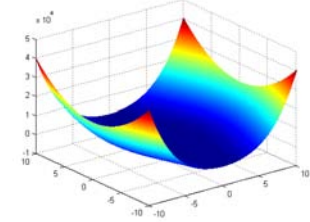
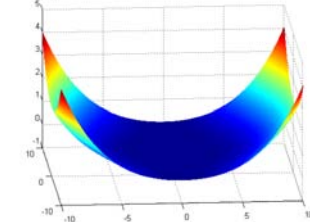


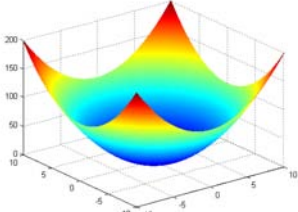
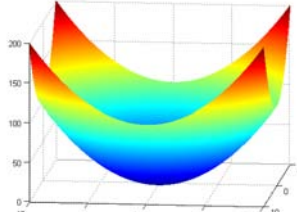
8. Bohachevsky's Function [Chen 1997]	
Objective Function	$f(x) = x_1^2 + 2x_2^2 - 0.3 \cos(3\pi x_1) - 0.4 \cos(4\pi x_2) + 0.7$
Feasible Region	$-2000 \leq x_1, x_2 \leq 2000$
Global Minima	$f(0,0) = 0$
Number of Global Minima	1
Function Images	
	

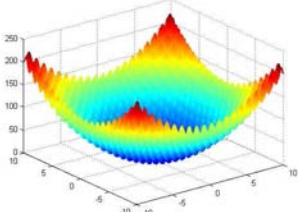
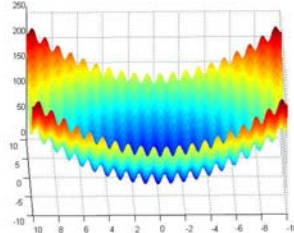
9. Powell's Function [Chen 1997]	
Objective Function	$f(x) = (x_1 + 10x_2)^2 + 5 \cdot (x_3 - x_4)^2 + (x_2 - 2x_3)^4 + 10 \cdot (x_1 - x_4)^4$
Feasible Region	$-2000 \leq x_1, x_2, x_3, x_4 \leq 2000$
Global Minima	$f(0,0,0,0) = 0$
Number of Global Minima	1
No function images are provided because its graph would be 5-dimensional.	

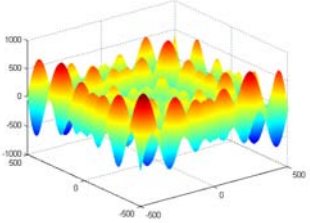
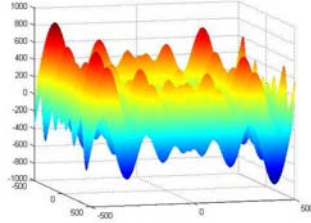
10. Wood's Function [Chen 1997]	
Objective Function	$f(x) = 100 \cdot (x_2 - x_1^2)^2 + (1 - x_1)^2 + 90 \cdot (x_4 - x_3^2)^2 + (1 - x_3)^2 + 10.1 \cdot [(x_2 - 1)^2 + (x_4 - 1)^2] + 19.8 \cdot (x_2 - 1) \cdot (x_4 - 1)$
Feasible Region	$-2000 \leq x_1, x_2, x_3, x_4 \leq 2000$
Global Minima	$f(1,1,1,1) = 0$
Number of Global Minima	1
No function images are provided because its graph would be 5-dimensional.	

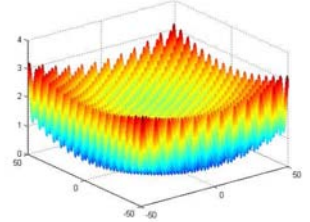
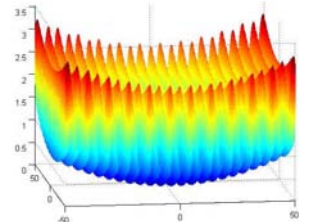
11. Beale's Function [Chen 1997]	
Objective Function	$f(x) = (1.5 - x_1 \cdot (1 - x_2))^2 + (2.25 - x_1 \cdot (1 - x_2^2))^2 + (2.625 - x_1 \cdot (1 - x_2^3))^2$
Feasible Region	$-2000 \leq x_1, x_2 \leq 2000$
Global Minima	$f(3, 0.5) = 0$
Number of Global Minima	1
Function Images	
	

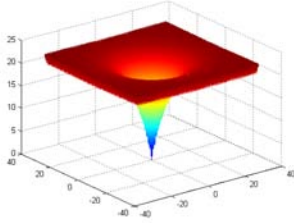
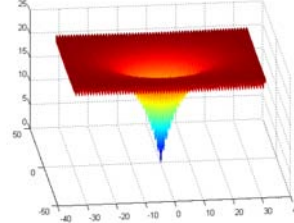
12. Engvall's Function [Chen 1997]	
Objective Function	$f(x) = x_1^4 + x_2^4 + 2x_1^2 \cdot x_2^2 - 4x_1 + 3$
Feasible Region	$-2000 \leq x_1, x_2 \leq 2000$
Global Minima	$f(1, 0) = 0$
Number of Global Minima	1
Function Images	
	

13. Generalized DeJong's (Spherical Contours) Function [Price et al. 2005]	
Objective Function	$f(x) = \sum_{i=1}^n x_i^2$
Feasible Region	$-10 \leq x_1, \dots, x_n \leq 10$
Global Minima	$f(0, \dots, 0) = 0$
Number of Global Minima	1
Function Images	
	

14. Generalized Rastrigin's Function [Price et al. 2005]	
Objective Function	$f(\mathbf{x}) = 10n + \sum_{i=1}^n (x_i^2 - 10 \cos(2\pi x_i))$
Feasible Region	$-10 \leq x_1, \dots, x_n \leq 10$
Global Minima	$f(0, \dots, 0) = 0$
Number of Global Minima	1
Function Images	
	

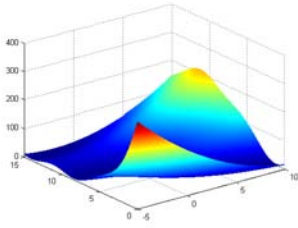
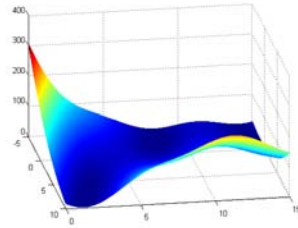
15. Generalized Schwefel's Function [Price et al. 2005]	
Objective Function	$f(\mathbf{x}) = \frac{1}{n} \sum_{i=1}^n (-x_i \sin(\sqrt{x_i}))$
Feasible Region	$-500 \leq x_1, \dots, x_n \leq 500$
Global Minima	$f(-418.983, \dots, -418.983) = 420.968746$
Number of Global Minima	1
Function Images	
	

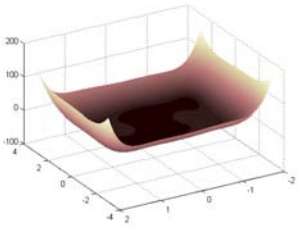
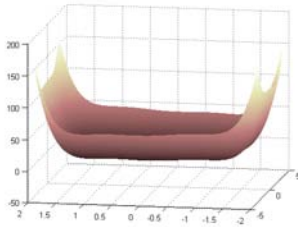
16. Griewangk's Function [GEATbx 2007]	
Objective Function	$f(x) = \sum_{i=1}^n \frac{x_i^2}{4000} - \prod_{i=1}^n \cos\left(\frac{x_i}{\sqrt{i}}\right) + 1$
Feasible Region	$-600 \leq x_i \leq 600$
Global Minima	$f(0, \dots, 0) = 0$
Number of Global Minima	1
Function Images	
	

17. Ackley's Path Function [GEATbx 2007]	
Objective Function	$f(x) = -20 \exp \left( -0.2 \sqrt{\frac{1}{n} \sum_{i=1}^n x_i^2} \right) - \exp \left( \frac{1}{n} \sum_{i=1}^n \cos(2\pi x_i) \right) + 20 + e$ $n = 2$
Feasible Region	$-32.768 \leq x_1, x_2 \leq 32.768$
Global Minima	$f(0,0) = 0$
Number of Global Minima	1
Function Images	
	

18. Modified Langermann's Function based on [Chen 1997]	
Objective Function	$f(x) = -\sum_{i=1}^m \left( c_i \cdot \exp \left( -\frac{1}{\pi} \sum_{j=1}^n (x_i - A_{i,j})^2 \right) \cdot \cos \left( \pi \sum_{j=1}^n (x_i - A_{i,j})^2 \right) \right)$ $m = 5, n = 5$ $A \text{ and } c \text{ are provided in [Chen 1997].}$
Feasible Region	$-10 \leq x_1, \dots, x_m \leq 10$
Global Minima	$f(???) = -1.5$ (assumed minimum)
Number of Global Minima	1
No function images are provided because its graph would be 6-dimensional.	

19. Michalewicz's Function [GEATbx 2007]	
Objective Function	$f(x) = -\sum_{i=1}^n \left( \sin(x_i) \cdot \sin \left( i \cdot x_i^{\frac{2}{m}} \right) \right)^{2m}$ $n, m = 10$
Feasible Region	$0 \leq x_1, \dots, x_{10} \leq \pi$
Global Minima	$f(???) = -9.66$
Number of Global Minima	1
No function images are provided because its graph would be 11-dimensional.	

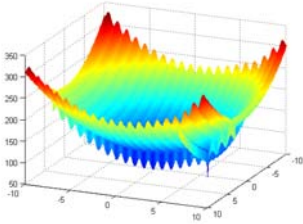
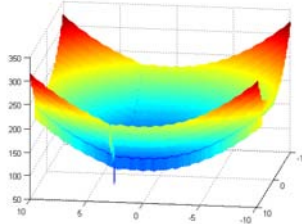
20. Branin's rcos Function [GEATbx 2007]	
Objective Function	$f(x) = a(x_2 - bx_1^2 + cx_1 - d)^2 + e(1 - f)\cos(x_1) + e$ $a = 1, b = \frac{5.1}{4\pi^2}, c = \frac{5}{\pi}, d = 6, e = 10, f = \frac{1}{8\pi}$
Feasible Region	$-5 \leq x_1 \leq 10, 0 \leq x_2 \leq 15$
Global Minima	$f(-\pi, 12.275) = 0.397887$ $f(\pi, 2.275) = 0.397887$ $f(9.42478, 2.475) = 0.397887$
Number of Global Minima	3
Function Images	
	

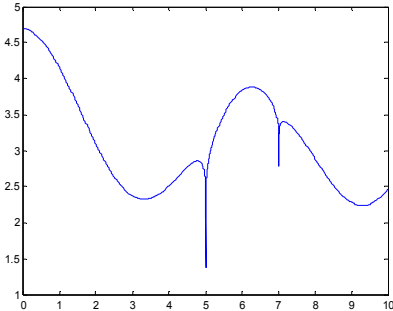
21. Six Hump Camel Back Function [GEATbx 2007]	
Objective Function	$f(x) = (4 - 2.1x_1^2 + \frac{x_1^4}{3})x_1^2 + x_1x_2 + (-4 + 4x_2^2)x_2^2$
Feasible Region	$-3 \leq x_1 \leq 3, -2 \leq x_2 \leq 2$
Global Minima	$f(-0.0898, 0.7126) = -1.0316$ $f(0.0898, -0.7126) = -1.0316$
Number of Global Minima	2
Function Images	
	

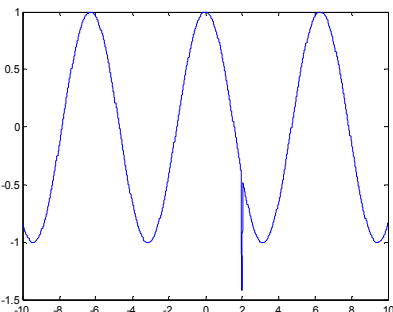
22. Osborne's Function 1 [Chen 1997]	
Objective Function	$f(x) = \sum_{i=1}^{33} ((x_1 + x_2 \exp(-x_4 t_i) + x_3 \exp(-x_5 t_i)) - y_i)^2$ $t = 10(i - 1)$ <p>Values for y are provided in [Chen 1997].</p>
Feasible Region	$0 \leq x_1, x_2, x_4, x_5 \leq 3, -3 \leq x_3 \leq 0$
Global Minima	$f(0.3753, 1.9358, -1.4647, 0.01287, 0.02212) = 5.46e - 5$
Number of Global Minima	1

No function images are provided because its graph would be 6-dimensional.

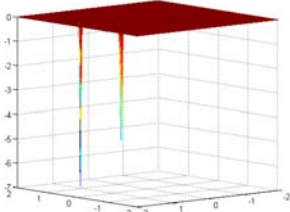
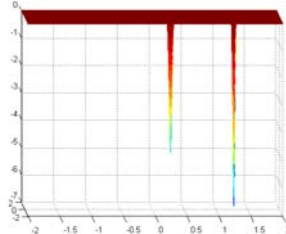
23. Osborne's Function 2 [Chen 1997]	
Objective Function	$f(x) = \sum_{i=1}^{65} (x_1 \exp(-x_5 t_i) + x_2 \exp(-x_6 (t_i - x_9)^2) + x_3 \exp(-x_7 (t_i - x_{10})^2) + x_4 \exp(-x_8 (t_i - x_{11})^2)) - y_i)^2$ $t = 10(i - 1)$ <p>Values for y are provided in [Chen 1997].</p>
Feasible Region	$0 \leq x_1, \dots, x_6, x_9 \leq 3, 0 \leq x_7 \leq 5,$ $4 \leq x_8 \leq 7, 2 \leq x_{10} \leq 5, 3 \leq x_{11} \leq 6$
Global Minima	$f(1.3100, 0.4315, 0.6336, 0.5993, 0.7539,$ $0.9056, 1.3651, 4.8248, 2.3988, 4.5689,$ $5.6754) = 0.0402$
Number of Global Minima	1
No function images are provided because its graph would be 12-dimensional.	

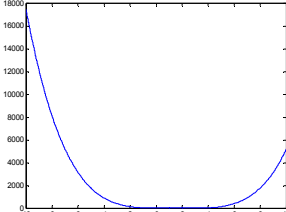
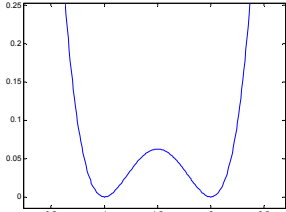
24. Modified Rastrigin's Function Based upon Rastrigin's Function from [Price et al. 2005].	
Objective Function	$f(x) = 20 + x_1^2 + x_2^2 - 10(\cos(2\pi x_1) + \cos(2\pi x_2)) + 40((7 - x_1)^{\frac{2}{15}} + (3 - x_2)^{\frac{2}{35}})$
Feasible Region	$-10 \leq x_1, x_2 \leq 10$
Global Minima	$f(0.9978, 3) = 60.79317$
Number of Global Minima	1
Function Images	
	

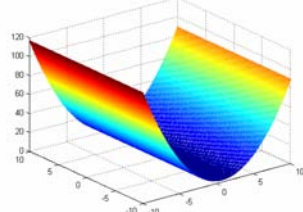
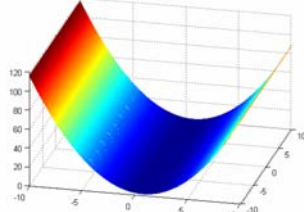
25. Mineshaft Function 1 [Monismith and Mayfield 2008]	
Objective Function	$f(x) = \cos(x) + (7-x)^{\frac{2}{15}} + 2(5-x)^{\frac{4}{35}}$
Feasible Region	$0 \leq x \leq 10$
Global Minima	$f(5) = 1.3805$
Number of Global Minima	1
Function Image	
	

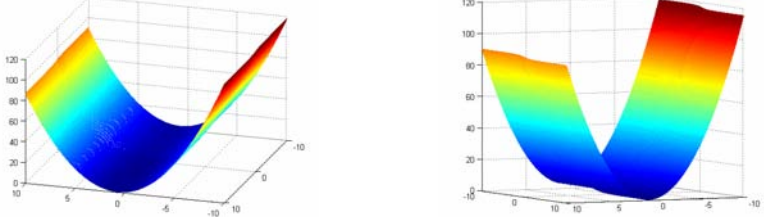
26. Mineshaft Function 2 [Monismith and Mayfield 2008]	
Objective Function	$f(x) = \cos(x) - e^{-1000(x-2)^2}$
Feasible Region	$-10 \leq x_1, x_2 \leq 10$
Global Minima	$f(2.000454648) = -1.41635352$
Number of Global Minima	1
Function Image	
	

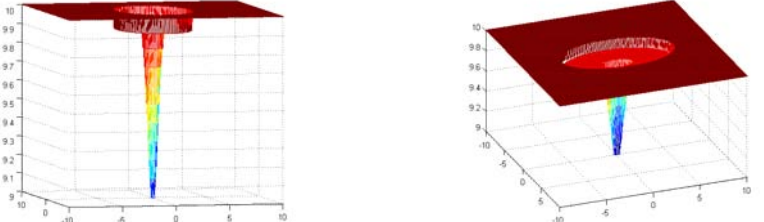


27. Mineshaft Function 3 [Monismith and Mayfield 2008]	
Objective Function	$f(x) = -5 \cdot e^{-1000(x_1-0.5)^2-1000(x_2-0.3)^2} - 7 \cdot e^{-2000(x_1-0.8)^2-2000(x_2-1.3)^2}$
Feasible Region	$-2 \leq x_1, x_2 \leq 2$
Global Minima	$f(0.8, 1.3) = -7$
Number of Global Minima	1
Function Images	
	

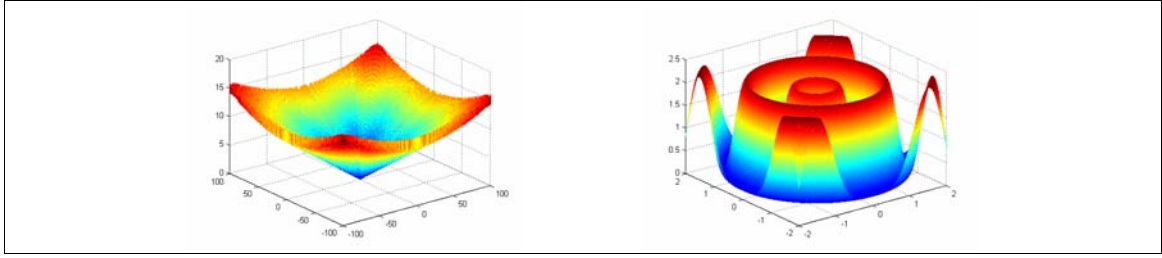
28. S1 [Choi and Mayfield 2009]	
Objective Function	$f(x) = (x-1)^2 \cdot (x-2)^2$
Feasible Region	$-10 \leq x \leq 10$
Global Minima	$f(1) = 0, f(2) = 0$
Number of Global Minima	2
	

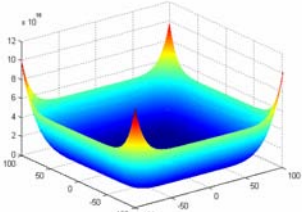
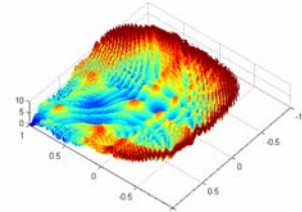
29. S2 [Choi and Mayfield 2009]	
Objective Function	$f(x_1, x_2) = 2.0 + (x_2 - 0.7)^2$
Feasible Region	$-10 \leq x_1, x_2 \leq 10$
Global Minima	$f(x_1, 0.7) = 2.0$
Number of Global Minima	Infinite
	

30. S3 [Choi and Mayfield 2009]	
Objective Function	$f(x_1, x_2) = 2.0 + (x_2 - 0.7)^2 - \arctan(x_1)$
Feasible Region	$-10 \leq x_1, x_2 \leq 10$
Global Minima	$f(10, 0.7) = 0.5289$
Number of Global Minima	1
	

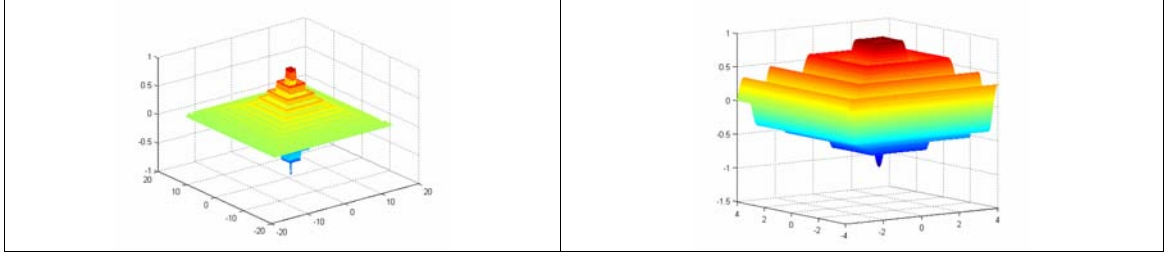
31. Downhill Step Function [Price et al. 2005]	
Objective Function	$f(x_1, x_2) = \frac{\text{floor}(10(10 - \exp(-x_1^2 - 3x_2^2)))}{10}$
Feasible Region	$-10 \leq x_1, x_2 \leq 10$
Global Minima	$f(0, 0) = 9$
Number of Global Minima	1
	

32. Salomon's Function [Price et al. 2005]	
Objective Function	$f(\mathbf{x}) = -\cos(2\pi \ \mathbf{x}\ ) + 0.1 \ \mathbf{x}\  + 1$ $\ \mathbf{x}\  = \sqrt{\sum_{j=0}^{N-1} x_j^2}$
Feasible Region	$-100 \leq x_j \leq 100$
Global Minima	$f(0, \dots, 0) = 0$
Number of Global Minima	1

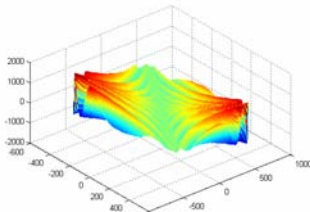
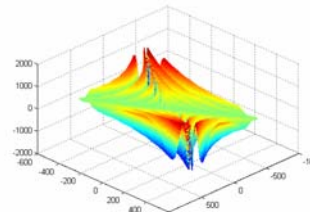


33. Whitley Function [Price et al. 2005]	
Objective Function	$f(\mathbf{x}) = \sum_{k=0}^{D-1} \sum_{j=0}^{D-1} \left( \frac{y_{j,k}^2}{4000} - \cos(y_{j,k}) + 1 \right)$ $y_{j,k} = 100 \cdot (x_k - x_j^2)^2 + (1 - x_j)^2$
Feasible Region	$-100 \leq x_j \leq 100$
Global Minima	$f(1, \dots, 1) = 0$
Number of Global Minima	1
Function Images	
	

34. Odd Square Function [Price et al. 2005]	
Objective Function	$f(x) = -\exp\left(\frac{-d}{2\pi}\right) \cdot \cos(d\pi) \cdot \left(1 + \frac{0.02 \cdot h}{d + 0.01}\right)$ $d = \sqrt{D \cdot \max_j ((x_j - b_j)^2)}$ $h = \sqrt{\sum_{j=0}^{D-1} (x_j - b_j)^2}$
Feasible Region	$-5\pi \leq x_j \leq 5\pi, j = 0, 1, \dots, D-1, D \leq 20, \varepsilon = 0.01$
Global Minima	$f(\mathbf{x}^*) = -1.14383, \mathbf{x}^* = \text{many solutions near } \mathbf{b}$ $\mathbf{b} = [1.0, 1.3, 0.8, -0.4, -1.3, 1.6, -0.2, -0.6, 0.5, 1.4, 1.0, 1.3, 0.8, -0.4, -1.3, 1.6, -0.2, -0.6, 0.5, 1.4]$
Number of Global Minima	Many minima near $\mathbf{b}$
Function Images	



35. Storn-Chebyshev Function [Price et al. 2005]	
Objective Function	$f(\mathbf{x}) = p_1 + p_2 + p_3$ $p_1 = \begin{cases} (u-d)^2 & \text{if } u < d \\ 0 & \text{otherwise} \end{cases}, \quad u = \sum_{j=0}^{D-1} x_j \cdot (1.2)^{D-1-j},$ $p_2 = \begin{cases} (v-d)^2 & \text{if } v < d \\ 0 & \text{otherwise} \end{cases}, \quad v = \sum_{j=0}^{D-1} x_j \cdot (-1.2)^{D-1-j},$ $p_k = \begin{cases} (w_k-1)^2 & \text{if } w_k > 1 \\ (w_k+1)^2 & \text{if } w_k < -1 \\ 0 & \text{otherwise} \end{cases}, \quad w_k = \sum_{j=0}^{D-1} x_j \cdot \left(\frac{2k}{m}-1\right)^{D-1-j},$ $p_3 = \sum_{k=0}^m p_k, \quad k = 0, 1, \dots, m, \quad m = 32 \cdot D,$ $d = T_{D-1}(1.2) \approx \begin{cases} 72.661 & \text{for } D = 9 \\ 10558.145 & \text{for } D = 17 \end{cases}$ $T_{D+1}(z) = 2z \cdot T_D(z) - T_{D-1}(z), \quad D > 0 \text{ and odd,}$ $T_0(z) = 1, \quad T_1(z) = z$
Feasible Region	$-2^D \leq x_j \leq 2^D, j = 0, 1, \dots, D-1, D > 1 \text{ and odd}$
Global Minima	$f(x^*) = 0$ $x^* = \begin{cases} [128, 0, -256, 0, 160, 0, -32, 0, 1] & \text{for } D = 9 \\ [32768, 0, -131072, 0, 212992, 0, -180224, \\ 0, 84480, 0, -21504, 0, 2688, 0, -128, 0, 1] & \text{for } D = 17. \end{cases}$
Number of Global Minima	1
Function Images	

36. Rana Function [Price et al. 2005]	
Objective Function	$f(\mathbf{x}) = \sum_{j=0}^{D-1} x_j \cdot \sin(\alpha) \cdot \cos(\beta) + x_{(j+1) \bmod D} \cdot \cos(\alpha) \cdot \sin(\beta),$ $\alpha = \sqrt{ x_{(j+1) \bmod D} + 1 - x_j }$ $\beta = \sqrt{ x_{(j+1) \bmod D} + 1 + x_j }$
Feasible Region	$-512 \leq x_j \leq 512$ $j = 0, 1, \dots, D-1$ $D > 1$
Global Minima	$f(\mathbf{x}^*) = -511.708,$ $x_j^* = -512$
Number of Global Minima	1
Function Images	
<div style="display: flex; justify-content: space-around; align-items: center;">   </div>	

# APPENDIX B1: SMOA AVERAGE RESULTS

	A50, N1	A50, N2	A50, N3	A50, N4	A100, N1	A100, N2	A100, N3	A100, N4	A250, N1	A250, N2	A250, N3	A250, N4	A500, N1	A500, N2	A500, N3	A500, N4	True Minima
Average Result (1M)	0.000402	0.000403	0.000402	0.000411	0.000411	0.000364	0.000411	0.000411	0.000411	0.000411	0.000411	0.000411	0.000246	0.000246	0.000246	0.000246	0
Rosenbrock (1)	-1.91322	-1.91322	-1.91322	-1.91322	-1.91322	-1.91322	-1.91322	-1.91322	-1.91322	-1.91322	-1.91322	-1.91322	-1.91322	-1.91322	-1.91322	-1.91322	-1.9133
McComic (2)	8.61E-08	8.61E-08	8.61E-08	4.08E-09	4.08E-09	3.53E-08	3.53E-08	3.53E-08	3.53E-08	3.53E-08	3.53E-08	3.53E-08	3.53E-08	3.53E-08	3.53E-08	3.53E-08	0
Box and Beits (3)	3.000012	3.000012	3.000012	3.000012	3.000012	3.000012	3.000012	3.000012	3.000012	3.000012	3.000012	3.000012	3.000012	3.000012	3.000012	3.000012	3
Goldstein (4)	-0.99928	-0.99928	-0.99928	-0.99931	-0.99931	-0.99931	-0.99931	-0.99931	-0.99931	-0.99931	-0.99931	-0.99931	-0.99931	-0.99931	-0.99931	-0.99931	-1
Easom (5)	0.027311	0.027311	0.027311	0.023993	0.023993	0.023993	0.023993	0.023993	0.023993	0.023993	0.023993	0.023993	0.023993	0.023993	0.023993	0.023993	0
Mod Rosenbrock 1 (6)	0.734808	0.734808	0.734808	0.734808	0.734808	0.734808	0.734808	0.734808	0.734808	0.734808	0.734808	0.734808	0.734808	0.734808	0.734808	0.734808	0
Mod Rosenbrock 2 (7)	0.664362	0.664362	0.664362	0.664362	0.664362	0.664362	0.664362	0.664362	0.664362	0.664362	0.664362	0.664362	0.664362	0.664362	0.664362	0.664362	0
Bohachevsky (8)	74968.98	74968.98	74968.98	66287.46	66287.46	26915.97	26915.97	26915.97	26915.97	26915.97	26915.97	26915.97	26915.97	26915.97	26915.97	26915.97	0
Powell (9)	186420.1	186420.1	186420.1	196599.2	196599.2	49440.49	49440.49	49440.49	49440.49	49440.49	49440.49	49440.49	49440.49	49440.49	49440.49	49440.49	0
Wood (10)	0.294941	0.320249	0.320249	0.294941	0.294941	0.294941	0.294941	0.294941	0.294941	0.294941	0.294941	0.294941	0.294941	0.294941	0.294941	0.294941	0
Beale (11)	0.350287	0.366319	0.350287	0.350287	0.350287	0.350287	0.350287	0.350287	0.350287	0.350287	0.350287	0.350287	0.350287	0.350287	0.350287	0.350287	0
Engvall (12)	2.28E-06	2.06E-06	2.28E-06	2.28E-06	2.28E-06	2.28E-06	2.28E-06	2.28E-06	2.28E-06	2.28E-06	2.28E-06	2.28E-06	2.28E-06	2.28E-06	2.28E-06	2.28E-06	0
DeJong (13)	0.000933	0.000802	0.000933	0.000933	0.000933	0.000933	0.000933	0.000933	0.000933	0.000933	0.000933	0.000933	0.000933	0.000933	0.000933	0.000933	0
Rastrigin (14)	-837.96	-837.959	-837.96	-837.96	-837.96	-837.96	-837.96	-837.96	-837.96	-837.96	-837.96	-837.96	-837.96	-837.96	-837.96	-837.96	0
Stiefel (15)	0.003327	0.003327	0.003327	0.003327	0.003327	0.003327	0.003327	0.003327	0.003327	0.003327	0.003327	0.003327	0.003327	0.003327	0.003327	0.003327	-837.9658
Griewangk (16)	0.015715	0.015715	0.015715	0.015715	0.015715	0.015715	0.015715	0.015715	0.015715	0.015715	0.015715	0.015715	0.015715	0.015715	0.015715	0.015715	0
Ackley (17)	-1.49631	-1.49631	-1.49631	-1.49631	-1.49631	-1.49631	-1.49631	-1.49631	-1.49631	-1.49631	-1.49631	-1.49631	-1.49631	-1.49631	-1.49631	-1.49631	0
Langerman (18)	-7.18443	-7.18443	-7.18443	-7.18443	-7.18443	-7.18443	-7.18443	-7.18443	-7.18443	-7.18443	-7.18443	-7.18443	-7.18443	-7.18443	-7.18443	-7.18443	-1.5
Michalewicz (19)	0.397891	0.397891	0.397891	0.397891	0.397891	0.397891	0.397891	0.397891	0.397891	0.397891	0.397891	0.397891	0.397891	0.397891	0.397891	0.397891	-9.66
Brannin (20)	-1.03163	-1.03163	-1.03163	-1.03163	-1.03163	-1.03163	-1.03163	-1.03163	-1.03163	-1.03163	-1.03163	-1.03163	-1.03163	-1.03163	-1.03163	-1.03163	0.397887
Six Hump Camel (21)	0.032072	0.032141	0.032072	0.032072	0.032072	0.032072	0.032072	0.032072	0.032072	0.032072	0.032072	0.032072	0.032072	0.032072	0.032072	0.032072	-1.03163
Osborne 1 (22)	0.01629	0.096655	0.01629	0.01629	0.01629	0.01629	0.01629	0.01629	0.01629	0.01629	0.01629	0.01629	0.01629	0.01629	0.01629	0.01629	0.03489
Osborne 2 (23)	82.726	82.726	82.726	82.726	82.726	82.726	82.726	82.726	82.726	82.726	82.726	82.726	82.726	82.726	82.726	82.726	58
Mod Rastrigin (24)	1.862575	1.745877	1.862575	1.862575	1.862575	1.862575	1.862575	1.862575	1.862575	1.862575	1.862575	1.862575	1.862575	1.862575	1.862575	1.862575	1.3805
Mineshaft 1 (25)	-1.41635	-1.35777	-1.41635	-1.41635	-1.41635	-1.41635	-1.41635	-1.41635	-1.41635	-1.41635	-1.41635	-1.41635	-1.41635	-1.41635	-1.41635	-1.41635	1.3805
Mineshaft 2 (26)	-6.96415	-6.93958	-6.96415	-6.96415	-6.96415	-6.96415	-6.96415	-6.96415	-6.96415	-6.96415	-6.96415	-6.96415	-6.96415	-6.96415	-6.96415	-6.96415	-1.4163535
Mineshaft 3 (27)	24.61982	25.10117	24.61982	24.61982	24.61982	24.61982	24.61982	24.61982	24.61982	24.61982	24.61982	24.61982	24.61982	24.61982	24.61982	24.61982	-7
Spherical Contours (28)	7.67E-14	0.001592	7.67E-14	7.67E-14	7.67E-14	7.67E-14	7.67E-14	7.67E-14	7.67E-14	7.67E-14	7.67E-14	7.67E-14	7.67E-14	7.67E-14	7.67E-14	7.67E-14	0
ST (29)	0.528872	0.528872	0.528872	0.528872	0.528872	0.528872	0.528872	0.528872	0.528872	0.528872	0.528872	0.528872	0.528872	0.528872	0.528872	0.528872	2
SZ (30)	0.0078	0.0078	0.0078	0.0078	0.0078	0.0078	0.0078	0.0078	0.0078	0.0078	0.0078	0.0078	0.0078	0.0078	0.0078	0.0078	9
S3 (31)	0.0078	0.0078	0.0078	0.0078	0.0078	0.0078	0.0078	0.0078	0.0078	0.0078	0.0078	0.0078	0.0078	0.0078	0.0078	0.0078	9
Downhill Step (32)	0.0078	0.0078	0.0078	0.0078	0.0078	0.0078	0.0078	0.0078	0.0078	0.0078	0.0078	0.0078	0.0078	0.0078	0.0078	0.0078	9
Salomon (33)	0.008011	0.007563	0.008011	0.008011	0.008011	0.008011	0.008011	0.008011	0.008011	0.008011	0.008011	0.008011	0.008011	0.008011	0.008011	0.008011	0
Whitley (34)	-1.00801	-1.00801	-1.00801	-1.00801	-1.00801	-1.00801	-1.00801	-1.00801	-1.00801	-1.00801	-1.00801	-1.00801	-1.00801	-1.00801	-1.00801	-1.00801	-1.4383
Odd Square (35)	17.17872	13.13723	9.98224	11.86194	24.47983	17.53931	11.44342	8.700355	16.86113	15.3333	16.39474	9.786629	15.2948	-1023.42	-1023.42	-1023.42	16.49638
Storn Chebyshev (36)	766.493	722.4747	596.8125	616.7109	741.1939	784.4724	670.7025	596.2125	745.57	798.971	782.423	688.4744	753.3015	768.6431	734.5859	693.2436	-1023.416
Rana (37)	215631.9	232480.2	114342.5	204009.4	244689.1	244689.1	135527.8	135527.8	175685.7	221299.4	165377.1	169411.9	169411.9	169411.9	22471.8	231971.3	0
Rosenbrock 10D (38)	724.2986	731.2287	626.7474	630.2497	712.1917	752.3544	692.0445	632.0441	718.5163	728.5996	689.4775	680.2817	713.0137	717.6882	722.0127	720.3334	0
Rosenbrock 30D (39)	19123.99	20040.35	14648.94	14648.94	18607.25	20184.18	15413.29	15413.29	17771.34	19241.05	17136.23	17141.65	19344.33	19201.11	19187.32	19207.04	0
Mod Rosenbrock 1	0.725363	0.68744	0.676156	0.674962	0.776318	0.764941	0.668965	0.672934	0.825972	0.758619	0.721543	0.628544	0.700211	0.712737	0.74573	0.766718	0
Mod Rosenbrock 2	0.731715	0.757984	0.652705	0.652705	0.718551	0.673812	0.689098	0.689098	0.697617	0.699729	0.733775	0.703081	0.707811	0.734572	0.682897	0.745933	0
Spherical Contours	0.573348	0.588785	0.486478	0.507552	0.567511	0.573723	0.529092	0.5223	0.57518	0.59563	0.562523	0.517418	0.541607	0.549564	0.537536	0.514582	0
Rastrigin 10D (44)	32.31205	30.98844	27.23783	27.23783	32.31205	32.31205	29.38652	26.64686	30.50488	32.49175	31.96937	27.5114	32.26534	32.45634	31.20856	29.9219	0
Rastrigin 30D (45)	256.5294	249.8531	215.3654	215.3654	249.8531	249.8531	215.3654	215.3654	235.6382	253.3823	232.7393	220.3587	250.0238	252.5157	247.4995	237.0287	0
Schwefel 10D (47)	-3208.83	-3239.22	-3127.16	-3088.67	-3229.78	-3279.87	-3207.89	-3070.77	-3176.27	-3316.88	-3252.76	-3091.07	-3227.63	-3281.36	-3290.49	-3136.39	-4189.829
Schwefel 30D (48)	-5876.36	-5950.71	-6057.5	-5953.55	-5953.55	-5953.55	-5953.55	-6004.64	-5953.92	-5976.06	-5982.65	-5942.89	-5787.05	-5927.63	-5892.16	-5892.16	-12569.487
Griewangk 10D (49)	1.509354	1.524128	1.448514	1.47859	1.512455	1.512455	1.509559	1.478292	1.494564	1.526658	1.536328	1.470864	1.51269	1.521907	1.526269	1.511917	0
Griewangk 30D (50)	19.08485	20.00746	14.85195	18.84433	20.70837	15.6535	15.6535	15.6535	17.9959	19.6212	17.07569	17.04924	20.10826	20.12751	20.18833	20.16099	0
Salomon 10D (51)	1.034537	1.04537	0.913313	0.913313	1.034537	1.034537	0.913313	0.913313	1.006648	1.006648	1.006648	0.96145	1.014156	1.005605	1.008794	0.989154	0
Salomon 30D (52)	5.10426	4.156946	4.156946	4.156946	5.10426	4.156946	4.156946	4.156946	4.723363	5.033435	4.699243	4.640203	5.002485	5.002485	4.989255	5.037555	0
Odd Square 10D (53)	-0.54328	-0.54396	-0.54328	-0.54328	-0.54328	-0.54328	-0.54328	-0.54328	-0.56674	-0.56674	-0.56674	-0.56674	-0.56674	-0.56674	-0.56674	-0.56674	-1.4383
Whitley 10D (54)	3378659	3585725	2153528	1.14E+08	3841405	4118895	3582727	2981665	3780291	3871799	4214695	2873089	3369248	3369248	3278458	3278458	0
Whitley 30D (55)	7.42E+11	8.66E+11	2.35E+11	6.09E+11	8.67E+11	2.79E+11	2.79E+11	2.79E+11	8.78E+11	5.4E+							







# APPENDIX B2: STANDARD DEVIATION FOR SMOA RESULTS

Results St. Dev. (1M)	A50, N1	A50, N2	A50, N3	A50, N4	A100, N1	A100, N2	A100, N3	A100, N4	A250, N1	A250, N2	A250, N3	A250, N4	A500, N1	A500, N2	A500, N3	A500, N4
Mod Rosenbrock (1)	0.000437	0.000384	0.000437	0.000437	0.000394	0.000394	0.000394	0.000394	0.000249	0.000123	0.000249	0.000249	0.000209	0.000209	0.000209	0.000209
McCormic (2)	2.40E-07	4.73E-08	2.40E-07	2.40E-07	9.12E-08	9.12E-08	9.12E-08	9.12E-08	1.15E-08	2.76E-09	1.45E-08	1.45E-08	4.39E-09	4.39E-09	4.39E-09	4.39E-09
Box and Betts (3)	5.54E-08	9.79E-09	1.21E-07	4.41E-08	3.29E-08	3.29E-08	3.29E-08	3.29E-08	1.65E-07	3.84E-06	1.09E-06	1.09E-06	7.50E-06	7.50E-06	7.50E-06	7.50E-06
Goldstein (4)	1.83E-05	9.55E-06	1.83E-05	1.83E-05	8.81E-06	8.81E-06	8.81E-06	8.81E-06	1.09E-06	1.87E-07	1.09E-06	1.09E-06	5.10E-07	5.10E-07	5.10E-07	5.10E-07
Easom (5)	0.000806	0.000801	0.000806	0.000806	0.000806	0.000806	0.000806	0.000806	0.000555	0.000564	0.000555	0.000555	0.000759	0.000759	0.000759	0.000759
Mod Rosenbrock 1 (6)	0.019627	0.020172	0.019627	0.019627	0.017049	0.017049	0.017049	0.017049	0.001314	0.009603	0.013314	0.013314	0.010117	0.010117	0.010117	0.010117
Mod Rosenbrock 2 (7)	0.296129	0.359734	0.296129	0.296129	0.348243	0.348243	0.348243	0.348243	0.35423	0.253084	0.350425	0.350425	0.265082	0.265082	0.265082	0.265082
Bohachevsky (8)	0.285133	0.252458	0.285133	0.285133	0.279267	0.279267	0.279267	0.279267	0.299992	0.252081	0.325081	0.325081	0.293778	0.293778	0.293778	0.293778
Powell (9)	51274	51274	46213.26	28629.98	39049.87	39049.87	39049.87	39049.87	26211.45	26211.45	35017.68	35017.68	42564.15	42564.15	36754.73	44358.76
Wood (10)	118376.1	118376.1	136333.2	39984.7	110385.9	110385.9	110385.9	108748.4	72063.37	72063.37	113672	113672	94209.75	94209.75	97168.61	138458.7
Beale (11)	0.224691	0.224691	0.224691	0.224691	0.177856	0.177856	0.177856	0.177856	0.180317	0.250809	0.176953	0.176953	0.181161	0.181161	0.181161	0.181161
Engvall (12)	0.317157	0.348493	0.317157	0.317157	0.338649	0.338649	0.338649	0.338649	0.430607	0.380675	0.430607	0.430607	0.31182	0.31182	0.31182	0.31182
DeJong (13)	2.46E-06	2.38E-06	2.46E-06	2.46E-06	2.89E-06	2.89E-06	2.89E-06	2.89E-06	5.76E-07	8.78E-08	5.76E-07	5.76E-07	3.10E-08	3.10E-08	1.83E-07	1.83E-07
Rastrigin (14)	0.001056	0.000084	0.001056	0.001056	0.000976	0.000976	0.000976	0.000976	0.000976	0.357481	0.000197	0.000197	0.003895	0.003895	0.003895	0.003895
Rastrigin (15)	0.009088	0.0013673	0.009088	0.009088	0.005981	0.005981	0.005981	0.005981	0.005349	0.007341	0.005349	0.005349	0.011325	0.009844	0.011325	0.011325
Griewangk (16)	0.002596	0.002658	0.002596	0.002596	0.002417	0.002417	0.002417	0.002417	0.002447	0.002447	0.002447	0.002447	0.002585	0.002585	0.002585	0.002585
Ackley (17)	0.009658	0.009658	0.009658	0.009658	0.009098	0.009098	0.009098	0.009098	0.008827	0.005175	0.008827	0.008827	0.007094	0.007094	0.007094	0.007094
Langerman (18)	0.001851	0.001622	0.001851	0.001851	0.001951	0.001951	0.001951	0.001951	0.002231	0.001811	0.001824	0.001824	0.002697	0.002697	0.002697	0.002697
Michalewicz (19)	0.474191	0.524754	0.474191	0.474191	0.448133	0.448133	0.448133	0.448133	0.509249	0.493068	0.434785	0.434785	0.404982	0.404982	0.404982	0.404982
Brannin (20)	3.22E-06	2.48E-06	3.22E-06	3.22E-06	2.44E-06	2.44E-06	2.44E-06	2.44E-06	6.38E-07	1.33E-07	6.38E-07	6.38E-07	1.49E-07	1.49E-07	1.49E-07	1.49E-07
Six Hump Camel (21)	3.87E-07	1.20E-07	3.87E-07	3.87E-07	1.30E-07	1.30E-07	1.30E-07	1.30E-07	1.93E-08	4.85E-09	1.93E-08	1.93E-08	9.36E-09	9.36E-09	9.36E-09	9.36E-09
Osborne 1 (22)	0.009487	0.009125	0.009487	0.009487	0.006825	0.006825	0.006825	0.006825	0.007996	0.007609	0.007996	0.007996	0.014464	0.00829	0.00829	0.00829
Osborne 2 (23)	0.001632	0.017976	0.001632	0.001632	0.015778	0.015778	0.015778	0.015778	0.021619	0.017109	0.021619	0.021619	0.018201	0.017597	0.017597	0.017597
Mod Rastrigin (24)	1.572467	1.435843	1.572467	1.572467	1.644803	1.644803	1.644803	1.644803	1.530131	3.569942	1.530131	1.530131	2.155697	2.809348	2.155697	2.155697
Mineshaft 1 (25)	0.144043	0.221727	0.144043	0.144043	0.075129	0.075129	0.075129	0.075129	0.048994	0.248315	0.045997	0.045997	0.065281	0.065281	0.065281	0.065281
Mineshaft 2 (26)	1.24E-06	0.141511	1.24E-06	1.24E-06	0.047463	0.047463	0.047463	0.047463	1.83E-09	0.150486	0.06008	0.06008	0.020859	0.161753	0.161753	0.161753
Mineshaft 3 (27)	0.140713	0.237416	0.140713	0.140713	0.009779	0.009779	0.009779	0.009779	1.83E-09	0.150486	0.06008	0.06008	0.020859	0.161753	0.161753	0.161753
Spherical Contours (28)	2.316279	2.21296	2.316279	2.316279	2.260339	2.260339	2.260339	2.260339	2.176073	2.214299	2.386694	2.386694	2.691502	3.668695	3.668695	3.668695
S1 (29)	1.88E-13	0.008996	1.88E-13	1.88E-13	1.24E-14	1.24E-14	1.24E-14	1.24E-14	8.15E-15	0.000161	8.15E-15	8.15E-15	3.41E-12	0.000478	0.000478	0.000478
S2 (30)	1.78E-11	1.04E-11	1.78E-11	1.04E-11	8.24E-12	8.24E-12	8.24E-12	8.24E-12	2.35E-12	2.58E-13	2.35E-12	2.35E-12	8.13E-13	8.13E-13	8.13E-13	8.13E-13
S3 (31)	9.22E-11	9.22E-11	9.22E-11	9.22E-11	1.60E-10	1.60E-10	1.60E-10	1.60E-10	1.46E-11	3.18E-12	1.46E-11	1.46E-11	1.26E-11	1.26E-11	1.26E-11	1.26E-11
Downhill Step (32)	0	0	0	0	0	0	0	0	0.039799	0	0.080474	0.080474	0	0.069649	0	0
Salomon (33)	0.007606	0.006057	0.007606	0.007606	0.006246	0.006246	0.006246	0.006246	0.007374	0.00676	0.007374	0.007374	0.005539	0.008213	0.005539	0.005539
Whitley (34)	0.01264	0.016101	0.01264	0.01264	0.010323	0.010323	0.010323	0.010323	0.017283	0.007378	0.017283	0.017283	0.009104	0.01586	0.009104	0.009104
Odd Square (35)	0.000312	0.000288	0.000312	0.000312	0.000255	0.000255	0.000255	0.000255	0.000207	0.000999	0.000207	0.000207	0.000156	0.09702	0.000156	0.000156
Stom Chebyshev (36)	28.23429	28.23429	17.48724	23.05748	35.47553	24.93495	22.9977	13.90026	26.60562	22.6578	24.2301	17.58457	20.73746	27.16827	27.16827	27.16827
Rana (37)	1.71E-12	1.71E-12	1.71E-12	1.71E-12	1.71E-12	1.71E-12	1.71E-12	1.71E-12	34.81094	1.71E-12	34.81094	34.81094	1.71E-12	1.71E-12	1.71E-12	1.71E-12
Rosenbrock 30D (38)	246.5233	224.1263	229.9829	220.6009	231.5705	240.9769	234.5566	202.3305	242.4529	237.388	253.4161	214.4771	227.475	242.7615	246.2663	213.9309
Rosenbrock 30D (39)	39785.29	51585.33	22228.96	22228.96	42220.61	52985.06	28159.6	28159.6	35173	41319.68	35073.88	31873.31	65249.3	47462.12	43556.92	48832.5
Mod Rosenbrock 1 10D (40)	145.373	119.141	113.2651	125.1624	130.8563	117.0223	117.7706	106.3879	127.0476	128.7352	144.6954	112.0421	131.2901	124.8997	118.8296	115.4838
Mod Rosenbrock 1 30D (41)	1665.994	1683.406	1626.561	1626.561	1728.878	1789.799	1691.59	1691.59	1759.453	1979.024	2015.454	1764.422	2302.889	2334.024	22210.516	2132.666
Mod Rosenbrock 2 10D (42)	0.31385	0.295638	0.289289	0.307031	0.362549	0.322219	0.294867	0.328345	0.326697	0.32948	0.334571	0.290418	0.319599	0.260012	0.314772	0.304611
Mod Rosenbrock 2 30D (43)	0.339468	0.307206	0.303298	0.303298	0.308544	0.275699	0.293461	0.293461	0.271014	0.296801	0.333813	0.291186	0.309105	0.306422	0.307735	0.329467
Spherical Contours 10D (44)	0.136282	0.134809	0.104814	0.12017	0.122002	0.139334	0.109729	0.127893	0.128079	0.13563	0.122283	0.119952	0.150376	0.148198	0.141052	0.143295
Rastrigin 10D (45)	4.141033	3.974505	3.921938	4.785566	4.604868	3.848777	3.650288	3.894978	3.708108	3.773467	3.773467	3.751131	4.090306	3.560041	4.142855	3.7753849
Rastrigin 30D (46)	12.16197	14.17906	11.33831	11.33831	12.67855	11.94253	12.9433	14.01134	12.49333	14.01134	10.60813	13.02565	13.44401	12.5956	9.915176	12.17534
Schwefel 10D (47)	147.1036	143.6883	261.4816	266.8263	130.1488	161.174	194.5188	232.9836	197.011	153.245	170.7773	159.3375	174.1463	169.8404	183.889	186.8393
Schwefel 30D (48)	350.5116	291.8257	343.4402	343.4402	241.9588	306.9538	364.7234	364.7234	292.9508	354.0479	326.8417	352.0194	284.7467	282.5303	305.0204	287.2805
Griewangk 10D (49)	0.140829	0.1472	0.108843	0.166442	0.118374	0.136513	0.126913	0.117344	0.114045	0.125358	0.130051	0.130643	0.111711	0.126248	0.121039	0.121039
Griewangk 30D (50)	1.757051	1.973438	1.482547	1.482547	1.786566	1.980831	1.845376	1.845376	1.625829	1.838516	1.793245	1.632179	1.761672	1.924008	1.965992	1.763186
Salomon 10D (51)	0.142015	0.117095	0.121526	0.112759	0.128949	0.121364	0.107272	0.107272	0.121296	0.138578	0.132315	0.109014	0.123248	0.134343	0.118612	0.131405
Salomon 30D (52)	0.269172	0.273527	0.23604	0.23604	0.271615	0.282089	0.22359	0.22359	0.24395	0.279696	0.24395	0.235967	0.252238	0.336557	0.32004	0.267942
Odd Square 10D (53)	0.03015	0.035421	0.080246	0.082187	0.05013	0.03659	0.072214	0.082494	0.085103	0.037741	0.052313	0.074461	0.042226	0.044102	0.028034	0.050544
Whitley 10D (54)	2364578	2852781	1806714	1.11E+09	3361426	2920139	3361426	2920139	2992812	3124692	3682742	2324133	2844082	3094068	2850511	2932680
Whitley 30D (55)	2.8E+11	3.43E+11	8.49E+10													

Results St. Dev. (500k)	A50, N1	A50, N2	A50, N3	A50, N4	A100, N1	A100, N2	A100, N3	A100, N4	A250, N1	A250, N2	A250, N3	A250, N4	A500, N1	A500, N2	A500, N3	A500, N4
Rosenbrock (1)	0.000756	0.001021	0.000756	0.000756	0.000535	0.000705	0.000535	0.000535	0.016207	0.000231	0.016207	0.016207	0.000404	0.000108	0.000404	A500, N4
McCormic (2)	4.66E-07	8.89E-08	4.66E-07	4.66E-07	1.60E-07	2.45E-08	1.60E-07	1.60E-07	2.75E-08	9.54E-09	2.75E-08	2.75E-08	5.44E-08	0.001188	5.44E-08	5.44E-08
Box and Betts (3)	1.32E-07	1.43E-08	1.32E-07	1.32E-07	1.71E-05	4.06E-06	1.71E-05	3.91E-08	1.69E-06	7.13E-06	2.71E-06	2.84E-06	8.32E-06	1.43E-05	8.57E-07	8.76E-06
Goldstein (4)	3.86E-05	1.08E-05	3.86E-05	3.86E-05	1.71E-05	4.06E-06	1.71E-05	1.71E-05	2.84E-06	1.77E-06	2.84E-06	2.84E-06	1.77E-06	1.005553	1.77E-06	1.77E-06
Easom (5)	0.001258	0.001637	0.001258	0.001258	0.001388	0.001466	0.001388	0.001388	0.001096	0.001436	0.001096	0.001096	0.001137	0.001751	0.001751	0.001751
Mod Rosenbrock 1 (6)	0.0033548	0.028089	0.0033548	0.0033548	0.002928	0.031019	0.002928	0.002928	0.029298	0.014084	0.029298	0.029298	0.018788	0.008379	0.018788	0.018788
Mod Rosenbrock 2 (7)	0.416064	0.426825	0.416064	0.416064	0.401015	0.472493	0.401015	0.401015	0.464774	0.323069	0.464774	0.464774	0.357422	0.237959	0.357422	0.357422
Bohachevsky (8)	0.42704	0.357941	0.42704	0.42704	0.405077	0.395993	0.405077	0.405077	0.405077	0.372534	0.405077	0.405077	0.389954	0.408339	0.389954	0.389954
Powell (9)	91484.43	91484.43	78868.13	45732.83	56293.06	56293.06	60932.05	72448.71	55667.27	55667.27	60997.87	77789.82	65463.17	65463.17	79997.6	70285.27
Wood (10)	201482	201482	184856.5	415946.2	229453.5	229453.5	237640.1	233075.2	287028.3	287028.3	233570.6	225014.8	201674.7	201674.7	273360	284447.3
Beale (11)	0.285671	0.350993	0.285671	0.285671	0.314958	0.456711	0.314958	0.314958	0.259253	0.406529	0.259253	0.259253	0.335294	0.3808	0.335294	0.335294
Engvall (12)	0.549128	0.623921	0.549128	0.549128	0.700467	0.579165	0.700467	0.700467	0.622752	0.662169	0.622752	0.622752	0.767395	0.811597	0.767395	0.767395
DeJong (13)	4.43E-06	4.60E-06	4.43E-06	4.43E-06	5.95E-06	1.31E-06	5.95E-06	5.95E-06	1.41E-06	2.06E-07	1.41E-06	1.41E-06	3.26E-07	7.46E-08	3.26E-07	3.26E-07
Rastrigin (14)	0.002195	0.00149	0.002195	0.002195	0.001606	0.001726	0.001606	0.001606	0.031997	0.357165	0.031997	0.031997	0.12018	0.383604	0.12018	0.12018
Schwefel (15)	0.016682	0.023531	0.016682	0.016682	0.022084	0.021574	0.022084	0.022084	0.015005	0.035108	0.033372	0.003372	0.030387	0.036806	0.019167	0.019167
Griewangk (16)	0.003311	0.003194	0.003311	0.003311	0.002987	0.00322	0.002987	0.002987	0.003372	0.003203	0.003372	0.003372	0.003087	0.003252	0.003087	0.003087
Langerman (18)	0.002913	0.0015134	0.002913	0.002913	0.002772	0.011914	0.002772	0.002772	0.013498	0.008106	0.013498	0.013498	0.010653	0.004841	0.010653	0.010653
Michalewicz (19)	0.437932	0.555375	0.437932	0.437932	0.4145	0.390654	0.4145	0.390654	0.003151	0.04046	0.003151	0.003151	0.003899	0.003867	0.003899	0.003899
Brannin (20)	1.76E-06	0.237394	1.76E-06	1.76E-06	6.93E-09	0.14317	6.93E-09	0.14317	0.439742	0.561614	0.439742	0.439742	0.353638	0.620254	0.547244	0.547244
Six Hump Camel (21)	1.10E-06	1.44E-07	1.10E-06	1.10E-06	1.10E-06	7.93E-06	1.10E-06	5.00E-06	8.76E-07	2.39E-07	8.76E-07	8.76E-07	4.35E-07	0.00717	4.35E-07	4.35E-07
Osborne 1 (22)	0.011156	0.010547	0.008841	0.011812	0.01086	0.008713	0.009302	0.008073	0.050026	0.010647	0.009622	0.011819	0.094278	0.003717	2.65E-08	2.65E-08
Osborne 2 (23)	0.018444	0.018518	0.031689	0.031689	0.019009	0.019157	0.022039	0.021289	0.028155	0.026556	0.028272	0.027274	0.025696	0.0248	0.025615	0.025615
Mod Rastrigin (24)	1.693458	1.482639	1.693458	1.693458	1.681425	1.831428	1.681425	1.681425	1.992592	3.390501	1.992592	1.992592	2.092007	2.748779	2.092007	2.092007
Mineshaft 1 (25)	0.159467	0.235351	0.143134	0.235351	0.070518	0.198024	0.070518	0.198024	0.045475	0.303635	0.099891	0.303635	0.113537	0.189193	0.283163	0.189193
Mineshaft 2 (26)	1.76E-06	0.165565	0.047463	0.165565	6.93E-09	0.14317	6.93E-09	0.14317	1.87E-09	0.17782	0.09662	0.17782	0.064847	0.165665	0.146946	0.146946
Mineshaft 3 (27)	0.141163	0.237394	0.141163	0.141163	0.009825	0.011204	0.009825	0.009825	0.001064	9.26E-05	0.001064	0.001064	0.001113	0.000172	0.001113	0.001113
Spherical Contours (28)	2.138468	2.401463	1.945076	1.945076	2.643557	2.489723	2.245526	2.245526	2.479205	2.338717	2.490693	2.338717	3.510566	3.510566	3.510566	3.510566
S1 (29)	4.78E-13	0.009055	3.47E-14	0.009055	6.48E-14	0.0005	9.90E-15	0.0005	3.73E-07	0.000838	0.000136	0.000838	0.00186	0.00497	0.000244	0.000497
S2 (30)	4.28E-11	3.18E-11	3.18E-11	3.18E-11	3.13E-10	9.68E-12	4.27E-11	4.27E-11	9.34E-12	1.59E-12	9.34E-12	9.34E-12	1.05E-10	7.33E-12	2.81E-12	2.81E-12
S3 (31)	2.43E-10	2.85E-10	2.43E-10	2.43E-10	3.13E-10	5.62E-11	3.13E-10	3.13E-10	1.06E-10	8.49E-11	1.06E-10	1.02815	1.05E-10	0.093772	1.05E-10	1.05E-10
Downhill Step (32)	0	0	0	0	0	0.039799	0	0	0.102815	0	0.102815	0.102815	0.024166	0.089649	0.024166	0.024166
Salomon (33)	0.015735	0.012631	0.015735	0.015735	0.014919	0.014873	0.014919	0.014919	0.01284	0.012219	0.01284	0.01284	0.01366	0.016193	0.01366	0.01366
Whitley (34)	0.042911	0.037759	0.042911	0.042911	0.026428	0.044325	0.026428	0.026428	0.039414	0.03161	0.039414	0.039414	0.025024	0.029495	0.025024	0.025024
Odd Square (35)	0.000475	0.000405	0.000475	0.000475	0.000409	0.000268	0.000409	0.000409	0.000313	0.001226	0.000313	0.000313	0.000455	0.09857	0.000455	0.000455
Storn Chebyshev (36)	46.44464	52.01753	41.87516	41.87516	39.27005	55.28197	39.27005	44.45229	60.40485	58.56539	51.52476	54.02611	229.7484	235.4666	48.52442	229.6639
Rana (37)	1.71E-12	1.71E-12	1.71E-12	1.71E-12	1.71E-12	20.76725	1.71E-12	20.76725	34.81094	303.2965	289.1212	283.7867	317.6501	7.867985	18.83067	18.83067
Rosenbrock 10D (38)	283.1568	326.7291	277.5191	303.365	306.6709	296.363	295.4585	297.2113	34.81094	303.2965	289.1212	283.7867	316.9756	7.867985	328.489	319.0554
Mod Rosenbrock 1 10D (40)	49290.32	53501.86	62496.98	62496.98	42361.24	58210.43	36716.7	36716.7	74575.26	47671.3	160.0957	134.2883	134491.9	148.68	134491.9	134491.9
Mod Rosenbrock 1 30D (41)	172.0327	152.6001	126.9216	131.6014	161.3865	138.7985	127.7054	151.448	142.9299	144.602	160.0957	134.2883	146.625	148.68	150.0513	149.4953
Mod Rosenbrock 1 10D (42)	1872.757	1895.906	2150.75	2150.75	2079.416	1966.351	1892.392	1892.392	1963.623	2064.532	2058.752	2101.691	2485.18	2485.18	2485.18	2485.18
Mod Rosenbrock 2 10D (43)	0.378009	0.441916	0.428236	0.389868	0.435787	0.409904	0.387595	0.438606	0.432662	0.437287	0.452299	0.433493	0.45863	0.410275	0.436822	0.448681
Mod Rosenbrock 2 30D (44)	0.408267	0.409574	0.406398	0.406398	0.419137	0.37593	0.458955	0.458955	0.365964	0.361523	0.412087	0.353928	0.46405	0.445902	0.448234	0.445116
Spherical Contours 10D (44)	0.161016	0.156973	0.125477	0.134335	0.144894	0.160651	0.13077	0.173359	0.14547	0.142937	0.153744	0.130692	0.192281	0.19339	0.191203	0.192029
Rastrigin 10D (45)	4.212124	4.410785	3.93059	4.800373	4.851406	3.993777	4.097455	3.51081	4.441527	3.564378	3.971872	4.293398	4.029398	3.988342	4.1198	4.608105
Rastrigin 30D (46)	14.2301	15.88953	11.06821	11.06821	14.43895	9.877303	9.877303	9.877303	12.64218	13.20751	13.6093	12.32588	16.73687	16.14214	22.57886	16.5837
Schwefel 10D (47)	168.8363	154.4088	263.3138	267.9654	148.5298	159.2169	205.8597	201.043	202.7064	147.0821	169.0713	137.9735	155.8784	165.5839	185.6357	190.0388
Schwefel 30D (48)	332.0435	319.3247	401.8298	401.8298	275.2647	336.4802	402.1975	402.1975	280.6042	280.4425	362.399	293.0126	268.942	323.4649	300.0566	300.0566
Griewangk 10D (49)	0.158881	0.161348	0.130199	0.168696	0.135724	0.143567	0.150323	0.134	0.146008	0.134822	0.135434	0.144402	0.15083	0.148991	0.145054	0.148857
Griewangk 30D (50)	1.86182	2.093944	2.093175	1.962253	1.743155	1.914879	1.743155	1.743155	2.087682	2.090606	2.049338	1.968108	2.63062	2.63062	2.63062	2.63062
Salomon 10D (51)	0.132549	0.125566	0.138015	0.120635	0.134464	0.136163	0.129774	0.125148	0.145865	0.1404381	0.140381	0.107726	0.153391	0.146234	0.151146	0.153905
Salomon 30D (52)	0.293693	0.292423	0.233612	0.292823	0.292823	0.282171	0.240855	0.240855	0.285416	0.294164	0.339419	0.289379	0.470059	0.470668	0.470668	0.470226
Odd Square 10D (53)	0.020814	0.035905	0.067289	0.075562	0.041027	0.021729	0.053348	0.060916	0.040699	0.026784	0.04135	0.052192	0.03386	0.030671	0.020078	0.039486
Whitley 10D (54)	4767272	4824064	77893541	1.11E+09	5293312	4507284	4394149	8870866	6272193	9192743	6172813	4535093	5297034	537713	5627969	5357754
Whitley 30D (55)	3.9E+11	3.97E+11	2.77E+11	2.77E+11	4.14E+11	4.57E+11	2.78E+11	2.78E+11	6.9E+11	4.58E+11	6.1E+11	5.87E+11	2.41E+12	5.3E+12	1.9E+12	1.49E+13
Rana 10D (56)	178.0522	174.5713	237.4377	252.0443	169.1452	180.4416	228.8966</									

Results St. Dev. (100k)

	A500_N1	A500_N2	A500_N3	A500_N4	A100_N1	A100_N2	A100_N3	A100_N4	A250_N1	A250_N2	A250_N3	A250_N4	A500_N1	A500_N2	A500_N3	A500_N4
Rosenbrock (1)	0.002838	0.003349	0.002838	0.002838	0.003682	0.003682	0.003682	0.003682	0.016315	0.001747	0.016315	0.016315	0.003032	0.003032	0.003032	A500_N4
McCormic (2)	2.47E-06	6.09E-07	2.47E-06	2.47E-06	7.89E-06	7.89E-06	7.89E-06	7.89E-06	6.67E-07	0.002864	6.67E-07	6.67E-07	4.60E-06	0.025841	4.60E-06	4.60E-06
Box and Betts (3)	3.80E-06	3.31E-06	2.14E-05	7.32E-07	1.80E-05	7.87E-06	1.14E-06	1.17E-05	6.19E-06	1.81E-05	6.19E-06	6.19E-06	3.10E-05	3.00E-05	2.14E-05	1.35E-05
Goldstein (4)	0.000175	0.000175	0.000175	0.000175	0.000269	3.614992	0.00269	0.00269	0.001045	1.788555	0.001045	0.001045	2.965234	2.965234	0.840233	0.840233
Easom (5)	0.006828	0.006828	0.006828	0.006828	0.006828	0.006828	0.006828	0.006828	0.005417	0.005417	0.005417	0.005417	0.018758	0.018758	0.018758	0.018758
Mod Rosenbrock 1 (6)	0.075177	0.093308	0.075177	0.075177	0.083478	0.083126	0.083478	0.083478	0.070926	0.054883	0.070926	0.070926	0.068096	0.068096	0.094713	0.094713
Mod Rosenbrock 2 (7)	0.738723	0.823507	0.738723	0.738723	0.831269	0.831269	0.831269	0.831269	0.821032	0.708311	0.821032	0.821032	0.944103	0.944103	0.944103	0.944103
Bohachevsky (8)	1.530798	1.493051	1.530798	1.530798	1.528111	1.480907	1.528111	1.528111	1.571858	1.591045	1.571858	1.571858	1.850036	1.850036	1.850036	1.850036
Powell (9)	231592.3	210423	231592.3	214135.1	332881.8	332881.8	257340.7	246307.7	368338.7	366338.7	373490	371418.4	466316.6	466316.6	466316.6	466316.6
Wood (10)	765814	765814	724098.6	1336975	1102980	1102980	964704.1	964704.1	1651301	1651301	1625699	1625699	1283857	1283857	1283857	1283857
Beale (11)	4.701599	5.872243	4.701599	4.701599	4.280269	8.116981	4.280269	4.280269	787.8959	787.8959	787.8959	787.8959	14.27274	14.27274	14.27274	14.27274
Engvall (12)	5.970906	4.574465	5.970906	5.970906	6.148214	2.875119	6.148214	6.148214	3.724247	3.724247	3.724247	3.724247	4.342884	4.342884	4.342884	4.342884
DeJong (13)	2.42E-05	2.42E-05	2.42E-05	2.42E-05	6.19E-06	6.19E-06	2.26E-05	2.26E-05	1.31E-05	2.19E-06	1.31E-05	1.31E-05	3.49E-05	3.49E-05	1.35E-05	1.35E-05
Rastrigin (14)	0.009252	0.006957	0.009252	0.009252	0.007517	0.007517	0.007517	0.007517	0.135133	0.030211	0.135133	0.135133	0.492697	0.492697	0.713365	0.713365
Schwefel (15)	13.83863	0.331049	13.83863	13.83863	6.206651	6.206651	3.960933	3.960933	2.455792	2.455792	2.455792	2.455792	0.232482	0.232482	0.232482	0.232482
Griewangk (16)	0.00563	0.00563	0.00563	0.00563	0.006283	0.006283	0.006283	0.006283	0.006465	0.006465	0.006465	0.006465	0.006055	0.006055	0.006055	0.006055
Ackley (17)	0.026917	0.038854	0.026917	0.026917	0.032993	0.032993	0.032993	0.032993	0.039174	0.039174	0.039174	0.039174	0.050048	0.050048	0.050048	0.050048
Langerman (18)	0.009487	0.009412	0.009487	0.009412	0.033961	0.074271	0.011145	0.030766	0.030479	0.030211	0.030512	0.030323	0.076777	0.076777	0.076777	0.076777
Michalewicz (19)	0.391912	0.597608	0.391912	0.597608	0.539895	0.492511	0.636854	0.500768	0.420983	0.652411	0.667338	0.425107	0.345368	0.417608	0.494556	0.321203
Branin (20)	2.97E-05	2.37E-05	2.97E-05	2.97E-05	2.98E-05	2.98E-05	2.96E-05	2.96E-05	6.94E-06	3.21E-06	6.94E-06	6.94E-06	1.06E-05	1.06E-05	1.06E-05	1.06E-05
Six Hump Camel (21)	5.15E-06	4.81E-06	5.15E-06	5.15E-06	2.15E-06	1.15E-06	2.15E-06	2.15E-06	1.36E-06	0.00678	1.36E-06	1.36E-06	0.009545	0.009545	0.009545	0.009545
Osborne 1 (22)	0.03322	0.033962	0.026389	0.084138	0.03444	0.057156	0.038263	0.048643	0.069075	0.067863	0.068706	0.068632	0.121728	0.121728	0.121728	0.121728
Osborne 2 (23)	0.034968	0.037203	0.037601	0.038174	0.064717	0.064548	0.0613	0.061092	0.073641	0.073641	0.073641	0.073641	0.268108	0.268108	0.268108	0.268108
Mod Rastrigin (24)	1.761468	1.83463	1.761468	1.761468	1.70829	1.881452	1.70829	1.757045	3.165864	3.165864	1.757045	1.757045	2.428702	2.428702	2.428702	2.428702
Mineshaft 1 (25)	0.142259	0.247955	0.1555	0.247955	0.085692	0.232135	0.131124	0.232135	0.118667	0.109911	0.216083	0.109911	0.195876	0.169604	0.12406	0.169604
Mineshaft 2 (26)	0.0003	0.196887	0.074392	0.196887	0.000752	0.185411	0.106206	0.185411	0.11364	0.171838	0.172527	0.171838	0.14573	0.161448	0.161448	0.161448
Mineshaft 3 (27)	0.168102	0.237116	0.168102	0.168102	0.172973	0.198016	0.172973	0.172973	0.901165	0.701755	0.901165	0.901165	0.022708	0.183814	0.022708	0.022708
Spherical Contours (28)	4.292402	4.292402	4.281148	4.281148	4.687166	4.687166	4.687166	4.687166	8.536318	8.536318	8.536318	8.536318	30.41852	30.41852	30.41852	30.41852
S1 (29)	1.747E-11	0.036352	9.70E-12	0.036352	1.40E-11	0.006812	3.35E-07	0.006812	0.00102	0.00102	0.000954	0.00102	0.000297	0.000494	0.000478	0.000494
S2 (30)	9.96E-10	7.01E-10	9.96E-10	9.96E-10	6.93E-10	6.93E-10	6.93E-10	6.93E-10	4.54E-10	4.54E-10	3.11E-08	3.11E-08	2.63E-10	2.63E-10	2.63E-10	2.63E-10
S3 (31)	4.77E-09	5.02E-08	4.77E-09	4.77E-09	9.36E-09	9.36E-09	9.36E-09	9.36E-09	3.11E-08	0.006519	3.11E-08	3.11E-08	0.000451	0.000451	0.000451	0.000451
Downhill Step (32)	0	0	0	0	0	0	0	0	0.144537	0.23731	0.144537	0.144537	0.179042	0.179042	0.113508	0.113508
Salomon (33)	0.034551	0.034551	0.034551	0.034551	0.036091	0.036091	0.036091	0.036091	0.034964	0.034964	0.034964	0.034964	0.034206	0.034206	0.034206	0.034206
Whitley (34)	0.20766	0.144338	0.20766	0.20766	0.221556	0.168407	0.221556	0.221556	0.197661	0.196573	0.197661	0.197661	0.188254	0.188254	0.188254	0.188254
Odd Square (35)	0.000955	0.001239	0.000955	0.000955	0.001065	0.000818	0.001065	0.001065	0.001039	0.091589	0.001039	0.001039	0.036299	0.036299	0.036299	0.036299
Storn Chebyshev (36)	245.9555	280.3621	323.4736	330.8224	285.6606	313.3876	310.1396	302.1664	2964.053	2964.222	2963.801	2964.081	829.6967	829.6967	829.6967	829.6967
Rana (37)	16.13413	22.19053	16.13413	16.13413	50.759	55.12045	50.759	50.759	35.3259	35.3259	35.3259	35.3259	20.27776	20.27776	20.27776	20.27776
Rosenbrock 10D (38)	544.2668	561.8502	526.9612	408455.5	694.8093	695.9515	696.0262	695.8187	1581.916	1581.916	1581.916	1581.916	1719.795	1719.795	1719.795	1719.795
Rosenbrock 30D (39)	17571717	1756056	1757254	1757254	507159.3	505662.7	505633.6	505633.6	3287020	3287020	3287020	3287020	14520913	14520913	14520913	14520913
Mod Rosenbrock 1 10D (40)	196.7557	199.4282	176.8484	188.2609	199.9633	200.3262	200.2455	200.9121	274.1576	274.1576	274.1576	274.1576	399.4616	399.4616	399.4616	399.4616
Mod Rosenbrock 1 30D (41)	3023.376	2945.106	3062.871	3062.871	5560.662	5560.662	5560.662	5560.662	18166.14	18166.14	18166.14	18166.14	17195.34	17195.34	17195.34	17195.34
Mod Rosenbrock 2 10D (42)	0.828299	0.76647	0.859053	0.760965	0.995211	0.835469	0.892004	0.845518	0.889317	0.810037	0.870069	0.882541	0.807257	0.807257	0.797844	0.807257
Mod Rosenbrock 2 30D (43)	0.86417	0.698242	0.837304	0.837304	0.775481	0.84195	0.875478	0.875478	0.899512	0.864116	0.918118	0.846655	0.933929	0.933929	0.933929	0.933929
Spherical Contours 10D (44)	0.206261	0.211533	0.195081	0.205429	0.27877	0.27877	0.27877	0.27877	0.280287	0.280287	0.280287	0.280287	0.747876	0.747876	0.747876	0.747876
Rastrigin 10D (45)	4.657461	5.750572	4.477706	6.033524	5.116071	5.947132	5.45526	5.335982	5.604763	5.967367	5.58317	5.933979	9.525192	9.525192	9.525192	9.525192
Rastrigin 30D (46)	19.00832	21.76841	17.45189	17.45189	26.1127	20.0227	27.45634	27.45634	29.8035	29.8035	29.8035	29.8035	32.84805	32.84805	31.57321	31.57321
Schwefel 10D (47)	175.1269	188.3229	277.9913	251.028	185.3319	189.2527	185.5074	138.8914	135.0754	138.8914	140.2418	141.5972	182.4222	178.3132	176.1503	180.7593
Schwefel 30D (48)	342.123	270.9085	395.064	395.064	289.5095	289.5095	329.3383	329.3383	297.2975	271.3189	327.4972	282.3059	257.1318	263.7628	260.0343	260.0343
Griewangk 10D (49)	0.195053	0.204844	0.206788	0.226351	0.233878	0.233878	0.233878	0.233878	1.002004	1.002004	1.002004	1.002004	0.522338	0.522338	0.522338	0.522338
Griewangk 30D (50)	2.843025	2.782216	2.842258	2.842258	5.193139	5.193139	5.193139	5.193139	8.931615	8.931615	8.931615	8.931615	20.86054	20.86054	20.86054	20.86054
Salomon 10D (51)	0.161632	0.161632	0.158974	0.158974	0.19557	0.19557	0.19557	0.19557	0.183994	0.183994	0.183994	0.183994	0.365103	0.365103	0.365103	0.365103
Salomon 30D (52)	0.426315	0.382995	0.347839	0.347839	0.449924	0.449924	0.447747	0.447747	0.973472	0.973472	0.973472	0.973472	1.559823	1.559823	1.559823	1.559823
Odd Square 10D (53)	0.056366	0.047269	0.032975	0.042577	0.06664	0.068216	0.059171	0.061553	0.070339	0.071846	0.073289	0.070483	0.061163	0.061163	0.060678	0.060678
Whitley 10D (54)	2.56E+08	2.57E+08	1.13E+09	1.13E+09	24438408	24421204	24438408	24438408	41082708	41082708	41082708	41082708	4.66E+08	4.66E+08	4.66E+08	4.66E+08
Whitley 30D (55)	3.11E+13	3.1E+13	3.1E+13	3.1E+13	6.68E+12	6.38E+12	6.68E+12	6.68E+12	8.87E+15	8.87E+15	8.87E+15	8.87E+15	1.99E+16			







## APPENDIX C1: SMOA AVG. RESULTS FROM VARYING PSEUDOPODS

Results	Z Pseudopods												4+ Pseudopods												A500, N1	A500, N2	A500, N3	A500, N4	A500, N5	A500, N6	A500, N7	A500, N8	A500, N9	A500, N10	A500, N11	A500, N12	A500, N13	A500, N14	A500, N15	A500, N16	A500, N17	A500, N18	A500, N19	A500, N20	A500, N21	A500, N22	A500, N23	A500, N24	A500, N25	A500, N26	A500, N27	A500, N28	A500, N29	A500, N30	A500, N31	A500, N32	A500, N33	A500, N34	A500, N35	A500, N36	A500, N37	A500, N38	A500, N39	A500, N40	A500, N41	A500, N42	A500, N43	A500, N44	A500, N45	A500, N46	A500, N47	A500, N48	A500, N49	A500, N50	A500, N51	A500, N52	A500, N53	A500, N54	A500, N55	A500, N56	A500, N57	A500, N58	A500, N59	A500, N60	A500, N61	A500, N62	A500, N63	A500, N64	A500, N65	A500, N66	A500, N67	A500, N68	A500, N69	A500, N70	A500, N71	A500, N72	A500, N73	A500, N74	A500, N75	A500, N76	A500, N77	A500, N78	A500, N79	A500, N80	A500, N81	A500, N82	A500, N83	A500, N84	A500, N85	A500, N86	A500, N87	A500, N88	A500, N89	A500, N90	A500, N91	A500, N92	A500, N93	A500, N94	A500, N95	A500, N96	A500, N97	A500, N98	A500, N99	A500, N100	A500, N101	A500, N102	A500, N103	A500, N104	A500, N105	A500, N106	A500, N107	A500, N108	A500, N109	A500, N110	A500, N111	A500, N112	A500, N113	A500, N114	A500, N115	A500, N116	A500, N117	A500, N118	A500, N119	A500, N120	A500, N121	A500, N122	A500, N123	A500, N124	A500, N125	A500, N126	A500, N127	A500, N128	A500, N129	A500, N130	A500, N131	A500, N132	A500, N133	A500, N134	A500, N135	A500, N136	A500, N137	A500, N138	A500, N139	A500, N140	A500, N141	A500, N142	A500, N143	A500, N144	A500, N145	A500, N146	A500, N147	A500, N148	A500, N149	A500, N150	A500, N151	A500, N152	A500, N153	A500, N154	A500, N155	A500, N156	A500, N157	A500, N158	A500, N159	A500, N160	A500, N161	A500, N162	A500, N163	A500, N164	A500, N165	A500, N166	A500, N167	A500, N168	A500, N169	A500, N170	A500, N171	A500, N172	A500, N173	A500, N174	A500, N175	A500, N176	A500, N177	A500, N178	A500, N179	A500, N180	A500, N181	A500, N182	A500, N183	A500, N184	A500, N185	A500, N186	A500, N187	A500, N188	A500, N189	A500, N190	A500, N191	A500, N192	A500, N193	A500, N194	A500, N195	A500, N196	A500, N197	A500, N198	A500, N199	A500, N200	A500, N201	A500, N202	A500, N203	A500, N204	A500, N205	A500, N206	A500, N207	A500, N208	A500, N209	A500, N210	A500, N211	A500, N212	A500, N213	A500, N214	A500, N215	A500, N216	A500, N217	A500, N218	A500, N219	A500, N220	A500, N221	A500, N222	A500, N223	A500, N224	A500, N225	A500, N226	A500, N227	A500, N228	A500, N229	A500, N230	A500, N231	A500, N232	A500, N233	A500, N234	A500, N235	A500, N236	A500, N237	A500, N238	A500, N239	A500, N240	A500, N241	A500, N242	A500, N243	A500, N244	A500, N245
---------	--------------	--	--	--	--	--	--	--	--	--	--	--	---------------	--	--	--	--	--	--	--	--	--	--	--	----------	----------	----------	----------	----------	----------	----------	----------	----------	-----------	-----------	-----------	-----------	-----------	-----------	-----------	-----------	-----------	-----------	-----------	-----------	-----------	-----------	-----------	-----------	-----------	-----------	-----------	-----------	-----------	-----------	-----------	-----------	-----------	-----------	-----------	-----------	-----------	-----------	-----------	-----------	-----------	-----------	-----------	-----------	-----------	-----------	-----------	-----------	-----------	-----------	-----------	-----------	-----------	-----------	-----------	-----------	-----------	-----------	-----------	-----------	-----------	-----------	-----------	-----------	-----------	-----------	-----------	-----------	-----------	-----------	-----------	-----------	-----------	-----------	-----------	-----------	-----------	-----------	-----------	-----------	-----------	-----------	-----------	-----------	-----------	-----------	-----------	-----------	-----------	-----------	-----------	-----------	-----------	-----------	-----------	-----------	-----------	-----------	------------	------------	------------	------------	------------	------------	------------	------------	------------	------------	------------	------------	------------	------------	------------	------------	------------	------------	------------	------------	------------	------------	------------	------------	------------	------------	------------	------------	------------	------------	------------	------------	------------	------------	------------	------------	------------	------------	------------	------------	------------	------------	------------	------------	------------	------------	------------	------------	------------	------------	------------	------------	------------	------------	------------	------------	------------	------------	------------	------------	------------	------------	------------	------------	------------	------------	------------	------------	------------	------------	------------	------------	------------	------------	------------	------------	------------	------------	------------	------------	------------	------------	------------	------------	------------	------------	------------	------------	------------	------------	------------	------------	------------	------------	------------	------------	------------	------------	------------	------------	------------	------------	------------	------------	------------	------------	------------	------------	------------	------------	------------	------------	------------	------------	------------	------------	------------	------------	------------	------------	------------	------------	------------	------------	------------	------------	------------	------------	------------	------------	------------	------------	------------	------------	------------	------------	------------	------------	------------	------------	------------	------------	------------	------------	------------	------------

128



Results Avgs. (500k)	A50, N1	A50, N2	A50, N3	10 Pseudopods		A50, N1	A50, N2	A50, N3	A50, N4
Rosenbrock (1)	0.0005173	0.0005796	-0.913222	0.0005173	0.0004784	0.000135	0.000135	0.0004784	0.0004784
McCormic (2)	-1.913222	-1.913222	-1.913222	-1.913222	-1.913222	-1.913174	-1.913174	-1.913222	-1.913222
Box and Betts (3)	3.02E-007	6.80E-008	2.22E-008	1.82E-008	1.70E-006	2.60E-006	7.19E-007	1.89E-007	1.89E-007
Goldstein (4)	3.0000212	3.0000061	3.0000212	3.0000212	3.021183	3.2877212	3.021183	3.021183	3.021183
Easom (5)	-0.99893	-0.99876	-0.99893	-0.99893	-0.998631	-0.998654	-0.998631	-0.998631	-0.998631
Mod Rosenbrock 1 (6)	0.039484	0.0392951	0.039484	0.039484	0.031345	0.0136327	0.031345	0.031345	0.031345
Mod Rosenbrock 2 (7)	0.8886352	0.9388832	0.8886352	0.8886352	0.8436484	0.5849233	0.8436484	0.8436484	0.8436484
Bohachevsky (8)	0.8375542	0.8939457	0.8375542	0.8375542	0.8516058	0.8539168	0.8516058	0.8516058	0.8516058
Powell (9)	76567.049	76567.049	71014.659	45928.479	118063.75	118063.75	118474.82	112571.83	112571.83
Wood (10)	201400.42	201400.42	186187.8	123009.71	403469.86	403469.86	403405.12	396081.04	396081.04
Beale (11)	0.4042946	0.5063336	0.4042946	0.4042946	0.6446515	0.6277064	0.6446515	0.6446515	0.6446515
Engvall (12)	0.6818518	0.6714933	0.6818518	0.6818518	0.7055988	0.7151354	0.7055988	0.7055988	0.7055988
DeJong (13)	4.92E-006	3.73E-006	4.92E-006	4.92E-006	5.36E-007	2.06E-007	5.36E-007	5.36E-007	5.36E-007
Rastrigin (14)	0.0009993	0.0010605	0.0009993	0.0009993	0.1688059	0.1688059	0.1688059	0.1688059	0.1688059
Schwefel (15)	-837.9576	-837.9576	-837.9576	-837.9576	-837.9435	-837.9389	-837.9389	-837.9389	-837.9389
Griewangk (16)	0.0047848	0.0049647	0.0047848	0.0047848	0.0048087	0.0047536	0.0048087	0.0048087	0.0048087
Ackley (17)	0.0210264	0.0202563	0.0210264	0.0210264	0.0205172	0.0106471	0.0205172	0.0205172	0.0205172
Langman (18)	-1.495844	-1.495767	-1.495892	-1.494948	-1.490861	-1.490782	-1.490815	-1.490743	-1.490743
Michalewicz (19)	-6.951505	-7.37319	-7.400179	-7.371684	-6.716209	-6.836357	-7.204594	-6.815297	-6.815297
Brannin (20)	0.3978938	0.3978903	0.3978938	0.3978938	0.3978878	0.3978875	0.3978878	0.3978878	0.3978878
Six Hump Camel (21)	-1.031628	-1.031628	-1.031628	-1.031628	-1.030488	-1.031628	-1.031628	-1.031628	-1.031628
Osborne 1 (22)	0.0308825	0.030226	0.0299776	0.0285964	0.0496613	0.0495464	0.0482054	0.0483372	0.0483372
Osborne 2 (23)	0.1024268	0.1010214	0.1105587	0.1159103	0.1472314	0.1472314	0.1472314	0.1472314	0.1472314
Mod Rastrigin (24)	83.302921	83.469887	83.302921	83.302921	85.058089	84.870976	85.058089	85.058089	85.058089
Mineshaft 1 (25)	1.87631	1.8518492	1.8378123	1.8518492	1.7850446	2.2976931	2.0899637	2.2976931	2.2976931
Mineshaft 2 (26)	-1.416353	-1.312604	-1.411884	-1.312604	-1.390517	-1.234492	-1.234492	-1.234492	-1.234492
Mineshaft 3 (27)	-6.984874	-6.986863	-6.984874	-6.984874	-6.999941	-6.999941	-6.999941	-6.999941	-6.999941
Spherical Contours (28)	23.297244	23.134779	21.363141	21.363141	37.141543	37.141543	37.141543	37.141543	37.141543
S1 (29)	3.39E-013	0.0064042	1.41E-014	0.0064042	1.55E-005	0.0002023	0.0001182	0.0002023	0.0002023
S2 (30)	2	2	2	2	2	2	2	2	2
S3 (31)	0.5288723	0.5288723	0.5288723	0.5288723	0.5288723	0.5288926	0.5288723	0.5288723	0.5288723
Downhill Step (32)	9	9	9	9	9.017	9.028	9.017	9.017	9.017
Salomon (33)	0.0111416	0.0135296	0.0111416	0.0111416	0.0131991	0.0130009	0.0131991	0.0131991	0.0131991
Whitley (34)	0.0157282	0.0170988	0.0157282	0.0157282	0.0202845	0.0164709	0.0202845	0.0202845	0.0202845
Odd Square (35)	-1.007856	-1.00791	-1.007856	-1.007856	-1.00767	-0.900818	-1.00767	-1.00767	-1.00767
Storn Chebyshev (36)	43.897955	35.045745	44.983149	52.04174	58.047556	58.192231	58.192231	58.192231	58.192231
Rana (37)	-1023.415	-1023.415	-1023.415	-1023.415	-1018.69	-1018.69	-1018.69	-1018.69	-1018.69
Rosenbrock 10D (38)	840.52	859.90229	750.36333	787.38753	1000.9787	1000.9787	1000.9787	1000.9787	1000.9787
Rosenbrock 30D (39)	129249.64	134346.69	121367.14	121367.14	382962.88	382962.88	382962.88	382962.88	382962.88
Mod Rosenbrock 1 10D (40)	690.12406	679.38593	661.12815	674.36462	761.50618	761.50618	761.50618	761.50618	761.50618
Mod Rosenbrock 1 30D (41)	18365.336	18492.402	17388.935	17388.935	28137.731	28137.731	28137.731	28137.731	28137.731
Mod Rosenbrock 2 10D (42)	0.9731461	0.928161	0.8815863	0.9139779	0.9046704	0.9303185	0.9236981	0.8991565	0.8991565
Mod Rosenbrock 2 30D (43)	0.9677003	0.8903888	0.9755474	0.9755474	1.0000904	0.9837482	0.9894645	0.9577823	0.9577823
Spherical Contours 10D (44)	0.4942146	0.5066767	0.4882896	0.4882896	0.5836408	0.5836408	0.5836408	0.5836408	0.5836408
Rastrigin 10D (45)	32.706796	32.87367	29.904197	29.641127	37.32679	37.32679	37.32679	37.32679	37.32679
Rastrigin 30D (46)	250.32011	246.38267	229.28576	229.28576	299.52098	299.52098	299.52098	299.52098	299.52098
Schwefel 10D (47)	-3150.598	-3157.397	-3033.731	-3025.83	-3028.596	-3044.003	-3053.772	-3031.061	-3031.061
Schwefel 30D (48)	-5808.899	-5856.398	-5871.401	-5871.401	-5781.794	-5718.376	-5728.893	-5730.517	-5730.517
Griewangk 10D (49)	1.4937351	1.4740899	1.4523469	1.477656	1.5515463	1.5515463	1.5515463	1.5515463	1.5515463
Griewangk 30D (50)	18.671223	18.427207	17.301573	17.301573	29.707615	29.707615	29.707615	29.707615	29.707615
Salomon 10D (51)	1.0631545	1.07975	1.0174733	1.0210911	1.1931783	1.1931783	1.1931783	1.1931783	1.1931783
Salomon 30D (52)	4.7224267	4.7065711	4.5112812	4.5112812	6.3227755	6.3227755	6.3227755	6.3227755	6.3227755
Odd Square 10D (53)	-0.571977	-0.593948	-0.590199	-0.584652	-0.51955	-0.520373	-0.520373	-0.520373	-0.520373
Whitley 10D (54)	5641993.4	5423974.4	4969907.8	5418845.4	7977932.3	7977932.3	7977932.3	7977932.3	7977932.3
Whitley 30D (55)	5.713E+11	6.053E+11	7.09E+11	7.09E+11	7.84E+12	7.84E+12	7.84E+12	7.84E+12	7.84E+12
Rana 10D (56)	-3392.982	-3414.131	-3393.954	-3391.886	-3376.711	-3356.652	-3377.814	-3361.737	-3361.737
Rana 30D (57)	-5785.587	-5751.792	-5770.707	-5770.707	-5780.67	-5696.714	-5797.546	-5728.21	-5728.21

[illegible]

131

Result St. Dev. (500k)

Rosenbrock (1)	A50, N1	A50, N2	A50, N3	10 Pseudopods		A50, N4	A500, N2	A500, N3	A500, N4
Mod Rosenbrock 1 (6)	0.000471	0.000594	0.000471	A50, N1	A500, N1	0.000471	0.000172	0.000552	0.000552
Mod Rosenbrock 2 (7)	5.92E-07	6.93E-08	5.92E-07	5.92E-07	3.34E-08	5.92E-07	0.000484	3.34E-08	3.34E-08
Bohachevsky (8)	2.89E-06	3.45E-06	1.59E-08	1.12E-08	7.62E-06	1.12E-05	3.34E-06	8.07E-07	8.07E-07
Powell (9)	2.49E-05	5.88E-06	2.49E-05	2.49E-05	0.210725	1.7616	0.210725	0.210725	0.210725
Wood (10)	0.000934	0.001356	0.000934	0.000934	0.001309	0.001421	0.001309	0.001309	0.001309
Mod Rosenbrock 1 (6)	0.02586	0.026869	0.02586	0.02586	0.021009	0.008658	0.021009	0.021009	0.021009
Mod Rosenbrock 2 (7)	0.414455	0.414455	0.414455	0.414455	0.325964	0.300508	0.325964	0.325964	0.325964
Bohachevsky (8)	0.391537	0.379622	0.391537	0.391537	0.323693	0.325521	0.323693	0.323693	0.323693
Powell (9)	50785.77	50785.77	50928.29	31757.97	74006.1	74006.1	383439.6	384667.3	384667.3
Wood (10)	138484.2	138484.2	139250.7	132909.9	389649.1	389649.1	0.572009	0.572009	0.572009
Beale (11)	0.269944	0.269944	0.269944	0.269944	0.572009	0.504469	0.572009	0.572009	0.572009
Engvall (12)	0.624774	0.624774	0.624774	0.624774	0.67679	0.67679	0.67679	0.67679	0.67679
DeJong (13)	4.55E-06	3.64E-06	4.55E-06	4.55E-06	5.09E-07	5.09E-07	5.09E-07	5.09E-07	5.09E-07
Rastrigin (14)	0.000898	0.000938	0.000898	0.000898	0.301363	0.301363	0.301363	0.301363	0.301363
Schwefel (15)	0.00387	0.008967	0.008387	0.008387	0.048736	0.048736	0.048736	0.048736	0.048736
Griewangk (16)	0.002945	0.003119	0.002945	0.002945	0.003112	0.003112	0.003112	0.003112	0.003112
Ackley (17)	0.01286	0.011742	0.01286	0.01286	0.010011	0.005992	0.010011	0.010011	0.010011
Langeman (18)	0.002194	0.002199	0.001631	0.002983	0.014855	0.014887	0.014646	0.014677	0.014677
Michalewicz (19)	0.31883	0.426673	0.445843	0.347047	0.384977	0.497245	0.54146	0.383701	0.383701
Brannin (20)	5.93E-06	3.11E-06	5.93E-06	5.93E-06	4.86E-07	1.8E-07	4.86E-07	4.86E-07	4.86E-07
Six Hump Camel (21)	1.06E-06	2.05E-07	1.06E-06	1.06E-06	5.42E-08	0.010464	5.42E-08	5.42E-08	5.42E-08
Osborne 1 (22)	0.007457	0.008354	0.007322	0.008166	0.029483	0.029085	0.020044	0.020263	0.020263
Osborne 2 (23)	0.015037	0.016776	0.021259	0.021745	0.026777	0.026777	0.026777	0.026777	0.026777
Mod Rastrigin (24)	1.408835	1.463579	1.408835	1.408835	1.765085	2.590538	1.765085	1.765085	1.765085
Mineshaft 1 (25)	0.12033	0.258444	0.157707	0.256444	0.125875	0.122861	0.267806	0.122861	0.122861
Mineshaft 2 (26)	6.13E-07	0.174262	0.03765	0.174262	0.089942	0.162722	0.168111	0.162722	0.162722
Mineshaft 3 (27)	0.043886	0.198855	0.043886	0.043886	6.97E-05	0.000143	6.97E-05	6.97E-05	6.97E-05
Spherical Contours (28)	2.216066	2.406677	2.543593	3.071966	3.071966	3.071966	3.071966	3.071966	3.071966
S1 (29)	9.91E-13	0.033802	2.83E-14	0.033802	0.000131	0.000495	0.000471	0.000495	0.000495
S2 (30)	2.97E-11	2.97E-11	2.93E-11	2.93E-11	1.6E-12	2.23E-12	2.23E-12	2.23E-12	2.23E-12
S3 (31)	2.66E-10	1.11E-10	2.66E-10	2.66E-10	6.67E-10	6.67E-10	6.67E-10	6.67E-10	6.67E-10
Dowhill Step (32)	0	0	0	0	0.064892	0.105906	0.064892	0.064892	0.064892
Salomon (33)	0.009388	0.013461	0.009388	0.009388	0.010129	0.011302	0.010129	0.010129	0.010129
Whitley (34)	0.030812	0.024382	0.030812	0.030812	0.029209	0.025517	0.029209	0.029209	0.029209
Odd Square (35)	0.00034	0.000344	0.00034	0.00034	0.000594	0.11311	0.000594	0.000594	0.000594
Storn Chebyshev (36)	52.69176	47.90423	109.9014	115.5886	85.43672	85.43672	85.43672	85.43672	85.43672
Rana (37)	1.71E-12	1.71E-12	1.71E-12	1.71E-12	21.44097	21.44097	21.44097	21.44097	21.44097
Rosenbrock 10D (38)	310.3719	287.5006	275.9039	263.4484	343.4386	343.4386	343.4386	343.4386	343.4386
Rosenbrock 30D (39)	20436.51	21665.49	29241.37	29241.37	88405.76	88405.76	88405.76	88405.76	88405.76
Mod Rosenbrock 1 10D (40)	113.4953	105.6971	128.2219	137.0013	148.6025	148.6025	148.6025	148.6025	148.6025
Mod Rosenbrock 1 30D (41)	2019.024	2009.756	1878.183	1878.183	2906.613	2906.613	2906.613	2906.613	2906.613
Mod Rosenbrock 2 10D (42)	0.436776	0.338221	0.379541	0.40212	0.400697	0.406313	0.409342	0.400208	0.400208
Mod Rosenbrock 2 30D (43)	0.3939	0.369174	0.389296	0.389296	0.420238	0.432723	0.419845	0.433057	0.433057
Spherical Contours 10D (44)	0.126383	0.138639	0.128108	0.140767	0.147573	0.147573	0.147573	0.147573	0.147573
Rastrigin 10D (45)	3.828726	4.427177	4.019498	4.597968	4.061239	4.115808	4.11863	4.107151	4.107151
Rastrigin 30D (46)	12.40516	12.54119	11.44259	14.28009	14.34087	14.51643	14.19616	14.19616	14.19616
Schwefel 10D (47)	198.0844	194.0897	260.5126	259.1012	137.1414	151.3654	149.6903	144.0855	144.0855
Schwefel 30D (48)	292.0999	291.8634	363.545	363.545	274.9801	274.9801	258.6574	231.1468	231.1468
Griewangk 10D (49)	0.117618	0.105535	0.106485	0.102087	0.129957	0.129957	0.129957	0.129957	0.129957
Griewangk 30D (50)	1.799744	1.992991	1.79589	3.278212	3.278212	3.278212	3.278212	3.278212	3.278212
Salomon 10D (51)	0.124715	0.134333	0.113734	0.13587	0.119309	0.119309	0.119309	0.119309	0.119309
Salomon 30D (52)	0.248284	0.244432	0.263811	0.263811	0.645282	0.645282	0.645282	0.645282	0.645282
Odd Square 10D (53)	0.066425	0.052018	0.07686	0.06971	0.04822	0.04671	0.04671	0.04671	0.04671
Whitley 10D (54)	3848213	4862680	4037592	4712612	6745201	6745201	6745201	6745201	6745201
Whitley 30D (55)	3.01E+11	2.32E+11	2.87E+12	2.87E+12	3.44E+13	3.44E+13	3.44E+13	3.44E+13	3.44E+13
Rana 10D (56)	177.1926	181.4633	222.3315	249.0385	187.519	173.4844	192.4755	185.3861	185.3861
Rana 30D (57)	362.3248	302.0619	409.6435	409.6435	332.979	317.7074	317.7074	317.7074	317.7074





Avg. Times (s) for 500k									
10 Pseudopods	A50, N1	A50, N2	A50, N3	A50, N4	A500, N1	A500, N2	A500, N3	A500, N4	
	1.652288	1.587666	1.535932	1.761453	1.173716	1.0291	1.021111	1.076757	
	Rosenbrock (1)	0.886199	1.055019	0.964796	0.962621	1.016635	0.978423	1.078228	
	McCormic (2)	1.803487	1.725344	1.879489	2.086168	1.738566	1.736307	1.736307	
	Box and Betts (3)	1.335522	1.059978	1.444333	1.339928	0.657716	0.626005	0.599873	0.725015
	Goldstein (4)	1.757823	1.79738	1.966994	1.749433	1.69449	1.520346	1.868192	1.894342
	Easom (5)	1.539082	1.519074	1.481364	1.589231	1.030103	1.049349	1.16148	1.035925
	Mod Rosenbrock 1 (6)	1.2921	1.363302	1.270935	1.356308	1.032674	1.127451	1.156738	1.028152
	Mod Rosenbrock 2 (7)	1.302745	1.19755	1.261109	1.357058	1.028246	1.133816	1.033285	1.078413
	Bohachevsky (8)	1.912028	2.004899	2.251261	3.759447	1.28202	1.350753	1.321472	1.427456
Spherical Contours (28)	Wood (10)	1.978085	2.063296	2.337419	3.622404	1.183233	1.189234	1.297928	1.334043
	Wood (11)	1.585145	1.518923	1.554062	1.238227	0.973546	0.936533	1.036729	0.956894
	Engvall (12)	1.710441	1.569719	1.597268	1.563894	1.051464	1.032385	1.086317	1.106969
	DeJong (13)	1.228539	1.126822	1.196316	1.366721	0.947706	0.85569	0.981246	0.914196
	Rastrigin (14)	1.243851	1.021825	1.290064	1.296615	1.087368	1.013657	1.116875	1.00118
	Schweifel (15)	1.30683	1.192203	1.279259	1.150578	1.209476	1.195006	1.183879	1.093619
	Griewangk (16)	1.306062	1.215995	1.318614	1.077406	0.957866	1.040603	1.017034	0.938479
	Ackley (17)	1.331395	1.330738	1.335929	1.138964	1.075142	1.056933	1.019763	0.986119
	Langman (18)	2.043332	2.139164	2.402897	3.46569	1.514444	1.461287	1.570947	1.54874
	Michalewicz (19)	4.136682	4.511612	5.508782	4.676256	9.574647	9.477914	8.541031	12.14914
Downhill Step (32)	Brannin (20)	0.861535	0.89413	0.631571	0.489407	0.769859	0.718438	0.74721	0.486288
	Six Hump Camel (21)	0.758038	0.723627	0.610298	0.520157	0.763109	0.776809	0.80601	0.527355
	Osborne 1 (22)	3.124206	3.203295	3.195071	3.566605	3.134367	3.166421	3.213055	2.97439
	Osborne 2 (23)	9.055923	9.216701	10.20961	10.80893	8.751568	8.787067	8.850807	9.111796
	Mod Rastrigin (24)	0.976321	0.99776	0.924958	1.541459	0.66401	0.61592	0.645653	0.709009
	Mineshaft 1 (25)	0.749786	0.601553	0.804371	0.948667	0.629249	0.596756	0.604592	0.64757
	Mineshaft 2 (26)	0.508889	0.377105	0.529065	0.663999	0.452521	0.387197	0.418332	0.367811
	Mineshaft 3 (27)	0.705868	0.618628	0.964818	0.84876	0.766962	0.784723	0.834348	0.625088
	Spherical Contours (28)	3.689709	3.806372	5.496512	4.424187	3.215783	3.205687	3.317483	3.856107
	S1 (29)	0.780628	0.54792	0.319763	0.221351	0.485701	0.295815	0.446588	0.730636
Spherical Contours (28)	S2 (30)	1.326926	1.112979	0.532025	0.401674	0.582743	0.542442	0.586496	0.819599
	S3 (31)	1.19849	1.085637	0.585197	0.348883	0.624392	0.58597	0.626	0.760198
	Downhill Step (32)	1.139009	1.285637	0.513389	0.513389	1.556228	1.121714	1.483068	1.280398
	Salomon (33)	0.70093	0.712194	0.430806	0.374561	0.965429	0.676053	0.969329	0.503805
	Whitley (34)	0.819976	0.748592	0.534118	0.470834	0.925157	0.974949	0.995405	0.589907
	Odd Square (35)	0.60517	0.719453	0.5487	0.410841	0.810629	1.032147	0.792412	0.545173
	Storn Chebyshev (36)	110.0809	110.6102	111.206	111.2438	110.804	111.2777	111.2331	111.0782
	Rana (37)	0.765444	0.630744	0.720573	0.790685	0.494651	0.420802	0.508827	0.635352
	Rosenbrock 10D (38)	1.439424	1.653632	2.347183	2.602705	0.957757	1.009022	1.010809	1.312977
	Rosenbrock 30D (39)	3.097626	3.296654	4.695704	4.826502	2.919139	2.854683	3.040111	3.259971
Spherical Contours (28)	Mod Rosenbrock 1 30D (41)	2.074299	2.258507	3.206218	3.329658	1.620275	1.708489	1.713863	1.940454
	Mod Rosenbrock 1 10D (40)	5.127109	5.372779	6.55227	6.538274	4.762478	4.73372	4.879756	5.269397
	Mod Rosenbrock 2 10D (42)	2.572237	3.025688	3.83876	4.52236	2.741213	2.885202	2.972244	3.667177
	Mod Rosenbrock 2 30D (43)	6.092649	6.659937	9.762769	9.780447	7.408168	7.440367	7.869666	9.008563
	Mod Rosenbrock 10D (44)	1.474762	1.736212	2.969752	3.14926	1.65419	1.215956	1.246293	1.614434
	Rastrigin 10D (45)	1.951104	2.533597	3.761043	3.384694	1.456686	1.523017	1.565553	1.968148
	Rastrigin 30D (46)	4.830776	5.2339043	6.46077	6.402276	3.785	3.767446	4.007235	4.435857
	Schweifel 10D (47)	2.668993	2.792176	3.65441	3.708668	5.181255	5.784582	5.50395	8.112289
	Schweifel 30D (48)	5.311278	5.99978	7.368573	6.89473	11.66679	10.55872	12.24267	16.40529
	Griewangk 10D (49)	2.226263	2.299223	2.35343	1.60302	1.716284	1.632784	1.538602	1.538602
Odd Square 10D (53)	Griewangk 30D (50)	4.511517	4.48062	4.842526	4.881197	4.061791	4.089547	4.190418	3.94982
	Salomon 10D (51)	1.589076	1.872191	2.041228	2.111867	1.269741	1.286219	1.349118	1.207056
	Salomon 30D (52)	3.368417	3.665413	4.179954	4.027339	3.140949	3.179816	3.182891	3.025329
	Odd Square 10D (53)	1.705554	1.873026	2.028919	2.148582	1.398003	1.481314	1.395385	1.355451
	Whitley 10D (54)	4.940133	4.809714	5.02324	4.939917	4.455708	4.53161	4.345904	4.323864
	Whitley 30D (55)	30.15141	30.20839	32.64665	32.7992	29.87458	29.96699	30.84656	30.84656
	Rana 10D (56)	2.33994	3.373608	3.649446	3.686519	6.948161	6.730818	6.730818	9.649686
	Rana 30D (57)	7.030908	7.403769	8.525557	8.468066	16.16661	14.18463	17.36994	26.12307





Average Results (500k)	A50_N1	A50_N2	A50_N3	A50_N4	A100_N1	A100_N2	A100_N3	A100_N4	A250_N1	A250_N2	A250_N3	A250_N4	A500_N1	A500_N2	A500_N3	A500_N4	True Minima
Rosenbrock (1)	0.003103	0.004071	0.003103	0.003103	0.002952	0.003838	0.002952	0.002952	0.004722	0.001991	0.004722	0.004722	0.002433	0.000745	0.002433	0.002433	0
McCormick (2)	-1.91322	-1.91322	-1.91322	-1.91322	-1.91322	-1.91322	-1.91322	-1.91322	-1.91322	-1.91322	-1.91322	-1.91322	-1.91322	-1.91322	-1.91322	-1.91322	-1.91322
Box and Betts (3)	1.60E-08	7.92E-09	2.74E-08	4.11E-08	5.02E-09	2.65E-09	9.93E-09	1.82E-08	1.42E-09	8.41E-10	2.84E-09	5.04E-09	1.26E-09	7.73E-10	1.55E-09	2.41E-09	0
Goldstein (4)	3.000195	3.000064	3.000195	3.000195	3.00007	3.00007	3.00007	3.00007	3.000018	3.000003	3.000018	3.000018	3.000004	3.000001	3.000004	3.000004	3
Easom (5)	-0.99058	-0.99058	-0.99058	-0.99058	-0.98855	-0.98855	-0.98855	-0.98855	-0.99116	-0.98943	-0.99116	-0.99116	-0.99275	-0.99	-0.99275	-0.99275	-1
Mod Rosenbrock 1 (6)	0.103371	0.118717	0.103371	0.103371	0.101515	0.10827	0.101515	0.101515	0.11264	0.078093	0.11264	0.11264	0.077788	0.034866	0.077788	0.077788	0
Mod Rosenbrock 2 (7)	1.609354	1.865767	1.609354	1.609354	1.548259	1.778427	1.548259	1.548259	1.638526	1.305264	1.638526	1.638526	1.437713	1.040032	1.437713	1.437713	0
Bohachevsky (8)	2.057183	0.845318	2.057183	2.057183	2.36895	1.783636	2.36895	2.36895	2.988851	1.282916	2.988851	2.988851	2.315651	0.979606	2.315651	2.315651	0
Powell (9)	334641.8	334641.8	306086.1	333889.5	346363.9	346363.9	261974.1	252444.9	308141.6	148069.9	308141.6	264614.3	353240.4	353240.4	345437.4	300504.2	0
Wood (10)	15625.6	15625.6	152387.5	177527.2	153299.4	153299.4	136857	144931	148069.9	148069.9	148069.9	146880.1	160016.1	160016.1	157758.1	148177.5	0
Beale (11)	1.010008	1.010008	1.010008	1.010008	1.008326	1.163811	1.008326	1.008326	1.008326	1.008326	1.008326	1.008326	1.008326	1.008326	1.008326	1.008326	0
Engvall (12)	3.812513	3.166476	3.812513	3.812513	4.019079	3.69155	4.019079	4.019079	6.100946	4.14202	6.100946	6.100946	9.596502	3.523968	9.596502	9.596502	0
DeJong (13)	1.90E-05	3.89E-05	1.90E-05	1.90E-05	2.35E-05	1.26E-05	2.35E-05	2.35E-05	1.25E-05	1.74E-06	1.25E-05	1.25E-05	2.79E-06	5.10E-07	2.79E-06	2.79E-06	0
Rastrigin (14)	0.007214	0.007214	0.007214	0.007214	0.005747	0.005747	0.005747	0.005747	0.001979	0.001979	0.001979	0.001979	0.03256	0.03256	0.03256	0.03256	0
Schwefel (15)	-837.944	-837.939	-837.944	-837.944	-837.946	-837.935	-837.946	-837.946	-837.946	-837.941	-837.939	-837.939	-837.935	-837.935	-837.935	-837.935	-837.9658
Greiwangk (16)	0.010396	0.004314	0.010396	0.010396	0.006948	0.006948	0.006948	0.006948	0.01883	0.01883	0.01883	0.01883	0.011625	0.004291	0.011625	0.011625	0
Ackley (17)	0.049757	0.065405	0.049757	0.049757	0.049368	0.063679	0.049368	0.049368	0.056512	0.041881	0.056512	0.056512	0.042332	0.021293	0.042332	0.042332	0
Langman (18)	-1.46197	-1.46531	-1.47468	-1.46122	-1.46881	-1.46592	-1.47131	-1.46393	-1.45315	-1.46594	-1.47876	-1.47876	-1.45029	-1.4489	-1.45361	-1.47825	-1.5
Michalewicz (19)	-7.56018	-7.70489	-7.62024	-7.5703	-7.57177	-7.73343	-7.76551	-7.64992	-7.58501	-7.75205	-7.93507	-7.64076	-7.57952	-7.66925	-7.86296	-7.69616	-9.66
Brannin (20)	0.39791	0.397915	0.39791	0.39791	0.397915	0.397895	0.397915	0.397915	0.397895	0.397895	0.397895	0.397895	0.397889	0.397889	0.397889	0.397889	0.397887
Six Hump Camel (21)	-1.03163	-1.03163	-1.03163	-1.03163	-1.03163	-1.03163	-1.03163	-1.03163	-1.03163	-1.03163	-1.03163	-1.03163	-1.03163	-1.03163	-1.03163	-1.03163	-1.03163
Osborne 1 (22)	0.018524	0.020291	0.018524	0.017317	0.020261	0.020261	0.018954	0.019677	0.018602	0.019381	0.019283	0.020263	0.020657	0.021244	0.020249	0.021244	0.021244
Osborne 2 (23)	0.08072	0.079939	0.08072	0.08072	0.082568	0.080747	0.082568	0.082568	0.083507	0.083507	0.083507	0.083507	0.083507	0.083507	0.083507	0.083507	0.083507
Mod Rastrigin (24)	84.32059	84.6378	84.32059	84.32059	83.99599	83.72299	83.99599	83.99599	84.52851	87.92877	84.52851	84.52851	83.95172	87.25	83.95172	83.95172	58
Mineshaft 1 (25)	1.996568	1.837093	1.950505	1.837093	1.873964	1.745339	1.833244	1.745339	1.80949	1.690242	1.742145	1.690242	1.734571	1.777222	1.723452	1.777222	1.3805
Mineshaft 2 (26)	-1.38613	-1.40695	-1.41605	-1.40695	-1.40695	-1.403	-1.41635	-1.403	-1.41111	-1.41111	-1.41111	-1.41111	-1.41111	-1.41111	-1.41111	-1.41111	-1.41111
Mineshaft 3 (27)	-6.83501	-6.73754	-6.73754	-6.73754	-6.94582	-6.97606	-6.94582	-6.94582	-6.97606	-6.9929	-6.97606	-6.97606	-6.9929	-6.9929	-6.9929	-6.9929	-7
Spherical Contours (28)	5.19985	5.293559	5.293559	5.293559	5.293559	5.221978	5.229533	5.229533	5.229533	5.229533	5.229533	5.229533	5.229533	5.229533	5.229533	5.229533	5.229533
St (29)	7.29E-12	6.07E-11	9.87E-13	6.07E-11	9.99E-13	5.66E-13	5.66E-13	5.66E-13	7.40E-14	6.37E-07	5.66E-13	6.37E-07	5.66E-13	6.37E-07	5.66E-13	6.37E-07	5.66E-13
S2 (30)	0.528878	0.528928	0.528878	0.528878	0.528898	0.528903	0.528898	0.528898	0.528898	0.528898	0.528898	0.528898	0.528898	0.528898	0.528898	0.528898	0.528898
S3 (31)	0.049952	0.023286	0.049952	0.049952	0.049952	0.049952	0.049952	0.049952	0.049952	0.049952	0.049952	0.049952	0.049952	0.049952	0.049952	0.049952	0.049952
Downhill Step (32)	0.142096	0.142096	0.142096	0.142096	0.142096	0.142096	0.142096	0.142096	0.142096	0.142096	0.142096	0.142096	0.142096	0.142096	0.142096	0.142096	0.142096
Salomon (33)	-1.0063	-1.00647	-1.0063	-1.0063	-1.0063	-1.0063	-1.0063	-1.0063	-1.0063	-1.0063	-1.0063	-1.0063	-1.0063	-1.0063	-1.0063	-1.0063	-1.0063
Whitley (34)	104.1171	805.4443	104.1171	104.1171	899.2648	842.9661	745.1562	951.9698	1085.782	776.5357	655.7771	1341.333	1286.065	1377.325	1053.538	1181.463	0
Odd Square (35)	607.1979	577.2208	15051.4	15051.4	15051.4	15051.4	15051.4	15051.4	15051.4	15051.4	15051.4	15051.4	15051.4	15051.4	15051.4	15051.4	15051.4
Storn Chebyshev (36)	15325.97	15325.97	15325.97	15325.97	15325.97	15325.97	15325.97	15325.97	15325.97	15325.97	15325.97	15325.97	15325.97	15325.97	15325.97	15325.97	15325.97
Rana (37)	569.151	569.151	569.151	569.151	569.151	569.151	569.151	569.151	569.151	569.151	569.151	569.151	569.151	569.151	569.151	569.151	569.151
Rosenbrock 10D (38)	569.151	569.151	569.151	569.151	569.151	569.151	569.151	569.151	569.151	569.151	569.151	569.151	569.151	569.151	569.151	569.151	569.151
Mod Rosenbrock 30D (39)	569.151	569.151	569.151	569.151	569.151	569.151	569.151	569.151	569.151	569.151	569.151	569.151	569.151	569.151	569.151	569.151	569.151
Rosenbrock 100D (40)	569.151	569.151	569.151	569.151	569.151	569.151	569.151	569.151	569.151	569.151	569.151	569.151	569.151	569.151	569.151	569.151	569.151
Mod Rosenbrock 100D (41)	569.151	569.151	569.151	569.151	569.151	569.151	569.151	569.151	569.151	569.151	569.151	569.151	569.151	569.151	569.151	569.151	569.151
Mod Rosenbrock 100D (42)	569.151	569.151	569.151	569.151	569.151	569.151	569.151	569.151	569.151	569.151	569.151	569.151	569.151	569.151	569.151	569.151	569.151
Mod Rosenbrock 200D (43)	569.151	569.151	569.151	569.151	569.151	569.151	569.151	569.151	569.151	569.151	569.151	569.151	569.151	569.151	569.151	569.151	569.151
Spherical Contours 10D (44)	0.499048	0.497702	0.499048	0.499048	0.499048	0.499048	0.499048	0.499048	0.499048	0.499048	0.499048	0.499048	0.499048	0.499048	0.499048	0.499048	0.499048
Rastrigin 10D (45)	28.8054	28.3444	27.94229	28.12935	27.73721	27.73721	28.03062	27.81685	27.93084	27.57163	26.79416	26.79416	26.93062	26.93062	26.93062	27.01307	0
Rastrigin 30D (46)	180.5292	180.5292	180.5292	180.5292	179.8564	183.0733	183.0733	183.0733	183.0733	183.0733	183.0733	183.0733	183.0733	183.0733	183.0733	183.0733	183.0733
Rastrigin 100D (47)	-3787.76	-3832.12	-3852.57	-3852.57	-3852.57	-3852.57	-3852.57	-3852.57	-3852.57	-3852.57	-3852.57	-3852.57	-3852.57	-3852.57	-3852.57	-3852.57	-3852.57
Schwefel 100D (48)	-8313.56	-8313.56	-8313.56	-8313.56	-8313.56	-8313.56	-8313.56	-8313.56	-8313.56	-8313.56	-8313.56	-8313.56	-8313.56	-8313.56	-8313.56	-8313.56	-8313.56
Griewangk 30D (49)	1.449689	1.443719	1.439963	1.439963	1.439963	1.439963	1.439963	1.439963	1.439963	1.439963	1.439963	1.439963	1.439963	1.439963	1.439963	1.439963	1.439963
Griewangk 30D (50)	5.314835	5.280795	5.332219	5.332219	5.264853	5.262369	5.264853	5.264853	5.264853	5.264853	5.264853	5.264853	5.264853	5.264853	5.264853	5.264853	5.264853
Salomon 10D (51)	1.008712	0.99896	1.00996	1.00996	0.99896	0.99896	0.99896	0.99896	0.99896	0.99896	0.99896	0.99896	0.99896	0.99896	0.99896	0.99896	0.99896
Salomon 30D (52)	4.459036	4.432628	4.372628	4.372628	4.296511	4.296511	4.296511	4.296511	4.296511	4.296511	4.296511	4.296511	4.296511	4.296511	4.296511	4.296511	4.296511
Odd Square 10D (53)	0.16396	-0.32624	-0.32624	-0.32624	-0.32624	-0.32624	-0.32624	-0.32624	-0.32624	-0.32624	-0.32624	-0.32624	-0.32624	-0.32624	-0.32624	-0.32624	-0.32624
Whitley 10D (54)	3517912	4191487	3993711	4014109</													

















# APPENDIX E1: AVG. RESULTS FOR SMOA WITH SIMPLEX VEG. STATE

	A50_N1	A50_N2	A50_N3	A50_N4	A100_N1	A100_N2	A100_N3	A100_N4	A250_N1	A250_N2	A250_N3	A250_N4	A500_N1	A500_N2	A500_N3	A500_N4	True Minima
Average Results (1M)																	
Rosenbrock (1)	5.71925	6.430246	5.71925	5.71925	0.333629	0.506339	0.333629	0.333629	0.347691	0.126845	0.347691	0.347691	0.071773	0.325206	0.071773	0.071773	0
McCormic (2)	-1.91322	-1.90927	-1.91322	-1.91322	-1.91322	-1.91205	-1.91322	-1.91322	-1.90664	-1.90664	-1.91301	-1.91301	-1.91293	-1.90616	-1.91293	-1.91293	-1.9133
Box and Betts (3)	6.00E-05	8.22E-05	5.44E-05	3.12E-05	3.62E-05	5.93E-05	2.96E-05	2.51E-05	2.58E-05	2.42E-05	1.81E-05	8.35E-06	1.83E-05	2.88E-05	9.52E-06	7.01E-06	0
Goldstein (4)	3	4.979294	3	3.12E-05	3.014856	3.546343	3.014856	3.014856	3.203862	3.842159	3.203862	3.203862	3.055906	4.243938	3.055906	3.055906	3
Easom (5)	-0.98532	-0.97542	-0.98532	-0.98532	-0.98867	-0.97931	-0.98867	-0.98867	-0.98867	-0.98867	-0.98867	-0.98867	-0.97933	-0.94372	-0.97933	-0.97933	-1
Mod Rosenbrock 1 (6)	0.004598	0.01134	0.004598	0.004598	0.008621	0.259123	0.008621	0.008621	0.028829	0.104769	0.028829	0.028829	0.102666	0.692315	0.102666	0.102666	0
Mod Rosenbrock 2 (7)	0.016098	0.061151	0.016098	0.016098	0.326659	0.650664	0.326659	0.326659	0.148164	0.265396	0.148164	0.148164	0.278731	0.998177	0.278731	0.278731	0
Bohachevsky (8)	0	9.53E-11	0	1.53E-11	3.25E-07	1.53E-11	1.53E-11	1.53E-11	1.27E-05	0.144593	1.27E-05	1.27E-05	0.025032	0.025251	0.025032	0.025032	0
Powell (9)	7064622	7064622	7064622	7064622	2994029	15655596	14236744	16028046	6921145	6921145	6921145	6921145	415785.7	415785.7	415785.7	415785.7	0
Wood (10)	4.43E+08	4.43E+08	4.43E+08	4.43E+08	649.7706	9.12E-09	649.7706	649.7706	2.585032	2.585032	2.585032	2.585032	8.61965	8.61965	8.61965	8.61965	0
Beale (11)	941.9017	941.9017	941.9017	941.9017	9.12E-07	9.12E-07	9.12E-07	9.12E-07	1.07E-07	1.07E-07	1.07E-07	1.07E-07	4.31E-08	4.31E-08	4.31E-08	4.31E-08	0
Engvall (12)	0	1.33E-17	0	0	6.81E-18	1.21E-17	6.81E-18	6.81E-18	2.87E-17	2.87E-17	2.87E-17	2.87E-17	1.85E-17	1.85E-17	1.85E-17	1.85E-17	0
DeJong (13)	6.76E-18	8.63E-18	6.76E-18	6.76E-18	0.04303	0.467511	0.04303	0.04303	0.590448	1.163442	0.590448	0.590448	0.70897	0.754688	0.70897	0.70897	0
Rastrigin (14)	0.01316	0.104444	0.01316	0.01316	-837.966	-837.966	-837.966	-837.966	-837.966	-837.966	-837.966	-837.966	-837.966	-837.966	-837.966	-837.966	-837.966
Schwefel (15)	-836.699	-831.076	-836.699	-836.699	0.00187	0.001833	0.00187	0.00187	0.008024	0.008024	0.008024	0.008024	0.013279	0.012655	0.013279	0.013279	0
Griewangk (16)	0.00187	0.001833	0.00187	0.00187	1.74E-12	4.28E-12	1.74E-12	1.74E-12	7.69E-07	7.69E-07	7.69E-07	7.69E-07	0.036614	0.019651	0.036614	0.036614	0
Ackley (17)	4.44E-16	4.44E-16	4.44E-16	4.44E-16	-0.54883	-0.54883	-0.54883	-0.54883	-0.54883	-0.54883	-0.54883	-0.54883	-0.63108	-0.63108	-0.63108	-0.63108	-1.5
Langman (18)	-0.48029	-0.57164	-0.48029	-0.48029	-0.60694	-0.60694	-0.60694	-0.60694	-0.60694	-0.60694	-0.60694	-0.60694	-0.60694	-0.60694	-0.60694	-0.60694	-0.60694
Michalewicz (19)	-5.25918	-5.67577	-5.25918	-5.25918	-5.81572	-6.0101	-5.81572	-5.81572	-6.0101	-6.129	-6.0101	-6.0101	-6.129	-6.0101	-6.129	-6.129	-6.129
Bratin (20)	0.397887	0.397887	0.397887	0.397887	0.402672	0.399437	0.402672	0.402672	0.39793	0.396066	0.39793	0.39793	0.39793	0.399363	0.39793	0.39793	0.397887
Six Hump Camel (21)	-1.03163	-1.02949	-1.03163	-1.03163	-1.03163	-1.03163	-1.03163	-1.03163	-1.03141	-1.03141	-1.03141	-1.03141	-1.03135	-1.02539	-1.03135	-1.03135	-1.0316
Osborne 1 (22)	1.065767	1.065302	1.068818	1.068818	1.008359	1.004042	1.008359	1.008359	0.889724	0.889724	0.889724	0.889724	0.795275	0.729511	0.795275	0.795275	0.795275
Osborne 2 (23)	2.27667	1.979744	1.90211	2.192205	1.324019	1.059813	1.324019	1.324019	0.495702	0.495702	0.495702	0.495702	0.441517	0.402699	0.441517	0.441517	0.402699
Mod Rastrigin (24)	60.82758	61.24061	60.82758	60.82758	60.81281	60.81281	60.81281	60.81281	61.39277	68.87264	61.39277	61.39277	64.53013	66.34871	64.53013	64.53013	58
Mineshaft 1 (25)	1.427722	2.008509	1.610372	2.008509	1.523942	2.208399	1.91734	2.208399	1.695217	2.262597	2.039713	2.262597	1.830054	2.239913	2.223343	2.239913	1.3805
Mineshaft 2 (26)	-1.39697	-1.25805	-1.38183	-1.25805	-1.39383	-1.16345	-1.2687	-1.16345	-1.35342	-1.27735	-1.27735	-1.27735	-1.34968	-1.35764	-1.28517	-1.35764	-1.4163555
Mineshaft 3 (27)	-6.17221	-4.07246	-6.17221	-6.17221	-5.89468	-6.39274	-5.89468	-5.89468	-6.39274	-6.39274	-6.39274	-6.39274	-6.39274	-6.39274	-6.39274	-6.39274	-6.39274
Spherical Contours (28)	166.6615	151.1821	166.4667	166.4667	5.90E-05	0.005969	128.7658	128.7658	100.9274	22.87757	89.3173	86.10068	71.47292	16.29965	36.97578	66.22102	0
S1 (29)	5.90E-05	0.000524	5.90E-05	5.90E-05	3.25E-06	0.000169	0.001005	0.000169	2.25E-05	2.25E-05	2.25E-05	2.25E-05	1.94E-05	9.22E-06	9.07E-05	9.22E-06	0
S2 (30)	2	2	2	2	2	2	2	2	2.000005	2.00001	2.000005	2.000005	2.000003	2.000003	2.000003	2.000003	2
S3 (31)	0.543429	0.562731	0.543429	0.543429	0.538762	0.542729	0.538762	0.538762	0.53625	0.53625	0.53625	0.53625	0.531747	0.533163	0.531747	0.531747	0.5289
Downhill Step (32)	9	9.016	9	9	9	9.049	9	9	9.019	9.019	9.019	9.019	9	9.048	9	9	9
Salomon (33)	0.073428	0.073937	0.073428	0.073428	0.059847	0.061034	0.059847	0.059847	0.084881	0.080066	0.084881	0.084881	0.092818	0.090474	0.092818	0.092818	0
Whitley (34)	0.068414	0.128892	0.068414	0.068414	0.011623	0.021317	0.011623	0.011623	0.001405	0.001132	0.001405	0.001405	-0.94724	-0.84285	-0.94724	-0.94724	-1.14383
Odd Square (35)	-0.98099	-0.92423	-0.98099	-0.98099	-0.97118	-0.87139	-0.97118	-0.97118	-0.95523	-0.80389	-0.95523	-0.95523	-0.94724	-0.84285	-0.94724	-0.94724	-0.94724
Storn Chebyshev (36)	246685.1	236049.3	281329.5	237209.9	136897	136971.2	13374.9	126371.5	50693.71	52845.35	52237.92	49778.33	8852.954	16093.39	16533.31	10213.68	0
Rana (37)	-912.348	-890.488	-912.348	-912.348	-936.351	-920.18	-936.351	-936.351	-958.33	-950.223	-958.33	-958.33	-972.952	-966.183	-972.952	-972.952	-1023.416
Rosenbrock 10D (38)	999257.8	852779.1	698395.9	517122.5	55654.94	14783.68	25967.77	117584.7	123.8326	144.4054	748.4898	346.6201	63.38196	12.19135	4316.886	7130.904	0
Rosenbrock 30D (39)	17036226	15385246	13298451	13298451	8929816	3553343	8607557	8607557	3698814	414144.2	5072870	4583556	3198035	189435.8	371007.2	3087984	0
Mod Rosenbrock 1 10D (40)	5529.514	4332.924	2674.968	2949.714	1633.49	2524.594	1264.562	2336.666	462.5994	781.3919	686.2013	680.0253	317.4758	246.5524	384.3532	330.8152	0
Mod Rosenbrock 1 30D (41)	147583.5	148008.8	143909.5	143909.5	118534	84547.15	98968.76	98968.76	56357.01	25124.98	59110.76	64038.82	47570.83	24858.89	44877.35	55225.51	0
Mod Rosenbrock 2 10D (42)	7.389795	6.534509	8.370551	7.389795	2.391558	3.159784	2.544374	2.163157	1.606749	4.292219	1.606749	1.606749	2.325334	0.331351	0.494818	0.871287	0
Mod Rosenbrock 2 30D (43)	4.582732	3.611158	7.783732	4.582732	2.710691	2.386913	5.13334	5.13334	1.762726	1.345021	1.844195	2.671944	1.67811	1.499332	1.606879	2.585766	0
Spherical Contours 10D (44)	0.288197	1.248027	1.403077	1.142813	6.96E-08	1.13E-08	4.88E-05	8.24E-12	0.007667	8.32E-12	9.19E-16	0.619323	8.43E-16	8.41E-16	8.46E-16	8.71E-16	0
Rastrigin 10D (45)	100.8853	96.68617	96.36191	92.30648	87.8834	63.32863	79.68325	78.90729	72.94699	46.181	41.68278	53.83201	61.65795	37.0766	35.55448	40.07102	0
Rastrigin 30D (46)	428.8088	2646.17	400.926	400.926	395.505	334.528	379.4556	379.4556	391.288	294.4175	270.5268	349.8121	345.3397	260.8311	216.4292	318.2817	0
Schwefel 10D (47)	-2538.28	-2646.17	-2625.2	-2582.33	-2805.81	-2739.29	-2804.36	-2745.9	-2961.22	-2965.57	-2965.1	-2965.1	-3070.73	-3044.37	-3063.51	-3031.83	-4189.829
Schwefel 30D (48)	-5006.98	-4914.4	-4785.15	-4785.15	-5552.36	-5644.59	-5352.88	-5352.88	-6150.91	-6057.21	-6295.12	-5668.12	-6057.21	-6007.73	-6174.04	-6271.78	-12569.487
Griewangk 10D (49)	0.338405	0.780375	0.554305	0.819576	0.195024	0.106038	0.23341	1.481827	0.043042	0.330673	0.051591	0.05054	0.032082	0.053848	0.038509	0.019521	0
Griewangk 30D (50)	148.1552	146.3882	144.9383	144.9383	101.8887	55.76118	92.37471	92.37471	67.81963	1.0265	68.49633	66.50014	55.81955	10.10948	27.4715	52.18428	0
Salomon 10D (51)	2.777451	1.977969	2.306428	2.514784	2.928204	2.13018	2.098167	4.271618	2.487501	1.747262	1.61202	3.943255	1.885866	1.525056	1.431969	2.80092	0
Salomon 30D (52)	12.02822	8.854137	9.456537	9.456537	10.46848	7.648776	8.259926	8.259926	10.55434	6.351501	5.067376	8.964623	6.903407	5.266752	4.553302	9.195895	0
Odd Square 10D (53)	-0.06199	-0.11517	-0.0942	-0.0925	-0.0781	-0.17504	-0.24836	-0.24836	-0.09988	-0.25181	-0.36284	-0.18221	-0.12834	-0.34585	-0.42408	-0.29621	-1.14383
Whitley 10D (54)	2.74E+14	2.63E+14	2.63E+14	1.91E+14	1.77E+14	3.9E+13	3.67E+13	3.67E+13	1.16E+09	1.							

Average Results (500k)	A50_N1	A50_N2	A50_N3	A50_N4	A100_N1	A100_N2	A100_N3	A100_N4	A250_N1	A250_N2	A250_N3	A250_N4	A500_N1	A500_N2	A500_N3	A500_N4	True Minima
Rosenbrock (1)	8.693761	6.507592	8.693761	8.693761	0.34613	1.156063	0.34613	0.34613	0.364039	0.128728	0.364039	0.364039	0.077676	0.331594	0.077676	0.077676	0
McCormic (2)	-1.91322	-1.90927	-1.91322	-1.91322	-1.91322	5.93E-05	-1.91322	-1.91322	-1.91301	-1.90664	-1.91301	-1.91301	-1.91293	-1.90616	-1.91293	-1.91293	-1.9133
Box and Betts (3)	6.00E-05	8.33E-05	5.44E-05	3.22E-05	3.62E-05	5.93E-05	2.96E-05	2.70E-05	2.58E-05	2.90E-05	2.58E-05	2.58E-05	1.85E-05	2.90E-05	1.85E-05	9.55E-06	8.08E-06
Goldstein (4)	3	5.019214	3	3	3	3.014856	3.014856	3.014856	3.014856	3.99175	3.203862	3.203862	3.203862	3.055906	3.055906	3.055906	3
Easom (5)	-0.96065	-0.935	-0.96065	-0.96065	-0.97076	-0.92858	-0.97076	-0.97076	-0.97076	-0.86726	-0.91312	-0.91312	-0.91312	-0.93207	-0.93207	-0.93207	-1
Mod Rosenbrock 1 (6)	0.015023	0.027853	0.015023	0.015023	0.228864	0.966437	0.228864	0.228864	0.78481	0.235994	0.78481	0.78481	0.138617	0.695192	0.138617	0.138617	0
Mod Rosenbrock 2 (7)	0.102851	0.15343	0.102851	0.102851	0.298143	0.228813	0.298143	0.298143	0.347038	0.735653	0.347038	0.347038	0.381745	1.001947	0.381745	0.381745	0
Bohachevsky (8)	3.33E-18	1.03E-09	3.33E-18	3.33E-18	4.41E-07	3.33E-07	4.41E-07	4.41E-07	1.27E-05	0.144596	1.27E-05	1.27E-05	0.025032	0.025251	0.025032	0.025032	0
Powell (9)	7004622	7004622	7004622	6806486	2994029	2994029	2994029	2994029	596976.1	596976.1	596976.1	596976.1	687890.1	415785.7	687890.1	415785.7	0
Wood (10)	4.43E+08	4.43E+08	4.43E+08	4.44E+08	47826.81	15655596	14236744	16028046	6921145	6921145	6921145	6921145	10724215	10724215	10719521	10694623	0
Beale (11)	6622.922	6622.922	6622.922	6622.922	4.7828.34	47826.81	47828.34	47828.34	2.659997	2.77877	2.659997	2.659997	8.61965	8.61965	8.61965	8.61965	0
Engvall (12)	0	9.52E-18	0	9.52E-18	7.88E-07	8.86E-17	7.88E-07	7.88E-07	0.000217	3.88E-06	0.000217	0.000217	4.31E-08	4.30E-08	4.31E-08	4.31E-08	0
DeJong (13)	0	1.24E-16	0	1.24E-16	0	0	0	0	1.79E-09	2.87E-17	1.79E-09	1.79E-09	1.86E-17	1.96E-17	1.86E-17	1.86E-17	0
Rastrigin (14)	0.027847	0.027847	0.027847	0.027847	0.28735	0.775381	0.28735	0.28735	0.758914	1.375346	0.758914	0.758914	0.758914	0.836617	0.754478	0.754478	0
Schwefel (15)	-833.588	-826.738	-833.588	-833.588	-836.103	-836.108	-836.108	-836.108	-837.912	-837.963	-837.912	-837.912	-837.966	-837.966	-837.966	-837.966	-837.9658
Griewangk (16)	0.003885	0.004351	0.003885	0.003885	0.010043	0.008342	0.010043	0.010043	0.018835	0.01557	0.018835	0.018835	0.013663	0.013024	0.013663	0.013663	0
Ackley (17)	3.47E-07	5.51E-16	3.47E-07	3.47E-07	7.75E-11	6.23E-08	7.75E-11	7.75E-11	7.69E-07	0.003014	7.69E-07	7.69E-07	0.036614	0.019851	0.036614	0.036614	0
Langman (18)	-0.43056	-0.52908	-0.57662	-0.56613	-0.45764	-0.4995	-0.68939	-0.61797	-0.53145	-0.55095	-0.66583	-0.71164	-0.58532	-0.60492	-0.66752	-0.84073	-1.5
Michalewicz (19)	-5.23109	-5.61928	-5.83049	-5.72357	-5.76326	-5.94671	-6.04806	-6.19231	-6.41087	-6.54511	-6.67265	-6.71145	-6.62867	-6.76435	-7.00593	-7.0582	-9.66
Brannin (20)	0.397887	0.397887	0.397887	0.397887	0.403178	0.399437	0.403178	0.403178	0.39793	0.398066	0.39793	0.39793	0.3979	0.393963	0.3979	0.3979	0.397887
Six Hump Camel (21)	-1.03163	-1.02949	-1.03163	-1.03163	-1.03163	-1.03134	-1.03163	-1.03163	-1.03141	-1.0243	-1.03141	-1.03141	-1.03135	-1.02538	-1.03135	-1.03135	-1.0316
Osborne 1 (22)	1.066367	1.065302	1.068818	1.069663	1.008359	1.000402	0.997421	1.00396	0.889724	0.892939	0.889793	0.890718	0.795725	0.731618	0.764425	0.739566	5.46E-05
Osborne 2 (23)	2.2667	1.979744	1.900211	1.922205	1.388521	1.06772	1.055201	1.158441	0.510809	0.630688	0.443994	0.787399	0.432119	0.425723	0.392258	0.395281	0.0402
Mod Rastrigin (24)	60.8702	60.8702	60.8702	61.40923	69.61056	61.40923	61.40923	61.40923	64.81563	71.44996	64.81563	64.81563	64.84966	67.23444	64.84966	64.84966	58
Mineshaft 1 (25)	1.427722	2.24147	1.73892	2.24147	1.543395	2.212828	1.91734	2.212828	1.704275	2.263818	2.039889	2.263818	1.830054	2.241417	2.262224	2.241417	1.3805
Mineshaft 2 (26)	-1.39606	-1.10161	-1.33856	-1.10161	-1.37913	-1.14666	-1.26544	-1.14666	-1.35164	-1.27304	-1.21439	-1.27304	-1.34968	-1.3565	-1.2651	-1.3565	-1.4163535
Mineshaft 3 (27)	-6.09221	-0.05246	-6.09221	-6.09221	-5.77479	-3.77479	-5.77479	-5.77479	-4.29922	-3.56896	-4.29922	-4.29922	-5.0928	-4.18593	-5.0928	-5.0928	-7
Spherical Contours (28)	166.7803	154.7766	166.4691	166.4691	112.4073	76.46544	130.0627	130.0627	107.0929	105.4382	132.5818	132.5818	33.51228	51.15185	97.52896	97.52896	0
S1 (29)	3.58E-22	0.00186	0.007241	0.00186	3.25E-06	0.00959	0.001015	0.00959	2.25E-05	9.20E-05	0.002056	9.20E-05	1.39E-05	1.29E-05	2.000003	2.000003	2
S2 (30)	0.547226	0.539546	0.547226	0.547226	0.539546	0.547226	0.539546	0.539546	0.539546	0.539546	0.539546	0.539546	0.539546	0.539546	0.539546	0.539546	0.5289
S3 (31)	0.547226	0.539546	0.547226	0.547226	0.539546	0.547226	0.539546	0.539546	0.539546	0.539546	0.539546	0.539546	0.539546	0.539546	0.539546	0.539546	0.5289
Downhill Step (32)	0.08657	0.097063	0.08657	0.08657	0.08657	0.08657	0.08657	0.08657	0.08657	0.08657	0.08657	0.08657	0.08657	0.08657	0.08657	0.08657	9
Salomon (33)	0.09883	0.148817	0.09883	0.09883	0.012023	0.055102	0.012023	0.012023	0.001406	0.005191	0.001406	0.001406	0.013682	0.002182	0.013682	0.013682	0
Whitley (34)	-0.92459	-0.85218	-0.92459	-0.92459	-0.92459	-0.92459	-0.92459	-0.92459	-0.92459	-0.92459	-0.92459	-0.92459	-0.92459	-0.92459	-0.92459	-0.92459	-1.14383
Odd Square (35)	246685.1	236049.3	281329.5	236049.3	281329.5	236049.3	281329.5	236049.3	281329.5	236049.3	281329.5	281329.5	281329.5	236049.3	281329.5	281329.5	0
Storn Chebyshev (36)	-902.541	-882.511	-902.541	-902.541	-902.541	-902.541	-902.541	-902.541	-902.541	-902.541	-902.541	-902.541	-902.541	-902.541	-902.541	-902.541	-1023.416
Rana (37)	999257.8	852779.1	698395.9	520177.4	55654.94	14783.68	25967.77	117584.7	123.8326	144.4566	748.4898	348.719	67.56159	12.55008	4316.976	7132.304	0
Rosenbrock 10D (38)	17044957	15418172	13369281	13369281	9762241	3728512	8876080	8876080	6595924	5224051	585.2013	585.2013	8531430	563895	1251348	4870246	0
Rosenbrock 30D (39)	5542.603	4332.924	2674.968	2949.714	1660.648	2524.594	1264.562	2336.666	462.5994	781.5445	586.2013	685.8687	322.7228	247.2759	385.7646	336.3267	0
Mod Rosenbrock 1 10D (40)	148936.6	148589.8	144035.3	144035.3	121280.6	85638.27	102341.4	102341.4	78769.74	30596.89	82381.59	78443.19	106435.1	42600.82	69371.35	80276.4	0
Mod Rosenbrock 1 30D (41)	8.732877	7.394498	6.57824	8.370551	2.926819	2.926819	2.926819	2.926819	2.801467	4.303665	1.609378	2.325362	0.729114	0.334406	0.495688	0.871372	0
Mod Rosenbrock 2 10D (42)	4.760328	3.75623	8.485173	8.485173	3.040714	2.597069	5.437896	5.437896	3.108426	2.443423	2.499182	2.826391	3.014361	2.485662	2.944943	3.882828	0
Mod Rosenbrock 2 30D (43)	0.288197	1.248027	1.403077	1.142813	6.96E-08	1.13E-08	4.68E-05	8.24E-12	0.007667	8.32E-12	9.26E-16	0.619323	8.92E-16	8.81E-16	9.15E-16	2.67E-09	0
Spherical Contours 10D (44)	101.6058	97.3615	93.88642	88.38452	64.70054	82.0233	82.0233	82.0233	73.79282	46.45614	42.10208	55.52596	37.98271	36.22847	41.25168	41.25168	0
Rastrigin 10D (45)	429.1251	377.1341	401.2693	398.765	336.1478	381.3069	381.3069	381.3069	399.2552	297.5594	273.1063	353.175	365.2617	288.5935	245.1957	331.3118	0
Rastrigin 30D (46)	2538.28	2645.98	-2625.2	-2582.33	-2805.81	-2725.42	-2801.19	-2745.9	-2958.32	-2960.46	-2964.21	-2948.14	-3053.11	-3043.95	-3057.39	-3030.7	-4189.829
Schwefel 10D (47)	-5006.85	-4893.69	-4777.47	-4777.47	-4777.47	-4777.47	-4777.47	-4777.47	-4777.47	-4777.47	-4777.47	-4777.47	-4777.47	-4777.47	-4777.47	-4777.47	-12569.487
Schwefel 30D (48)	0.080375	0.080375	0.080375	0.080375	0.080375	0.080375	0.080375	0.080375	0.080375	0.080375	0.080375	0.080375	0.080375	0.080375	0.080375	0.080375	0
Griewangk 10D (49)	149.2662	146.6398	145.4176	145.4176	145.4176	145.4176	145.4176	145.4176	145.4176	145.4176	145.4176	145.4176	145.4176	145.4176	145.4176	145.4176	0
Griewangk 30D (50)	3.969749	2.664481	4.59826	5.020375	2.928204	2.130393	2.104266	4.607477	98.59677	21.08639	89.51036	82.62121	100.9833	25.6105	51.51071	74.18067	0
Salomon 10D (51)	12.02822	8.854137	9.514885	10.51124	7.656887	8.274674	8.274674	8.274674	10.57303	6.353849	5.145742	8.976707	7.032698	5.302349	4.561777	9.277582	0
Salomon 30D (52)	-0.0615	-0.11376	-0.09052	-0.0841	-0.17488	-0.24821	-0.24821	-0.24821	-0.17488	-0.25181	-0.17402	-0.17402	-0.17402	-0.34532	-0.42337	-0.28938	-1.14383
Odd Square 10D (53)	2.74E+14	2.63E+14	2.65E+14	2.65E+14	1.91E+14	1.77E+14	3.9E+13	3.67E+13	1.16E+09	1.05E+12	1.81E+11	2.49E+11	2.49E+11	5.66E+13	9.9E+14	17980198	0
Whitley 10D (54)	5.72E+15	1.80E+15	3.55E+15	3.55E+15	4.62E+14	4.62E+14	1.55E+15	1.55E+15	2.24E+15	5.66E+13	4.9E+14	6					

Average Results (100k)	A50_N1	A50_N2	A50_N3	A50_N4	A100_N1	A100_N2	A100_N3	A100_N4	A250_N1	A250_N2	A250_N3	A250_N4	A500_N1	A500_N2	A500_N3	A500_N4	True Minima
Rosenbrock (1)	8.733811	6.534812	8.733811	8.733811	0.458707	1.385009	0.458707	0.458707	0.587626	0.137834	0.587626	0.587626	0.097617	1.013599	0.097617	0.097617	0
McCormic (2)	-1.91322	-1.90335	-1.91322	-1.91322	-1.91322	-1.91205	-1.91322	-1.91322	-1.91301	-1.90629	-1.91301	-1.91301	-1.91288	-1.90451	-1.91288	-1.91288	-1.9133
Box and Betts (3)	6.22E-05	8.34E-05	5.48E-05	3.45E-05	3.75E-05	6.00E-05	3.24E-05	2.85E-05	3.16E-05	3.20E-05	2.19E-05	1.05E-05	2.50E-05	3.80E-05	1.05E-05	1.50E-05	0
Goldstein (4)	4.057764	6.046018	4.057764	4.057764	4.057764	4.437346	4.014856	3.014856	3.014856	3.203862	3.203862	3.203862	3.132947	4.615813	3.132947	3.132947	3
Easom (5)	-0.84938	-0.75361	-0.84938	-0.84938	-0.84938	-0.87342	-0.87342	-0.87342	-0.87342	-0.87342	-0.87342	-0.87342	-0.86895	-0.75042	-0.86895	-0.86895	-1
Mod Rosenbrock 1 (6)	5.043978	5.120915	5.043978	5.043978	5.043978	1.726498	1.726498	1.726498	1.726498	1.726498	0.785322	0.785322	0.186887	0.69572	0.186887	0.186887	0
Mod Rosenbrock 2 (7)	4.241897	4.510911	4.241897	4.241897	4.241897	1.729629	1.729629	1.729629	1.729629	1.729629	0.235997	0.235997	0.186887	0.69572	0.186887	0.186887	0
Bobachevsky (8)	0.013849	0.013849	0.013849	0.013849	0.005687	0.005687	0.005687	0.005687	0.005687	0.005687	0.348882	0.348882	0.413099	0.68768	0.413099	0.413099	0
Powell (9)	7004622	7004622	7004622	7004622	6806486	2994029	2994029	2994029	2994029	2994029	619403.2	619403.2	470465.4	470465.4	470465.4	470465.4	0
Wood (10)	4.43E+08	4.43E+08	4.43E+08	4.43E+08	15684317	15684317	14236744	14236744	6921145	6921145	6921145	6921145	10774919	10774919	10774919	10745013	0
Beale (11)	23116.49	8042.363	23116.49	23116.49	47828.92	47828.92	47828.92	47828.92	26.58685	26.58685	26.58685	26.58685	8.660151	8.660151	8.660151	8.660151	0
Engvall (12)	2.09E+08	2.09E+08	2.09E+08	2.09E+08	0.029512	1.18E-05	0.029512	0.029512	0.000217	0.000217	0.000217	0.000217	4.31E-08	4.30E-08	4.31E-08	4.31E-08	0
DeJong (13)	2.97E-09	9.05E-05	2.97E-09	2.97E-09	7.88E-07	9.24E-17	7.88E-07	7.88E-07	1.79E-09	1.79E-09	1.79E-09	1.79E-09	2.05E-17	2.05E-17	2.05E-17	2.05E-17	0
Rastrigin (14)	1.300161	1.891408	1.300161	1.300161	1.347032	2.006126	1.347032	1.347032	0.987612	0.987612	0.987612	0.987612	0.836547	0.845276	0.836547	0.836547	0
Schwefel (15)	-806.921	-795.207	-806.921	-806.921	-829.934	-827.941	-829.934	-829.934	-836.912	-837.819	-836.912	-836.912	-837.966	-836.774	-837.966	-837.966	-837.9658
Greiwangk (16)	0.05233	0.046952	0.05233	0.05233	0.043173	0.036284	0.043173	0.043173	0.019861	0.016929	0.019861	0.019861	0.014453	0.014453	0.014453	0.014453	0
Ackley (17)	0.000151	0.000209	0.000151	0.000151	6.39E-08	6.25E-08	6.39E-08	6.39E-08	7.72E-07	0.003014	7.72E-07	7.72E-07	0.052912	0.07888	0.052912	0.052912	0
Langeman (18)	-0.31775	-0.37415	-0.40055	-0.44277	-0.40018	-0.41113	-0.52256	-0.52605	-0.49119	-0.50213	-0.57157	-0.65698	-0.5186	-0.54068	-0.57129	-0.70405	-1.5
Michalewicz (19)	-5.14986	-5.39289	-5.57917	-5.42748	-5.68833	-5.69455	-5.7761	-5.74919	-6.1972	-6.21617	-6.00351	-6.00351	-5.52365	-5.97405	-6.40214	-5.75861	-9.66
Brannin (20)	0.419308	0.412768	0.419308	0.419308	0.399437	0.403178	0.403178	0.403178	0.39793	0.398066	0.39793	0.39793	0.3979	0.399363	0.3979	0.3979	0.397887
Six Hump Camel (21)	-1.03163	-1.01439	-1.03163	-1.03163	-1.03134	-1.03134	-1.03163	-1.03163	-1.03141	-1.02409	-1.03141	-1.03141	-1.03135	-1.02474	-1.03135	-1.03135	-1.0316
Osborne 1 (22)	1.066367	1.065652	1.069167	1.069663	1.003191	1.001338	1.001338	1.00336	0.897829	0.910211	0.91686	0.913145	0.849159	0.834375	0.856338	0.828166	5.46E-05
Osborne 2 (23)	2.27667	2.022382	1.931283	2.309363	1.461861	1.274652	1.190519	1.268005	0.972166	1.324128	0.915116	1.261285	1.621948	1.687301	1.540294	1.562009	0.0402
Mod Rastrigin (24)	71.17316	75.82064	71.17316	71.17316	68.3314	68.3314	68.3314	68.3314	72.37996	75.0089	72.37996	72.37996	77.90728	77.3971	77.90728	77.90728	58
Mineshaft 1 (25)	1.505628	2.247644	1.912828	2.247644	1.690044	2.21369	1.920639	1.21369	1.720952	2.272917	2.058074	2.272917	1.8385	2.273999	2.226424	2.273999	1.3805
Mineshaft 2 (26)	-1.37547	-1.09189	-1.3125	-1.348	-1.348	-1.13493	-1.26544	-1.13493	-1.34703	-1.24992	-1.2087	-1.24992	-1.34824	-1.34946	-1.28446	-1.34946	-1.4163535
Mineshaft 3 (27)	-7.8317	-2.98309	-4.78317	-4.78317	-4.78317	-2.44175	-4.37447	-4.37447	-4.15368	-3.36322	-4.15368	-4.15368	-4.487	-3.72016	-4.487	-4.487	-7
Spherical Contours (28)	183.7017	169.9385	174.288	174.288	177.8608	106.9693	147.2501	147.2501	194.4426	63.7373	137.7152	130.1522	174.3043	78.74274	94.75032	121.6056	0
S1 (29)	4.59E-06	0.014276	0.007241	0.014276	3.25E-06	0.00161	0.001015	0.00161	2.25E-05	2.000005	0.000258	0.000135	1.94E-05	1.73E-05	9.94E-05	1.73E-05	0
S2 (30)	2	2.000003	2	2	2.000014	2.000014	2.000014	2.000014	2.000005	2.00001	2.000005	2.000005	2.000003	2.000003	2.000003	2.000003	2
S3 (31)	0.550319	0.567699	0.550319	0.550319	0.548788	0.543725	0.548788	0.548788	0.534867	0.538362	0.538362	0.538362	0.534335	0.534335	0.534335	0.534335	0.5289
Downhill Step (32)	9	9.029	9	9	9.078	9.078	9	9	9.116	9.152	9.116	9.116	9.069	9.069	9.069	9.069	9
Salomon (33)	0.175129	0.232743	0.175129	0.175129	0.208928	0.227425	0.208928	0.208928	0.176679	0.184526	0.176679	0.176679	0.143498	0.155107	0.143498	0.143498	0
Whitley (34)	0.317088	0.336746	0.317088	0.317088	0.08855	0.085489	0.08855	0.08855	0.002264	0.007236	0.002264	0.002264	0.058944	0.037876	0.058944	0.058944	0
Odd Square (35)	-0.85531	-0.78514	-0.85531	-0.85531	-0.85882	-0.80482	-0.88882	-0.88882	-0.87947	-0.76806	-0.87947	-0.87947	-0.88285	-0.83823	-0.88285	-0.88285	-1.14383
Storn Chebyshev (36)	246685.1	239039.2	281614.2	238883.9	135944.2	137066.7	134629.6	126371.5	86595.45	87071.63	105438.4	79791.99	75755.28	67704.75	67335.16	69050.74	0
Rana (37)	-883.582	-867.679	-883.582	-883.582	-904.877	-896.994	-904.877	-904.877	-944.716	-938.071	-944.716	-944.716	-961.42	-959.576	-961.42	-961.42	-1023.416
Rosenbrock 10D (38)	999257.8	852779.1	698395.9	520182.9	55667.84	14796.78	25970.22	117867.5	1525.152	385.7047	1321.716	1352.026	191781.4	33165.39	235043.6	60714.76	0
Rosenbrock 30D (39)	1967891.1	1646402.1	1532704.0	14931864	6191315	10774149	16638050	3007218	9491500	8438932	15758794	3609461	4249258	7153496	0	0	0
Mod Rosenbrock 1 10D (40)	5549.365	4529.728	2675.409	2951.771	1742.819	2532.502	1268.211	2369.432	903.8052	806.2559	661.1551	747.7678	3077.651	2019.825	2883.475	2410.562	0
Mod Rosenbrock 1 30D (41)	170367.1	164586.6	150259.7	150259.7	159192	118575.6	129043.3	129043.3	157340.1	66348.82	116669.5	109036.2	510434	90857.42	106576.6	99212.15	0
Mod Rosenbrock 2 10D (42)	8.780211	7.459895	6.619547	8.41058	2.442525	3.166994	2.946276	2.40343	4.924816	3.063107	5.090162	5.090162	9.960865	11.2935	8.84355	9.325355	0
Mod Rosenbrock 2 30D (43)	7.355164	5.730425	11.30162	6.839081	5.946199	7.59988	7.59988	7.59988	7.541485	5.14466	5.929589	7.131956	6.093098	4.934047	8.431204	8.431204	0
Spherical Contours 10D (44)	0.811456	1.248027	1.598791	1.272283	0.081451	1.13E-08	0.264334	1.037246	7.188816	3.882462	4.166703	4.283447	11.07061	7.560248	6.879366	8.413953	0
Rastrigin 10D (45)	104.4968	99.45972	100.9335	96.72043	89.71338	66.51844	83.13564	83.80125	79.72599	50.89642	48.57552	35.77263	81.19068	59.93619	52.81084	65.84896	0
Rastrigin 30D (46)	431.5188	383.6689	406.1136	406.1136	401.1136	351.9507	385.4728	385.4728	416.5546	335.4558	318.4149	359.9527	396.0528	330.133	291.2128	346.6424	0
Box and Betts (47)	-2534.01	-2628.16	-2604	-2578.11	-2783.24	-2724.02	-2794.24	-2732.84	-2876.62	-2915.3	-2911.86	-2908.94	-2990.2	-2938.51	-2953.47	-2931.24	-4189.829
Schwefel 10D (48)	-4550.74	-4648.29	-4683.86	-4683.86	-4532.64	-4099.24	-4737.56	-4737.56	-3809.15	-4070.64	-4187.66	-3925.04	-3752.29	-4039.16	-4146.3	-3495.06	-12569.487
Greiwangk 30D (49)	2.348358	0.780957	0.55438	0.819858	0.208589	0.109971	0.236017	1.468531	0.711003	0.85273	1.552785	1.081064	5.13644	4.062326	4.916143	6.187114	0
Greiwangk 30D (50)	169.8376	158.9351	152.8305	152.8305	157.0457	93.51826	124.1981	124.1981	162.2106	58.70239	118.8107	109.5668	148.0204	85.47694	90.03661	101.0417	0
Salomon 10D (51)	4.003966	2.863405	5.026218	5.577034	3.022477	2.147623	2.162615	4.83007	3.014822	1.784316	1.64996	4.291278	2.62354	1.624024	1.549122	3.020011	0
Salomon 30D (52)	12.11175	8.87527	9.646904	9.646904	10.61845	7.910659	8.423978	8.423978	11.61623	6.539072	5.290962	9.311105	8.97273	5.703356	4.882822	9.526014	0
Odd Square 10D (53)	-0.05951	-0.10939	-0.08465	-0.08113	-0.07607	-0.17341	-0.2453	-0.1005	-0.09541	-0.2432	-0.35262	-0.14574	-0.11377	-0.30731	-0.39106	-0.26078	-1.14383
Whitley 10D (54)	2.74E+14	2.63E+14	2.65E+14	2.63E+14	1.91E+14	1.77E+14	3.9E+13	3.67E+13	8.57E+12	3.82E+13	1.54E+13	1.01E+13	4.08E+13	3.09E+			









Average Times (s) for 500k		A50, N1	A50, N2	A50, N3	A50, N4	A100, N1	A100, N2	A100, N3	A100, N4	A250, N1	A250, N2	A250, N3	A250, N4	A500, N1	A500, N2	A500, N3	A500, N4
Rosenbrock (1)	1.078831	0.656722	0.477856	0.602343	0.711809	0.473997	0.604695	0.578145	0.496982	0.650789	0.572721	0.627839	0.845276	0.690155	0.845276	0.923668	0.646753
		0.902049	0.707866	0.895778	1.007855	0.543462	0.742792	0.784873	0.528804	0.631737	0.621384	0.627363	0.799783	0.720784	0.720784	0.922538	0.653563
		2.090114	0.632603	1.963009	0.857778	0.508251	0.918114	1.884801	1.869744	1.942792	1.962251	2.254737	2.254737	2.197846	2.197846	2.247727	2.227804
		0.911752	0.784202	0.729082	0.673268	0.503825	0.864116	0.543496	0.570911	0.646988	0.575679	0.615099	0.734396	0.705917	0.705917	0.865475	0.704151
		1.9494	1.58666	1.729623	1.714295	1.188234	2.094611	1.316777	1.261814	1.433401	1.45982	1.532386	2.035904	1.663259	1.663259	1.837958	1.911168
Mod Rosenbrock 1 (6)	0.941672	0.904739	0.788283	0.788283	0.784557	0.690957	0.919624	0.619865	0.619865	0.569034	0.569034	0.569034	0.569034	0.569034	0.569034	0.647593	0.631871
		0.941672	0.904739	0.788283	0.784557	0.690957	0.919624	0.619865	0.619865	0.569034	0.569034	0.569034	0.569034	0.569034	0.569034	0.647593	0.631871
		0.941672	0.904739	0.788283	0.784557	0.690957	0.919624	0.619865	0.619865	0.569034	0.569034	0.569034	0.569034	0.569034	0.569034	0.647593	0.631871
		0.941672	0.904739	0.788283	0.784557	0.690957	0.919624	0.619865	0.619865	0.569034	0.569034	0.569034	0.569034	0.569034	0.569034	0.647593	0.631871
		0.941672	0.904739	0.788283	0.784557	0.690957	0.919624	0.619865	0.619865	0.569034	0.569034	0.569034	0.569034	0.569034	0.569034	0.647593	0.631871
Mod Rosenbrock 2 (7)	1.045944	0.989338	0.83419	0.986474	1.021213	0.878626	1.037359	0.822711	0.694286	0.667548	0.569734	0.638127	0.662432	0.612779	0.662432	0.655157	0.629736
		0.989338	0.83419	0.986474	1.021213	0.878626	1.037359	0.822711	0.694286	0.667548	0.569734	0.638127	0.662432	0.612779	0.662432	0.655157	0.629736
		0.989338	0.83419	0.986474	1.021213	0.878626	1.037359	0.822711	0.694286	0.667548	0.569734	0.638127	0.662432	0.612779	0.662432	0.655157	0.629736
		0.989338	0.83419	0.986474	1.021213	0.878626	1.037359	0.822711	0.694286	0.667548	0.569734	0.638127	0.662432	0.612779	0.662432	0.655157	0.629736
		0.989338	0.83419	0.986474	1.021213	0.878626	1.037359	0.822711	0.694286	0.667548	0.569734	0.638127	0.662432	0.612779	0.662432	0.655157	0.629736
Powell (9)	1.055374	0.903873	0.903873	1.055374	1.072688	0.961482	1.1197	1.06418	1.218824	1.229515	1.217436	1.31193	1.39411	1.342529	1.342529	1.435407	1.44919
		0.903873	0.903873	1.055374	1.072688	0.961482	1.1197	1.06418	1.218824	1.229515	1.217436	1.31193	1.39411	1.342529	1.342529	1.435407	1.44919
		0.903873	0.903873	1.055374	1.072688	0.961482	1.1197	1.06418	1.218824	1.229515	1.217436	1.31193	1.39411	1.342529	1.342529	1.435407	1.44919
		0.903873	0.903873	1.055374	1.072688	0.961482	1.1197	1.06418	1.218824	1.229515	1.217436	1.31193	1.39411	1.342529	1.342529	1.435407	1.44919
		0.903873	0.903873	1.055374	1.072688	0.961482	1.1197	1.06418	1.218824	1.229515	1.217436	1.31193	1.39411	1.342529	1.342529	1.435407	1.44919
Wood (10)	0.972534	0.988017	0.82782	1.032021	0.994288	1.037645	0.882994	0.983561	1.102047	1.143181	1.12528	1.167276	1.239377	1.298248	1.298248	1.362449	1.362449
		0.988017	0.82782	1.032021	0.994288	1.037645	0.882994	0.983561	1.102047	1.143181	1.12528	1.167276	1.239377	1.298248	1.298248	1.362449	1.362449
		0.988017	0.82782	1.032021	0.994288	1.037645	0.882994	0.983561	1.102047	1.143181	1.12528	1.167276	1.239377	1.298248	1.298248	1.362449	1.362449
		0.988017	0.82782	1.032021	0.994288	1.037645	0.882994	0.983561	1.102047	1.143181	1.12528	1.167276	1.239377	1.298248	1.298248	1.362449	1.362449
		0.988017	0.82782	1.032021	0.994288	1.037645	0.882994	0.983561	1.102047	1.143181	1.12528	1.167276	1.239377	1.298248	1.298248	1.362449	1.362449
Beale (11)	1.022264	1.026291	0.859322	1.072629	0.909677	1.104232	0.819416	0.867754	0.657635	0.53272	0.53272	0.667837	0.728602	0.682087	0.682087	0.872946	0.646549
		1.026291	0.859322	1.072629	0.909677	1.104232	0.819416	0.867754	0.657635	0.53272	0.53272	0.667837	0.728602	0.682087	0.682087	0.872946	0.646549
		1.026291	0.859322	1.072629	0.909677	1.104232	0.819416	0.867754	0.657635	0.53272	0.53272	0.667837	0.728602	0.682087	0.682087	0.872946	0.646549
		1.026291	0.859322	1.072629	0.909677	1.104232	0.819416	0.867754	0.657635	0.53272	0.53272	0.667837	0.728602	0.682087	0.682087	0.872946	0.646549
		1.026291	0.859322	1.072629	0.909677	1.104232	0.819416	0.867754	0.657635	0.53272	0.53272	0.667837	0.728602	0.682087	0.682087	0.872946	0.646549
Engvall (12)	1.143296	1.165652	1.008394	1.205727	1.093499	1.298627	0.941285	1.021806	0.787635	0.691118	0.663513	0.809272	0.711118	0.817857	0.817857	0.838845	0.809379
		1.165652	1.008394	1.205727	1.093499	1.298627	0.941285	1.021806	0.787635	0.691118	0.663513	0.809272	0.711118	0.817857	0.817857	0.838845	0.809379
		1.165652	1.008394	1.205727	1.093499	1.298627	0.941285	1.021806	0.787635	0.691118	0.663513	0.809272	0.711118	0.817857	0.817857	0.838845	0.809379
		1.165652	1.008394	1.205727	1.093499	1.298627	0.941285	1.021806	0.787635	0.691118	0.663513	0.809272	0.711118	0.817857	0.817857	0.838845	0.809379
		1.165652	1.008394	1.205727	1.093499	1.298627	0.941285	1.021806	0.787635	0.691118	0.663513	0.809272	0.711118	0.817857	0.817857	0.838845	0.809379
De Jong (13)	0.948158	0.963238	0.793435	0.968284	0.853385	1.067594	0.674858	0.705142	0.614457	0.619519	0.488441	0.629279	0.611098	0.746282	0.746282	0.659916	0.659916
		0.963238	0.793435	0.968284	0.853385	1.067594	0.674858	0.705142	0.614457	0.619519	0.488441	0.629279	0.611098	0.746282	0.746282	0.659916	0.659916
		0.963238	0.793435	0.968284	0.853385	1.067594	0.674858	0.705142	0.614457	0.619519	0.488441	0.629279	0.611098	0.746282	0.746282	0.659916	0.659916
		0.963238	0.793435	0.968284	0.853385	1.067594	0.674858	0.705142	0.614457	0.619519	0.488441	0.629279	0.611098	0.746282	0.746282	0.659916	0.659916
		0.963238	0.793435	0.968284	0.853385	1.067594	0.674858	0.705142	0.614457	0.619519	0.488441	0.629279	0.611098	0.746282	0.746282	0.659916	0.659916
Rastrigin (14)	1.007844	0.995085	0.84328	0.974314	0.874626	1.004169	0.690324	0.773253	0.63688	0.582879	0.587342	0.629483	0.581202	0.626202	0.626202	0.698158	0.613001
		0.995085	0.84328	0.974314	0.874626	1.004169	0.690324	0.773253	0.63688	0.582879	0.587342	0.629483	0.581202	0.626202	0.626202	0.698158	0.613001
		0.995085	0.84328	0.974314	0.874626	1.004169	0.690324	0.773253	0.63688	0.582879	0.587342	0.629483	0.581202	0.626202	0.626202	0.698158	0.613001
		0.995085	0.84328	0.974314	0.874626	1.004169	0.690324	0.773253	0.63688	0.582879	0.587342	0.629483	0.581202	0.626202	0.626202	0.698158	0.613001
		0.995085	0.84328	0.974314	0.874626	1.004169	0.690324	0.773253	0.63688	0.582879	0.587342	0.629483	0.581202	0.626202	0.626202	0.698158	0.613001
Schwefel (15)	0.960331	0.95088	0.766733	0.88483	0.871626	1.004169	0.690324	0.773253	0.63688	0.582879	0.587342	0.629483	0.581202	0.626202	0.626202	0.698158	0.613001
		0.95088	0.766733	0.88483	0.871626	1.004169	0.690324	0.773253	0.63688	0.582879	0.587342	0.629483	0.581202	0.626202	0.626202	0.698158	0.613001
		0.95088	0.766733	0.88483	0.871626	1.004169	0.690324	0.773253	0.63688	0.582879	0.587342	0.629483	0.581202	0.626202	0.626202	0.698158	0.613001
		0.95088	0.766733	0.88483	0.871626	1.004169	0.690324	0.773253	0.63688	0.582879	0.587342	0.629483	0.581202	0.626202	0.626202	0.698158	0.613001
		0.95088	0.766733	0.88483	0.871626	1.004169	0.690324	0.773253	0.63688	0.582879	0.587342	0.629483	0.581202	0.626202	0.626202	0.698158	0.613001
Griewangk (16)	1.032951	1.05341	0.777143	0.928586	0.873339	0.939885	0.674269	0.701165	0.599128	0.552046	0.546708	0.674241	0.60956	0.712373	0.712373	0.77675	0.632066
		1.05341	0.777143	0.928586	0.873339	0.939885	0.674269	0.701165	0.599128	0.552046	0.546708	0.674241	0.60956	0.712373	0.712		







Average Results (500k)	A50_N1	A50_N2	A50_N3	A50_N4	A100_N1	A100_N2	A100_N3	A100_N4	A250_N1	A250_N2	A250_N3	A250_N4	A500_N1	A500_N2	A500_N3	A500_N4	True Minima
Rosenbrock (1)	0.000776	0.000672	0.000776	0.000776	0.000628	0.000581	0.000628	0.000628	0.000652	0.000227	0.000652	0.000652	0.000498	9.31E-05	0.000498	0.000498	0
McCormic (2)	-1.91322	-1.91322	-1.91322	-1.91322	-1.91322	-1.91322	-1.91322	-1.91322	-1.91322	-1.91322	-1.91322	-1.91322	-1.91322	-1.91322	-1.91322	-1.91322	-1.91322
Box and Betts (3)	2.47E-08	1.08E-08	1.90E-08	1.70E-06	3.21E-08	1.61E-07	3.21E-08	2.03E-08	1.87E-07	1.00E-06	7.30E-08	1.71E-08	1.71E-06	2.89E-06	3.102066	3.000002	1.06E-06
Goldstein (4)	3.000023	3.000023	3.000023	3.000023	3.000009	3.000009	3.000009	3.000009	3.000002	3.000001	3.000002	3.000002	3.000002	3.000002	3.000002	3.000002	3
Easom (5)	-0.99908	-0.99908	-0.99908	-0.99908	-0.99909	-0.99902	-0.99909	-0.99909	-0.99901	-0.99902	-0.99901	-0.99901	-0.99901	-0.99906	-0.99906	-0.99906	-1
Mod Rosenbrock 1 (6)	0.030646	0.030646	0.030646	0.030646	0.030646	0.030646	0.030646	0.030646	0.030646	0.030646	0.030646	0.030646	0.030646	0.030646	0.030646	0.030646	0
Mod Rosenbrock 2 (7)	0.516174	0.516174	0.516174	0.516174	0.516174	0.516174	0.516174	0.516174	0.516174	0.516174	0.516174	0.516174	0.516174	0.516174	0.516174	0.516174	0
Bohachevsky (8)	0.77917	0.840887	0.77917	0.77917	0.906311	0.832202	0.906311	0.906311	0.861947	0.507588	0.861947	0.861947	0.861947	0.861947	0.861947	0.861947	0
Powell (9)	105611.3	105611.3	41427.51	41237.94	89647.89	89647.89	50944.19	5160.11	78045.36	78045.36	88547.97	7956.454	103797	103797	110509.4	33969.73	0
Wood (10)	319599.1	319599.1	93080.76	271461.7	271461.7	271461.7	101112.1	5020.948	183769	183769	192618.4	8122.754	299246.8	299246.8	286273.3	27752.1	0
Beale (11)	0.290398	0.38052	0.290398	0.290398	0.343688	0.341604	0.343688	0.400445	0.400445	0.400445	0.400445	0.400445	0.400445	0.400445	0.400445	0.400445	0
Engvall (12)	0.797297	0.745037	0.797297	0.797297	0.763627	0.647485	0.763627	0.763627	0.775825	0.39817	0.775825	0.775825	0.775825	0.775825	0.775825	0.775825	0
DeJong (13)	5.82E-06	3.14E-06	5.82E-06	5.82E-06	5.48E-06	1.00E-06	5.48E-06	5.48E-06	1.21E-06	1.79E-07	1.21E-06	1.21E-06	3.48E-07	8.56E-08	3.48E-07	3.48E-07	0
Rastrigin (14)	0.001411	0.001283	0.001411	0.001411	0.001436	0.000472	0.001436	0.001436	0.000468	0.137636	0.000468	0.000468	0.020398	0.059439	0.020398	0.020398	0
Schwefel (15)	-837.959	-837.961	-837.959	-837.959	-837.96	-837.96	-837.96	-837.96	-837.96	-837.957	-837.957	-837.957	-837.957	-837.962	-837.956	-837.956	-837.9658
Greiwangk (16)	0.005601	0.004895	0.005601	0.004895	0.004998	0.004998	0.004998	0.004998	0.005141	0.004307	0.005141	0.005141	0.00482	0.005194	0.00482	0.00482	0
Ackley (17)	0.018733	0.024858	0.018733	0.018733	0.022607	0.022423	0.022607	0.022607	0.02504	0.009278	0.02504	0.02504	0.012924	0.004805	0.012924	0.012924	0
Langman (18)	-6.77248	-1.49455	-1.49454	-1.49445	-1.49445	-1.49445	-1.49451	-1.49458	-1.49331	-1.4932	-1.49357	-1.49357	-1.49303	-1.493	-1.49303	-1.49223	-1.5
Michalewicz (19)	-7.52904	-8.25935	-7.52904	-7.47129	-6.77395	-8.35816	-7.72282	-7.31138	-7.50726	-8.12503	-7.99851	-7.20926	-7.48962	-7.79696	-7.93894	-7.11748	-9.66
Brannin (20)	0.397892	0.397891	0.397892	0.397892	0.397888	0.397892	0.397892	0.397892	0.397889	0.397888	0.397888	0.397888	0.397888	0.397888	0.397888	0.397888	0.397887
Six Hump Camel (21)	-1.03163	-1.03163	-1.03163	-1.03163	-1.03163	-1.03163	-1.03163	-1.03163	-1.03163	-1.03163	-1.03163	-1.03163	-1.03163	-1.03125	-1.03163	-1.03163	-1.0316
Osborne 1 (22)	0.037205	0.035101	0.030354	0.028176	0.034368	0.034758	0.032475	0.031539	0.039506	0.040396	0.03843	0.034308	0.054678	0.057136	0.048085	0.054425	5.46E-05
Osborne 2 (23)	0.118435	0.1051	0.119724	0.119073	0.123495	0.112132	0.126659	0.122491	0.133092	0.123111	0.119592	0.130879	0.14129	0.140948	0.141679	0.142024	0.0402
Mod Rastrigin (24)	81.54867	79.13218	81.54867	79.13218	81.96909	81.96909	81.96909	81.96909	83.14685	82.83151	83.14685	83.14685	82.88808	81.43853	82.88808	82.88808	58
Mineshaft 1 (25)	1.754727	1.83898	1.807361	1.83898	1.76767	1.787393	1.753839	1.747039	1.992637	1.4273	1.992637	1.992637	1.734469	2.260179	1.992109	2.260179	1.3805
Mineshaft 2 (26)	-1.41635	-1.41032	-1.33576	-1.33576	-1.41635	-1.34233	-1.41432	-1.41432	-1.28446	-1.28446	-1.28446	-1.28446	-1.4056	-1.26007	-1.34665	-1.26007	-1.4163535
Mineshaft 3 (27)	-6.98871	-6.98871	-6.98871	-6.98871	-6.98871	-6.98871	-6.98871	-6.98871	-6.98871	-6.98871	-6.98871	-6.98871	-6.98871	-6.98871	-6.98871	-6.98871	-7
Spherical Contours (28)	23.34782	24.19461	20.63753	20.63753	23.40344	25.30614	21.91096	21.91096	26.38852	26.44991	26.38852	26.38852	32.91937	32.91937	32.91937	32.91937	0
S1 (29)	1.19E-13	0.001762	1.56E-14	3.35E-14	8.33E-05	8.17E-15	8.33E-05	8.33E-05	3.39E-14	0.000228	1.84E-05	0.000228	1.84E-05	0.000228	1.84E-05	0.000228	0
S2 (30)	2	2	2	2	2	2	2	2	2	2	2	2	2	2	2	2	2
S3 (31)	0.528872	0.528872	0.528872	0.528872	0.528872	0.528872	0.528872	0.528872	0.528872	0.528872	0.528872	0.528872	0.528872	0.528872	0.528872	0.528872	0.5289
Downhill Step (32)	9	9	9	9	9	9	9	9	9.016	9.016	9.016	9.016	9.007	9.014	9.007	9.007	9
Salomon (33)	0.014037	0.017516	0.014037	0.014037	0.013903	0.015004	0.013903	0.013903	0.013664	0.01541	0.013664	0.013664	0.015619	0.012491	0.015619	0.015619	0
Whitley (34)	0.021271	0.022541	0.021271	0.021271	0.014088	0.017201	0.014088	0.014088	0.022981	0.0167	0.022981	0.022981	0.017191	0.01097	0.017191	0.017191	0
Odd Square (35)	-1.00777	-1.00778	-1.00777	-1.00777	-1.00786	-1.00803	-1.00786	-1.00786	-1.0081	-1.00414	-1.0081	-1.0081	-1.00797	-0.79718	-1.00797	-1.00797	-1.14383
Storn Chebyshev (36)	40.80173	10.57006	43.94857	48.67533	48.12192	5.931929	5.859969	31.52742	38.77751	29.02368	2.597565	43.86236	69.04352	82.40736	26.2826	74.62423	0
Rana (37)	-1023.42	-1023.42	-1023.42	-1023.42	-1023.42	-1023.42	-1023.42	-1023.42	-1023.42	-1023.42	-1023.42	-1023.42	-1023.42	-1023.42	-1023.42	-1023.42	-1023.416
Rosenbrock 10D (38)	854.1811	830.0601	690.5763	714.301	857.3875	911.3072	735.7911	789.2425	908.9694	977.3341	736.6232	869.8465	971.0684	968.885	967.7971	971.0683	0
Rosenbrock 30D (39)	201403.5	221437.9	150026.8	150026.8	198327.8	242992.1	175779.4	255904.1	258737.9	259865	256160.8	256160.8	507104.4	507104.4	507104.4	507104.4	0
Mod Rosenbrock 1 10D (40)	788.5139	738.4796	682.6546	697.0191	774.3249	786.1146	622.9925	744.2402	789.9867	790.7422	569.8011	784.6431	821.682	817.1932	821.3425	821.3425	0
Mod Rosenbrock 1 30D (41)	18378.38	19034.94	16223.9	16223.9	18968.35	20255.16	18022.99	18022.99	20523.16	20477.26	20368.01	20537.48	25223.52	25223.52	25223.52	25223.52	0
Mod Rosenbrock 2 10D (42)	0.639236	0.363844	0.962291	0.860631	0.919516	0.319287	0.710177	0.975512	0.489599	0.489599	0.639314	0.940223	0.946027	0.846291	0.736089	0.965171	0
Mod Rosenbrock 2 30D (43)	0.587038	0.359928	0.890388	0.979112	0.889658	0.281179	0.889658	0.889658	0.914371	0.594617	0.969994	0.916821	0.891053	0.845625	0.86672	0.993714	0
Spherical Contours 10D (44)	0.626531	0.612232	0.54511	0.622656	0.622656	0.622656	0.492055	0.568389	0.643401	0.65672	0.568389	0.568389	0.643433	0.643433	0.643433	0.643433	0
Rastrigin 10D (45)	33.33578	29.87455	29.88049	33.10619	29.24666	30.2831	32.41291	33.14987	32.21292	33.14987	32.21292	33.14987	34.19422	33.84409	34.33475	34.65795	0
Rastrigin 30D (46)	250.7989	238.6941	225.8756	245.3154	225.8756	229.7949	229.7949	257.551	249.4078	257.551	249.4078	246.1011	281.5002	279.2583	279.3113	279.3113	0
Box and Betts (3)	-3490.19	-3386.49	-3044.51	-3046.67	-3355.65	-3459.67	-3275.82	-3046.42	-3300.78	-3506.51	-3418.05	-3062.53	-3440.24	-3448.22	-3423.81	-3070.62	-4189.829
Schwefel 10D (47)	-6899.56	-6863.61	-5951.64	-5951.64	-6868.31	-6868.31	-5946.88	-5946.88	-6918.58	-6895.06	-6895.06	-5758.31	-6832.05	-6862.66	-6862.66	-6862.66	-12569.487
Griewangk 30D (48)	1.581811	1.551686	1.489028	1.519399	1.570948	1.562544	1.437001	1.524427	1.562598	1.584749	1.400229	1.563082	1.630711	1.630711	1.630711	1.630711	0
Griewangk 30D (50)	19.05578	19.56282	16.54641	16.54641	18.88788	20.3806	17.80893	17.80893	21.18915	21.21915	21.21915	21.16616	25.84642	25.84642	25.84642	25.84642	0
Salomon 10D (51)	1.091542	1.077758	0.979608	1.002171	1.075972	1.058209	1.032943	1.020515	1.101185	1.108821	1.069816	1.087883	1.114335	1.101174	1.111909	1.10421	0
Salomon 30D (52)	4.906982	5.009541	4.51926	4.895194	5.149522	4.706435	4.706435	5.179124	5.199422	5.160728	5.156453	5.994579	5.9901	5.9901	5.993119	5.992761	0
Odd Square 10D (53)	-0.5386	-0.5423	-0.59199	-0.59475	-0.5386	-0.54236	-0.55534	-0.57757	-0.54371	-0.53871	-0.53871	-0.5605	-0.5387	-0.53678	-0.53678	-0.53403	-1.14383
Whitley 10D (54)	5422338	5406995	1.23E+08	1.23E+08	5086759	5980773	4414587	5504989	6703457	7041453	5561806	5323664	6990138	7028678	7286276	7028364	0
Whitley 30D (55)	7.																

Average Results (100k)	A50, N1	A50, N2	A50, N3	A50, N4	A100, N1	A100, N2	A100, N3	A100, N4	A250, N1	A250, N2	A250, N3	A250, N4	A500, N1	A500, N2	A500, N3	A500, N4	True Minima
Rosenbrock (1)	0.003719	0.003539	0.003719	0.003719	0.003786	0.003579	0.003786	0.003786	0.0057	0.002071	0.0057	0.0057	0.004057	0.004057	0.004057	0.004057	0
McCormic (2)	-1.91322	-1.91322	-1.91322	-1.91322	-1.91322	-1.91322	-1.91322	-1.91322	-1.91322	-1.91322	-1.91322	-1.91322	-1.91322	-1.91322	-1.91322	-1.91322	-1.91322
Box and Betts (3)	2.14E-06	8.25E-07	4.83E-07	1.68E-07	1.99E-06	1.33E-06	6.76E-07	1.32E-06	1.89E-06	6.28E-06	2.11E-06	4.39E-07	1.92E-05	2.37E-05	1.01E-05	4.74E-06	0
Goldstein (4)	3.000167	3.000049	3.000167	3.000167	3.000116	3.504947	3.000116	3.000116	3.000174	3.000174	3.000174	3.000174	3.224086	3.156892	3.224086	3.224086	3
Easom (5)	-0.99331	-0.9928	-0.99331	-0.99331	-0.99213	-0.99599	-0.99213	-0.99213	-0.99407	-0.99687	-0.99407	-0.99407	-0.97311	-0.97512	-0.97311	-0.97311	-1
Mod Rosenbrock 1 (6)	0.11261	0.118302	0.11261	0.11261	0.120548	0.113057	0.120548	0.120548	0.115392	0.084471	0.115392	0.115392	0.117339	0.133214	0.117339	0.117339	0
Mod Rosenbrock 2 (7)	1.509149	1.822585	1.509149	1.509149	1.782731	1.822593	1.782731	1.782731	2.056043	2.056043	2.056043	2.056043	2.02553	2.101303	2.02553	2.02553	0
Bohachevsky (8)	2.269499	2.164355	2.269499	2.269499	2.014049	2.183515	2.014049	2.014049	2.309156	2.309156	2.309156	2.309156	2.78908	2.78908	2.78908	2.78908	0
Powell (9)	326514.2	326514.2	199511.5	300113.5	385731.3	385731.3	282161	260006.1	491923.7	491923.7	491923.7	491923.7	648778.6	648778.6	648778.6	648778.6	0
Wood (10)	1134891	1134891	576138.3	490899.4	1157531	1157531	794788.9	458407.5	1724791	1724791	1724791	1735243	1963031	1963031	1963031	1963031	0
Beale (11)	2.659759	2.659759	1.237617	1.237617	2.402608	2.415451	2.402608	2.402608	4.826361	4.826361	4.826361	4.826361	10.25196	10.25196	10.25196	10.25196	0
Engvall (12)	5.002165	5.002165	5.002165	5.002165	3.253983	3.406642	3.253983	3.253983	4.159679	4.117014	4.159679	4.159679	3.522215	3.522215	3.522215	3.522215	0
DeJong (13)	2.86E-05	1.83E-05	2.86E-05	2.86E-05	2.81E-05	5.63E-06	2.81E-05	2.81E-05	7.29E-06	1.88E-06	7.29E-06	7.29E-06	9.73E-06	9.73E-06	9.73E-06	9.73E-06	0
Rastrigin (14)	0.00861	0.007315	0.00861	0.00861	0.007543	0.005916	0.007543	0.007543	0.031931	0.608148	0.031931	0.031931	0.499535	0.580432	0.499535	0.499535	0
Schwefel (15)	-837.908	-837.911	-837.908	-837.908	-837.908	-837.824	-837.908	-837.908	-837.842	-837.357	-837.842	-837.842	-837.742	-837.742	-837.742	-837.742	0
Griewangk (16)	0.011015	0.011622	0.011015	0.011015	0.011168	0.011088	0.011168	0.011168	0.011276	0.011181	0.011276	0.011276	0.012465	0.012465	0.012465	0.012465	0
Ackley (17)	0.057493	0.069097	0.057493	0.057493	0.061296	0.059243	0.061296	0.061296	0.06257	0.084254	0.06257	0.06257	0.062469	0.062469	0.062469	0.062469	0
Langman (18)	-1.48383	-1.48443	-1.48602	-1.47661	-1.46772	-1.46682	-1.47474	-1.46819	-1.45955	-1.45955	-1.45955	-1.45955	-1.424	-1.424	-1.424	-1.424	-1.5
Michalewicz (19)	-6.30718	-7.76073	-7.13502	-6.912	-6.25667	-7.94698	-7.2661	-6.73415	-6.5581	-7.37832	-7.19338	-6.34976	-5.8426	-5.8426	-5.8426	-5.8426	-9.66
Bratin (20)	0.397925	0.397906	0.397925	0.397925	0.397914	0.397892	0.397914	0.397914	0.397895	0.39789	0.397895	0.397895	0.397896	0.397896	0.397896	0.397896	0.397887
Six Hump Camel (21)	-1.03162	-1.03162	-1.03162	-1.03162	-1.03162	-1.03162	-1.03162	-1.03162	-1.03163	-1.03076	-1.03163	-1.03163	-1.03035	-1.03035	-1.03035	-1.03035	-1.0316
Osborne 1 (22)	0.078983	0.06742	0.072231	0.07688	0.092688	0.102949	0.098343	0.089154	0.112339	0.112277	0.112339	0.112339	0.171489	0.171489	0.171489	0.171489	5.46E-05
Osborne 2 (23)	0.167625	0.16624	0.171616	0.170281	0.190588	0.190816	0.196367	0.192707	0.258226	0.258226	0.258226	0.258226	0.414724	0.414724	0.414724	0.414724	0.0402
Mod Rastrigin (24)	83.73278	85.31511	83.73278	83.73278	85.45783	85.37017	85.45783	86.40093	87.32495	86.40093	86.40093	86.40093	88.75725	87.56937	88.75725	88.75725	58
Mineshaft 1 (25)	1.937338	2.02507	1.927696	2.02507	1.888167	2.063715	1.862662	2.063715	1.892411	2.29222	2.025927	2.29222	2.080758	2.323916	2.280202	2.323916	1.3805
Mineshaft 2 (26)	-1.41808	-1.22494	-1.40341	-1.22494	-1.41628	-1.15741	-1.38021	-1.15741	-1.38067	-1.15695	-1.24531	-1.15695	-1.32732	-1.22442	-1.2417	-1.22442	-1.4163535
Mineshaft 3 (27)	-6.97031	-6.96008	-6.97031	-6.97031	-6.98263	-6.92964	-6.98263	-6.98263	-6.92837	-6.97097	-6.92837	-6.92837	-6.73943	-6.73943	-6.73943	-6.73943	-7
Spherical Contours (28)	30.87021	30.95735	30.83219	30.83219	37.52425	37.52425	37.52425	37.52425	62.52586	62.52586	62.52586	62.52586	121.1291	121.1291	121.1291	121.1291	0
S1 (29)	1.27E-12	0.009982	1.27E-12	0.009982	4.00E-12	0.002725	3.96E-05	0.002725	9.23E-07	0.00587	0.002036	0.00587	0.000019	0.000019	0.000019	0.000019	0
S2 (30)	0.528872	0.528872	0.528872	0.528872	0.528872	0.528872	0.528872	0.528872	0.528872	0.528872	0.528872	0.528872	0.528872	0.528872	0.528872	0.528872	2
S3 (31)	0.528872	0.528872	0.528872	0.528872	0.528872	0.528872	0.528872	0.528872	0.528872	0.528872	0.528872	0.528872	0.528872	0.528872	0.528872	0.528872	2
Downhill Step (32)	0.528872	0.528872	0.528872	0.528872	0.528872	0.528872	0.528872	0.528872	0.528872	0.528872	0.528872	0.528872	0.528872	0.528872	0.528872	0.528872	9
Salomon (33)	0.057458	0.057458	0.057458	0.057458	0.049184	0.046294	0.049184	0.049184	0.050563	0.051105	0.050563	0.050563	0.062391	0.059772	0.062391	0.062391	0
Whitley (34)	0.161554	0.177354	0.161554	0.161554	0.138244	0.130518	0.138244	0.138244	0.166362	0.166362	0.166362	0.166362	0.179894	0.192313	0.179894	0.179894	0
Odd Square (35)	-1.00677	-1.00677	-1.00677	-1.00677	-1.00684	-1.0073	-1.00684	-1.00684	-1.00665	-0.93191	-1.00665	-1.00665	-0.98783	-0.87124	-0.98783	-0.98783	-1.14383
Storn Chebyshev (36)	281.9294	183.2996	278.0215	264.5542	313.1659	242.6493	301.2619	292.7093	815.3117	815.3117	811.822	810.3418	1225.455	1225.455	1225.455	1225.455	0
Rana (37)	-1019.25	-1006.37	-1019.25	-1019.25	-992.871	-987.051	-992.871	-992.871	-1011.72	-1011.72	-1011.72	-1011.72	-1019.38	-1019.38	-1019.38	-1019.38	-1023.416
Rosenbrock 10D (38)	1493.422	1423.228	1475.732	42546.15	1591.557	1591.557	1574.751	1591.557	2768.679	2768.679	2768.679	2768.679	4656.455	4656.455	4656.455	4656.455	0
Rosenbrock 30D (39)	557572.3	554770.7	564532.2	564532.2	794939	797247.2	797247.2	797247.2	4542416	4542416	4542416	4542416	16226260	16226260	16226260	16226260	0
Mod Rosenbrock 1 10D (40)	1022.596	1012.23	978.6697	980.6449	1084.177	1084.329	1084.329	1084.329	1325.06	1325.06	1325.06	1325.06	1877.504	1877.504	1877.504	1877.504	0
Mod Rosenbrock 1 30D (41)	24251.35	24146.44	24243.25	24243.25	29083.57	29083.57	29083.57	29083.57	47748.25	47748.25	47748.25	47748.25	85427.94	85427.94	85427.94	85427.94	0
Mod Rosenbrock 2 10D (42)	1.608352	1.032925	1.921275	1.943575	1.961571	1.499006	1.775495	1.88269	1.929981	1.950481	1.929981	2.05832	2.169398	2.169398	2.169398	2.169398	0
Mod Rosenbrock 2 30D (43)	1.603208	1.059208	1.961374	1.961374	2.056881	1.354624	1.933383	1.933383	1.941167	1.87322	1.937336	1.954814	2.298725	2.298725	2.298725	2.298725	0
Spherical Contours 10D (44)	0.878944	0.874175	0.814164	0.853665	0.92424	0.92424	0.92424	0.92424	1.257534	1.257534	1.257534	1.257534	2.155032	2.155032	2.155032	2.155032	0
Rastrigin 10D (45)	40.8003	38.07945	39.24959	38.06889	40.98482	39.46908	40.79169	41.01127	48.1604	48.1604	48.1604	48.1604	58.15936	58.15936	58.15936	58.15936	0
Rastrigin 30D (46)	280.9433	269.0272	265.1899	265.1899	312.7547	312.4636	308.7531	308.7531	365.0024	365.4306	361.4041	361.4041	435.7895	435.7895	435.7895	435.7895	0
Schwefel 10D (47)	-3279.22	-3210.92	-2851.26	-2851.26	-3269.38	-3142.56	-3030.24	-2870.72	-2955.42	-2955.42	-2955.42	-2955.42	-2820.52	-2820.52	-2820.52	-2820.52	-4189.829
Schwefel 30D (48)	-6324.37	-6099.08	-5522.37	-5522.37	-6400.52	-6198.06	-5370.04	-5370.04	-5520.84	-5520.84	-5520.84	-5520.84	-5204.84	-5204.84	-5204.84	-5204.84	-12569.487
Griewangk 10D (49)	1.817236	1.797318	1.795732	1.818037	1.8804	1.8804	1.884204	1.8804	2.277633	2.277633	2.277633	2.277633	3.032524	3.032524	3.032524	3.032524	0
Griewangk 30D (50)	24.22766	24.22766	24.30302	24.30302	30.21411	30.21411	30.21411	30.21411	48.74501	48.74501	48.74501	48.74501	94.43771	94.43771	94.43771	94.43771	0
Salomon 10D (51)	1.200709	1.263991	1.240492	1.240492	1.303596	1.296861	1.300562	1.299224	1.560916	1.560916	1.560916	1.560916	2.099224	2.099224	2.099224	2.099224	0
Salomon 30D (52)	5.686977	5.67497	5.671804	5.671804	6.475221	6.475221	6.475221	6.475221	8.928658	8.928658	8.928658	8.928658	12.48599	12.48599	12.48599	12.48599	0
Odd Square 10D (53)	-0.4945	-0.50885	-0.52745	-0.52745	-0.47	-0.45618	-0.477895	-0.46649	-0.31582	-0.31582	-0.31582	-0.31582	-0.1926	-0.1926	-0.1926	-0.1926	-1.14383
Whitley 10D (54)	28895561	1.64E+08	1.66E+08	1.66E+08	2297752												

# APPENDIX F2: ST. DEV. FOR SMOA-HTDE

Results St. Dev. (1M)	A50, N1	A50, N2	A50, N3	A50, N4	A100, N1	A100, N2	A100, N3	A100, N4	A250, N1	A250, N2	A250, N3	A250, N4	A500, N1	A500, N2	A500, N3	A500, N4
Rosenbrock (1)	0.000307	0.000318	0.000307	0.000307	0.000322	0.00027	0.00027	0.00027	0.000288	0.00012	0.000288	0.000288	0.000288	0.000202	0.000202	0.000202
McCormick (2)	2.03E-07	2.03E-07	2.03E-07	2.03E-07	2.03E-07	2.03E-07	2.03E-07	2.03E-07	2.03E-07	2.03E-07	2.03E-07	2.03E-07	2.03E-07	2.03E-07	2.03E-07	2.03E-07
Box and Betts (3)	1.79E-08	4.28E-09	2.52E-08	2.52E-08	2.52E-08	2.52E-08	2.52E-08	2.52E-08	2.52E-08	2.52E-08	2.52E-08	2.52E-08	2.52E-08	2.52E-08	2.52E-08	2.52E-08
Goldstein (4)	1.10E-05	3.99E-06	1.10E-05	1.10E-05	1.10E-05	1.10E-05	1.10E-05	1.10E-05	1.10E-05	1.10E-05	1.10E-05	1.10E-05	1.10E-05	1.10E-05	1.10E-05	1.10E-05
Easom (5)	0.000513	0.0000513	0.000513	0.000513	0.000513	0.000513	0.000513	0.000513	0.000513	0.000513	0.000513	0.000513	0.000513	0.000513	0.000513	0.000513
Mod Rosenbrock 1 (6)	0.018743	0.014496	0.018743	0.018743	0.018743	0.018743	0.018743	0.018743	0.018743	0.018743	0.018743	0.018743	0.018743	0.018743	0.018743	0.018743
Mod Rosenbrock 2 (7)	0.311908	0.388841	0.311908	0.311908	0.311908	0.311908	0.311908	0.311908	0.311908	0.311908	0.311908	0.311908	0.311908	0.311908	0.311908	0.311908
Bohachevsky (8)	0.334739	0.334739	0.334739	0.334739	0.334739	0.334739	0.334739	0.334739	0.334739	0.334739	0.334739	0.334739	0.334739	0.334739	0.334739	0.334739
Powell (9)	4.1414.71	4.1414.71	4.1414.71	4.1414.71	4.1414.71	4.1414.71	4.1414.71	4.1414.71	4.1414.71	4.1414.71	4.1414.71	4.1414.71	4.1414.71	4.1414.71	4.1414.71	4.1414.71
Wood (10)	135577.7	135577.7	135577.7	135577.7	135577.7	135577.7	135577.7	135577.7	135577.7	135577.7	135577.7	135577.7	135577.7	135577.7	135577.7	135577.7
Beale (11)	0.162886	0.162886	0.162886	0.162886	0.162886	0.162886	0.162886	0.162886	0.162886	0.162886	0.162886	0.162886	0.162886	0.162886	0.162886	0.162886
Engvall (12)	0.294959	0.317852	0.294959	0.294959	0.294959	0.294959	0.294959	0.294959	0.294959	0.294959	0.294959	0.294959	0.294959	0.294959	0.294959	0.294959
DeJong (13)	2.20E-06	1.78E-06	2.20E-06	2.20E-06	2.20E-06	2.20E-06	2.20E-06	2.20E-06	2.20E-06	2.20E-06	2.20E-06	2.20E-06	2.20E-06	2.20E-06	2.20E-06	2.20E-06
Rastrigin (14)	0.000795	0.000618	0.000795	0.000795	0.000795	0.000795	0.000795	0.000795	0.000795	0.000795	0.000795	0.000795	0.000795	0.000795	0.000795	0.000795
Griewangk (15)	0.004407	0.00292	0.004407	0.004407	0.004407	0.004407	0.004407	0.004407	0.004407	0.004407	0.004407	0.004407	0.004407	0.004407	0.004407	0.004407
Ackley (16)	0.002641	0.002586	0.002641	0.002641	0.002641	0.002641	0.002641	0.002641	0.002641	0.002641	0.002641	0.002641	0.002641	0.002641	0.002641	0.002641
Langerman (18)	0.002034	0.001774	0.001586	0.001586	0.001586	0.001586	0.001586	0.001586	0.001586	0.001586	0.001586	0.001586	0.001586	0.001586	0.001586	0.001586
Michalewicz (19)	0.316243	0.327444	0.408829	0.353477	0.325599	0.325599	0.325599	0.325599	0.325599	0.325599	0.325599	0.325599	0.325599	0.325599	0.325599	0.325599
Brannin (20)	3.09E-06	2.07E-06	3.09E-06	3.09E-06	3.09E-06	3.09E-06	3.09E-06	3.09E-06	3.09E-06	3.09E-06	3.09E-06	3.09E-06	3.09E-06	3.09E-06	3.09E-06	3.09E-06
Six Hump Camel (21)	6.02E-07	7.70E-07	6.02E-07	6.02E-07	6.02E-07	6.02E-07	6.02E-07	6.02E-07	6.02E-07	6.02E-07	6.02E-07	6.02E-07	6.02E-07	6.02E-07	6.02E-07	6.02E-07
Osborne 1 (22)	0.006967	0.008828	0.008851	0.00882	0.00882	0.00882	0.00882	0.00882	0.00882	0.00882	0.00882	0.00882	0.00882	0.00882	0.00882	0.00882
Osborne 2 (23)	0.015282	0.01556	0.021836	0.019351	0.015002	0.016061	0.015684	0.034713	0.024941	0.017259	0.018921	0.017957	0.017957	0.017957	0.017957	0.017957
Mod Rastigrin (24)	3.608104	3.742744	3.608104	3.608104	3.608104	3.608104	3.608104	3.608104	3.608104	3.608104	3.608104	3.608104	3.608104	3.608104	3.608104	3.608104
Mineshaft 1 (25)	0.231163	0.242054	0.140767	0.242054	0.15921	0.172595	0.050117	0.172595	0.062243	0.275532	0.1678528	0.1678528	0.1678528	0.1678528	0.1678528	0.1678528
Mineshaft 2 (26)	5.76E-07	0.13947	0.023587	0.13947	0.102895	1.02E-08	4.31E-11	0.150416	0.036986	0.150416	0.036986	0.150416	0.150416	0.150416	0.150416	0.150416
Mineshaft 3 (27)	0.003121	0.003121	0.014718	0.014718	0.01477	0.000509	0.001477	0.001477	0.001477	0.001477	0.001477	0.001477	0.001477	0.001477	0.001477	0.001477
Spherical Contours (28)	2.178067	1.626606	1.626606	1.626606	1.626606	1.626606	1.626606	1.626606	1.626606	1.626606	1.626606	1.626606	1.626606	1.626606	1.626606	1.626606
S1 (29)	6.85E-14	0.008994	2.91E-14	0.008994	2.91E-14	0.008994	2.91E-14	0.008994	2.91E-14	0.008994	2.91E-14	0.008994	2.91E-14	0.008994	2.91E-14	0.008994
S2 (30)	2.94E-12	0	0	0	0	0	0	0	0	0	0	0	0	0	0	0
S3 (31)	4.01E-11	3.85E-11	4.01E-11	4.01E-11	4.01E-11	4.01E-11	4.01E-11	4.01E-11	4.01E-11	4.01E-11	4.01E-11	4.01E-11	4.01E-11	4.01E-11	4.01E-11	4.01E-11
Downhill Step (32)	0	0	0	0	0	0	0	0	0	0	0	0	0	0	0	0
Salomon (33)	0.007252	0.007415	0.007252	0.007252	0.007252	0.007252	0.007252	0.007252	0.007252	0.007252	0.007252	0.007252	0.007252	0.007252	0.007252	0.007252
Whitley (34)	0.009421	0.009421	0.009421	0.009421	0.009421	0.009421	0.009421	0.009421	0.009421	0.009421	0.009421	0.009421	0.009421	0.009421	0.009421	0.009421
Odd Square (35)	0.000276	0.000276	0.000276	0.000276	0.000276	0.000276	0.000276	0.000276	0.000276	0.000276	0.000276	0.000276	0.000276	0.000276	0.000276	0.000276
Storn Chebyshev (36)	23.29153	5.32589	13.87507	16.28878	23.69721	1.382097	4.862997	16.53017	18.15813	18.17421	1.786396	21.46312	19.73274	19.21866	1.762901	225.828
Rana (37)	1.71E-12	1.71E-12	1.71E-12	1.71E-12	1.71E-12	1.71E-12	1.71E-12	1.71E-12	1.71E-12	1.71E-12	1.71E-12	1.71E-12	1.71E-12	1.71E-12	1.71E-12	1.71E-12
Rosenbrock 10D (38)	217.3042	230.3305	187.9664	195.2453	267.4521	252.2162	231.2002	228.9008	217.2144	237.5201	266.3089	207.8625	219.8819	217.1602	273.8847	211.6849
Rosenbrock 30D (39)	40708.14	41318.06	29136.98	29136.98	32629.77	40425.99	29351.73	29351.73	37653.95	40321.04	37411.85	37411.85	43699.42	44570.2	45796.61	48229.69
Mod Rosenbrock 1 10D (40)	129.2781	147.4957	125.0784	123.077	118.2696	160.3991	154.5099	154.5099	117.4365	132.7173	150.6909	127.8867	111.8914	120.1281	162.935	136.4074
Mod Rosenbrock 1 30D (41)	1696.444	2114.439	1451.999	1451.999	1729.504	1894.073	1392.555	1392.555	1777.212	1732.451	2032.062	1818.887	2056.898	1987.639	1950.938	2041.206
Mod Rosenbrock 2 10D (42)	0.366734	0.136452	0.274406	0.34906	0.350406	0.122698	0.289315	0.272427	0.313261	0.124857	0.195883	0.32491	0.321779	0.311181	0.230536	0.285847
Mod Rosenbrock 2 30D (43)	0.362667	0.122393	0.277712	0.277712	0.408525	0.134203	0.289763	0.289763	0.318638	0.236065	0.360304	0.32363	0.276242	0.352676	0.285994	0.332669
Spherical Contours 10D (44)	0.111995	0.143396	0.126954	0.127931	0.107545	0.13252	0.178944	0.275017	0.114588	0.133011	0.161653	0.130383	0.14015	0.141659	0.176444	0.14273
Rastrigin 10D (45)	3.594738	5.044592	3.789704	3.756153	3.864114	4.75427	3.846435	3.863727	3.832011	5.270562	4.026834	3.216063	3.999821	4.5045	4.180427	3.994107
Rastrigin 30D (46)	12.344	16.04493	10.9809	10.9809	13.1257	19.08223	9.281153	9.281153	14.78485	11.3366	10.9821	12.8066	12.79729	12.8066	13.05385	12.60066
Schwefel 10D (47)	102.6061	160.2401	260.2853	293.2839	89.91938	163.4934	220.084	226.034	258.8402	109.8138	186.8554	184.8625	130.2179	133.3553	165.4847	149.9314
Schwefel 30D (48)	316.9808	419.4869	478.4665	478.4665	331.3564	373.1279	370.4348	370.4348	294.6744	307.0243	494.9968	301.3769	292.8625	305.8772	350.3684	281.309
Griewangk 10D (49)	0.111057	0.124152	0.129368	0.112491	0.112069	0.146805	0.175135	0.119118	0.115619	0.12328	0.170179	0.116731	0.118151	0.1297	0.168754	0.141561
Griewangk 30D (50)	1.598808	1.841664	1.32692	1.32692	1.585077	1.829976	1.494744	1.494744	1.701168	1.646999	1.821455	1.994324	2.094793	2.180435	2.157859	2.095577
Salomon 10D (51)	0.102366	0.125539	0.112904	0.103876	0.122558	0.115434	0.119155	0.108493	0.107252	0.123347	0.140973	0.120655	0.126033	0.127279	0.141262	0.122004
Salomon 30D (52)	0.265647	0.276739	0.239194	0.239194	0.226056	0.188108	0.188108	0.188108	0.269583	0.227435	0.276435	0.22022	0.249681	0.278787	0.251496	0.381325
Odd Square 10D (53)	0.058929	0.058929	0.071698	0.081334	0.039939	0.026156	0.017091	0.078022	0.05976	0.04038	0.039152	0.08385	0.029826	0.044146	0.035168	0.052835
Whitley 10D (54)	2045522	2604460	78015538	3031878	1890845	2378926	2938534	2544105	2337130	2442704	3347130	2442704	3231051	2755655	3052807	2089246
Whitley 30D (55)	2.3E+11	2.71E+11	1.31E+11	1.31E+11	1.78E+11	1.72E+11	1.72E+11	1.72E+11	2.15E+11	1.99E+11	1.99E+11	2.54E+11	1.03E+11	3.28E+11	4.37E+11	3.58E+11
Rana 10D (56)	274.4108	286.1826	262.0122	288.24	269.461	334.9216	295.1612	250.5919	414.7407	270.471	290.471</					



Results St. Dev. (100k)	A50, N1	A50, N2	A50, N3	A50, N4	A100, N1	A100, N2	A100, N3	A100, N4	A250, N1	A250, N2	A250, N3	A250, N4	A500, N1	A500, N2	A500, N3	A500, N4
Rosenbrock (1)	0.003351	0.00371	0.00351	0.00351	0.00353	0.003587	0.00353	0.00353	0.016458	0.002232	0.016458	0.016458	0.004011	0.002941	0.004011	0.004011
McCormic (2)	2.97E-06	7.22E-07	2.97E-06	2.97E-06	7.91E-06	2.48E-07	7.91E-06	7.91E-06	7.91E-06	0.002864	6.50E-07	6.50E-07	6.50E-07	0.002584	6.50E-07	6.50E-07
Box and Beits (3)	8.92E-06	2.16E-06	1.23E-06	1.23E-06	1.63E-05	7.81E-06	1.63E-05	1.63E-05	1.63E-05	1.81E-05	0.001045	0.001045	0.001045	3.00E-05	1.30E-05	1.30E-05
Goldstein (4)	0.000217	0.000151	0.000217	0.000217	0.000271	3.614992	0.000271	0.000271	0.001045	0.001045	0.001045	0.001045	0.001045	0.001045	0.001045	0.001045
Easom (5)	0.00716	0.007695	0.00716	0.00716	0.009262	0.005447	0.009262	0.009262	0.003372	0.00675	0.003372	0.003372	0.003372	0.003372	0.003372	0.003372
Mod Rosenbrock 1 (6)	0.090207	0.092136	0.090207	0.090207	0.090207	0.087196	0.090207	0.090207	0.082421	0.058726	0.082421	0.082421	0.082421	0.082421	0.082421	0.082421
Mod Rosenbrock 2 (7)	0.945759	0.941672	0.945759	0.945759	0.945759	0.934742	0.945759	0.945759	0.934742	0.93375	0.93375	0.93375	0.934187	1.253961	0.934187	0.934187
Bohachevsky (8)	1.668626	1.525626	1.668626	1.668626	1.668626	1.668626	1.668626	1.668626	1.668626	1.668626	1.668626	1.668626	1.668626	1.668626	1.668626	1.668626
Powell (9)	272380.1	272380.1	194569.9	413263.4	357388.9	357388.9	357388.9	357388.9	357388.9	357388.9	357388.9	357388.9	357388.9	357388.9	357388.9	357388.9
Wood (10)	931193.6	621732.2	433811.9	849174	700168.3	2096928	700168.3	700168.3	2096928	2096928	2096928	2096928	2096928	2096928	2096928	2096928
Beale (11)	3.680284	6.546745	3.680284	3.680284	3.509965	4.036273	3.509965	3.509965	9.627236	9.627236	9.627236	9.627236	28.06499	28.06499	28.06499	28.06499
Engvall (12)	8.125644	4.744431	8.125644	8.125644	3.218156	3.218156	3.218156	3.218156	5.514785	5.514785	5.514785	5.514785	4.101723	4.101723	4.101723	4.101723
DeJong (13)	3.08E-05	2.07E-05	3.08E-05	3.08E-05	2.50E-05	5.58E-06	2.50E-05	2.50E-05	7.01E-06	7.01E-06	7.01E-06	7.01E-06	1.44E-05	0.004572	1.44E-05	1.44E-05
Rastrigin (14)	0.008669	0.008323	0.008669	0.008669	0.005903	0.007679	0.005903	0.005903	0.076243	0.719393	0.076243	0.076243	0.484122	0.714999	0.484122	0.484122
Schwefel (15)	0.077186	0.093307	0.077186	0.077186	0.071113	0.066878	0.071113	0.071113	0.123635	3.15282	0.123635	0.123635	0.21028	0.21028	0.21028	0.21028
Griewangk (16)	0.005521	0.006364	0.005521	0.005521	0.005221	0.005471	0.005221	0.005221	0.006528	0.006528	0.006528	0.006528	0.005568	0.005568	0.005568	0.005568
Ackley (17)	0.040271	0.044498	0.040271	0.040271	0.039701	0.037941	0.039701	0.039701	0.034117	0.381666	0.034117	0.034117	0.040351	0.035427	0.040351	0.040351
Langenman (18)	0.010019	0.009415	0.008157	0.008157	0.068201	0.081411	0.068201	0.068201	0.051596	0.051596	0.051596	0.051596	0.065795	0.065795	0.065795	0.065795
Michalewicz (19)	0.374456	0.479419	0.64218	0.514902	0.354524	0.46527	0.568423	0.36165	0.593487	0.574367	0.592506	0.328586	0.341035	0.341035	0.341035	0.341035
Bratlin (20)	3.97E-05	1.81E-05	3.97E-05	3.97E-05	3.28E-05	4.09E-06	3.28E-05	3.28E-05	7.59E-06	7.59E-06	7.59E-06	7.59E-06	1.03E-05	0.007201	1.03E-05	1.03E-05
Six Hump Camel (21)	7.82E-06	4.94E-06	7.82E-06	7.82E-06	2.50E-05	1.08E-06	2.50E-05	2.50E-05	1.82E-06	0.00678	1.82E-06	1.82E-06	0.009545	0.02913	0.009545	0.009545
Osborne 1 (22)	0.10423	0.026561	0.07722	0.076414	0.077857	0.086835	0.106546	0.057226	0.058789	0.058789	0.058789	0.058789	0.058789	0.058789	0.058789	0.058789
Osborne 2 (23)	0.037971	0.036672	0.041729	0.036044	0.057931	0.057856	0.066041	0.062046	0.070409	0.070409	0.070409	0.070409	0.068505	0.068505	0.068505	0.068505
Mod Rastrigin (24)	3.836512	2.513368	3.836512	3.836512	2.274385	2.274385	2.274385	2.274385	1.661451	1.661451	1.661451	1.661451	2.407466	2.738888	2.407466	2.407466
Mineshaft 1 (25)	0.207792	0.249713	0.160201	0.249713	0.081897	0.236123	0.118727	0.236123	0.119335	0.119335	0.119335	0.119335	0.119335	0.119335	0.119335	0.119335
Mineshaft 2 (26)	0.002695	0.197476	0.05896	0.197476	0.000752	0.178724	0.101407	0.178724	0.096204	0.175209	0.175209	0.175209	0.160723	0.160723	0.160723	0.160723
Mineshaft 3 (27)	0.047576	0.180189	0.047576	0.047576	0.008493	0.074361	0.008493	0.008493	0.696338	0.705041	0.696338	0.696338	1.248096	2.466138	1.248096	1.248096
Spherical Contours (28)	3.881627	3.932635	3.932635	3.932635	4.687166	4.687166	4.687166	4.687166	8.536318	8.536318	8.536318	8.536318	30.41852	30.41852	30.41852	30.41852
S1 (29)	1.33E-11	0.036352	2.41E-12	0.036352	8.30E-12	0.006813	8.30E-12	8.30E-12	0.00102	0.000854	0.00102	0.00102	0.000297	0.000494	0.000494	0.000494
S2 (30)	5.16E-10	5.16E-08	5.16E-10	5.16E-10	2.07E-10	2.07E-10	2.07E-10	2.07E-10	1.91E-09	1.91E-09	1.91E-09	1.91E-09	6.47E-10	6.47E-10	6.47E-10	6.47E-10
S3 (31)	1.80E-08	1.94E-08	1.60E-08	1.60E-08	1.13E-06	2.79E-09	1.13E-06	1.13E-06	1.54E-08	0.006519	1.54E-08	1.54E-08	0.000451	0.0044	0.000451	0.000451
Downhill Step (32)	0	0	0	0	0	0	0	0	0.136715	0.219463	0.136715	0.136715	0.140513	0.140513	0.140513	0.140513
Salomon (33)	0.036696	0.033982	0.036696	0.036696	0.033505	0.034957	0.033505	0.033505	0.036331	0.036331	0.036331	0.036331	0.035645	0.037488	0.035645	0.035645
Whitley (34)	0.217441	0.170997	0.217441	0.217441	0.162739	0.159866	0.162739	0.162739	0.170306	0.170306	0.170306	0.170306	0.192486	0.200334	0.192486	0.192486
Odd Square (35)	0.001003	0.001191	0.001003	0.001003	0.001174	0.000701	0.001174	0.001174	0.001068	0.001068	0.001068	0.001068	0.043293	0.106424	0.043293	0.043293
Storn Chebyshev (36)	292.5495	311.4895	367.3218	351.2086	273.184	266.3224	335.3326	304.5303	2959.976	2959.976	2959.976	2959.976	2709.907	2709.907	2709.907	2709.907
Rana (37)	24.79684	46.58653	24.79684	24.79684	53.84518	56.73861	53.84518	53.84518	35.3259	35.3259	35.3259	35.3259	20.27776	20.27776	20.27776	20.27776
Rosenbrock 10D (38)	540.4067	515.8669	581.4181	408457.7	570.2309	569.7199	570.2309	569.7199	1579.246	1579.246	1579.246	1579.246	1719.795	1719.795	1719.795	1719.795
Rosenbrock 30D (39)	1756885	1757268	1758909	1758909	504834.9	504834.9	504834.9	504834.9	3287020	3287020	3287020	3287020	14520913	14520913	14520913	14520913
Mod Rosenbrock 1 10D (40)	224.5054	219.9974	239.046	217.1349	208.3191	208.5737	208.5737	208.5737	275.0985	275.0985	275.0985	275.0985	399.4616	399.4616	399.4616	399.4616
Mod Rosenbrock 1 30D (41)	2800.592	2818.703	2910.547	2910.547	5560.662	5560.662	5560.662	5560.662	18166.14	18166.14	18166.14	18166.14	17195.34	17195.34	17195.34	17195.34
Mod Rosenbrock 2 10D (42)	0.986514	0.721361	1.010997	0.957996	0.790669	0.664453	0.913418	0.801535	0.891816	0.982384	0.911703	0.959474	0.883104	0.883104	0.883104	0.883104
Mod Rosenbrock 2 30D (43)	1.0153	0.667337	0.93516	0.93516	0.986059	0.926619	0.836993	0.793268	0.739447	0.799809	0.813932	0.813932	1.015218	1.015218	1.015218	1.015218
Spherical Contours 10D (44)	0.217506	0.226473	0.249506	0.225105	0.285347	0.285347	0.285347	0.285347	0.280287	0.280287	0.280287	0.280287	0.747876	0.747876	0.747876	0.747876
Rastrigin 10D (45)	4.574538	5.77205	5.244224	5.491665	5.271861	6.484666	5.989542	5.352133	7.903638	7.903638	7.903638	7.903638	6.99626	6.99626	6.99626	6.99626
Rastrigin 30D (46)	16.71133	21.27324	18.80427	18.80427	26.19195	20.30815	24.58501	24.58501	28.07731	28.18518	27.39898	25.76213	31.80102	31.80102	31.80102	31.80102
Schwefel 10D (47)	115.2902	214.4069	321.302	322.9689	167.4295	207.9802	272.1125	208.9884	200.665	189.0501	227.15	185.3078	172.0348	172.0348	172.0348	172.0348
Schwefel 30D (48)	328.6991	461.652	453.4439	523.4439	387.135	554.2985	434.978	434.978	366.853	384.4306	451.4802	263.9187	261.1423	261.1423	261.1423	261.1423
Griewangk 10D (49)	0.191766	0.224213	0.278913	0.236337	0.230225	0.230225	0.230225	0.230225	1.002004	1.002004	1.002004	1.002004	0.522338	0.522338	0.522338	0.522338
Griewangk 30D (50)	2.721659	2.739612	2.741282	2.741282	5.193139	5.193139	5.193139	5.193139	8.931615	8.931615	8.931615	8.931615	20.86054	20.86054	20.86054	20.86054
Salomon 10D (51)	0.161748	0.163882	0.177408	0.153915	0.18758	0.19322	0.186931	0.191023	0.183994	0.183994	0.183994	0.183994	0.364181	0.364181	0.364181	0.364181
Salomon 30D (52)	0.395756	0.398025	0.384203	0.384203	0.447699	0.447699	0.447699	0.447699	0.973472	0.973472	0.973472	0.973472	1.561221	1.561221	1.561221	1.561221
Odd Square 10D (53)	0.054685	0.042378	0.045685	0.0287	0.072463	0.06792	0.06792	0.06792	0.067661	0.067661	0.067661	0.067661	0.057783	0.057783	0.057783	0.057783
Whitley 10D (54)	23084616	1.13E+09	1.13E+09	1.13E+09	8.28E+12	21247497	21247497	21247497	41082708	41082708	41082708	41082708	4.66E+08	4.66E+08	4.66E+08	4.66E+08
Whitley 30D (55)	4.79E+14	4.79E+14	4.79E+14	4.79E+14	7.58E+12											

















167











# APPENDIX H1: EA AVERAGE RESULTS

Average Results	1M Evals				500K Evals				100K Evals			
	SGA	PSO	DE	HJ	SGA	PSO	DE	HJ	SGA	PSO	DE	HJ
Rosenbrock (1)	7.42E-06	-1.91322	-1.91322	0	1.28E-022	1.14E-05	-1.91322	0	1.28E-022	1.62E-05	0	8.08E-013
McCormic (2)	-1.91322	-1.91322	-1.91322	-1.91322	-1.91322	-1.91322	-1.91322	-1.91322	-1.91322	-1.91322	-1.91322	-1.91322
Box and Betts (3)	5.10E-17	6.29E-33	6.29E-33	3	2.60E-025	2.08E-13	6.29E-33	3	2.60E-025	1.98E-10	6.29E-33	3
Goldstein (4)	3	3	3	3	3	3	3	3	3	3	3	3
Easom (5)	-1	-1	-1	-1	-0.96	-1	-1	-1	-0.96	-1	-1	-1
Mod Rosenbrock 1 (6)	0.029463	0.067461	7.83E-005	0.12562	0.008204	0.029463	0.067466	0.000278	0.008204	0.029463	0.068211	0.00574
Mod Rosenbrock 2 (7)	0.554649	1.026444	0.12562	0.12562	0.007147	0.554649	1.042706	0.186451	0.007147	0.554649	1.080681	0.478551
Bohachevsky (8)	0	0	0	0	0	0	0	0	0	0	0	0
Powell (9)	0.07962	225149.3	1.37E-010	1.37E-010	1.31E-018	2918.928	225149.3	7.65E-010	1.76E-017	36223.6	227915	32467.1
Wood (10)	0.055115	1.895501	1.62E-020	1.62E-020	4.11E-021	0.114644	1.895501	4.62E-011	4.11E-021	0.185459	2.191786	0.002877
Beale (11)	0	0.104137	0	0	1.10E-023	0	0.104137	0	1.11E-023	0	0.133885	0
Engvall (12)	0	0	0	0	0	0	0	0	0	0	0	0
DeJong (13)	0	0	0	5.50E-035	1.45E-023	0	6.69E-220	5.50E-035	1.45E-023	3.50E-100	5.17E-48	5.50E-035
Rastrigin (14)	0	0	0	0	0	0	0	0	0	0	0	0
Schweifel (15)	-837.966	-810.725	-837.966	-837.966	-837.966	-837.966	-809.541	-837.966	-837.966	-837.966	-807.172	-837.966
Griewangk (16)	0.00076	7.40E-05	7.40E-05	0	0.006435	0.00076	7.40E-05	0	0.006435	0.00076	0.000518	7.91E-007
Ackley (17)	4.44E-16	4.44E-16	4.44E-16	4.44E-016	9.05E-012	4.44E-16	4.44E-16	4.44E-016	9.05E-012	4.44E-16	4.44E-016	9.05E-012
Langerman (18)	-1.5	-1.5	-1.5	-1.5	-0.84904	-1.5	-1.5	-1.5	-0.84904	-1.5	-1.5	-1.5
Michalewicz (19)	-9.41956	-8.38134	-8.58054	-8.58054	-8.98162	-9.41956	-8.37332	-8.15419	-8.98162	-9.41956	-8.34146	-6.91792
Brannin (20)	0.397887	0.397887	0.397887	0.397887	0.397887	0.397887	0.397887	0.397887	0.397887	0.397887	0.397887	0.397887
Six Hump Camel (21)	-1.03163	-1.03163	-1.03163	-1.03163	-1.03163	-1.03163	-1.03163	-1.03163	-1.03163	-1.03163	-1.03163	-1.03163
Osborne 1 (22)	0.000431	0.500993	7.44E-005	7.44E-005	5.46E-005	0.000576	0.500993	0.000107	5.46E-005	0.001788	0.519239	0.000136
Osborne 2 (23)	0.040192	0.338392	0.040138	0.040138	0.040138	0.040138	0.338393	0.040138	0.040138	0.049142	0.339375	0.040136
Mod Rastrigin (24)	61.91701	66.03951	60.79753	60.79753	69.65214	61.91701	66.03951	60.79753	69.65214	61.91701	66.10381	73.32614
Mineshaff 1 (25)	2.108147	1.759376	1.833253	1.833253	2.252252	2.108147	1.759376	1.976885	2.252252	2.108147	1.759376	2.191939
Mineshaff 2 (26)	-1.41635	-1.40803	-1.41635	-1.41635	-1.3539	-1.41635	-1.40803	-1.41635	-1.3539	-1.41635	-1.40803	-1.41635
Mineshaff 3 (27)	-6.19856	-5.78	-6.9423	-6.9423	-6.19856	-6.19856	-5.72	-6.9064	-7	-6.19856	-5.68	-6.86802
Spherical Contours (28)	1.73E-142	0.00139	4.29E-031	4.29E-031	1.55E-70	1.55E-70	0.00139	4.29E-031	7.06E-021	1.44E-13	0.001593	6.23E-007
S1 (29)	0	0	0	0	3.11E-025	0	0	0	3.11E-025	0	0	3.11E-025
S2 (30)	2	2	2	2	2	2	2	2	2	2	2	2
S3 (31)	0.528872	0.528872	0.528872	0.528872	0.528872	0.528872	0.528872	0.528872	0.528872	0.528872	0.528872	0.528872
Downhill Step (32)	9	9	9	9	9	9	9	9	9	9	9	9
Salomon (33)	0.000999	0.000999	0	0	0.000999	0.000999	0.00513	0	0.056928	0.000999	0	0.056928
Whitley (34)	0.004735	0.004735	0	0	0.002368	0.002368	0	0	0.002368	0.005919	0	0
Odd Square (35)	-1.00847	-1.00847	-1.00847	-1.00847	-1.00847	-1.00847	-1.00847	-1.00847	-1.00847	-1.00847	-1.00847	-1.00847
Storn Chebyshev (36)	48.48605	48.48605	0	0.000633	48.48605	48.48605	0	0.30974	48.48605	48.48605	0	82.10315
Rana (37)	-999.075	-1009.3	-1023.42	-1023.42	-1004.01	-1000.53	-1009.3	-1023.42	-1004.01	-1000.05	-1009.3	-1004.01
Rosenbrock 10D (38)	3.271653	32.03413	0.018428	0.018428	2.47E-019	5.091197	32.03421	0.337704	8.70E-017	6.834324	32.45678	4.487699
Rosenbrock 30D (39)	27.83797	1130.247	0.005003	0.005003	3.28E-006	30.34245	1130.463	9.016813	0.098478	36.58164	1134.681	26.41671
Mod Rosenbrock 1 10D (40)	118.1656	7.866659	0.724829	0.724829	9.328353	118.1656	118.1656	8.025103	0.74089	9.328464	127.4822	8.368693
Mod Rosenbrock 1 30D (41)	55.65867	520.0627	28.07968	28.07968	21.173	55.65867	520.087	28.29864	21.24531	55.66621	546.9679	32.35948
Mod Rosenbrock 2 10D (42)	0.48398	0.869415	0.124351	0.124351	0.007811	0.48398	0.869415	0.176551	0.007811	0.48398	0.983523	0.542867
Mod Rosenbrock 2 30D (43)	0.533107	0.859063	0.118276	0.118276	0.007532	0.533107	0.861324	0.172092	0.007572	0.533107	1.017408	0.504374
Spherical Contours 10D (44)	0	0	4.50E-032	4.50E-032	1.27E-021	1.24E-165	5.97E-214	4.50E-032	1.27E-021	3.82E-32	7.28E-46	5.25E-032
Rastrigin 10D (45)	2.706289	16.22776	11.91103	11.91103	1.591934	2.706289	16.25761	14.67694	1.591934	2.706414	16.51629	22.75599
Rastrigin 30D (46)	22.82435	100.5741	161.7422	161.7422	9.591405	22.82435	100.5752	169.8472	9.591405	22.85317	100.576	198.794
Schweifel 10D (47)	-3881.3	-2813.98	-2815.25	-2815.25	-3598.4	-3881.3	-2813.98	-2719.13	-3598.4	-3881.3	-2812.78	-2465.1
Schweifel 30D (48)	-9057.22	-6954.17	-4831.07	-4831.07	-9361.55	-9057.22	-6954.17	-4681.46	-9361.55	-9055.4	-6954.12	-4305.95
Griewangk 10D (49)	0.008468	0.137772	0.132389	0.132389	0.000222	0.008468	0.138289	0.177611	0.000222	0.008468	0.139594	0.273462
Griewangk 30D (50)	0.00037	0.073024	0	0	0.00037	0.00037	0.073024	0	0	0.00037	0.083133	0.001387
Salomon 10D (51)	0.099873	0.184873	0.099873	0.099873	0.687873	0.099873	0.184873	0.099873	0.687873	0.099873	0.185873	0.099873
Salomon 30D (52)	0.217893	2.068873	0.121959	0.121959	2.458873	0.217893	2.068873	0.153587	2.458873	0.217893	2.069873	0.501882
Odd Square 10D (53)	-0.73712	-0.48034	-0.74049	-0.74049	-0.02058	-0.73712	-0.48033	-0.74026	-0.02058	-0.73712	-0.48027	-0.7395
Whitley 10D (54)	26.1428	30.44494	38.86195	38.86195	0	26.19969	42.90359	40.4026	0	26.48996	30.45603	51.15253
Whitley 30D (55)	275.6891	7844.236	590.4345	590.4345	0	276.0691	7844.236	625.7617	0	277.5687	8342.14	733.4363
Rana 10D (56)	-3040.95	-3615.7	-5114.47	-5114.47	-4502.87	-3109.41	-3612.96	-5114.29	-4501.14	-2970.85	-3585.25	-5076.73
Rana 30D (57)	-5973.06	-8415.67	-13998.6	-13998.6	-11992.9	-6177.16	-8402.75	-12901.2	-11772.6	-5781.02	-8333.76	-8053.51

# APPENDIX H2: EA ST. DEV. OF RESULTS

Results St. Dev.	SGA	PSO	1M Evals DE	HJ	SGA	PSO	500k Evals DE	HJ	SGA	PSO	100k Evals DE	HJ
Rosenbrock (1)	0.000063	0	4.00E-15	0	1.58E-022	0.000096	0	0	1.58E-022	0.000137	0	1.47E-012
McCormic (2)	0	4.00E-15	4.00E-015	0	4.00E-015	0	4.00E-15	4.00E-015	4.00E-015	4.00E-015	4.00E-015	4.00E-015
Box and Betts (3)	0	2.66E-32	0	0	1.85E-025	0	2.66E-32	0	1.85E-025	0	2.66E-32	0
Goldstein (4)	0	9.01E-16	8.88E-016	0	3.66E-015	0	8.98E-16	8.88E-016	3.66E-015	0	8.68E-16	0
Easom (5)	0	0	0	0	0.195943	0	0	0	0.195943	0	0	0
Mod Rosenbrock 1 (6)	0.044651	0.252745	5.70E-005	5.70E-005	0.044651	0.044651	0.252744	0.000209	0.044651	0.044651	0.253561	0.004461
Mod Rosenbrock 2 (7)	0.324284	2.067343	0.054968	0.054968	0.324284	0.324284	2.090583	0.07273	0.324284	0.324284	0.215632	0.01077
Bohachevsky (8)	0	0	0	0	0	0	0	0	0	0	0	0
Powell (9)	0.794879	2145012	1.03E-010	1.03E-010	17907.51	17907.51	2145012	5.45E-010	138455.9	138455.9	2146120	28471.41
Wood (10)	0.296656	14.54911	3.82E-020	3.82E-020	0.44573	0.44573	14.54911	7.35E-011	0.54884	0.54884	17.47995	0.002059
Beale (11)	0	0.19054	0	0	1.22E-023	0	0.19054	0	1.22E-023	0	0.203776	0
Engvall (12)	0	0	0	0	1.55E-023	0	0	0	1.55E-023	0	1.02E-47	1.84E-034
DeJong (13)	0	0	0	0	2.16E-012	0	0	0	2.16E-012	0	0	0
Rastrigin (14)	0	49.8427	0	0	0.005988	0	50.58301	2.16E-012	0.005988	0.002232	51.95111	2.16E-012
Schwefel (15)	0.002232	0.000736	0	0	4.56E-012	0	0.000736	0	4.56E-012	0	0.001887	2.57E-006
Griewangk (16)	0	0	0	0	0.155603	0	0.286011	2.22E-016	0.155603	0	0.285088	3.43E-016
Ackley (17)	0	0.286011	0	0	0.197975	0.157387	0.763187	0.300465	0.197975	0.157387	0.768329	0.374973
Langerman (18)	0.157387	0.759209	0.238737	0.238737	0	0	0	0	0	0	0	0
Michalewicz (19)	0	1.33E-15	0	0	1.27E-015	0	1.33E-15	1.33E-015	1.27E-015	0	1.33E-15	1.27E-015
Six Hump Camel (21)	0	0.000205	1.81E-006	1.81E-006	0.000364	0.000364	0.482557	3.82E-006	0.000937	0.000937	0.496403	0.000216
Osborne 1 (22)	0.000103	0.312003	3.71E-017	3.71E-017	0.001767	0.001767	0.312005	5.00E-017	0.006231	0.006231	0.313051	0.000845
Osborne 2 (23)	5.755315	11.92076	0.014792	0.014792	5.755315	5.755315	11.92076	0.014792	5.755315	5.755315	11.99384	3.966187
Mod Rastrigin (24)	0.392745	0.464042	0.466305	0.466305	0.392745	0.392745	0.464042	0.391092	0.392745	0.392745	0.464042	0.158571
Mineshaft 1 (25)	0.058289	0.058289	1.33E-015	1.33E-015	0.146668	0.146668	0.058289	1.33E-015	0.146668	0.146668	0.058289	0.238943
Mineshaft 2 (26)	0.9755	0.30168	0	0	6.64E-022	0.93892	0.96	0.376568	0.93892	0.93892	0.947418	0.405928
Mineshaft 3 (27)	0.002743	1.03E-031	0	0	7.54E-025	0	0.002743	1.03E-031	6.64E-022	0.002995	1.52E-007	3.73E-005
Spherical Contours (28)	0	0	0	0	5.25E-015	0	0	0	5.25E-015	0	0	5.25E-015
S1 (29)	0	6.66E-16	6.66E-016	6.66E-016	0.049445	0	6.66E-16	6.66E-016	0.049445	0	6.66E-16	6.66E-016
S2 (30)	0	0	0	0	0.049445	0	0	0	0.049445	0	0	0
S3 (31)	0	0.012823	0	0	0.126913	0	0.01327	0	0.126913	0	0.01409	0
Downhill Step (32)	0.009987	6.34E-09	3.08E-009	3.08E-009	0.009418	0.009418	7.52E-09	1.15E-008	0.009987	0.009987	1.79E-08	3.91E-007
Salomon (33)	0.009418	0	0	0	173.6254	173.6254	0	1.271737	0.009418	0.009418	0	100.6916
Whitley (34)	0	0	0.006155	0.006155	11.50347	11.50347	12.50943	1.71E-012	173.6254	173.6254	12.50943	1.71E-012
Odd Square (35)	14.26028	12.50943	1.71E-012	1.71E-012	0.686242	0.686242	79.12802	0.083821	11.70672	11.70672	12.50943	1.71E-012
Storn Chebyshev (36)	0.800642	79.12805	0.006282	0.006282	15.91657	15.91657	8947.351	0.665747	0.587817	0.587817	81.46991	0.432216
Rana (37)	14.90065	8947.371	0.001629	0.001629	9.687551	9.687551	314.901	0.042138	21.43761	21.43761	8947.183	0.140335
Rosenbrock 30D (38)	9.687551	314.901	0.031629	0.031629	45.69274	45.69274	334.0535	0.024738	9.687544	9.687544	318.168	0.061401
Rosenbrock 100D (39)	45.69274	334.041	0.022442	0.022442	6.185837	6.185837	1.832608	0.07152	45.69502	45.69502	350.0611	0.642863
Mod Rosenbrock 1 10D (40)	0.376667	1.82757	0.052302	0.052302	0.014619	0.014619	1.832608	0.07152	0.376667	0.376667	2.155357	0.225003
Mod Rosenbrock 1 30D (41)	0.383134	1.719927	0.054468	0.054468	0.010463	0.010463	1.71906	0.08702	0.383134	0.383134	2.022665	0.238489
Mod Rosenbrock 2 10D (42)	0	2.85E-032	2.85E-032	2.85E-032	3.15E-022	3.15E-022	0	2.85E-032	0.010441	0.010441	3.11E-032	8.24E-018
Mod Rosenbrock 2 30D (43)	6.5826	6.549642	1.996652	1.996652	2.015283	2.015283	6.584022	2.225028	2.015176	2.015176	6.88607	3.427226
Spherical Contours 10D (44)	26.154	26.02242	8.79619	8.79619	7.207864	7.207864	26.0213	9.545773	2.015176	2.015176	26.02068	9.487318
Rastrigin 10D (45)	228.6542	326.6097	114.3907	114.3907	142.7457	142.7457	326.6097	128.4158	228.6542	228.6542	329.2317	131.8472
Rastrigin 30D (46)	784.5893	744.3764	201.2209	201.2209	784.5893	784.5893	744.3764	222.3171	786.0776	786.0776	744.3378	281.2943
Schwefel 10D (47)	0.017456	0.073298	0.038384	0.038384	0.001262	0.001262	0.074168	0.041646	0.017456	0.017456	0.075464	0.05994
Griewangk 10D (48)	0.001866	0.097188	0	0	0.001866	0.001866	0.097188	0	0.001866	0.001866	0.109041	0.010733
Griewangk 30D (49)	8.60E-012	0.063836	8.60E-012	8.60E-012	0.176227	0.176227	0.063836	3.65E-011	0.001866	0.001866	0.064838	4.21E-009
Salomon 10D (50)	0.041087	0.482752	0.030311	0.030311	0.250637	0.250637	0.482752	0.040536	0.041087	0.041087	0.483789	0.031814
Salomon 30D (52)	0.032639	0.118679	0.000216	0.000216	0.016301	0.016301	0.118674	0.000248	0.032639	0.032639	0.118664	0.000327
Odd Square 10D (53)	3.817087	11.21451	3.817087	3.817087	13.22542	13.22542	11.21451	3.979878	0.032639	0.032639	11.22504	0.000327
Whitley 10D (54)	94.78674	39082.2	94.78674	94.78674	94.41092	94.41092	39082.2	14.40303	93.16561	93.16561	16.65185	2.74E-009
Whitley 30D (55)	567.8693	427.3699	7.393179	7.393179	150.1853	150.1853	427.3699	8.506968	540.2387	540.2387	452.5264	82.70786
Rana 10D (56)	2498.725	1061.921	1178.774	1178.774	316.3914	316.3914	1067.271	1535.417	1969.486	1969.486	1085.752	146.1392
Rana 30D (57)												295.192



# APPENDIX I: PARAMETER VALUE LIST FOR SMOA AND VARIANTS

Parameter Values from Section 3.2: Vegetative State		
Parameter	Value	Description
$c$	0.5	Scaling factor for random movement.
MIN_SEARCH_TIME	30	Minimum number of time steps an amoeba must spend in the Vegetative State.
NUM_PSEUDOPODS	4	The number of pseudopods (searches) an amoeba uses during a time step in the Vegetative State.

Parameter Values from Section 3.3: Aggregative State		
Parameter	Value	Description
$c_1$	0.2	Scaling factor for previous timestep velocity.
$c_2$	0.4	Scaling factor for the direction of the neighboring vertex with the most cAMP.
$c_3$	0.4	Scaling factor for the direction of the pacemaker.
$c_4$	0.4	Scaling factor for the random movement in the velocity update equation.
$k$	256	Maximum amount of cAMP allowed at a vertex.
$c$	8	Maximum cAMP deposit allowed by an amoeba.
$\epsilon$	0.05	Allowed error in $\epsilon$ -ANN
minAggregateCount	50, (0.5* aggregateCountThreshold if originally greater than or equal to 50)	Minimum number of amoeba in an aggregate (slug)
aggregateCountThreshold	NUM_AMOEBAE / NUM_NEIGHBORS	Minimum preferred number of amoeba in an aggregate. Not effective if NUM_NEIGHBORS is large
MAX_AG_TIME	30	Maximum amount of time an amoeba may spend aggregating before reverting to the vegetative state.

Parameter Values from Section 3.6: Slug State		
Parameter	Value	Description
$c_1$	0.2	Scaling factor for previous timestep velocity in slug.
$c_2$	0.2	Scaling factor for the direction of the neighboring amoeba with the best objective function value.
$c_3$	0.4	Scaling factor for the direction of the head.
$c_4$	0.4	Scaling factor for the random movement in the slug velocity update equation.
MIN_SLUG_UPDATES	30	Minimum number of timesteps an amoeba must spend in the slug state. Unnamed in Section 3.6.

Parameter Values from Section 3.7: Slime Mold Optimization Algorithm		
Parameter	Value	Description
NUM_AMOEBAE	50, 100, 250, or 500	Number of amoebae in the population
NUM_EVALS	100,000, 500,000, or 1,000,000	Number of objective function evaluations to be used in the algorithm.
NUM_NEIGHBORS	Based on neighbor strategy	Number of neighbors used in the $\epsilon$ -ANN data structures.

Parameter Values from Section 4.1.1: Simplex Vegetative State		
Parameter	Value	Description
ALLOWED_ERROR	0.05	The probability of making a random point in the simplex the reflected point.
$\lambda$	2	Scaling factor for the size of the reflected Simplex. A value of 2 produces a symmetric reflection.

Parameter Values from Section 4.1.2: Razor Search Vegetative State		
Parameter	Value	Description
$\epsilon_{\min}$	$10^{-10}$	Overall smallest allowable step size during Razor Search.
$\epsilon_{\text{razor}}$	Average distance between amoebae	Initial smallest allowable step size
MAX_PATTERN_EVALS	100	The maximum number of pattern iterations.
$\kappa$	7	The maximum number of Razor Search iterations.



Parameter Values from Section 4.2: DE+Followers (HTDE) Slug State		
Parameter	Value(s)	Description
F	0.5	DE constant for mutation factor
CR	0.9	DE constant for crossover probability
MINIMUM_SIZE_FOR_DE	4	Fewest number of amoebae that may be in the slug for DE to work.
PERCENT_HEAD	0.20	The appropriate percentage of amoebae to put in the head of the slug.

## VITA

David R. Monismith Jr.

Candidate for the Degree of

Doctor of Philosophy

Dissertation: THE USES OF THE SLIME MOLD LIFECYCLE AS A MODEL FOR  
NUMERICAL OPTIMIZATION

Major Field: Computer Science

Biographical:

Education:

Completed the requirements for the Master of Science in Electrical Engineering at Oklahoma State University, Stillwater, Oklahoma in July 2008.

Completed the requirements for the Bachelor of Science in Computer Science at Tulane University, New Orleans, Louisiana in December 2001.

Experience:

Teaching Assistant at Tulane University from January 2001 to December 2001.

Research Assistant at Oklahoma State University from August 2004 to December 2004.

Teaching Assistant at Oklahoma State University from January 2002 to July 2008.

Professional Memberships:

Member of IEEE and ACM.

Name: David R. Monismith Jr.

Date of Degree: July 2010

Institution: Oklahoma State University

Location: Stillwater, Oklahoma

Title of Study: THE USES OF THE SLIME MOLD LIFECYCLE AS A MODEL FOR  
NUMERICAL OPTIMIZATION

Pages in Study: 177

Candidate for the Degree of Doctor of Philosophy

Major Field: Computer Science

Scope and Method of Study:

This work provides a discussion of the lifecycle of the cellular slime mold, *Dictyostelium discoideum* (Dd), as it may be used for numerical optimization with emphasis on its use as an Evolutionary Algorithm. The study begins with a review of a number of existing numerical optimization algorithms that make use of direct search methodology (i.e. they do not require the computation of a derivative to perform optimization) such as Pattern Search, Downhill Simplex, and Razor Search. These algorithms are of interest because they were precursors to Evolutionary Optimization, and their search strategies, in some cases, are similar to amoeboid movement. Next, a review of some existing Evolutionary Algorithms is provided. This includes a review of Differential Evolution, Particle Swarm Optimization, and a Real-Coded Genetic Algorithm. The second part of the review is of Dd lifecycle, biological computation, and simulations thereof. With simulations in hand, several data structures are introduced to handle the transition from simulation to optimization. Then, the Slime Mold Optimization Algorithm is introduced. It follows the lifecycle of Dd, using vegetative, aggregative, mound, slug, and dispersive states to perform optimization. Thereafter, several variants of the Slime Mold Optimization Algorithm are created.

Findings and Conclusions:

The Slime Mold Optimization Algorithm and its variants were tested on a comprehensive function suite consisting of objective functions of varying difficulty, dimensionality, and modality. Results were compared by varying parameters of the algorithm including number of amoebae and maximum numbers of objective function values. Results were also compared to those of existing Evolutionary Algorithms. These results show promise and in some cases are better than existing Evolutionary Algorithms, though work is needed to make the algorithm better suited to extremely large search spaces and problems with high dimensionality. Variants of the algorithm were also tested showing improvement over the original version of the Slime Mold Optimization Algorithm.

ADVISER'S APPROVAL: Dr. Blayne E. Mayfield

---